



UNIVERSIDADE D
COIMBRA

Ana Catarina Sousa Lobo

**IMMUNOLOGICAL EFFECTS OF
PHOTODYNAMIC THERAPY**

Tese no âmbito do doutoramento em Química, ramo de Química Médica, orientada pelo Professor Doutor Luís Guilherme da Silva Arnaut Moreira e pelo Professor Doutor Mário José Ferreira Calvete e apresentada ao Departamento de Química, Faculdade de Ciências e Tecnologia da Universidade de Coimbra.

Dezembro de 2020

Faculdade de Ciências e Tecnologia da Universidade de Coimbra

IMMUNOLOGICAL EFFECTS OF PHOTODYNAMIC THERAPY

Ana Catarina Sousa Lobo

Dissertação de Doutoramento na área científica Química, ramo de Química Médica orientada pelo Professor Doutor Luís Guilherme da Silva Arnaut Moreira e pelo Professor Doutor Mário José Ferreira Calvete e apresentada ao Departamento de Química da Faculdade de Ciências e Tecnologia da Universidade de Coimbra

Dezembro de 2020



UNIVERSIDADE D
COIMBRA

The studies presented in this thesis were performed at Chemistry Department of Faculty of Sciences and Technology of University of Coimbra, Centre for Neuroscience and Cell Biology of University of Coimbra (CNC), Institute of Nuclear Sciences Applied to Health (ICNAS), Coimbra Institute for Clinical and Biomedical Research (iCBR), Immunology Institute and Anatomic Pathology Department of Faculty of Medicine of University of Coimbra. The work was funded by the grants PD/BD/132524/2017, PTDC/QEQ-MED/3521/2014 and from the European Union's Horizon 2020 research and innovation programme under the Marie Skłodowska-Curie grant agreement number 764837 (Polythea—How light can save lives). The Coimbra Chemistry Center is supported by the Fundação para a Ciência e a Tecnologia (FCT) through the project Pest-OE/QUID/QUI/00313/2019. Luzitin S.A. provided redaporfin for this work.



“If we knew what it was we were doing, it would not be called research, would it?”

Albert Einstein

TABLE OF CONTENTS

I.	ACKNOWLEDGEMENTS.....	1
II.	THESIS ABSTRACT	4
III.	RESUMO DA TESE.....	7
IV.	LIST OF PHOTOSENSITIZERS	11
V.	DEFINITION OF TERMS	13
1	GENERAL INTRODUCTION.....	21
1.1	PHOTODYNAMIC THERAPY.....	21
1.1.1	Photochemistry	21
1.1.2	Photosensitizers	22
1.1.3	Light.....	24
1.1.4	PDT protocols and cell death mechanisms.....	25
1.1.5	Tumor associated antigens	28
1.2	SYSTEMIC ANTITUMOR IMMUNITY ELICITED BY PDT.....	30
1.2.1	PDT and innate immunity	33
1.2.1.1	Acute Inflammation: From local to systemic.....	33
1.2.1.2	Complement activation.....	35
1.2.1.3	Neutrophils.....	36
1.2.1.4	Natural Killer cells.....	38
1.2.1.5	Macrophages	39
1.2.1.6	Dendritic cells	42
1.2.2	PDT and adaptive immunity	43
1.2.2.1	Helper T cells.....	45
1.2.2.2	Cytotoxic T cells.....	46
1.2.2.3	Regulatory T cells.....	47
1.2.2.4	B cells.....	48
1.3	COMBINATORIAL APPROACHES TO STIMULATE IMMUNE RESPONSES.....	50
1.3.1	Non-specific immunotherapies and PDT.....	50
1.3.1.1	Exogeneous and microbial immunostimulants	51
1.3.1.2	Cytokines, growth factors and other modulators	53
1.3.2	Specific/Cell-based immunotherapies + PDT	55
1.3.2.1	Adoptive transfers and PDT-generated vaccines.....	55

1.3.2.2	Monoclonal antibodies.....	57
1.3.2.3	Immune checkpoint blockers (ICB).....	60
2	OBJECTIVES AND OUTLINES.....	66
3	IMMUNE RESPONSES AFTER VASCULAR PDT WITH REDAPORFIN	69
3.1	ABSTRACT.....	70
3.1.1	Graphical Abstract.....	70
3.2	INTRODUCTION.....	71
3.3	MATERIAL AND METHODS	74
3.3.1	Cell line.....	74
3.3.2	Mouse tumor model and PDT	74
3.3.3	Lymphocyte analysis by flow cytometry	74
3.3.4	Quantification of blood cytokines.....	74
3.3.5	Analysis of blood lymphocytes expressing TNF- α , IFN- γ , IL-4 or IL-17A by flow cytometry	75
3.3.6	In vivo depletion of neutrophils and CD4 ⁺ or CD8 ⁺ T lymphocytes	75
3.3.7	Histology and Immunohistochemistry (IHC).....	75
3.3.8	Statistical analysis.....	76
3.4	RESULTS AND DISCUSSION.....	77
3.4.1	Redaporfin-PDT induces accentuated neutrophilia and increased levels of the pro-inflammatory cytokine IL-6.....	77
3.4.2	Redaporfin-PDT activates the adaptive immune system and depends on CD8 ⁺ T cells for tumor eradication.....	79
3.4.3	Redaporfin-PDT changes T cells population in the tumor bed but not B cells.....	83
3.5	CONCLUSION.....	87
3.6	SUPPLEMENTARY MATERIAL	88
4	OPTIMIZATION OF REDAPORFIN-PDT OF IMMUNOSSUPPRESSIVE TUMOR MODELS.....	90
4.1	ABSTRACT.....	90
4.2	INTRODUCTION.....	91
4.3	MATERIAL AND METHODS	93
4.3.1	Chemicals.....	93
4.3.2	Cell lines	93
4.3.3	Animal tumor models and PDT protocol.....	93
4.3.4	Photoacoustic Tomography	94
4.3.5	Statistical Analysis	94

4.4	RESULTS AND DISCUSSION.....	96
4.4.1	PDT optimization of melanoma and mammary carcinoma animal models	96
4.4.2	Accumulation profile of redaporfin is dependent on the tumor models	102
4.5	CONCLUSION.....	104
4.6	SUPPLEMENTARY MATERIAL	105
5	COMBINATORIAL APPROACHES OF REDAPORFIN-PDT AND IMMUNOTHERAPY.....	107
5.1	ABSTRACT.....	107
5.2	INTRODUCTION.....	108
5.3	MATERIAL AND METHODS	109
5.3.1	Chemicals.....	109
5.3.2	Cell lines	109
5.3.3	Mouse tumor model and PDT	109
5.3.4	Immune checkpoint blockade with monoclonal antibodies	110
5.3.5	IVIS Imaging	110
5.3.6	In vitro PDT protocol	111
5.3.7	Flow cytometry.....	111
5.3.8	Statistical Analysis	112
5.4	RESULTS AND DISCUSSION.....	113
5.4.1	Combinatorial approaches of redaporfin-PDT and immune checkpoint blockers	113
5.4.2	Redaporfin-PDT alters the expression of immune molecules by tumor cells	120
5.5	CONCLUSION.....	126
6	GENERAL CONCLUSIONS AND FINAL REMARKS	128
7	APPENDIX.....	133
I.	REDAPORFIN IN VIVO FORMULATION	133
II.	LIGHT DELIVERY LASER.....	133
III.	LIST OF FIGURES	135
IV.	LIST OF TABLES.....	140
8	REFERENCES	141

i. Acknowledgements

The accomplishment of this doctoral thesis was an amazing adventure which started in 2016. I would like to thank all the ones involved in the development of this project, without whom it would not be possible to accomplish.

First and foremost, I would like to express my sincere gratitude to my supervisor Professor Luis Arnaut. To express one of the most important things that I have learned I echo the words of Claude Levi-Strauss, “The scientist is not a person who gives the right answers, he's one who asks the right questions”. I am thankful for the continuous guidance and support over this project, for the shared wisdom and the opportunity to develop my PhD project in his research group.

I am also deeply grateful to Dr. Lúcia Silva, for all the support given over the last years, even when from a few hundred kms away. For all the scientific discussions, for the help with the experiments, for sharing the enthusiasm for science and for being a huge inspiration.

I would like to extend my sincere thanks to Professor Mário Calvete, for the support and availability to always find the best solution for the faced challenges.

I would also like to thank Professor Carlos Serpa and Dr. Fábio Schaberle for the insightful ideas, for the help in the spectroscopic fields but also for all the conversations that kept us thinking out of the box.

Special thanks to all my research group colleagues and friends for the support whenever it was needed. Particularly to Alexandre for being a lab partner and friend for almost a decade, to Maria Inês for being my friend, my mum, and my shrink at the same time. To Hélder, Diogo, Bernardo, Amílcar, Claire and Piotr, for listening all my PhD dramas, and for the countless scientific discussions that end up with nonscientific solutions.

I thank the Portuguese Foundation for Science and the MedChemTrain programme for the funding that financially supported this research project (PD/BD/132524/2017 and PTDC/QEQ-MED/3521/2014), to *Centro de Química de Coimbra* (Pest-OE/QUID/QUI/00313/2019), to Polythea and all the institutions involved in this project. I also thank Luzitin S.A. for providing the compound for these studies.

Last but not the least, to my family, a toda a minha família Sousa Lobo, pelo apoio incondicional e por conseguirem controlar a ansiedade de perguntar quando é que estaria terminada a tese. Aos meus pais, Céu e Luís, pela prova diária de superação, com toda a certeza nada disto seria possível sem vós. Às minhas irmãs, Raquel e Andreia, por estarem sempre presentes, por me fazerem olhar para cima e seguir em frente, sempre. À avó Maria, pela persistência e esforço em tentar perceber o tema da minha tese. À Rita e ao Cristiano, por provarem que há sempre tempo para tudo, principalmente para sonhar mais alto. E aos três presentes mais recentes da minha vida, os meus sobrinhos, Miguel, Afonso e Inês, por serem as estrelas do meu dia-a-dia e transformarem a minha vida.

ii. Thesis Abstract

Photodynamic therapy (PDT) relies on the administration of a photosensitizer (PS) that is activated on the target tissue after the irradiation with light of a specific wavelength absorbed by the PS. Redaporfin is a recently developed photosensitizer for PDT that is currently in phase 2 clinical trials (NCT02070432). Redaporfin is a photostable bacteriochlorin with intense infrared absorption, high yield of ROS generation, high phototoxicity, low skin photosensitivity and favorable pharmacokinetics. A vascular protocol of redaporfin-PDT with mice bearing CT26.WT tumors not only destroys the primary tumor but also reduces the development of metastasis, thus suggesting antitumor immunity.

This work characterizes the immune response triggered by this vascular-PDT protocol. At different timepoints after tumor irradiation, blood samples were collected, and distinct immune cell populations and cytokines were quantified. Redaporfin-PDT leads to a strong neutrophilia, with systemic increase of IL-6, increased percentage of CD4⁺ and CD8⁺ T cells producing IFN- γ or CD69⁺ and increased CD4⁺/CD8⁺ T cell ratio. We also showed that at the tumor bed, T cell tumor infiltration disappeared after PDT but reappeared with a much higher incidence one day later. The depletion of specific immune populations suggested that neutrophils and cytotoxic T cells have a major role in the development of the antitumor immune response elicited by redaporfin-PDT, while helper T cells may just have a supportive role.

Regarding this, we hypothesize that the combination of redaporfin-PDT with an immune therapy may potentiate the efficacy of both therapies, namely by increasing the response rates of immunotherapies and strengthening the systemic effects of PDT, especially in difficult tumors to treat. The tumor models were selected taking in consideration that redaporfin-PDT is capable of eliciting immunogenic cell death (ICD) and may be able to enhance the immunogenicity of tumor cells.

Melanoma and mammary carcinoma tumors are recognized to be more aggressive and difficult to treat than most mouse tumor models, namely colon carcinoma. The response to redaporfin-PDT was evaluated in mouse mammary carcinoma expressing luciferase (4T1-luc2) and in mouse skin melanoma (B16F10) tumor models, and PDT parameters were optimized to maximize the impact on tumors while minimizing treatment lethality.

A significant edema that later progressed to necrosis was observed in both tumor models. However, cures were only achieved with the B16F10 tumor model. Imaging with photoacoustic tomography suggested that the lower content of redaporfin in 4T1 tumors is the main reason for the challenging behavior of this orthotopic 4T1 model.

The antitumor effect elicited by PDT is in some cases opposed by the immunosuppressive mechanisms elicited by tumor cells which makes the treatment ineffective. Thus, immunotherapies that have as major goal the alleviation of this immunosuppressive tumor environment are interesting for combination therapies, increasing the efficacy with better antitumoral and antimetastatic effects. We reported a combination of redaporfin-PDT with immunotherapies using CTLA-4 and PD-1 in three different tumor models. Treatment outcomes were evaluated by survival, tumor growth kinetics and, for the carcinoma model, observation of metastasis development by bioluminescent imaging. Furthermore, we evaluated the changes on expression of several immune checkpoint molecules triggered by redaporfin-PDT *in vitro*.

Combination of redaporfin-PDT with CTLA-4 immunotherapy, but not with PD-1, led to a significant improvement of survival and a higher cure rate in the colon carcinoma animal model. However, the same was not achieved with the melanoma and breast carcinoma animal models. Expression of immune checkpoint molecules was induced in tumor cells treated *in vitro* with redaporfin-PDT. The most notable changes were observed for CD80 and PD-L1. These results demonstrate that the combination of photodynamic therapy with immunotherapy may improve the treatment of malignant diseases that represent a challenge to immunotherapies alone and highlights the fact that a global therapeutic strategy may not be ideal for every tumor model. Combinatorial approaches are not universal and have to be tailored to the specificities of each clinical case.

Keywords:

photodynamic therapy, redaporfin, cancer, antitumor immune response, immunotherapy, immune checkpoint blockers, metastasis, medicinal chemistry

iii. Resumo da Tese

A terapia fotodinâmica (PDT, do inglês, *photodynamic therapy*) consiste na administração de um fotossensibilizador (PS, do inglês, *photosensitizer*) que é ativado no tecido alvo após a irradiação com luz com um comprimento de onda absorvido pelo PS. A redaporfin é um fotossensibilizador desenvolvido recentemente para a PDT e que está atualmente em ensaios clínicos fase 2 (NCT02070432). A redaporfin é uma bacterioclorina fotoestável com intensa absorção no infravermelho próximo, elevado rendimento de formação de espécies reativas de oxigênio (ROS, do inglês, *reactive oxygen species*), elevada fototoxicidade, baixa fotossensibilidade da pele e uma farmacocinética favorável. A aplicação de um protocolo de PDT vascular com redaporfin em murganhos com tumores de carcinoma do cólon (CT26.WT) não só destrói o tumor primário como também reduz o desenvolvimento de metástases, sugerindo assim o aparecimento de imunidade anti-tumoral.

Este trabalho caracteriza a resposta imunitária desencadeada através deste protocolo de PDT vascular. Em tempos pré-determinados após a irradiação do tumor foram feitas colheitas de sangue e foram quantificadas as diferentes populações de células imunes e citocinas envolvidas na resposta imunitária. A PDT com a redaporfin provoca uma forte neutrófilia, um aumento sistêmico da IL-6, um aumento da percentagem de células CD4⁺ e CD8⁺ T que produtoras de IFN- γ ou CD69⁺ e um aumento do rácio de células T CD4⁺/CD8⁺. Ao nível do leito tumoral, a infiltração de linfócitos T desaparece após a PDT, mas reaparece com muito maior incidência 24 h mais tarde. A depleção de populações de células imunes específicas demonstrou que os neutrófilos e as células T citotóxicas desempenham um papel importante no desenvolvimento da resposta imune anti-tumoral desencadeada pela PDT com redaporfin, enquanto que as células T auxiliares parecem desempenhar apenas um papel de suporte.

Tendo isto em consideração, propomos que a combinação da PDT com a redaporfin e a imunoterapia pode potenciar a eficácia de ambos os tratamentos, nomeadamente através do aumento da taxa de resposta às imunoterapias bem como o reforço do efeito sistêmico da PDT, especialmente em tumores difíceis de tratar. Os modelos tumorais utilizados nestes estudos foram seleccionados tendo em conta que a PDT com a redaporfin é capaz de gerar morte celular imunogénica e aumentar a imunogenicidade das células tumorais tratadas.

Os melanomas e carcinomas mamários são reconhecidos por serem bastante mais agressivos e difíceis de tratar do que a maioria dos modelos tumorais de murganho usados, como o carcinoma do cólon. A resposta à PDT com redaporfin foi avaliada em murganhos com modelos tumorais de carcinoma mamário que expressa luciferase (4T1-luc2) e de melanoma da pele (B16F10). Os parâmetros da PDT foram otimizados para maximizar o impacto no tumor primário e minimizar a letalidade do tratamento. Em ambos os modelos foi observado edema que posteriormente evoluiu para necrose, contudo, apenas foram obtidas curas no modelo de melanoma. Recorrendo a tomografia fotoacústica verificou-se que o baixo conteúdo de redaporfin que consegue aceder ao tumor pode ser a principal razão para a falta de eficácia no modelo ortotópico de 4T1.

A resposta anti-tumoral desencadeada pela PDT é por vezes neutralizada por mecanismos imunossupressores desencadeados pelas células tumorais que diminuem a eficácia do tratamento. Deste modo, as imunoterapias que têm como função atenuar o ambiente tumoral imunossupressor aparentam ser promissoras em terapias combinatórias que ambicionam aumentar a eficácia dos efeitos anti-tumorais e anti-metastáticos. Neste estudo, reportamos a combinação da PDT com redaporfin e as imunoterapias usando a CTLA-4 e a PD-1 em três modelos tumorais diferentes. Os resultados dos tratamentos foram avaliados através do tempo de sobrevida, da cinética de crescimento tumoral e, para o caso do modelo do carcinoma mamário, do desenvolvimento das metástases analisado através de imagiologia de bioluminescência. Posteriormente, as alterações da expressão de diferentes moléculas dos checkpoints imunitários em células tumorais foram avaliadas após a PDT *in vitro*.

A combinação da PDT com a redaporfin e a imunoterapia com CTLA-4, mas não com a PD-1, originou uma melhoria significativa da sobrevida e um aumento da taxa de curas no modelo de carcinoma do cólon de murganhos. Contudo, o mesmo não se verificou para os modelos de melanoma e de carcinoma mamário.

O aumento da expressão de moléculas dos checkpoints imunitários foi induzido de forma significativa nas células tumorais após o tratamento de PDT *in vitro*. As alterações mais notáveis foram observadas para CD80 e PD-L1. Os resultados sugerem que a combinação de PDT com imunoterapia pode ser eficaz no tratamento de tumores que são um maior desafio para a imunoterapia como tratamento isolado. Isto salienta a ideia de que uma estratégia terapêutica global pode não ser a ideal para todos os modelos tumorais. As

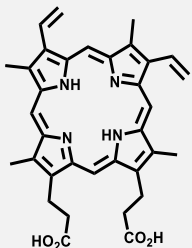
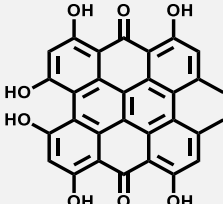
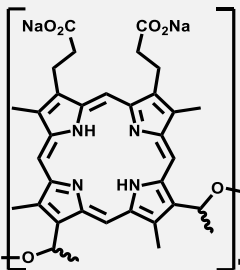
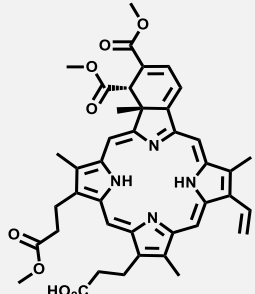
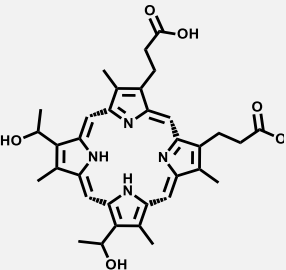
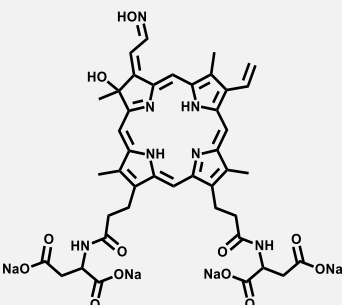
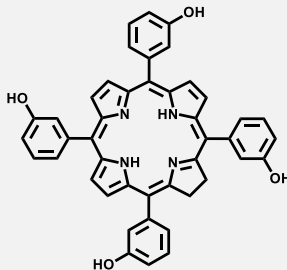
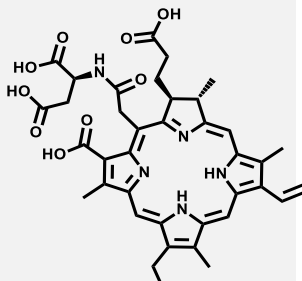
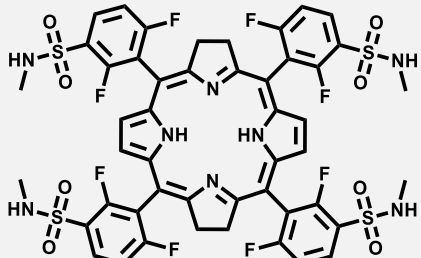
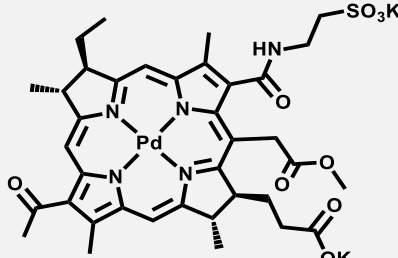
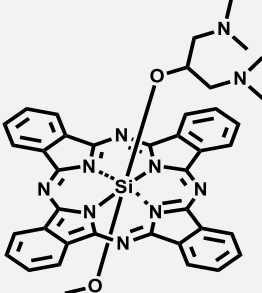
estratégias combinatórias não são universais e necessitam de ser adaptadas às especificações de cada caso clínico.

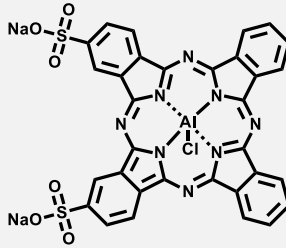
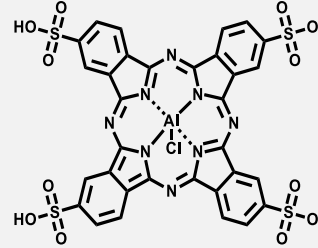
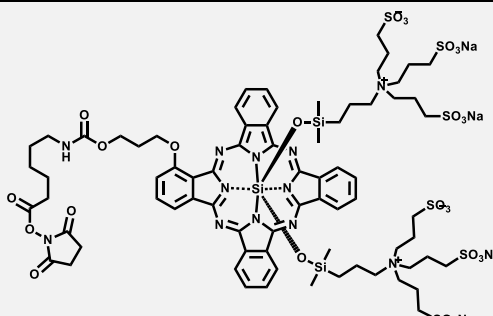
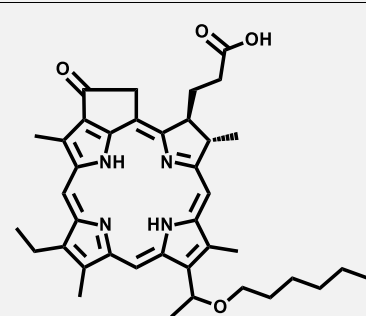
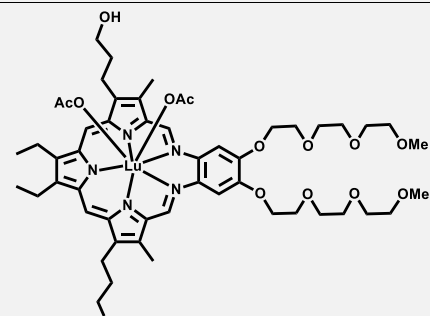
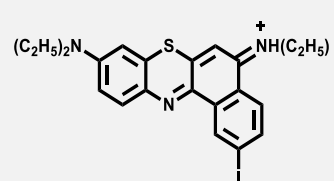
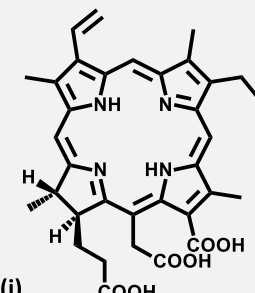
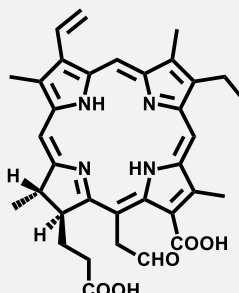
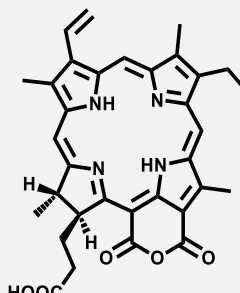
Palavras chave:

terapia fotodinâmica, redaporfin, cancro, resposta imune anti tumoral, imunoterapia, bloqueadores de checkpoints imunitários, metástases, química medicinal

iv. List of Photosensitizers

Table 1. Molecular structures of some photosensitizers for PDT, as well as their excitation wavelength.

PpIX	Hypericin	Photofrin/ Porfimer Sodium	Verteporfin/ BPD/ Visudyne
Porphyrin	Naphthodianthrone	Porphyrin	Porphyrin
630 nm	595 nm	630 nm	690 nm
			
PS-3/ Photosan-3	ATX-S10(Na)	mTHPC/ Temoporfin/ Foscan	Talaporfin/ NPe6/ Laserphyrin
Porphyrin	Porphyrin	Chlorin	Chlorin
670 nm	670 nm	652 nm	660 nm
			
Redaporfin/ LUZ11/ F2BMet	WST11/ Padeliporfin/ Tookad Soluble	BAM-SiPc	
Bacteriochlorin	Bacteriochlorin	Phthalocyanine	
749 nm	762 nm	676 nm	
			

AlS₂Pc	CIAISPc	IR700
Phthalocyanine	Phthalocyanine	Phthalocyanine
670 nm	675 nm	690 nm
		
HPPH/ Photochlor	MLu / Lutetium texaphyrin	2I-EtNBS
Pyropheophorbide-A	Texaphyrin	Phenothiazine
665 nm	732 nm	654 nm
		
Bremachlorin		
Mixture of chlorin e6 (i), purpurin 5 (ii) and chlorin p6 (iii)		
662 nm		
		
(i)	(ii)	(iii)

v. Definition of Terms

Table 2. Description of terms and abbreviations referred over this thesis.

Term	Definition
17.1A	monoclonal antibody specific for the epithelial cell adhesion molecule antigen
ADCC	antibody-dependent cellular cytotoxicity
ANXA1	annexin A1, DAMP, hallmark of ICD
AP-1	activator protein 1, a transcription factor that regulates gene expression
APC	antigen presenting cell
ATP	adenosine triphosphate
B7-1/B7-2	the same of CD80/CD86, membrane protein found in activated APCs
BCG	Bacillus Calmette-Guérin, live bacteria vaccine
BCR	B cell receptor
C225	mAb anti-epidermal growth factor receptor
C3	component 3, most important and abundant complement protein
C3a, C5a	proteins formed by the cleavage of other complement components
CD11b/c	glycoproteins only expressed in monocytes, macrophages, NK cells, neutrophils and granulocytes
CD152	same as CTLA-4
CD19	expressed in all B lineage cells
CD25	IL-2 receptor alpha chain, plays a critical role in the development and maintenance of Tregs
CD274	same as PD-L1
CD279	same as PD-1
CD28	protein expressed on T cells that provide co-stimulatory signals required for T cell activation and survival
CD3	protein complex and T cell receptor involved in T cells activation
CD4	glycoprotein found on the surface of immune cells, such as T helper cells, monocytes, macrophages, and DCs
CD40	co-stimulatory protein expressed by APCs, required for their activation
CD49	adhesion molecule of the integrin family, upregulated on armed effector T cells needed for both migration and activation of these cells
CD69	early activation marker that is expressed in hematopoietic stem cells, T cells, and other immune cells
CD8	glycoprotein found on the surface of cytotoxic T cells
CD80 /CD86	also designated as B7-1/2, expressed by APCs, co-stimulatory signal for T cell activation by interaction with CD28
CF	Complete Freund adjuvant, solution of antigen
CP	<i>Corynebacterium parvum</i> adjuvant, an anaerobic diphtheroid
CpG-ODN	CpG oligodeoxynucleotide, adjuvant
CRT	calreticulin, soluble ER protein that binds to misfolded proteins

CTL	cytotoxic T lymphocyte		that stimulates granulocytes and stem cells production
CTLA-4	cytotoxic T lymphocyte-associated antigen 4, immune checkpoint, negative regulator of T-cell immune function	GFP	green fluorescence protein
CY	cyclophosphamide, type of alkylating agent	GM-CSF	granulocyte macrophage-colony stimulating factor, cytokine, white blood cell growth factor
Cy5.5	near infrared fluorescent dye	Gr1	granulocytic marker, made up of Ly6C and Ly6G
DAMP	danger associated molecular pattern	HER1	epidermal growth factor receptor in humans
DBPMAF	D3-binding protein-derived macrophage activating factor	HER2-ECD	human epidermal receptor-2 extracellular domain
DC	dendritic cell	Hip1	huntingtin-interacting protein 1 – tumor antigen
DD	drug dose	HMGB1	high mobility group box 1 protein, released during cell injury or inflammation
DLI	drug-to-light interval, time between PS injection and irradiation	HSP	heat shock protein, chaperone proteins and cellular marker of stress
DMXAA	5,6-dimethylxanthenone-4-acetic acid, a vascular disrupting agent	HpD	Hematoporphyrin derivative
DTx	diphtheria toxin, an exotoxin secreted by <i>Corynebacterium</i>	i.m.	intramuscular
EGFR	epidermal growth factor receptor	i.p.	intraperitoneal
ER	endoplasmic reticulum, organelle responsible for folding of proteins and transport to GA	i.v.	intravenous
FDA	Food and Drug Administration	ICAM-1	adhesion molecule, cell surface receptor that mediates interaction between cells
FOXP3	forkhead box P3, protein regulator of Tregs development and function	ICB	immune checkpoint blockers
GA	Golgi apparatus, organelle involved in protein and lipid transport, and lysosome formation	ICD	immunogenic cell death
GC	glycated chitosan, galactose molecules attached to the chitosan molecule	ICG	Indocyanine green
G-CSF	granulocyte colony-stimulating factor, cytokine and hormone, glycoprotein	ICD	immunogenic cell death
		iDC	immature dendritic cell
		IDO	indoleamine 2,3-dioxygenase, immune checkpoint
		IF	Incomplete Freund, immune modulator
		IFN-γ	interferon gamma, soluble cytokine
		IgG	immunoglobulin G, type of antibody

IL	interleukin, group of cytokines
IMQ	imiquimod, immune modulator
iNOS	inducible nitric oxide synthase
KD	knockdown
LD	light dose
LDL	low density lipoprotein
LRP1/CD91	low density lipoprotein receptor-related protein 1 or cluster of differentiation 91, involved in receptor-mediated endocytosis
LT	lymphotoxin, cytokines that regulate growth and function of lymphocytes
Ly6G/Ly6C	markers for identifying neutrophils, eosinophils, and subsets of monocytes/macrophages
M1/2 macrophage	classification of macrophages according to their functionality
mAb	monoclonal antibody
MAC	membrane attack complex, formed on cell membranes and caused by complement activation
MAF	macrophage-activating factor, lymphokine
MHC	major histocompatibility complex
MIP-2	macrophage inflammatory protein 2
NFκB	nuclear factor kappa B, transcriptional factor
NIR	near infrared
NK	natural killer
OC125	antigen expressed in 80 % of the non-mucinous ovarian cancers
OK-432	Streptococcal preparation
o.t.	orthotopic

p16	protein that slows cell division and act as a tumor suppressor
P1A	tumor antigen only expressed in tumor cells
p40	protein, subunit of IL-12 and IL-23 cytokines
p53	tumor protein p53 or cellular tumor antigen p53 – act as a tumor suppressor
PA	photoacoustic
PBMC	peripheral blood mononuclear cell
PD-1	programmed death 1, immune checkpoint, negative regulator of T-cell immune function
PD-L1	programmed death ligand 1, immune checkpoint, negative regulator of T-cell immune function
PDT	photodynamic therapy
PIT	photoimmunotherapy, combines PDT and immunotherapy
PRR	pattern-recognition receptor
PS	photosensitizer
ROS	reactive oxygen species
s.c.	subcutaneous
siRNA	small interfering RNA, class of double-stranded non-coding RNA molecules
SLP	synthetic long peptides, personalized peptide vaccine
SPG	Schizophyllan, immune modulator
TAA	tumor associated antigen
TAM	tumor associated macrophages
TDLN	tumor draining lymph node
TGF-β	transforming growth factor beta, cytokine
Th1/2/17	subtypes of helper T cell

TIL	tumor infiltrate lymphocyte
TLR	toll-like receptor, class of proteins expressed on the membrane of leukocytes
TNF-α	tumor necrosis factor alpha, cytokine that promotes inflammation
Treg	regulatory T cell, a subpopulation of CD4 ⁺ T lymphocytes associated with immunosuppressive mechanisms
Trp	tryptophan
VEGF	vascular endothelial growth factor, angiogenic factor

Table 3. **Cell lines description.** Description of several cell lines implemented in vitro and in vivo experiments to evaluate the efficacy of photodynamic therapy and reported in this thesis.

Cell Line	Description
4T1	murine mammary carcinoma cell line from a BALB/cfC3H mouse, mimics stage IV human breast cancer
4T1-fluc/ 4T1-luc2	4T1 cell line transfected with the luciferase gene
A431	human epidermoid carcinoma cell line, HER1 overexpressing cell line
AsPC-1	human pancreatic ductal adenocarcinoma cell line
B16F1/B16F10	murine melanoma producing melanin from C57BL/6J mouse
CT26.WT/ CT26/ Colo26	murine colon carcinoma cell line from BALB/c mouse
CT26.CL25	CT26 stably transduced with the retroviral vector LXSJN that contains the lacZ gene encoding the model TAA beta-galactosidase
DA3	murine lymphoma cell line from DBA/2 mouse
ECA109	human esophageal squamous cell carcinoma cell line
E0771	murine malignant neoplasms of the C57BL/6 mouse mammary gland
EMT6	murine mammary carcinoma cell line from BALB/cCrgl mouse
FaDu	human hypopharyngeal squamous cell carcinoma cell line
FSaR	murine fibrosarcoma from C3H mouse
H460	human lung large cell carcinoma cell line
HepG2	human hepatoblastoma cell line
HT29	human colon adenocarcinoma cell line
J774	murine monocyte/macrophage (reticulum cell sarcoma) cell line from BALB/cN mouse
LLC	murine Lewis lung carcinoma cell line from C57BL mouse
M2R	mouse melanoma cell line, a clone of transplantable B16 melanoma cells
MB-49-luc	murine urinary bladder carcinoma from C57BL6 mouse
MC38	murine colon adenocarcinoma cell line from C57BL6 mouse
MGH	human lung squamous cell carcinoma
MKN45	human gastric cancer cell line
MS-2	human pleural malignant mesothelioma cell line (fibrosarcoma)
NK92MI	human IL-2 independent Natural Killer cell line from the NK-92 cell line
NXS2	murine neuroblastoma cell line derived from A/J mice
OVCAR3	human high grade ovarian serous adenocarcinoma cell line
P1.204	P1A antigen-negative murine mastocytoma cell line derived from P815
P815	murine mastocytoma cell line from DBA/2 mouse, P1A antigen-positive
Panc-1	human pancreatic ductal adenocarcinoma cell line
PECA	murine squamous cell carcinoma of the NMRI mouse skin
RIF-1	murine fibrosarcoma cell line from C3H mouse

TABLE OF CONTENTS

RIF-1 EGFP	RIF-1 cell line expressing GFP
S91	mouse melanoma from DBA mouse
SCC	human squamous carcinoma cell line
SCCVII	murine squamous carcinoma cell line from C3H mouse
SiHa	human papillomavirus-related cervical squamous cell carcinoma cell line
SQ2	murine anaplastic cell line generated from an SCC tumor that developed spontaneously in a male BALB/c mouse
TC1	tumor cell line derived from primary lung epithelial cells of C57BL/6 mice
TRAMP-C2	murine carcinoma of the C57BL/6-TgN mouse prostate gland cell line
TUBO	murine mammary carcinoma cell line from BALB/neuT mouse
NPC	human nasopharyngeal carcinoma cell line

Table 4. **List of animal models.** Description of animal models implemented in photodynamic therapy in vivo experiments and reported over this thesis.

Animal Model	Description
A/J	inbred albino strain of mouse model, frequently used in cancer research, has a strong tendency to develop tumors when presented with common carcinogens
BALB/c	inbred strain of laboratory albino mice, with white coat; ideal for general multipurpose model, hybridoma development, monoclonal antibody production and infectious disease
C57BL/6	inbred strain of laboratory mice, with dark brown coat: ideal for general multipurpose model, diet-induced obesity, transgenic/knockout model development, safety and efficacy testing and immunology
DBA/2	inbred strain of laboratory mice, with dilute brown coat; oldest of all the inbred strains of mice, ideal for safety and efficacy testing, immunology and audiogenic seizures
C3H	inbred strain of laboratory mice, with dilute brown coat; ideal for safety and efficacy testing, oncology, neurological disorders, and retinal degeneration
NMRI	outbred model used as an experimental animal in the fields of biology, pharmacology and toxicology; develops a wide variety of spontaneous tumors and with an increasing incidence of renal disease with age
nude	the first immunocompromised mouse strain used in cancer research, hairless athymic mice that lack a normal immune system and thymus gland, thus with greatly reduced T cell production; ideal for tumor and tissue studies; available on both BALB/c and C57BL/6 background
scid	severe combined immune deficiency, mice with a genetic immune deficiency that affects their B and T cells; ideal for xenoengraftment of human cells and tissue, and hairless models to tumor imaging and measurements; available on both BALB/c and C57BL/6 background

1 GENERAL INTRODUCTION

1.1 Photodynamic Therapy

Light has been studied for its therapeutic properties for thousands of years, but the concept of “photodynamic action” was developed in the beginning of the last century (1903)¹. Photodynamic Therapy (PDT) combines three main components: light, molecular oxygen, and a non-toxic dye (photosensitizer, PS). Individually none of them presents toxicity, but when combined they generate damage in the surrounding environment. The PS, that should present selectivity to the tumor, is activated by visible light delivered commonly by a laser with a specific wavelength usually matching the lowest energy absorption band of the PS. PDT effect is dependent on the localization of the PS and on the local delivery of light. This dual specificity represents a major advantage to minimize the side effects on unwanted tissues.

1.1.1 Photochemistry

The absorption of a photon with the appropriate wavelength activates the PS to an excited singlet state ($^1\text{PS}^*$) by exciting one electron into an orbital with higher energy. This unstable excited state can lose the excess of energy by fluorescence or internal conversion to the ground state (^1PS). The excited state can also undergo an intersystem crossing process with spin inversion to form a long-lived excited triplet state ($^3\text{PS}^*$), according to the Jablonski diagram (Figure 1). The photochemical reactions that arise from the interaction of this triplet state with molecular oxygen generate reactive oxygen species (ROS) that cause the cytotoxic effect on the nearby cells. ROS may be generated by two types of mechanisms, type I and type II, which occur simultaneously and, in a ratio that is dependent on the treatment conditions. By type I mechanism the $^3\text{PS}^*$ undergoes

electron transfer reactions directly with a substrate to form radicals or radical ions, which further react with molecular oxygen and generates superoxide radical anion ($O_2^{\bullet-}$), hydrogen peroxide (H_2O_2) and hydroxyl radical (HO^{\bullet}). In some cases, namely when the PS has a sufficiently low oxidation potential, direct electron transfer from $^3PS^*$ to molecular oxygen to generate the superoxide ion is also possible². Following the type II mechanism, the PS triplet state can transfer its energy to other triplet state molecules, such as molecular oxygen (O_2) and generates the singlet oxygen (1O_2)³⁻⁵.

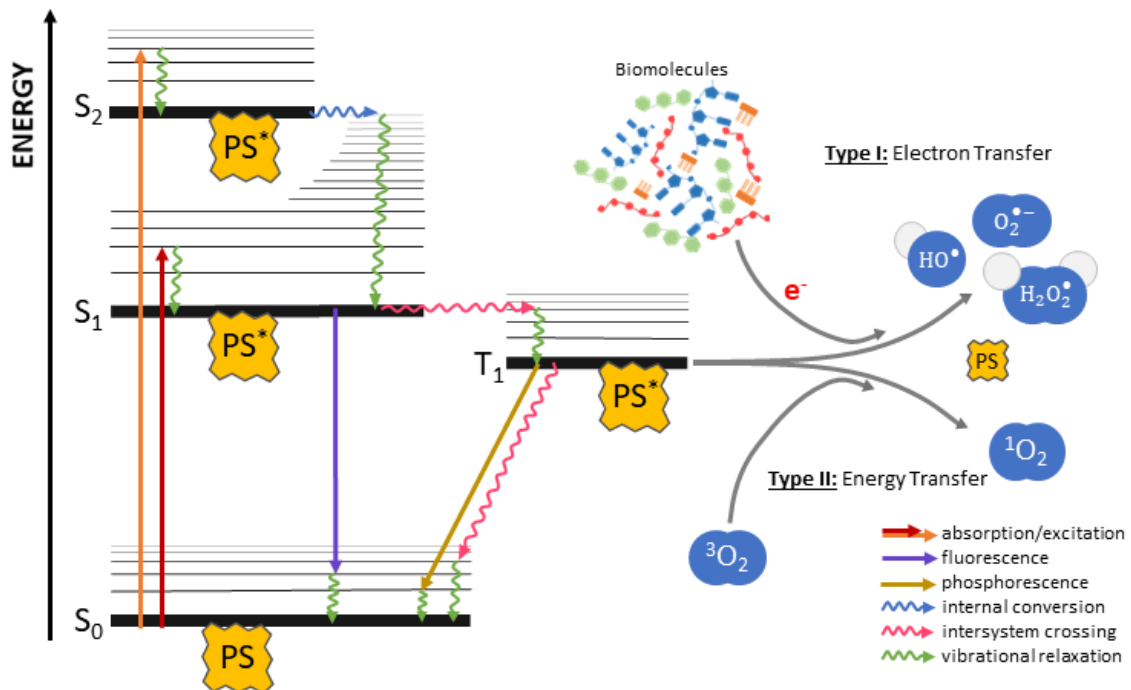


Figure 1. **Jablonski energy diagram illustrating the main events of PDT mechanism, leading to the generation of reactive oxygen species (ROS).** The photosensitizer molecule (PS) is excited from ground state to excited singlet states (S_1, S_2, \dots) by the absorption of light at a specific wavelength. The excited molecule (PS^*) can either decay to the ground state by radiative (fluorescence and/or phosphorescence) or nonradiative processes (internal conversion and/or intersystem crossing to the triplet state). The PS triplet excited state (T_1) can further trigger the local production of cytotoxic ROS, such as singlet oxygen (1O_2), superoxide radical anion ($O_2^{\bullet-}$), hydrogen peroxide (H_2O_2) and hydroxyl radical (HO^{\bullet}).

1.1.2 Photosensitizers

The ideal PS for PDT should have a manufacturing method with low cost and yield a high purity compound with a long shelf-life. It should have no toxicity in the dark and relative rapid clearance from the healthy tissues to minimize the phototoxic side effects. PSs should present absorption bands in the phototherapeutic window: higher than 650 nm where the tissues are more transparent and lower than 800 nm because longer wavelengths

does not have enough energy to excite oxygen molecules. PSs should also present long-lived triplet with high triplet quantum yield, indicative of high capacity to generate ROS⁴. Most of the PSs studies are based on a tetrapyrrole structure, such as porphyrins, chlorins, bacteriochlorins or phthalocyanines.

The first generation of PSs are hematoporphyrin and its derivatives (**HpD**). **Photofrin** – porfimer sodium –, a purified HpD, was the first PS approved for PDT in 1993 and is still the most widely used PS⁶. **Photofrin** presents a weak band at 630 nm, which is used for clinical treatments due to the skin penetration for longer wavelengths. However, due to the weak absorption at this wavelength high light doses are required for effective tumor control (100-200 J/cm²). The drug doses required also lead to skin photosensitivity for 4-12 weeks. **ALA** was the second molecule to receive treatment approval for PDT cancer treatment in 1999. **ALA** is the precursor of a natural PS, protoporphyrin IX (**PpIX**) which is then converted by ferrochelatase to heme. As tumors present lower ferrochelatase activity compared to other tissues, after **ALA** administration there is an accumulation of **PpIX** in tumor cells. Compared to **photofrin**, **ALA** has a more rapid clearance and a greater tumor selectivity that is attained by being topically or orally administered. However, the strong hydrophilicity of **ALA** prevents it from entering the cells and several alkyl ester derivatives have been developed to infiltrate the cell easier^{7,8}. **mTHPC** is a meso-tetra-hydroxyphenylchlorin and was approved for PDT cancer treatment in 2001. **mTHPC** presents a much higher absorption at longer wavelengths (652 nm), which turns it into a more potent PS and increases the tissue depth penetration of light^{9,10}. In a similar manner, **Talaporfin** is a second-generation chlorin based photosensitizer with absorption at 664 nm and is associated with lower skin phototoxicity compared to the previous¹¹. **Verteporfin**, a benzoporphyrin derivative monoacid ring A, is activated by 689 nm light and presents specificity for high expression of low-density lipoprotein (LDL) receptors, such as in tumor cells. **Verteporfin** is rapidly cleared from the blood and follows a biphasic clearance¹². The first phase of clearance from plasma has a half-life less than 20 minutes and the slower second phase has a half-life less than 8 h¹³.

Several improvements have been achieved in the development of PSs, but the current clinical approved PSs still present complications related to the clearance of the PS and the penetration of light which severely impact the treatment efficacy and the life quality of the patients. Over the last years, new photosensitizers based on a bacteriochlorin backbone seem to overcome some of these problems and revealed promising results.

WST11 is a negatively charged water-soluble palladium-bacteriochlorophyll derivative with absorption at 762 nm. **WST11** presents a rapid clearance from circulation ($t_{1/2}=1.65$ min) after i.v. injection, which reduces the risk of photosensitivity but requires short DLI to achieve effectiveness^{14,15}. **Redaporfin** is a synthetic amphiphilic bacteriochlorin with strong absorption in the phototherapeutic window (749 nm) and elevated generation of ROS. **Redaporfin** presents a 8 h plasma half-life and its pharmacokinetics profile allows to perform both cellular and vascular PDT protocols¹⁶⁻¹⁸.

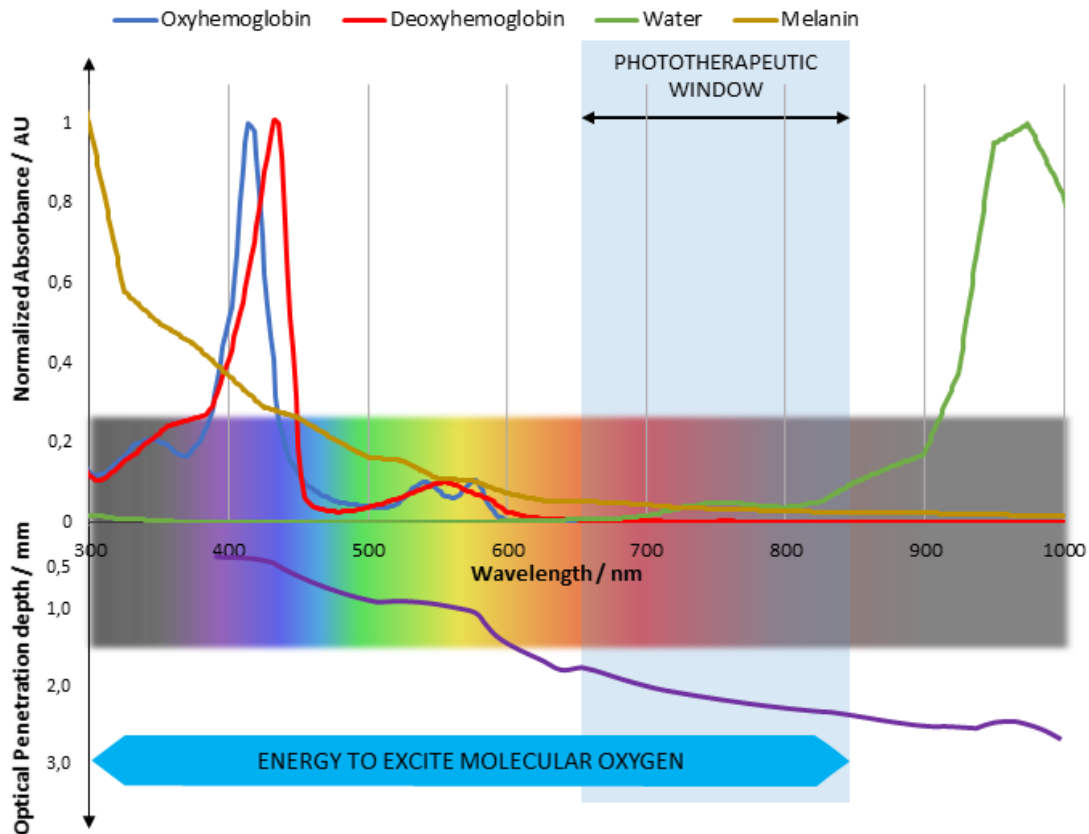


Figure 2. **Phototherapeutic window for PDT.** Endogenous chromophores, such as hemoglobin and melanin have absorption until the 650 nm, while water absorbs from the 900 nm. Over 850 nm, light does not present enough energy to excite the molecular oxygen and generate ROS. These facts lead to the definition of the phototherapeutic window, from 650 to 850 nm, which is also corroborated by the optical penetration depth of light into skin. Adapted from¹⁹.

1.1.3 Light

Activation of PS in the target tissue requires that light penetrates the skin and reaches the localization of the lesion intended to be treated, and that it delivers enough energy to generate the ROS. Many efforts have been made to understand how light penetrates tissues, and to modulate light parameters and maximize the light dose²⁰. Light can be reflected, refracted, scattered, or absorbed, depending on the tissue components.

Scattering and absorption are the most pronounced effects. Scattering is responsible for widening of the light beam and changes of its direction. Scatter increases for lower wavelengths⁵. Absorption is the most relevant process in terms of loss of light intensity with penetration. Tissues have endogenous chromophores that are responsible for the light absorption. For visible light, chromophores such as hemoglobin, myoglobin, melanin, and cytochromes play an important role. Regarding near infrared light, for wavelengths higher than 1300 nm, water has strong absorption bands. While at 600 nm the optical penetration depth into skin is about 1 mm, at 850 nm it is about 2.5 mm^{5,19}. These limitations led to the designation of the “phototherapeutic window” between 650 and 850 nm (Figure 2) where tissues present less absorption, and the penetration depth is higher. Many efforts have been made to design new PSs that present high absorption coefficients within this window⁴.

1.1.4 PDT protocols and cell death mechanisms

The efficacy of PDT depends on several parameters, such as the type of molecule, the PS concentration, the localization of PS, the light dose (fluence, $\text{J}\cdot\text{cm}^{-2}$), the dose rate (fluence rate, $\text{mW}\cdot\text{cm}^{-2}$), the drug-to-light interval (DLI), the oxygen availability and the tumor margins²¹.

The effect of PDT on the tumor is then a result of several mechanisms that cause tumor destruction. These mechanisms are: **a)** the direct cytotoxic effect of ROS in the tumor cells, that is dependent on the localization of the PS and availability of oxygen; **b)** the damage caused in the vasculature that lead to tumor hypoxia and anoxia; and **c)** the activation of an immune response against the tumor cells. These mechanisms complement each other and are crucial for the long-term tumor control¹. ROS have a brief lifetime which means that their diffusion area is limited^{22,23}. The lifetime of singlet oxygen in cells and its associated diffusion radius were recently established²⁴: 3 μs , which corresponds to a diffusion radius of 200 nm over a period of 5 lifetimes. This also means that oxidative damage caused by PDT reflect the localization of the photosensitizer at the time of irradiation.

In cases where illumination is performed briefly after PS administration, shorter DLI, the molecule is still on the vasculature (vascular-PDT), where the main damage will occur and usually leads to extensive necrosis. With longer DLI, illumination of lesions is performed when the PS had already had enough time for redistribution and was

internalized by cells (cellular-PDT). In this case, the cytotoxicity effect occurs directly in tumor cells, and the subcellular PS localization will determine the cell death mechanism. More hydrophobic PS tend to accumulate in endoplasmic reticulum (ER), Golgi Apparatus (GA) and/or mitochondria, while hydrophilic PSs usually follow the endocytic pathway and can be observed in lysosomes²⁵.

Under photooxidative stress, cell triggers several mechanisms that could result in removing/repairing the damaged material or in cell death, which depends on the severity of the damages. Survival mechanisms are usually regulated by transcription factors and intend to recover the cell homeostasis^{26,27}. For example, ER stress usually culminates with the shutdown of protein synthesis caused by the accumulation of misfolded proteins. Transcription factors may be activated to mediate the expression of genes that restore the normal protein synthesis. Another reported survival mechanism is by the expression of genes and proteins responsible for destroying the oxidized biomolecules and electrophilic agents, such as antioxidant enzymes and multidrug transporters. Inhibitors of these feedback mechanisms, have been studied for improving PDT efficacy²⁷.

However, if the stress originated is too severe and repairing is not achievable, cell death mechanisms are triggered instead. Cell death mechanisms are complex and, in many situations, very difficult to identify due to the overlap of pathways and characteristics that occur among them. Necrosis, apoptosis and autophagy are the three best known and reported mechanisms of cell death in PDT, even though several other mechanisms are also well described²⁵. In general, high photodamage protocols (high LD and/or high PS concentration) induce necrosis, moderate protocols induce apoptosis, while regimens leading to minor damage induce autophagy. The same PS can generate different cell death mechanisms and the same PDT protocol is likely to trigger more than one sort of cell death modality. Recently, Rocha et al. reported an *in vivo* study evaluating the necrosis depth in livers of rats after PDT with the PS **redaporfin**. The authors described the relation between the light dose and the depth of necrosis, with frontal and interstitial illumination. The authors were able to determine a “photodynamic threshold dose” of 1.5×10^{19} photons.cm⁻³, which is defined as the number of photons absorbed by the photosensitizer per unit volume of tissue that produce tissue necrosis, and which is in agreement with the values for other photosensitizers²⁸. These evidences are very useful in the clinical to improve the planning of protocols.

Necrosis is usually associated with PSs that present tropism for the cell membrane. Upon light activation, loss of membrane integrity, swelling and release of cellular contents occur, triggering a strong inflammation. Short periods of incubation may also contribute to trigger necrosis because the PS does not have time to internalize in the target organelles and is localized in the cytosol or in the membrane.

Apoptosis is recognized as a regulated cell death mechanism, very complex and may be triggered with intracellular or extracellular perturbations. The mitochondrial pathway is the most reported in PDT and involves the permeabilization of the outer membrane of mitochondria. All the pathways end in activation of effector caspases, with formation of apoptotic bodies that are rapidly cleared by immune cells. Not just the PSs that accumulate in the mitochondria can trigger apoptosis, it is also reported that PSs with tropism for ER-Golgi activate this mitochondrial apoptosis mechanism.

Autophagy is described as a survival mechanism, by clearing the damaged material, and as a death mechanism, in conditions where the clearing process ends up with permanent damages on organelles. Morphologically, autophagy is recognized by the formation of autophagosomes (double layer membrane vesicles) that engulf the damaged cellular content and degrade it after fusion with lysosomes. This process allows for the removal of damaged contents and reuse of the lysed contents for new processes.

Immunogenic cell death (ICD) is described by the nomenclature committee on Cell Death 2018²⁹ as an independent type of cell death mechanism that presents a spatial-temporal controlled manner of releasing ICD markers, a specific set of molecules. These ICD markers are danger-associated molecular patterns (DAMPs) that are released/expressed by cells after stress with the ability to be recognized by immune cells and stimulate an immune response. DAMPs include calreticulin (CRT), heat shock proteins (HSP), adenosine triphosphate (ATP), interferon (IFN), high-mobility group box-1 (HMGB1) and annexin A1 (ANXA1). It was proposed by Kroemer et al. that ICD must satisfy two criteria: a) *in vitro* treated cancer cells must trigger an immune response *in vivo*, in the absence of any adjuvant, and give protection against rechallenge to the same type of cancer cells.; b) when occurring *in vivo* must trigger a local immune response with recruitment into the tumor bed of immune cells of both arms of the immune system, and thereby inhibit the tumor growth by immune mechanisms³⁰. Several PS have already been described to be ICD inducers through the reported expression of these ICD hallmarks^{25,31}.

1.1.5 Tumor associated antigens

The efficacy of photodynamic therapy depends on the immune system response of the host. This elicited immune response has been studied over the last years, motivated by positive outcomes observed in clinical cares³², and many advances have been made in the understanding of the mechanisms responsible for this response. The development of new antitumoral strategies aims to find methodologies that can create long-term survival capable of eliminate any remaining tumor cells after the tumor ablation. Targeting tumor associated antigens (TAAs) and taking advantage of their capacity to stimulate an immune response have been described in several studies. Tumor antigens activate DCs and allow the CD8⁺ T cells to recognize and destroy tumor cells, triggering an adaptive antitumoral response. However, most of the tumors may decrease or even lose the expression of both MHC molecules and tumor antigens, or present mechanisms that inhibit the costimulatory signal required for APC / CTL effective function, thus reducing their immunogenicity, and avoiding the immune surveillance.

According to their expressions, tumor antigens that trigger immune response can be categorized in four main categories: **a)** unique tumor-specific antigens, caused by somatic mutations in genes, such as p53 and p16; **b)** antigens which are present both in normal cells and tumor cells; **c)** tumor-antigens, present in several types of tumors but not in normal cells, such as P1A; **d)** antigens of viral etiology, such as Epstein-Barr virus, Hepatitis B virus^{33,34}.

One way of exploring this antigen-dependent immune response is to transduce tumor cell lines with tumor antigens, which will allow the immune system to recognize and selectively identify distant tumor lesions. GFP was used as a foreign antigen in GFP-expressing tumors to evaluate if the PDT outcome would be different in comparison with the wildtype cell line. The results showed 100% cure rate of RIF-1 EGFP tumors after **verteporfin**-PDT, whereas the RIF-1 wildtype tumors all recurred. Cured mice were also resistant to RIF-1 EGFP and rechallenge with RIF-1 cells showed a decreased growth kinetic³⁵. These results suggest that the presence of GFP as a foreign antigen potentiated the antitumor immune response and generated a long-term memory immune response. The same strategy was later tested with CT26 cell line and CT26.CL25, which express β -galactosidase as tumor antigen and animals were treated with vascular **verteporfin**-PDT³⁶. All the animals with CT26.CL25 tumors were cured and showed resistance to rechallenge, but the animals with wildtype tumors did not. The isolated T lymphocytes

from cured animals were able to recognize and selectively destroy antigen-positive cells. A similar approach was used for P1A antigen, which is a naturally antigen expressed by mouse mastocytoma P815. PDT-induced antitumor immunity was evaluated in P815 tumor model and P1.204, which is derived from P815 but is P1A antigen negative³⁷. The results demonstrated that the lack of the antigen lead to significantly reduced survivals and lower rejection to tumor rechallenge when compared with the wildtype tumor model. CD4⁺ and CD8⁺ T cells also presented higher levels of intracellular cytokines in the antigen-positive model, revealing the antigen- and epitope-specific immune response elicited by **verteporfin**-PDT.

Gollnick and coworkers reported in a clinical setting that PDT of basal cell carcinoma led to increased systemic immune response to Hip1, a tumor antigen associated with this tumor type³². Recognition of Hip1 by lymphocytes was increased in PDT treated patients, compared to surgery. These clinical evidences demonstrated that local PDT treatment could enhance the systemic antitumor immunity in patients.

1.2 Systemic antitumor immunity elicited by PDT

The efficacy of PDT in oncology depends both on its capacity to eradicate the local tumor and in its ability to induce a systemic immune response capable of detect and eliminate distant cancer lesions without causing damages in the healthy tissues³⁸. Canti et al. reported in 1994 that PDT triggered an antitumor immunity, by demonstrating that cells isolated from lymph nodes of PDT-treated animals were able to inhibit the tumor growth when transferred to naïve hosts and that PDT-cured animals were able to resist a tumor rechallenge³⁹. Several studies of PDT treatments with scid and nude mice have demonstrated the role of the immune system in the efficacy of treatments, providing no long-term cures or even no cures^{17,40-46}.

PDT is a promising alternative to conventional therapies, such as surgery and chemotherapy since it produces an acute inflammation and recruits immune cells to the illuminated area and also to distant tumors⁴⁷. PDT can trigger an immune response either by the stress/cytotoxicity elicited in tumor cells and/or by the direct effect on the immune cell populations. As illustrated in Figure 3, PDT-treated cells produce danger signals (DAMPs) that increase the presentation of antigen by APC and increase the recruitment of T cells to the treated area. These activated T cells may recognize and destroy the remaining tumor cells of the illuminated area or create an immune memory to recognize this type of cells in the future or in a distant part of the organism, namely in metastases.

DAMPs, danger associated molecular patterns, can be any molecule or a breakdown product of a molecule that is abnormally exposed or displayed in a wrong location due to damage that occur in the cell. DAMPs originated from PDT may be categorized in three major groups: cell derived molecules, extracellular matrix degradation products and extravasated plasma proteins⁴⁸. Several studies have described the expression and/or release of DAMPs after PDT, such as heat shock proteins (HSP)⁴⁹, products of cellular membranes⁵⁰, intracellular molecules that are released, fragments of extracellular matrix, fibrinogen and extravasated plasma proteins⁵¹. DAMPs are further recognized by pattern-recognition receptors (PRR), the recognition part of the innate system. Upon engagement between the DAMP and the PRR, the effector cells become activated and capable of performing their activity immediately. PRR can also be classified as: **a)** signaling (TLRS)⁴⁹; **b)** endocytic (macrophage scavenger receptor); **c)** soluble receptors (complement proteins and pentraxins)^{52,53}.

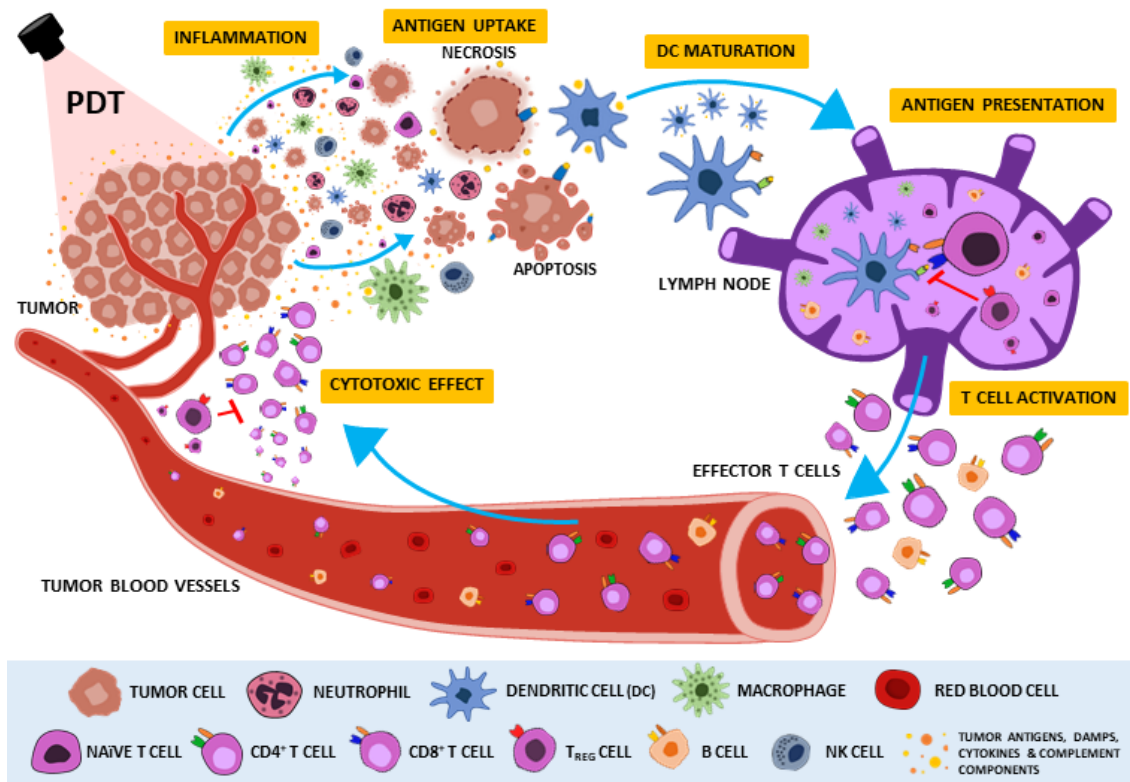


Figure 3. **Antitumor immune mechanism triggered by Photodynamic Therapy.** The cytotoxic effect of PDT induces a local inflammation, with recruitment of innate immune cells to the illuminated area. Innate immune cells, such as DCs, phagocytize tumor antigens and DAMPS released by damaged tumor cells and present them to T cells in the lymph nodes. This stimulation activates the adaptive arm of the immune system, generating the proliferation of effector T cells capable of recognize and destroy the remaining tumor cells.

One of the major advantages of PDT is the possibility to elicit an antitumor immune response with one treatment that initiates with an acute non-specific inflammation that further evolves to a systemic immune response. This fulfills with the ability of the immune system to recognize tumor cells in a different part of the body or in a future event. Several studies have investigated how antitumor response prompted by PDT develops and how far can we take this advantage. These studies include rechallenge with cancer cells, immunization of the host with PDT treated cells, and, most importantly, to assess the ability of PDT to control the development of metastasis. Table 5 summarizes numerous of these *in vivo* experiments that have been reported with different photosensitizers and with different tumor models.

Table 5. PDT protocols with several photosensitizers and tumor models uncovering the importance of the immune system for the outcome of the treatment. Rechallenge refers to the ability of PDT treated animals acquire immune memory and reject a rechallenge with untreated tumor cells. Immunization refers to experiments where PDT treated cancer cells are administered to healthy animals and confer protection to rechallenge. Percentages refers to percentage of cures.

Photosensitizer	Local Treatment	Rechallenge	Immunization with cancer cells	Impact on distant lesions
ALA	s.c. NPC ⁵⁴ induced SCC ⁵⁵ s.c. SCC ⁵⁶ o.t. TRAMP-C2 ⁵⁷		PECA (100 %) ^{58,59} SCC (100 %) ^{55,60}	
Hypericin	s.c. CT26 (100 %) ⁶¹ s.c. DA3 ⁶² s.c. LLC ⁶³ s.c. MGH ⁶⁴ s.c. SQ2 ⁶²	CT26 (100 %) ⁶¹ LLC ⁶³		DA3 ⁶² SQ2 ⁶²
Photofrin	s.c. 4T1 ⁶⁵ s.c. Colo26 ⁶⁶ s.c. Eca109 ⁶⁷ s.c. EMT6 ^{40,45,68,69} s.c. FsaR ⁷⁰ s.c. LLC (100 %) ⁷¹ s.c. OVCAR3 (100%) ⁷² s.c. RIF1 ⁷³ s.c. SCCVII ⁶⁸	4T1 ⁶⁶ Colo26 ⁶⁶	EMT6 ^{40,69}	4T1 ^{65,66} EMT6 ⁶⁹ LLC ⁷¹
Verteporfin	s.c. 4T1 ⁷⁴ o.t. 4T1 ⁷⁵ o.t. AsPC-1&Panc-1 ⁷⁶ s.c. CT26 ⁷⁷ s.c. CT26.CL25 (100 %) ³⁶ o.t. E0771 ⁷⁵ s.c. J774 ⁷⁸ s.c. OVCAR5 ⁷⁹ s.c. P815(82%) ³⁷ s.c. RIF-1-GFP (100 %) ³⁵	CT26 ⁷⁷ CT26.CL25 (100 %) ³⁶ J774 ⁷⁸ P815 (91 %) ³⁷ RIF-1 (100 %) ³⁵	P815 ³⁷ SCCVII ⁸⁰	J774 ⁷⁸
HPPH	o.t. 4T1 ⁶⁶ s.c. Colo26 ^{66,43} s.c. Eca109 ⁶⁷ s.c. FaDu (60 %) ⁸¹ s.c. H460 ⁸² s.c. NXS2 ⁸¹	4T1 ⁶⁶ Colo26 ⁶⁶		NXS2 (50 %) ⁸¹
mTHPC	s.c. EMT6 ^{68,83} s.c. HT29 ⁸³ s.c. SCCVII ^{68,84} s.c. SiHa ⁸³			
Redaporfin	s.c. B16F10 (100 %) ⁸⁵ s.c. CT26 (85 %) ^{17,86} s.c. LLC (67 %) ⁸⁷ s.c. S91 (44 %) ⁸⁸	CT26 (67 %) ¹⁷		CT26 ¹⁷
WST11	s.c. 4T1 ⁸⁹ s.c. CT26 (>70 %) ⁸⁹ s.c. MB-49-luc (12 %) ⁹⁰ s.c. M2R (70 %) ¹⁵	4T1 ⁸⁹ CT26 ⁸⁹ MB-49-luc ⁹⁰	CT26 ⁸⁹	4T1 ⁸⁹ CT26 ⁸⁹ MB-49-luc ⁹⁰
BAM-SiPc	s.c. CT26 (70 %) ⁹¹ s.c. HepG2 ⁹² s.c. HT29 ⁹²	CT26 ⁹¹		
ATX-S10(Na)	s.c. CT26 ⁹³	CT26 ⁹³		
AlS₂Pc	s.c. MS-2 ³⁹	MS-2 ³⁹		

1.2.1 PDT and innate immunity

Innate immunity is the first line of defense of the immune system, represented by mechanisms that do not present immunologic memory. Regardless the number of the times that the antigen is found, it will not change the response by innate immune cells. While adaptive immune responses usually take time to be effective, innate responses are critical in the first hours and days to protect the host from infection. This innate arm of the immune system reacts to pathogenic invaders by cytokine release, recruitment and activation of phagocytes (macrophages, neutrophils and dendritic cells), natural killer (NK) cells and by activating the complement cascade⁹⁴.

PDT triggers an oxidative stress in the illuminated area causing damage in the nearby cells. Damaged and dying cells release DAMPs into extracellular matrix or present them on the cellular surface. DAMPs are recognized and neutralized by innate immune phagocytes, leading to the removal of the cellular debris, and inducing the inflammatory response. This response is then followed by the secretion of pro-inflammatory mediators, activation of complement and accumulation of inflammatory cells in the treated area to destroy the remaining tumor cells^{47,48,63,94}.

1.2.1.1 Acute Inflammation: From local to systemic

One of the first signs of the immune stimulation elicited by PDT is the local acute inflammation revealed a few hours after tumor illumination. The damage caused by PDT has been described as a massive and rapid invasion of several activated inflammatory cells^{41,47,95,96}. Inflammation is responsible for the expression of several pro-inflammatory mediators, enhancing the expression of vascular adhesion molecules and the synthesis of chemokines required for the neutrophil extravasation⁹⁶⁻⁹⁹.

PDT has an impact in the illuminated area and triggers an acute phase response with systemic effects, as illustrated in Figure 4. PDT is well described for triggering a systemic response characterized by induction of acute phase reactants^{53,68,96,100}, complement proteins expression¹⁰¹⁻¹⁰³, systemic neutrophilia⁶⁸ and expression of several cytokines^{68,96,104-108}, that all together will help in the phagocytosis, removal of cell debris and local healing^{53,100}. Immune stimulation by PDT has been described to activate NFκB and AP-1¹⁰⁹, which control the expression of dozens of cytokines – most remarkably IL-1β, IL-1, IL-6, IL-10, TNF-α, TGF-β – but also Granulocyte colony-stimulating factor

(G-CSF), thromboxane, prostaglandins, leukotrienes, histamine and several coagulation factors^{42,96,97,99,105,110–112}.

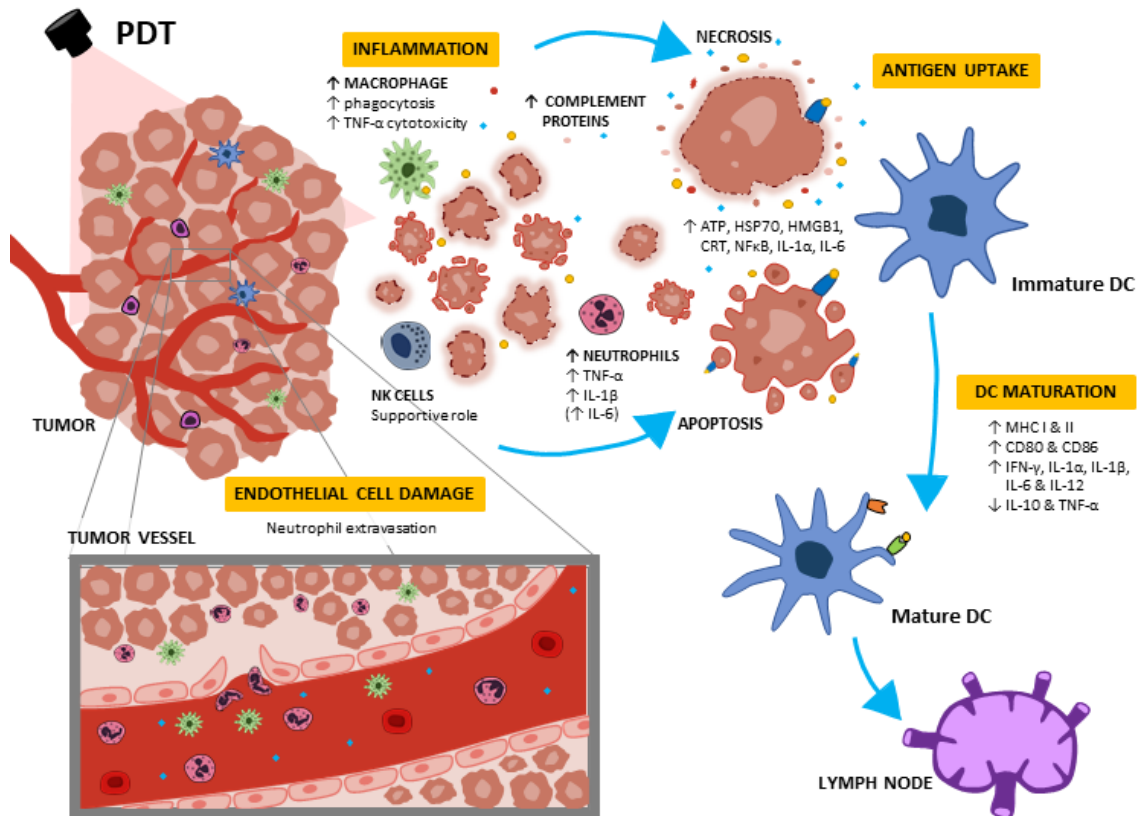


Figure 4. **Innate immune response mechanism triggered by Photodynamic Therapy.** Shortly after the light activation, the release of DAMPs, cytokines and other components lead to the development of a strong inflammation with infiltration of innate immune cells, such as macrophages, neutrophils, dendritic cells (DCs) and NK cells. The recognition of the tumor antigens by APCs and further presentation to T cells in the lymph nodes activated the adaptive immune response.

Among the expressed mediators, IL-6 and IL-1β seem to have an important role on the development of inflammation after **photofrin**, **HPPH** or **mTHPC-PDT**^{96,113}. On the other hand, IL-10 and TGF-β were shown to have impact in hampering this response. Several studies have evaluated the impact of selectively blocking these expressed mediators on the efficacy of PDT. Sun et al. demonstrated that the IL-1β neutralization diminished PDT cure rates that was not observed with IL-6 and TNF-α neutralization¹¹³. Blocking the function of some adhesion molecules expressed during inflammation also decreased the efficacy of treatment^{96,113}. Additionally, selective blockade of IL-10 and TGF-β were described to improve PDT outcome⁴⁸.

PDT also induces several changes in the vasculature of tumors, damaging the endothelial cells, creating vessel constriction, platelet aggregation, blood occlusion and hemorrhages.

These changes make vessels more permeable to blood proteins and pro-adhesive for inflammatory cells, through the over-expression of several adhesion molecules⁴⁸. The damage caused in the vasculature also induces the activation of complement, which acts as direct mediator of inflammation and stimulate cells to release other inflammatory mediators¹⁰⁵.

When inflammation is the result of trauma, ischemia-reperfusion or chemically induced injury, as is the case with PDT, inflammation occurs without the presence of any microorganism, and is named “sterile inflammation”¹¹⁴. Induction of these sterile inflammation is crucial for the initiation of antitumor adaptive immunity after PDT as it increases the neutrophil entry into the tumor-draining lymph nodes (TDLNs). Brackett et al. reported that this enhanced neutrophil infiltration into TDLNs following induction of sterile inflammation by **HPPH**-PDT is regulated by IL-17:IL17RA¹¹⁵.

1.2.1.2 Complement activation

The complement system is made up of large number of proteins that circulate in the blood and tissue fluids. Complement proteins are the major effector arm of the innate immunity and only become active in response to a trigger that will start a cascade of enzymatically cleavages that sequentially activate different proteins. Apart from the capacity to stimulate an inflammatory response, the main roles of complement are to mark pathogens to be destroyed by phagocytes and to recruit leukocytes to the local, increasing the cytotoxic effects of inflammation¹¹⁶.

The stimulation of the complement system was reported to be crucial to neutrophil infiltration, because its inhibition completely prevented the development of neutrophilia induced by PDT⁶⁸. PDT triggers the complement system by a non-antibody mediated pathway as its activation was still detected in PDT-treated scid mice lacking B cells¹⁰⁵.

Complement component 3 (C3) is a protein that plays a central role in the activation of complement. Its stimulation was reported to be dependent on the photosensitizer and the PDT regimen¹¹⁷. Also, the mechanism by which PDT activates the complement system is suggested to be through the release of C3a and C5a proteins, which work as chemoattractants/activators not only for neutrophils but also to monocytes, B-cells, macrophages and mast cells¹⁰³. Indeed, blockade of complement factors has been described to have a negative impact on PDT-mediated tumor cures⁴⁸ and also to lead to neutropenia¹¹⁸.

Complement may have both positive and negative impact on the efficacy of PDT. It has been suggested by Cecic et al. that according to the localization of the photosensitizer, activation of complement may differ¹¹⁷. Rapid complement activation during **photofrin**-PDT illumination leads to the generation of the membrane attack complex (MAC) on vascular endothelial cells, collapse of blood vessels and consequent enhanced decline in tumor oxygenation, which negatively affects the efficiency of PDT. On the other hand, PDT with **verteporfin** does not present significant decreases in tumor oxygenation. These conclusions inspired approaches that could block temporarily the complement activity, during illumination, to improve the outcome of PDT. Several studies have reported combinatory therapies with PDT that stimulate the activation of the complement system and have revealed increased animal cure rate¹¹⁹⁻¹²².

1.2.1.3 Neutrophils

Neutrophils are the most abundant type of leukocytes and are an important part of the innate immune system. They have relevant functions in the regulation of inflammation by secreting proinflammatory cytokines (eg IL-6, IL-1 β , IL-4 and IL-12,) and other inflammatory mediators (eg leukotrienes and prostaglandins), which potentiate the inflammatory response by recruiting and activating other immune cells. Neutrophils are also able to directly kill pathogens and under these circumstances work as APCs, presenting the antigens via MHC class II¹²³.

Neutrophils have been reported to have an important role in the development of the antitumor immunity after PDT. The mechanisms involved in this modulation are still not completely understood, but some aspects have been postulated over the years. Neutrophils secrete chemokines and granule proteins which further recruit monocytes. The activation of DCs is by cell-to-cell contact and is accompanied by the secretion of TNF- α , which also stimulates the differentiation of monocytes and T cells¹²⁴.

The increased levels of neutrophils in the peripheral blood and in the tumor area after PDT have been described in several studies^{68,89,96,104,123,125,126}. Following **photofrin**-PDT of rhabdomyosarcoma rat tumor model, neutrophilia appears as early as 4 h post-illumination and is maintained for at least 24 h, while for example the high levels of lymphocytes returns to basal levels in 2 h¹⁰⁴. Krosli et al. described that **photofrin**-PDT of squamous cell carcinoma mouse tumor model lead to 200-fold increase in the content of neutrophils within 5 minutes after tumor illumination and further studies reported that

this effect is dependent on neutrophils and mediated by complement^{41,68,125}. According to Gollnick et al., the percentage of neutrophils in the treated tumor was significantly increased 4 h after **HPPH**-PDT when compared to the nonilluminated control and remained high for at least 72 h post-treatment. The number of infiltrating neutrophils into the treated tumor after **HPPH**-PDT was less when compared to **photofrin**-PDT (37 % of the total cells 24 h following **photofrin**-PDT vs 13.8% of the total cells 24 h following **HPPH**-PDT) which is consistent with the lower degree of inflammation observed for **HPPH**-PDT⁹⁶. The vascular-PDT modality is also associated with neutrophilia and/or tumor infiltrating neutrophils. Salomon and coworkers reported a massive neutrophil infiltration in the tumor rim and interface 1 h after **WST11**-PDT (but not in the tumor core), that returned to basal levels in 24 h⁸⁹. A pronounced neutrophilia was also observed 2 to 24 h after **redaporfin**-vascular-PDT, which was shown to significantly contribute for its efficacy as cure rates decrease from 100 to 62.5% when neutrophils were systemically depleted¹²⁷. This observation will be discussed in detail later in this work.

The migration of neutrophils to the tumor after **HPPH**-PDT was reported to be dependent on the local increase of chemokines (eg macrophage inflammatory protein 2, MIP2) and vascular endothelial adhesion molecules E-selectin and ICAM-1, which facilitate neutrophil extravasation through the vasculature^{96,126}. Sun et al. implemented a different approach to evaluate the importance of neutrophils in **photofrin**- and **mTHPC**-PDT. By administering anti-ICAM-1, which prevents neutrophils migration into the tumor, there was a markedly reduction of the tumor cure rate¹¹³.

Several studies have reported that local administration of granulocyte-colony stimulating factor (G-CSF) or granulocyte-macrophage colony-stimulating factor (GM-CSF) led to a specific increase in the number of circulating neutrophils which significantly potentiates the antitumor response^{44,128,129}.

The neutrophils migration to the tumor bed has also been associated with cell surface expression of TNF- α and their subsequent accumulation in the TDLN¹²⁶. In the lymph nodes, neutrophils directly interact with DCs, further promoting T cell activation. Although IL-6 has been highly associated with the induction of systemic neutrophilia by **photofrin**-PDT¹⁰⁵, neutralization of this cytokine did not significantly affect the neutrophils levels in the tumor, did not block the induction of E-selectin and ICAM-1 on tumor microvessels and also did not affect the long-term survival of **mTHPC**-PDT, while

IL-1 β was critical for the therapeutic outcome^{96,113}. Thus, role of IL-6 in prompting inflammation after PDT apparently depend on the photosensitizer and the tumor model.

The degree of neutrophil infiltration seems to be dependent on the PDT regimen applied. Shams et al. demonstrated that PDT with low dose light (48 J/cm² given at 14 mW/cm²), considered an immune enhancing protocol, led to a higher neutrophil infiltration, both in the tumor tissue and in the TDLN, when compared with an high dose light regimen (132 J/cm² given at 14 mW/cm²) that was considered a tumor controlling protocol⁶⁶. Also, the number of activated CD8⁺ T cell increased in the low dose light regimen, but the combination of both regimens triggered even higher levels of cytotoxic T lymphocytes (CTLs). Apart from demonstrating that fluence rate influences the inflammatory response associated with PDT, Henderson et al. also reported that the depletion of neutrophils only abolished curability of the maximal inflammatory regimen⁴³.

Numerous studies have shown that depletion of neutrophils diminished the curative effect of PDT^{41,43–45,104,126,129}. The specific depletion of neutrophils was reported to directly reduce the number of activated cytotoxic T cells in TDLN and in the tumor tissue, inhibiting the establishment of a strong antitumor CD8⁺ T cell response after **HPPH**-PDT in a high inflammatory regimen (48 J/cm² given at 7 mW/cm²)¹²⁶. Korbelik's group demonstrated that neutrophils depletion led to a 30 % drop in mice cured with **photofrin**-PDT from EMT6 mammary sarcoma tumors⁴⁵. However, depletion of neutrophils did not significantly changed the efficacy of **ALA**-PDT with rat rhabdomyosarcoma tumor model, suggesting that the magnitude of damage originated by **ALA**-PDT was not dependent on neutrophils as for other photosensitizers¹³⁰.

1.2.1.4 Natural Killer cells

Natural killer (NK) cells are lymphocytes of the innate immune system with the ability to directly kill infected cells or tumor cells. They can also work as regulators of immunity through reciprocal interactions with DCs, macrophages, T cells and endothelial cells, meaning that they can impair or exacerbate immune responses¹³¹.

The effect of PDT in NK cells was studied *in vivo* by Marshall et al.¹³². Their work showed that the activity of NK cells was significantly impaired by **ClAISPC**-PDT but not by **HpD**-PDT, suggesting that the impact of PDT in NK cells is dependent on the photosensitizer and/or the PDT regimen.

The importance of NK cells to the outcome of PDT was evaluated by Hendrzak et al.⁴⁶. Their work demonstrated that the selective depletion of NK cells reduced **2I-EtNBS**-PDT effect. NK cells obtained from PDT treated mice were not cytotoxic *in vitro* against tumor cells, suggesting that its effect *in vivo* occur by an indirect mechanism, rather by a direct cytotoxic effect on cancer cells. The contribution of NK cells to **photofrin**-PDT efficacy was evaluated by Korbelik and Dougherty by selectively depleting these cell population, both in immunocompetent and immunocompromised (scid) mice bearing Meth-A fibrosarcomas⁴². Their results demonstrated that NK depletion on scid mice significantly reduced the cure rate, while in BALB/c mice had no significant effect. These findings suggested that immunocompetent hosts maintain tumor control through PDT-activated T lymphocytes, whereas NK cells are required for tumor control in scid mice. However, this requirement may be dependent on the tumor type, namely in its susceptibility to NK cells. Later, Korbelik et al. reported that the combination of **mTHPC**-PDT with NK cell-based adoptive immunotherapy mediated better therapeutic outcomes than any of the therapies alone, thus showing the potential of this strategy for the control of solid tumors⁸³. Kabingu et al. reported that NK cells can also contribute to the antitumor immunity elicited by PDT⁶⁹. Their work showed that the number of EMT6 lung tumors per mouse were significantly higher in the NK-depleted animals. These results were further corroborated with studies with deficient scid mice replenished with CD8⁺ T and NK cells, suggesting that NK cells have an impact in antitumor immunity and affect the activity of CD8⁺ T cells after PDT. The previous findings suggest that NK cells play a supportive yet important role in the establishment of CD8⁺ T cell antitumor responses through activation of DCs.

1.2.1.5 Macrophages

Macrophages main functions consist in maintaining homeostasis and host defense through phagocytosis. These cells are also responsible for the production of several cytokines, chemokines and other mediators, representing an essential population in the development of inflammation after PDT treatment^{47,133}. Macrophages express a wide number of membrane receptors that can recognize several endogenous and exogenous ligands⁹⁵. According to their role, macrophages can be divided into two phenotypes, termed M1 and M2. M1 macrophages are proinflammatory innate immune effector cells, involved in immune activation and invader (pathogens or cancer cells) attack. Their tumoricidal activity can be exerted directly by phagocytosis and digestion of cancer cells

or indirectly by means of complement proteins and antibodies – antibody-dependent cellular cytotoxicity (ADCC). M1 macrophages also contribute for the activation of adaptive immunity as they can act as tumor-associated antigens (TAAs) presenters to lymphocytes^{133,134}.

After PDT, the generated hypoxia within the tumor bed facilitates the infiltration of monocytes, precursor cells of macrophages and myeloid dendritic cells. This invasion of macrophages into the tumor with **photofrin**-PDT occurs within the first 2 h after tumor irradiation, achieving a 2-3-fold increase in the percentage of macrophages over a 24 h period^{99,125}. Macrophages secrete lysophosphatidylcholine that triggers the release of MAF by B and T lymphocytes. This lymphokine/cytokine promotes an amplification of the response by activating additional macrophages that can destroy cancer cells³³. Once they have engulfed and processed the cancer cells debris, macrophages present TAAs on their membranes through MHC class II molecules, thus working as APC. The recognition of TAAs by T cells triggers a tumor-specific immune response^{41,135}. At this point, macrophages may also be reprogrammed to produce anti-inflammatory cytokines (such as IL-10 and TGF- β) and proangiogenic factors that promote tissue repair and consequently tumor growth⁴⁸. Regarding this, one strategy to increase the efficacy of PDT is to block anti-inflammatory cytokines, postponing the resolution of the inflammation triggered by PDT, enhancing the infiltration of monocytes and thus, improving the eradication of treated lesions⁴⁸. Some reports have also demonstrated that there is an increased expression of angiogenic factors following the proinflammatory phase, such as VEGF, and its inhibition also improves the therapy outcome⁴⁸.

Numerous studies show that selective depletion of macrophages immediately after PDT has a substantial impact in the outcome of treatment, decreasing its curative effect⁴⁵. Moreover, it has been reported that the proliferation and activation of this immune population by means of D3-binding protein-derived macrophage-activating factor (DBPMAF)¹³⁶ and granulocyte-macrophage colony-stimulating factor (GM-CSF)¹²⁸ can markedly improve the therapeutic effect of **photofrin**-PDT in mouse models of cancer.

PDT has shown to decrease the viability of macrophages in *in vitro* studies, as well as *in vivo* when high doses of light and/or PS are used^{132,137–139}. In contrast, several studies reported that at low doses of light and/or PS, macrophages are activated increasing their phagocytic activity both *in vitro* and *in vivo*^{97,125,140–145}, although their number does not change significantly⁹⁶.

For instance, Yamamoto et al. demonstrated that the enrichment of the Fc-receptor (phagocytosis-mediator) in murine macrophages was attained with low doses of **HpD** or **photofrin** and very short periods of illumination¹⁴². Similarly, Korbelik et al. also demonstrated that macrophages submitted to a sublethal dose of **PS-3-PDT** have preferential cytotoxicity towards tumor cells¹³⁸.

Many studies have reported that PDT-treated macrophages release several cytokines. **Photofrin**-PDT treated macrophages release prostaglandin-E2¹⁴⁶ and TNF- α ⁹⁷. This last one was suggested to significantly contribute to the antitumor immunity elicited by PDT. Similarly, *in vitro* macrophages (differentiated from a monocyte cell line) subjected to sub-lethal **mTHPC**-PDT had an enhancement on the phagocytic capacity, TNF- α production and NO release¹⁴¹.

The mechanisms by which macrophages become more proficient in phagocytosing tumor cells after PDT is not yet clear, but two mechanisms were proposed. One of them, suggests that macrophages are indirectly activated by PDT-treated cancer cells while the other hypothesizes that they are directly activated. Some studies showed that macrophages directly treated with PDT did not exhibit cytotoxicity against cancer cells whereas co-incubation of PDT-treated cancer cells with macrophages activate their tumoricidal functions and induce the production of several pro-inflammatory cytokines and immune mediators^{49,135,138,147,148}. It was suggested that DAMPs released/expressed by PDT-treated cells, namely HSP70, trigger TLR-2 and 4 signaling pathways in macrophages that induces NF κ B-dependent nitric oxide synthase (iNOS). The latter promotes the release of high levels of nitric oxide and more reactive nitrogen species that are toxic to cancer cells of different histological origin¹⁴⁹. Alternatively, some studies support the hypothesis that PDT may directly activate macrophages. Indeed, the work of Yamamoto et al. showed that *in vitro* PDT-treated macrophages presented higher phagocytic activity¹⁴⁴. However, this was only observed when macrophages were co-incubated with lymphocytes during PDT.

With an opposite role, M2 macrophages are important for tumor progression and damage healing. M2 macrophages produce growth factors, extracellular matrix degrading enzymes, proangiogenic mediators, which altogether contribute to tumor survival and invasion^{133,150}. Tumor-associated macrophages (TAMs) are a subset of M2 macrophages that can suppress antitumor immune responses. New strategies that target this subset of macrophages have been under investigation for antitumor therapies. Selective destruction

of TAMs was reported by Hamblin's group by attaching photosensitizers to ligands of the scavenger receptor. They should lead to a selective accumulation of photosensitizer in TAMs and to their preferential killing upon irradiation¹⁵⁰. Hayashi et al. synthesized a mannose-conjugated chlorin, designated to bind the mannose receptors highly expressed on TAMs. The conjugate produced strong cytotoxicity against both cancer cells and TAMs in the cancer stroma¹⁵¹.

1.2.1.6 Dendritic cells

Dendritic cells (DCs) act as linkers between the innate and adaptive immune system. DCs are the most representative antigen-presenting cells (APC) and are responsible to perform an important task in priming naïve T and NK lymphocytes. Their main role is to process TAAs and present them on its cell surface to lymphocytes initiating an adaptive immune response¹⁵². Immature DCs respond to inflammatory chemotactic factors and migrate to the inflamed tissues. The antigen uptake promotes the maturation of DCs, which become less responsive to the locally chemotactic factors and consequently, migrate to the secondary lymphoid organs¹⁵³. In the lymph nodes, DCs present antigens, through MHC molecules, to T and B lymphocytes, which promotes their maturation¹⁵⁴⁻¹⁵⁶.

PDT creates an environment that facilitates tumor antigen loading and allows activation of DCs. The latter is facilitated by DAMPs exposed/released by PDT-treated tumor cells, which are recognized by receptors present in APCs (eg LRP1/CD91¹⁵⁷ and CD40¹⁵⁸). Maturation of DCs by cell-lysates generated by PDT was associated with the expression of IL-1 α , IL-1 β , IL-6, IL-12 and inhibition of TNF- α ¹⁵⁹⁻¹⁶¹. These cytokines promote TAAs loading by DCs as well as the expression of peptide-MHC complexes and costimulatory molecules (CD80 and CD86) at the cell surface⁹⁵. Several studies have demonstrated that through local inflammation, PDT promotes DCs maturation and migration to the lymph nodes, which contributes for the antitumor immunity elicited by PDT^{124,159,162,163}. In the absence of inflammation, DCs remain in an immature state and although they can migrate to the lymph nodes to present antigens to T cells without costimulation, these T cells are eliminated or generate regulatory T cells, Treg⁹⁵.

The importance of DCs for the induction on antitumor immunity has been demonstrated by several studies. The selective depletion of DCs with diphtheria toxin (DTx) resulted in higher tumor recurrence rates after **WST11**-vascular-PDT, which was observed for both local and systemic depletion⁸⁹. PDT-treated LLC cells co-cultured with immature

DCs were then used to stimulate T cell population. This mediated a potent stimulation of IFN- γ -secreting CD8⁺ T cells and a remarkable depression of Treg cells⁶³. Recent studies that studied the generation of transient intracellular ROS of **hematoporphyrin**-PDT *in vitro* and *in vivo*, demonstrated effective maturation of DCs¹⁶⁴. Furthermore, these intracellular ROS-stimulated DCs enhanced antigen specific T-cell responses *in vitro* and *in vivo*, which led to delayed tumor growth and prolonged survival of tumor-bearing mice when immunized with a specific tumor antigen.

However, PDT also appears to have a negative impact on the surface receptor expression of DCs. Treatment with **verteporfin**-PDT reduced DCs levels of MHC class I and II, ICAM-1, costimulatory molecules B7-1 and B7-2 among other molecules crucial to the activation of T cells¹⁶⁵. These findings were in agreement with the study of Hryhorenko et al., that demonstrated that **ALA**-PDT-treated peripheral blood mononuclear cells (PBMC) reduced their ability to activate lymphocytes, thus, suggesting the impairment of APCs function¹⁶⁶.

Therapeutic strategies that involve the combination of PDT with the administration of DCs have recently demonstrated to improve the outcome of the treatments. Intratumoral injection of naïve DCs immediately after local **ATX-S10 Na(II)**-PDT significantly improved the overall survival when compared with any of the individual therapies⁹³. Jalili et al. demonstrated that the inoculation of immature DCs into the **photofrin**-PDT-treated tumors resulted in effective migration to the lymph nodes and consequent stimulation of the cytotoxic activity of T and NK cells¹⁶⁷. Then authors also showed that PDT-treated cancer cells were efficiently engulfed by DCs in *in vitro* co-culture studies¹⁶⁷.

These findings demonstrate the importance of DCs for the development of the antitumoral response after PDT and supports the hypothesis that intratumoral administration of DCs may be a promising combinatory therapy for PDT⁹⁴.

1.2.2 PDT and adaptive immunity

In contrast to innate immunity, the adaptive immune system is highly specific to certain antigens and provides immunological memory. The activation of the adaptive part of the immune system is initiated with TAAs presentation by APC to naïve T cells (CD4⁺ and/or CD8⁺), which ends in the production of cytotoxic tumor-specific T cells and/or antibodies production by B cells.

Maturation of DCs, the main responsible for the linkage between innate and adaptive immunity, upregulates surface MHC I and II molecules and costimulatory molecules CD80 and CD86. This allows DCs to efficiently prime CD4⁺ and CD8⁺ T cells and induce B cells to produce antigen-specific immunoglobulins (antibodies). This adaptive immune response creates immunological memory in the host system, giving protection in an antigen-specific manner¹⁶⁸.

In 1987, Murphree and coworkers reported that **photofrin**-PDT yielded partial or complete cure of s.c. LLC tumors in C57BL/6 mice and also decreased the number of lung metastasis⁷¹. The same effect was not achieved in mice treated by surgical removal of the primary tumor. The importance of the adaptive immune system for PDT efficacy was also later reported by Canti et al., by showing that although both normal and immunocompromised mice, bearing MS-2 fibrosarcoma tumors, were cured by **AlS₂Pc**-PDT, only the immunocompetent surviving animals were able to resist to a subsequent MS-2 rechallenge³⁹. Furthermore, Korbelyik and coworkers demonstrated that the adoptive transfer of splenic T lymphocytes from untreated BALB/c mice into immunocompromised scid mice 9 days before **photofrin**-PDT of EMT6 tumors delayed tumor growth⁴⁰. In addition, several other studies have proved the essential role of the host immune system for a higher efficacy of PDT treatments, showing reduced cured rates in immunocompromised mice^{17,36,46,89}.

A substantial recruitment of lymphocytes into the tumor bed was reported by Preise et al. 24 h after **WST11**-PDT, most of them located in the tumor rim rather than in the tumor core⁸⁹. There was a complete absence of CD3⁺ T cells immediately after the illumination, indicating their destruction by PDT⁸⁹. This lymphocyte destruction is thought to be advantageous, once tumor infiltrating lymphocytes (TILs), the type of lymphocytes normally present in tumors, suppress antitumor responses and may inhibit the inflammatory responses. CD3⁺ T cells have a drastic rise in 24 h and go back to the basal levels in 48 h.

Antitumor immunity has been proposed to have a conceivable contribution for the inhibition of metastasis and this is of utmost importance as metastasis are the leading cause of death in cancer patients. In the PDT field, numerous works have highlighted the importance of adaptive immunity for the control of both the primary tumor and distant (non-irradiated) metastasis. Shams et al. implemented a two-step PDT strategy that combines an immune enhancing protocol (low light dose) followed by a tumor controlling

protocol (high light dose). The first activates antitumor immunity with impact in non-irradiated metastasis whereas the later eradicates the primary tumor⁶⁶.

Similar results have been described using a single protocol of PDT. For instance, **photofrin**-PDT had a positive impact in the irradiated EMT6 primary tumor and significantly reduced lung metastasis that were induced by i.v. injection of cancer cells (pseudo-metastatic model)⁶⁹. **Verteporfin**-PDT treatments of mice bearing one CT26.CL25 tumor in each flank (bilateral tumor model) revealed that the irradiation of only one of the tumors led to complete tumor regression of the non-irradiated tumor in 78 % of the treated mice³⁶. Similar results were also attained with **redaporfin**-PDT but with CT26.WT tumor. **Redaporfin**-PDT significantly reduced the number and/or size of non-irradiated pseudo-metastatic lesions¹⁷.

Korbelik et al. reported that antitumor immunity triggered by PDT is able to mount an immunological memory, showing that adoptive transfer of splenocytes from **Photofrin**-PDT-cured mice to immunocompromised scid mice had a strong effect on EMT6 tumors⁴². CTL were identified the main immune effector cells responsible for this effect, which were also demonstrated with other photosensitizers and/or tumor models^{61,69,127}.

1.2.2.1 Helper T cells

Helper T cells, also known as CD4⁺ T cells, main function is to regulate the activity of other immune cells by secreting cytokines that will assist the clearance of pathogens and tumor cells. They support activated B cells to secrete antibodies and cytotoxic T cells to kill target cells and help macrophages to destroy ingested cells. They can differentiate into different helper T cell types depending on the cytokines present in the surrounding environment. Thus, CD4⁺ effector T cells can be divided in several subsets according to their functions. The most relevant are: Th1, Th2 and Th17. Th1 cells, recognized by the secretion of IFN- γ , GM-CSF, IL-2 and lymphotoxin (LT), promote cell-mediated inflammatory responses, phagocytic activity by numerous mechanisms and regulate macrophages functions. Th2 subset favors predominantly the humoral response and are recognized for producing several cytokines (IL-4, IL-5, IL-6 and IL-10). Th2 cells trigger immune responses mediated by mast cells and eosinophils and increase degranulation processes. Finally, Th17 cells are characterized by the production of IL-6, IL-17 and TNF- α and induction of other cytokines and chemokines production. Th17 cells are also

associated with the increased infiltration of neutrophils and with the activation of cell-mediated inflammation^{169,170}.

The importance of CD4⁺ T cells for anti-cancer PDT is not yet completely understood, and some of the studies present controversial effects for this immune population. Solomon and coworkers reported that lymphocytes isolated from cured mice several months after **WST11**-PDT secreted IFN- γ upon the re-stimulation with *in vitro* photosensitized cells⁸⁹, suggesting the triggering of a proinflammatory Th1 response. Prior evidence that IL-17 promotes neutrophil migration to the infected sites motivated Brackett and coworkers to further study the induction of sterile inflammation with **HPPH**-PDT. Their results revealed a rapid accumulation of IL-17 producing Th17 cells in the TDLN after PDT¹¹⁵.

The cure rate of EMT6 tumors treated by **photofrin**-PDT was reduced by ~25% and 50% after the administration of monoclonal antibodies against CD4 and CD8, respectively⁴⁵. Similar results were reported by Korbelik et al., implementing the adoptive transfer of splenocytes from immunocompromised PDT-treated mice to reestablish the curative effect on scid mice. When CD4⁺ T cells were depleted from donor splenocytes, the curative effect of **photofrin**-PDT of EMT6 tumor model⁴² partially but significantly decreased. In contrast, other studies have suggested that PDT does not require CD4⁺ T cells to mount antitumor immunity. Indeed, PDT with **photofrin** of a s.c. EMT6 tumor model⁶⁹ and with **redaporfin** of a s.c. CT26.WT tumor model¹²⁷ are not affected by CD4⁺ T cells specific depletion with monoclonal antibodies, suggesting that CD8⁺ T cells activation is possible in some cases even in the absence of CD4⁺ T cells.

1.2.2.2 Cytotoxic T cells

Cytotoxic T lymphocytes (also known as CD8⁺ T cells or CTL) play an important role in identifying and eliminating cancer cells. After DCs maturation, these migrate to the lymph nodes where they present TAAs to CTL through MHC class I. This leads to CD8⁺ T cells activation and recruitment to the treated tissues, where they can exert their cytotoxic activity together with the secretion of IFN- γ .

Gollnick and coworkers hypothesized that the systemic antitumor response elicited by **photofrin**-PDT might have impact in distant cancer lesions that were not inside of the illuminated area⁶⁹. PDT was delivered to s.c. tumors of mice bearing both s.c. tumor and lung tumors. An infiltration of CD8⁺ T cells into untreated tumors was reported and these

immune cells presence was critical for the inhibition of tumor growth outside the illuminated area. In this study it was also demonstrated that this CD8⁺ T cell antitumor immunity was dependent on NK cells, instead of CD4⁺ T cells. Korbelik et al. selectively inhibited CD4⁺ and CD8⁺ T cell population to better understand their relevance for the treatment outcome⁴⁵. Depletion of CD8⁺ T cells resulted in a severe reduction of the cure rate, while CD4⁺ T cell depletion just led to a less pronounced reduction of the curative effect. Several other studies have also reported that depletion of CD8⁺ T cells led to reduced cure rates^{46,171}, revealing the importance of this cell population to the efficacy of PDT treatment. Saji et al. reported that adoptive transfer of splenocytes from CT26 cured mice with **ATX-S10 Na(II)**-PDT gave protection to naïve mice from a rechallenge with CT26 and this was mainly due to CD8⁺ T lymphocytes⁹³. Similarly, CD8⁺ T cells depletion from splenocytes of **photofrin**-PDT-cured mice were used for an adoptive transfer procedure and the results revealed a complete abrogation of the curative effect^{42,89}, confirming the previously stated. Even though it is described that the generation and maintenance of effective memory CD8⁺ T cells requires the presence of helper T cells¹⁷², these findings suggest that the efficacy of the treatment is not affected by the absence of CD4⁺ T cells. Thus, although both populations participate in the antitumor elicited response, cytotoxic T cells appears to have a crucial role while helper T cells play a supportive role.

1.2.2.3 Regulatory T cells

Regulatory T cells (Tregs) are the main cell population suppressing the immune response and account for 5 % to 10 % of the CD4⁺ T cell population. Among all the regulatory T cells the most common are CD4⁺CD25⁺FOXP3⁺ T cells, which are responsible for tolerance of self-antigens and excessive inflammation, being crucial in autoimmune diseases prevention. In addition to this regulatory function, Tregs also have the capacity to suppress other cells activity, particularly effector T cells. This cell population is characterized by the constitutive expression of CD4, CD25, FoxP3 and CTLA-4 molecules and its proliferation is enhanced by IL-10 and TGF- β expression¹⁷³.

Tregs are recognized to have a great impact on the antitumor immunity, through the inhibition of T cells maturation to cytotoxic cells. This immune cell population is the predominant cell type that accumulate in the tumor and its immunosuppressive effect is associated with various mechanisms^{174,175}. Tregs can be categorized in two main

populations: natural Tregs (nTregs) and induced Tregs (iTregs). Natural Tregs are found in the thymus and are important to prevent autoimmune diseases. Induced Tregs are generated and differentiate in the periphery, for example through TGF- β stimulation in the tumor microenvironment¹⁷⁶. Inside tumors, Tregs can prevent the complete activation of effector T cell by sequestration of IL-2. Partially activated effector T cells are continuously producing IL-2, which is beneficial to Tregs, as it is also necessary to Tregs maintenance¹⁷⁷. TGF- β production by Tregs is another immunosuppressive mechanism triggered by these immune cell population and prevents the differentiation of cytotoxic effector T cells, keeping the memory CD8⁺ T cells in an inactive state and can lead to an increased number of Tregs¹⁷⁸.

PDT has a great impact on lymphocytes and consequently, also has an important impact on Tregs levels. Reginato et al. reported that **verteporfin**-PDT of CT26 tumors led to a significant increase in CD4⁺CD25⁺FOXP3⁺ Tregs in the spleen and in the lymph nodes between day 0 and day 4 after the treatment, which later dropped back to the normal values. The levels of TGF- β in serum were also elevated after PDT, suggesting the generation of an immunosuppressive microenvironment inside the tumor⁷⁷. On the other hand, **photofrin**-PDT abolished the suppressive activity of Tregs 7 days after the treatment, even though no impact was observed on Tregs levels³⁴. This abrogation of its immunosuppressive capacity was accompanied by a significant increase of DAMPs release and a rise of IL-6 levels observed after PDT, suggesting that these mediators may be responsible for the abolishment of Tregs functions after PDT. Zheng et al. also described a decrease of Tregs induction *in vitro* and *in vivo* when treated with DCs which had been pulsed with **hypericin**-PDT-treated LLC cells. Rechallenge with live LLC cells also led to a significant inhibition of tumor growth⁶³.

Induction of Tregs expansion by tumor cell microenvironment is a major barrier to PDT efficacy and appears to be dependent on the type of PDT regimen. There may be a need for external depletion of suppressor cells in protocols wherein PDT alone does not accomplish that depletion. Selective depletion of Tregs was studied in several studies and improvement of the treatment outcome was reported^{77,78}.

1.2.2.4 B cells

Adaptive immunity not only comprises the activation of T cells but also B lymphocytes, immune cells responsible for mounting the humoral immunity. The activation of B cells

occurs in the lymph nodes via the recognition of antigens by B cell receptors (BCR) present on their cell membrane. Activated B cells are then responsible for producing antigen-specific immunoglobulins, typically known as antibodies.

The contribution of humoral responses for PDT-mediated antitumor immunity was only rarely suggested. Korbelyk described the role of host lymphoid populations in **photofrin**-PDT efficacy⁴⁰. A 100% curative PDT protocol in immunocompetent mice was implemented in scid mice and nude mice. While scid mice have no mature T and B lymphocytes, nude mice have normal levels of B lymphocytes and NK cells. The implemented protocol produced no cures in either scid or nude mice. Preise et al. described a marked B-cell infiltration 24 h after **WST11**-PDT in the tumor rim and in the interface between tumor and skin. Also, increased levels of IgG were detected 1 week after PDT and the serum of cured mice conferred protection to naïve mice against tumor challenge⁸⁹. Even though PDT is generally accepted to trigger both cell-mediated and humoral adaptive antitumor responses, the mechanisms by which the humoral immunity impacts PDT remain unclear and further research is needed.

1.3 Combinatorial approaches to stimulate immune responses

Malignant diseases usually present a poor diagnosis and outcome caused by their invasiveness and difficulty to treat. PDT is a promising and effective cancer treatment, however some limitations occur when the ambition is to go beyond a local treatment and attempt to destroy isolated tumor cells and distant lesions, such as metastasis. This is a difficulty found in other oncology treatments. Therefore, several combinatorial approaches have been tested to improve the therapeutic efficacies and reduce the side effects. Treatment combinations usually include chemotherapy, radiotherapy, immunotherapy, and other therapies.

The cell death originated by PDT creates a source of TAAs and thus, combinatory approaches with immunotherapy are promising strategies that could potentiate the antigen uptake, activation of T cells and consequent trigger a specific antitumoral response. The ability of tumors to evade PDT cytotoxic, such as immune cell dysfunction and suppression are also some of the reasons proposed for PDT ineffectiveness, and synergistic approaches that tackle these problems have also been reported over the past few years.

1.3.1 Non-specific immunotherapies and PDT

Immunotherapies which do not present specificity to just one antigen, but to several instead, are considered non-specific immunotherapies. They do not trigger a specific response regarding the infection or type of cancer but are capable of broadly boosting the immune system. Some of these immunotherapies are usually used alone while others are combined with other strategies.

Immunostimulants are described as any non-specific substances that modulate immune responses, boosting the protection for a specific disease. The mechanisms of actions behind this modulation are not fully understood but are thought to be dependent on the interaction with pattern recognition receptors (PRRs), such as TLRs, expressed by several immune cells. Immune stimulation can occur as a result of several mechanisms of action, including formation of a depot by trapping antigens at the injection place, extension of the presence of the TAAs in the blood, recruitment of immune cells, enhancement of TAAs uptake/presentation and/or induction of cytokines/chemokines production¹⁷⁹.

The stress caused by PDT in cancer cells triggers the release of TAAs which initiates an inflammatory process, further generating an antitumoral response. However, most of the tumors are described as low immunogenic, meaning that the host response to the tumor is not enough to eliminate alone the remaining tumor cells. The presence of an immunomodulator at the local of treatment may enhance the immune responses triggered against tumor cells, improving the treatment outcome.

1.3.1.1 Exogeneous and microbial immunostimulants

Myers et al. reported the benefits of combining PDT with immunoadjuvants in 1989¹⁸⁰. The combination of **HpD**-PDT and a preparation of *Corynebacterium parvum* (CP) in a mouse model of s.c. bladder cancer prolonged the animal survival, while either one of the treatments alone only exerted marginal control of the tumor. The administration of mycobacterium-cell wall extract immediately after PDT with several PSs (**photofrin**, **verteporfin**, **mTHPC** and **ZnPc**) also elicited a local inflammatory response, indicated by neutrophil infiltration and potentiated the curative effect in EMT6 tumor model¹⁸¹

Later, Korbelik et al. tested the combination of PDT with Bacillus Calmette-Guérin (BCG) vaccine in a s.c. EMT6 mouse tumor model with six PSs: **photofrin**, **BPD**, **mTHPC**, **talaporfin**, **MLu** and **ZnPc**¹⁸². Apart from the improvement of the cure rate, the number of memory T cells in the TDLNs was also significantly increased. In agreement with this studies, Cho et al. described that **HpD**-PDT combined with intravesical BCG was more effective than any of the treatments alone¹⁸³. Preliminary clinical results revealed that patients subjected to a combinatory approach of PDT with BCG resulted in an improved response, with total destruction of the tumor tissue or lowering of its staging¹⁸⁴.

Uehara et al. studied the antitumor effect of **HpD**-PDT and the administration of a streptococcal preparation designated OK-432¹⁸⁵. The combination confirmed the potentiation of the antitumor effect, but only when OK-432 was administered before PDT, possibly caused by the impaired blood flow into the tumor which prevent the infiltration of inflammatory cells. The same observations were obtained by Krosli et al. when combining PDT with daily intramuscular (i.m.) administrations of Schizophyllan (SPG). SPG is a β -D-glucan polysaccharide derived from fungal cells and has the capability to stimulate both humoral and cell immune responses. The combination approach generated a three times higher cure rate, and increased the PS retention in tumor cells¹⁸⁶. Chen et al.

tested the combination of four different immunoadjuvants (Glycated chitosan (GC), Complete Freund (CF) adjuvant, incomplete Freund (IF) adjuvant and *Corynebacterium parvum* (CP)) individually with PDT with two photosensitizers, **photofrin** and **mTHPC**, and a light-absorbing dye, ICG. All the combinations with these immunoadjuvants enhanced the treatment efficacy of the tumors and increased the long-term survival of the laser cancer treatments¹⁸⁷. Korbely and coworkers used a very aggressive, metastatic, and poorly immunogenic orthotopic tumor model, 4T1 breast tumor, to evaluate the impact of **verteporfin**-PDT combination with CpG oligodeoxynucleotides (CpG-ODN). CpG-ODN are short single-stranded synthetic DNA molecules that contains unmethylated CpG dinucleotides (CpG motifs) that act as immunostimulants. The combination increased the levels of activated DCs and the tumor response to PDT, enhancing the overall survival¹⁸⁸. More recently, Korbely and coworkers published a study showing that combination of N-dihydrogalactochitosan with the administration of treated cells enhances the therapeutic effect obtained with PDT vaccines as well as reduces the numbers of myeloid-derived suppressor cells¹⁸⁹. The intratumoral administration of γ -inulin, a potent classical complement activator, immediately after PDT led to a delay in tumor recurrence with several PSs¹²⁰. Even though each treatment alone increased the levels of C3 protein, the combination allowed to attain even higher amounts, suggesting the magnification of complement system activation and the development of specific T cell mediated antitumor response. Imiquimod (IMQ) is another immunoadjuvant that acts by activating APCs and by inducing the production of several cytokines such as IFN- γ , TNF- α , IL-1, IL-6, IL-8, IL-10, IL-12, p40, G-CSF and GM-CSF. Bhatta and coworkers reported that the combination of IMQ with **ALA**-PDT enhanced the efficacy of each treatment alone of cutaneous squamous cell carcinoma⁵⁶. The presence of a greater number of apoptotic cells in this combination was assigned to be due to the increased number of cytotoxic T cells.

Similar approaches have been reported using nanoparticles as delivery strategies, engulfing both the PS and the immunoadjuvant. Dhar and coworkers combined CpG-ODN and **ZnPc** in a single nanoparticle construct for the treatment of 4T1 mice tumors. The incubation of the treated cells with bone marrow derived immature DCs revealed a synergistic increase in the production of several proinflammatory cytokines¹⁹⁰. Im et al. applied a hypoxia-responsive transforming carrier to improve the delivery at the same time the photosensitizer and the adjuvant, which boosts the antigen presentation by

dendritic cells. This approach revealed a significant inhibition of B16F1 tumor growth in an animal model¹⁹¹.

1.3.1.2 Cytokines, growth factors and other modulators

The inflammation observed after PDT is important to trigger antitumor immune responses and cytokines are recognized to be highly involved in this process. Several studies described the possibility of administering recombinant cytokines or inducers of these molecules as a strategy to potentiate PDT.

A single dose administration of recombinant human TNF- α as well as of DMXAA (5,6-dimethylxanthenone-4-acetic acid), an inducer of TNF- α , statistically enhanced the tumoricidal response to **photofrin**-PDT, allowing for drug dose reduction to avoid side effects, without losing efficacy^{192,193}. Administration of the granulocyte colony-stimulating factor (G-CSF) led to a significant increase in the number of circulating neutrophils, followed by a delay of tumor growth^{44,129}. Following a similar strategy, granulocyte-macrophage colony-stimulating factor (GM-CSF) immunotherapy is based on the injection of lethally irradiated granulocyte-macrophage colony-stimulating factor-producing tumor cells. The combination of this therapy with **photofrin**-PDT increased the toxicity of tumor-associated macrophages and substantially potentiated tumor control¹²⁸. Adoptive transfer of highly cytotoxic NK92MI cells, natural killer cells that were genetically modified to express IL-2, was implemented as an adjuvant immunotherapy with PDT⁸³. This treatment modality led to an improvement of PDT efficacy and was dependent on the IL-2 expression. The major concern with adoptive immunotherapies is the risk of allogeneic rejection, reactions triggered by the host against the transplanted cells from a genetically different recipient⁸³. However, in this study it was demonstrated that immunocompetent mice bearing PDT-treated EMT6 tumors showed a clear benefit of adjuvant NK92MI immunotherapy.

Another strategy to potentiate the antitumor effect after PDT is to stimulate/activate the immune cells responsible for the response observed after PDT. Serum vitamin D3-binding protein-derived macrophage-activating factor (DBPMAF) leads to activation of macrophages which raised to 100% **photofrin**-PDT cure rates in a mouse SCCVII tumor model¹³⁶.

Another approach to improve the antitumoral response is by increasing the concentration of DAMPs present on the tumor microenvironment, boosting the recognition of TAAs

released by PDT treated cells. From the all set of DAMPs induced after PDT (eg CRT, HSP70, HMGB1), Korbelik and coworkers injected CRT peritumorally immediately after **mTHPC**-PDT in SCCVII tumor-bearing immunocompetent mice. The results revealed that the administration of CRT enhanced the antitumor response and improved the treatment outcomes in comparison with PDT alone¹⁹⁴.

As an antitumor immune response is based on the concept of antigen-specificity, one possible immunotherapeutic strategy is the vaccination using synthetic long peptides (SLP) that will cover the epitopes of tumor antigens and increase the recognition by T cell. Ossendorp and coworkers implemented this concept in combination with **bremachlorin**-PDT in two independent aggressive tumor models and obtained higher percentage of cures and an increased overall survival in comparison with any of the treatments alone¹⁹⁵.

It is well known that cancer cells present several mechanisms to escape antitumor immune responses. One of them is related to the expression of tumor antigens that can be detected by the immune system of the host, commonly designated as high or low immunogenicity. Apart from that, even highly immunogenic tumors can still progressively growth meaning that somehow antigen recognition by T cells and any sort of response elicited by that recognition are being suppressed. The immunosuppressive tumor microenvironment is characterized by the presence of Tregs, the immunosuppressor T cells. Several studies demonstrated that inhibiting these immunosuppressor cells, namely, regulatory T cells, affects the kinetics of tumor growth¹⁹⁶. However, this seems to be only true when the depletion is started at the same time or even before tumor cell inoculation¹⁹⁶. Cyclophosphamide (CY) is an anticancer chemotherapeutic drug, which was discovered to have the ability to selectively deplete Tregs when used in low doses. The combination of **verteporfin**-PDT with low-dose CY resulted in 70 % permanent cures with a J774 mice tumor model where any of the treatments alone could only give a survival advantage but no cures⁷⁸. Analyses of spleens from cured mice revealed the presence of tumor-specific T cells and 71 % of cured animals rejected a rechallenge with tumor cells. The same conclusions were obtained by Reginato et al. where the same combination was applied to a different tumor model, CT26.WT tumors. Long-term survival was achieved in 90 % of the treated mice. Moreover, levels of Tregs and TGF- β , a known inducer of Tregs, were reduced compared to naïve mice levels⁷⁷. However, for this model the rejection of the rechallenge only occurred when a second dose of CY was administered

before rechallenge. These results suggest that the combination of PDT with low-dose CY depletes the regulatory T cells which leads to improve of PDT outcome and promote the establishment of a memory immunity.

1.3.2 Specific/Cell-based immunotherapies + PDT

Specific immunotherapies refer to strategies that aim to help the immune system recognize the TAAs and destroy the cancer cells, boosting host immune system to fight cancer. These strategies have reached a mature state with several therapeutic approaches in clinical use. The concept is based on enforcing cancer cells recognition by the immune system, such as increasing T cells survival and functions or modifying DCs to present TAAs to activated T cells¹⁹⁷.

1.3.2.1 Adoptive transfers and PDT-generated vaccines

The idea of potentiating the host antitumor immune response resorting to an external source of immune cells has been considered for many years. Adoptive cell therapies consist of activating, modifying, or expanding a specific population of immune cells and infuse them into the patient. Dougherty et. al tested adoptive transfer in mice with a compromised immune system, such as scid mice, in which the curative effect of **photofrin**-PDT is completely abolished⁴². The results revealed that adoptive transfer of splenocytes to scid mice was only effective when the hosts were engrafted with splenocytes from PDT-cured immunocompetent mice. In contrast, no benefit was observed if spleen cells were sensitized for a different tumor model of the host one.

PDT-vaccines were initially tested to understand the direct effect of PDT on tumor cells, rather than the surrounding tissues, and their contribution to the antitumor immunity. In comparison with traditional vaccine-generating strategies, PDT-vaccine of tumor cell lysates revealed to be more effective¹⁹⁸⁻²⁰⁰. Even though several strategies could initiate the maturation of DCs, only PDT was able to trigger DCs to produce IL-12, a critical cytokine for the cellular immune response. These studies showed that PDT alone triggers an immune response and that PDT is a promising strategy to generate vaccines¹⁹⁸. These findings have been corroborated by many other studies with different photosensitizers and tumor models^{63,80,199,200}, which reported increased numbers of DCs, B and T lymphocytes on the vaccinated mice, most importantly with effective engagement of the cytotoxic T lymphocytes. Wang and coworkers studied in vitro and in vivo the effect of

the major **ALA**-PDT generated DAMPs – calreticulin, HSP70 and HMGB1 – on immune cells. They showed that the enhanced levels of expression of these danger signals after **ALA**-PDT played an important role on the activation of DCs. Increased surface expression of MHC-II, CD80 and CD86 and enhanced ability to secrete IFN- γ and IL-12 resemble the phenotypic and functional maturation of DCs. Furthermore, the authors reported that the administration of PDT-treated cells ensured complete protection against cancer cells of the same origin⁵⁵. Several other strategies have also combined the inoculation of PDT-cell lysates with the administration of an immunoadjuvant to improve the therapeutic outcome through a synergic effect^{189,201}.

Cancer patients generally present significantly decreased numbers of circulating DCs in comparison with healthy people. Moreover, blood monocytes present reduced ability to process antigen and a low expression of costimulatory and MHC molecules. This decrease their ability to differentiate into immature monocyte-derived DCs and can even induce anergized/tolerized T cells²⁰². Regarding this, Jalili and coworkers tested the inoculation of immature DCs into PDT-treated tumors¹⁶⁷. The PDT-treated tumor cells were effectively endocytosed by immature DCs, leading to their activation, homing to lymph nodes and inducing an immune response. Even with more aggressive and invasive tumor models, the protocol approach based on the DCs cell administration immediately after PDT led to promising results²⁰³. This strategy represents one huge advantage, that is overriding the need for *in vitro* procedures with tumor antigens to prime the immune cells.

The effective priming of these immune cells *ex vivo* was reported to present greater impact on the outcomes, portraying it as a promising strategy by several studies over the last years. DCs vaccine using **ALA**-PDT-treated apoptotic cells revealed protection against SCC tumor growth with strong antitumor immunity^{58,60}. The mechanism proposed by the authors suggests that apoptotic cancer cells are the source of multiple danger signals triggering the maturation and activation of DCs. It has been severely discussed over the last few years which mechanism of cell death better triggers an effective antitumor immune response, and it is believed that it is essential to trigger an immunogenic cell death in order to trigger antitumoral immunity³¹.

Morphologic modifications of DCs were identified after **ALA**-PDT, with enlargement of the dendrites and an increased number of lysosomes. Furthermore, some phenotypic changes also arise, as upregulation of MHC II and costimulatory CD80 and CD86 molecules. Regarding the functional maturation, some variations in the secretion of

cytokines have also been described, as the high expression of IFN- γ and IL-12 and the absence of IL-10, critical for the development of the cellular immune response^{58,60}. All these factors are recognized to be potentiators of DCs maturation and consequently T cell proliferation. Garg et al. demonstrated that murine DCs co-incubated with **hypericin**-PDT-treated glioma cells led to significant phenotypic maturation of DCs. The authors described the induction of anti-glioma protective immunity by ICD-based DC vaccines. This response was dependent on ROS and some DAMPS but also on the presence of intact adaptive immune system and specially on CD8⁺ T cells²⁰⁴. In agreement with these, another study performed by Zheng et. al involving the same photosensitizer demonstrated that both PDT-DCs and PDT-tumor cells prepared by PDT showed potent antitumor responses against rechallenge⁶³.

Cell submitted to PDT with **DH-I-180-3**, a derivative of methylpheophorbide-a, secrete HSP70 and the exposition of DCs *in vitro* to tumor cell lysates treated with PDT increase the DCs expression of IL-2, a T cell growth factor²⁰⁵. To evaluate the *in vivo* immune response, tumor-bearing mice were vaccinated with PDT-stimulated DCs. The authors reported a great stimulation of IFN- γ -secreting CD8⁺ T cells, increased IFN- γ and decreased IL-4 expression levels, consistent with an antitumor response, even against established solid tumors and late-stage tumors. The authors also showed that this protocol was more effective than vaccination with PDT tumor lysates. Similar results were recently described for dendritic cells pulsed by **ALA**-PDT-treated skin squamous cell carcinoma⁵⁹. The authors reported that this strategy could increase the activity of CD4⁺ and CD8⁺ T cells present on the spleen of immunized mice. Increased levels of IL-12, IFN- γ and decreased levels of IL-10 were observed. Several other studies have been published describing the impact of PDT-based DCs vaccines on tumors, leading to regression of tumor growth, cures, including in distant metastasis⁹³.

1.3.2.2 Monoclonal antibodies

Disappointing PDT efficacy is usually associated with insufficient accumulation of PS, insufficient illumination to cause specific necrosis or tissue physical properties (hypoxic tissues). Taking this into consideration, several studies have proposed different strategies to tackle these problems, such as targeting specific tumor microenvironment features or creating optimal conditions for PDT to be effective.

Ferrario et. al reported that hypoxia and oxidative stress originated by **photofrin**-PDT *in vivo* could be involved in the overexpression of vascular endothelial growth factor, VEGF, which is described to affect angiogenesis and vascular permeability and the host immune response to tumors²⁰⁶. PDT combination with antiangiogenic therapies improved the tumoricidal responses compared to the treatments alone. Synergistic effects were also observed when **verteporfin**-PDT was combined with monoclonal (mAb) C225-based inhibition of epidermal growth factor receptor (EGFR), yielding lowest mean tumor burden and an approximately threefold greater survival in a mouse model of human ovarian cancer²⁰⁷. The authors suggested that combination of **verteporfin**, which causes damages in mitochondria, and EGFR-targeted therapy, that causes cell cycle arrest, enhances the efficacy of the therapy due to the non-overlapping mechanisms of action. Recently, Fisher et al. demonstrated that **PpIX**-PDT combined with a clinical EGFR inhibitor, lapatinib, led to a significant increase in PS accumulation and elicited stronger responses following PDT in two human glioma-derived tumors *in vivo*²⁰⁸. This coupling strategy emerges as a promising strategy that may improve tumor local control and resection rates, leading to an improved survival.

Similar studies with several PS have been describing the same accomplishments^{64,209,210}. Regarding a different target, interesting findings were reported by Korbely and coworkers related to the immunodepletion of granulocytes. Anti-Gr1 mAb administration had an opposite effect on mouse SCCVII tumors when administered immediately after **mTHPC**-PDT and 1 h after the treatment²¹¹. The authors suggest that neutrophils that are engaged immediately after irradiation are within one hour replaced with a different myeloid population that are responsible for hampering the antitumor immune effect elicited by PDT. Thus, depleting granulocytes 1 h after irradiation destroys these immunosuppressor granulocytes that are recruited to the tumor and enhances treatment outcome. These findings emphasize that optimization of conditions can have a huge impact in the efficacy of treatment combinations.

To improve the efficacy of PDT treatments through the conjugation of PS with antibodies is called as photoimmunotherapy (PIT). PIT is a therapeutic strategy that uses light activation of an antibody-photosensitizer conjugate to selectively destroy cancer cells²¹². The antibody is responsible for the selective targeting by binding to cancer cells and the photosensitizer is responsible for the cytotoxic through the generation of ROS. PIT can

provide highly specific cytotoxicity to tumor cells expressing specific antigens, to which the mAb binds.

To increase the targeting selectivity of ovarian cancer PDT treatment, the photosensitizer molecule chlorin e6 (**Ce6**) was conjugated to a mAb recognizing an antigen expressed in 80 % of the non-mucinous ovarian cancers, OC125. The reported results revealed a significant increased survival compared to the control group²¹³. mAb 17.1A was conjugated to **Ce6** and the efficacy of the conjugate was tested in an orthotopic murine xenograft²¹⁴. There was a highly significant reduction of tumor weights and the median survival was increased compared to free PS. These findings showed a promising strategy to overcome the limitations of PDT of liver tumors, minimizing the damages in the healthy liver tissue. Similarly, **IR700** conjugated to mAb targeting EGFR led to tumor shrinkage after the treatment. No phototoxicity was observed when the conjugate was not bound to the membrane, suggesting that the mechanism was different from conventional PDT²¹⁵. Several other studies have demonstrated the conjugation of **verteporfin** with chimeric mAb targeting EGFR and showed higher specificity for EGFR-overexpressing cell lines^{216–219}. Ishida et al. combined the molecular-targeted PIT with gene transfer technology to demonstrate a promising strategy to treat peritoneal dissemination in gastric cancer²²⁰. This involves trastuzumab-**IR700**-mediated PIT combined with adenoviral HER2-ECD gene transfer. This protocol inhibited peritoneal metastasis and improved the survival of mice bearing gastric tumors (MKN45). Soukos et al. studied the combination of the mAb C225 anti-EGFR for two purposes: either coupling to the NIR fluorescent dye Cy5.5 for detection or to the photosensitizer **Ce6** for therapy. With the same mAb, diagnostic and therapy was conducted and the authors demonstrated the potential of immunophotodiagnosis to follow up the efficacy of the treatment²²¹. Similarly, Mitsunaga et al. later described the implementation of panitumumab-**IR700** PIT for HER1-overexpressing tumor model (A431). Based on the redistribution of the conjugate evaluated by **IR700** fluorescence guidance, therapeutic effects were observed with fractionated administrations of the conjugate and NIR irradiations of the tumor bed²²².

Even though PIT has been initially designed to target and destroy cancer cells, some studies have also implemented the strategy to deplete specific subpopulation of immune cells within the tumor, mainly immunosuppressor cells population. CD25-targeted NIR PIT with **IR700** was implemented to selectively deplete tumor-infiltrating Tregs without disturbing the homeostasis in other organs²²³. This effect prompted a rapid activation of

CD8⁺ T and NK cells, systemic antitumor effects which affected the local tumor and the tumor growth of distant tumors.

There are still a few reasons that prevent PIT to succeed and further research is still important to solve some of these problems, such as the low extinction coefficients of PS which requires several PSs connected to each Ab; the hydrophobicity of PSs that complicates the conjugation with mAb; the PSs absorption on the visible region that limits light penetration²¹⁵.

1.3.2.3 Immune checkpoint blockers (ICB)

The low efficacy of treatments such as surgery, chemo and radiotherapy in some specific cancer diseases motivated the development of new strategies that could boost the antitumor immune response. Immunotherapy relies on the idea that the host immune system could detect and destroy cancer cells if correct priming of T cells occurred, without facing inhibitory stimulus. T cells are subjected to several suppressive mechanisms, including inhibition by Tregs, myeloid derived suppressor cells and several inhibitory checkpoint receptors.

Immune checkpoints comprise several immunosuppressive mechanisms that play essential roles in maintaining immune homeostasis and protect the host from exacerbated immune responses to pathogens or even against self-components. These pathways are usually co-opted by tumors as a mechanism to escape from the immune attack (Figure 5).

Programmed-cell death-1 (PD-1, CD279) is a transmembrane receptor expressed on the surface of activated T and B cells and in some cases in natural killer and myeloid cells, such as macrophages. PD-1 binds to its cognate ligands, PD-L1 and PD-L2. PD-L1, also described as B7-H1 or CD274, is expressed in various types of cells: leukocytes, nonhematopoietic cells and nonlymphoid tissues, such as many tumor cells. PD-L2, also described as B7-DC or CD273, is expressed mainly in DCs and monocytes. The binding connection of PD-1 to its ligand negatively regulates the immune system through impairment of attacking immune cells²²⁴. In a similar manner, cytotoxic T-lymphocyte-associated protein 4 (CTLA-4, CD152) protein receptor is expressed by activated T cells and is also constitutively expressed in Tregs. CTLA-4 is homologous to T cell co-stimulatory protein CD28. Both CD28 and CTLA-4 binds to CD80 (B7.1) and CD86 (B7.2) expressed on APCs, acting as co-stimulators of T cells. However, CTLA-4 has a

greater affinity to this binding, hence when expressed it prevents the co-stimulation of CD28 and transmits an inhibitory signal to T cells²²⁵.

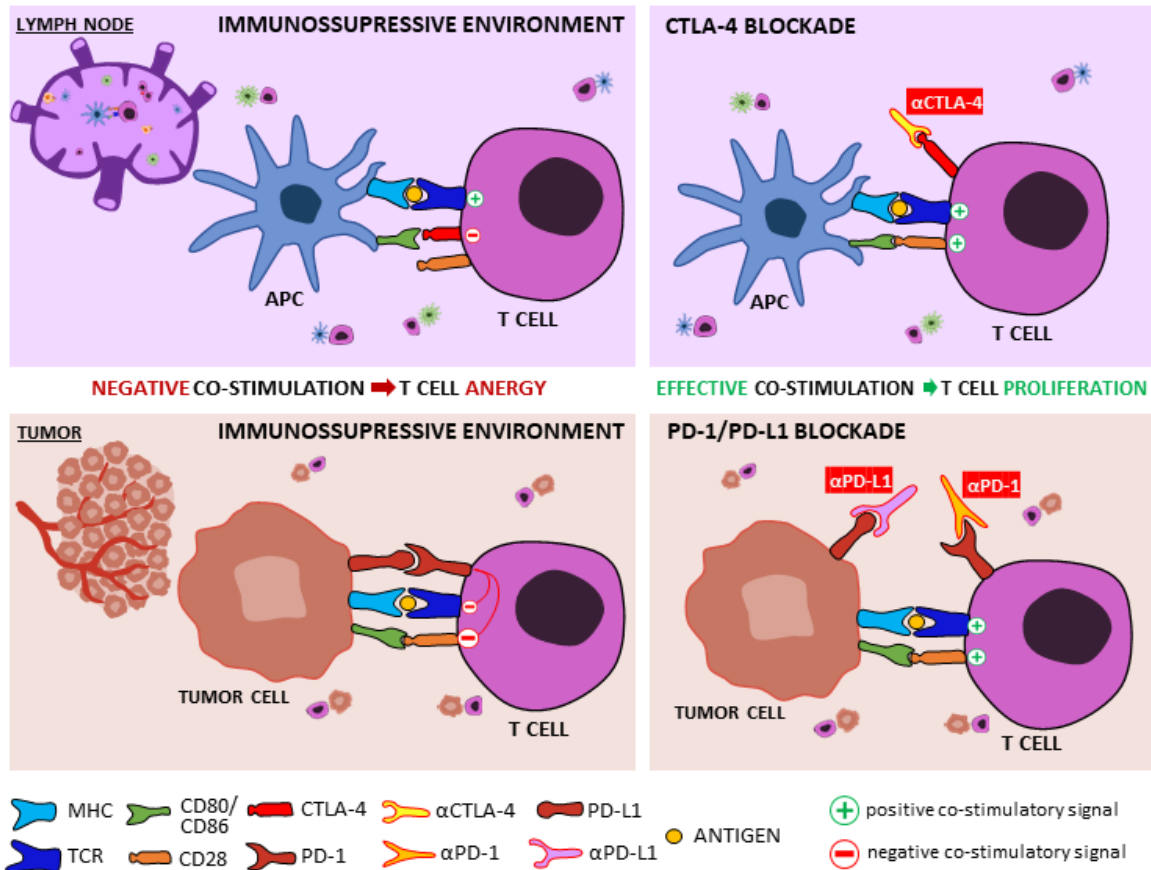


Figure 5. **Immune checkpoint mechanisms and respective blockade therapy.** T cell activity can be impaired by immune checkpoint protein to maintain the immune homeostasis of the organism. However, these mechanisms are exploited by tumor cells to evade antitumor immune responses. Binding of CTLA-4 to CD80/CD86 prevents the costimulation of CD28, crucial for effective T cell activation. In a similar manner, binding of PD-L1 to PD-1 generates a negative stimulation, causing T cell anergy. Blockade of these proteins with specific monoclonal antibodies represents a therapeutic strategy to increase the effector function of the immune system.

Several drugs that target these immune checkpoints are currently in clinical trials, and a small number have been already approved by FDA, such as: nivolumab, pembrolizumab and cemiplimab for PD-1; atezolizumab, avelumab and durvalumab for PD-L1; and ipilimumab for CTLA-4²²⁶. However, clinical evidence indicates that these strategies seem to be effective only in a small percentage of patients, typically leading to 20-40 % response rates³¹. Immune checkpoint blockade efficacy is usually dependent on the overexpression of the specific receptor which is highly variable between tumors and

among patients. Considering these, numerous approaches have been explored to combine ICBs with other therapies.

Several studies reported the administration of monoclonal antibodies against immune checkpoint molecules combined with PDT with several photosensitizers^{75,90,227,228}. Administration of anti-PD-L1 Abs potentiated the antitumor effects of **verteporfin**-PDT in a 4T1 mice model, as 50 % of mice had no tumor growth for more than 70 days of observation⁷⁵. The addition of lenalidomide, an inhibitor of lymphatic vessels regeneration, completely abrogated the antitumor efficacy, revealing the importance of lymphatic drainage and regeneration after PDT to achieve an antitumor response.

Combination therapy of **bremachlorin**-PDT and CTLA-4 blocking antibodies during the treatment phase also significantly improved the efficacy and survival of a double-tumor-bearing mice protocol with two independent tumor models (MC38 and CT26), which was further proved to be dependent on the systemic presence of CD8⁺ T cells²²⁷. PD-L1 expression was verified to be induced after **WST11**-PDT, which prompt the authors to evaluate the impact of the combination with PD-1/PD-L1 pathway inhibition. Treatment of an orthotopic Renca murine model with **WST11**-PDT and PD-1/PD-L1 antagonistic antibodies enabled the regression of primary tumors and prevented lung metastasis, which was not verified with any of the treatments alone. Further studies showed an increase in the ratios of effector T cells to regulatory T cells in primary tumors and inhibition of metastasis was associated with an increased T cell infiltration in the location of metastasis²²⁸. More recently, the combination of the same photosensitizer, **WST11**, with CTLA-4 inhibitor was also evaluated with a murine bladder tumor model. Tumor growth was significantly suppressed by the combination therapy, which also prevented lung metastasis and tumor recurrence⁹⁰.

PDT with a phthalocyanine targeting integrin $\alpha v \beta 6$ of tumors (**DSAB-HK**-PDT) combined with PD-1 immune checkpoint inhibitor also revealed to be effective in the treatment of 4T1-fluc tumor model with metastasis. The authors described that the treatment triggered the maturation of DCs, production of cytokines, and further migration of CTLs to the tumor bed. Irradiation of the primary tumor, suppressed the growth of a secondary nonirradiated s.c. tumor as well as slowed the growth of lung metastasis¹⁵⁹.

Numerous other strategies have been evaluating the combination of more than one therapy by loading different drugs in nanoparticles or micelles. A nanoscale metalorganic framework composed by iron clusters and porphyrin ligands was developed to overcome

tumor hypoxia and increase PDT efficacy. Fe-**TBP** combined with anti-PD-L1 mAbs elicited an abscopal effects with over 90 % of tumor regression in a mouse model of colorectal cancer²²⁹. Duan et al. demonstrated that Zn-pyrophosphate nanoparticles loaded with the photosensitizer pyrolipid (**ZnP@pyro**) induce phototoxicity upon irradiation, causing indirect vasculature disruption and increased tumor immunogenicity. Furthermore, they studied the combination of **ZnP@pyro**-PDT with mAb for PD-L1 for the treatment of orthotopic 4T1 tumor model²³⁰. The results showed an acute inflammation followed by eradication of the primary tumor and prevention of lung metastasis as well as inhibition of the preexisting ones. The same conclusions were validated in a second tumor model, TUBO bilateral syngeneic mouse model. Taking in consideration the hypoxia tumor environment, Shao et al. designed up conversion nanoparticles with a hypoxia-activated prodrug, tirapazamine, in nanopores of this metal-organic framework. This strategy induced PDT and hypoxia-activated chemotherapy, and when combined with anti-PD-L1 promotes specific tumor infiltration of cytotoxic T cells, completely inhibiting the growth of untreated distant tumors²³¹. Another potential strategy presented by Li and coworkers is to mediate cancer immunotherapy through the knockdown (KD) of these checkpoint molecules in tumor cells using small interfering RNA (siRNA). The authors designed an acid-activable cationic micelle, loaded with the photosensitizer pheophorbide-A and the siRNA responsible for the specific silencing of PD-L1 cell-surface and cytosolic expression on tumor cells. Tumor growth was efficiently inhibited, and the PDT-induced systemic immune memory response also prevented distant metastasis²³². A similar strategy aiming to silent PD-L1 was also recently described by Dai et al. in combination with a photosensitizer targeting the mitochondria²³³.

Indolamine-2,3-dioxygenase (IDO) is another immune checkpoint working as a regulatory enzyme that is highly expressed in tumors. IDO can deplete tryptophan (Trp) through its oxidative catabolism. This catalytic process prevents the clonal expansion of T cells, causing T cell anergy and apoptosis²³⁴. Even though some small molecules have been successfully developed as IDO-inhibitors, inhibiting the catabolism of Trp, its impact on tumor growth is mild due to the lack of antigen presentation and lack antitumoral responses. Lu et al. loaded a nanoscale metal-organic framework, **TBC-HF**, with an IDO inhibitor and used this system to combine PDT with IDOi-based immunotherapy²³⁵. The

results showed the eradication of the treated primary tumor and rejection of the untreated distant tumors in two syngeneic colorectal cancer models.

2 OBJECTIVES AND OUTLINES

As referred in the previous chapter, immune responses elicited by PDT are extremely important for the outcome of the treatment. The mechanism behind this stimulation have been studied and described over the last years, however, there are still many mechanisms that are not fully understood. The uncover of these gaps opens new opportunities to future strategies that might solve many of the clinical problems that are being faced today.

Redaporfin is a promising molecule used for PDT treatment with a remarkable effect in primary tumor which depends on the immune system response. Regarding this we aim to contribute to better understand the mechanisms behind the efficacy that turns this localized therapy into a systemic therapeutic response. Study of this immune response was studied over this thesis and new strategies to improve treatment efficacy was tested.

This thesis is divided in four parts, from chapter 3 to chapter 6.

Chapter 3 refers to an extensive characterization of immune responses triggered by the previously optimized vascular protocol of redaporfin-PDT of a colon carcinoma animal model. This study enabled to characterize the main immune events that occur post-PDT, from the strong inflammation to the abolition of the primary tumor. Several immune cell populations and molecules were investigated and its influence on the efficacy of the treatment is discussed.

Based on the promising results with the colon carcinoma model, the motivation was to further apply and evaluate the efficacy of redaporfin-PDT to treat other tumor models. Regarding this, **Chapter 4** refers to the optimization process used to find the best PDT conditions to treat each model. This process involved the optimization of several parameters such as drug and light doses, drug-to-light interval, fluence rate, safety margins. Furthermore, the content of redaporfin inside tumors over time was also assessed

by photoacoustic tomography to elucidate about the distribution behavior of the photosensitizer in different tumors.

In **Chapter 5** it is proposed that currently approved immunotherapies could increase or enrich the antitumor immune responses triggered by redaporfin-PDT. Two combinatory approaches with immune checkpoint blockers immunotherapies were tested in three tumor models and the outcomes are reported in this chapter.

Finally, general conclusions are summarized in **Chapter 6**.

3

IMMUNE RESPONSES AFTER VASCULAR PDT WITH REDAPORFIN

The work presented in this chapter was published in:

[J. Clin. Med. 2020, 9\(1\), 104; https://doi.org/10.3390/jcm9010104](https://doi.org/10.3390/jcm9010104)

Immune Responses after Vascular Photodynamic Therapy with Redaporfin

Ana Catarina S. Lobo¹, Lígia C. Gomes-da-Silva¹, Paulo Rodrigues-Santos^{2,3,4,5,6}, António Cabrita⁷, Manuel Santos-Rosa^{2,4,5,6} and Luís G. Arnaut¹

¹ CQC, Chemistry Department, University of Coimbra, 3004-535 Coimbra, Portugal

² Immunology Institute, Faculty of Medicine, University of Coimbra, 3004-504 Coimbra, Portugal

³ Laboratory of Immunology and Oncology, Center for Neuroscience and Cell Biology (CNC), University of Coimbra, 3004-504 Coimbra, Portugal

⁴ Center of Investigation in Environment, Genetics and Oncobiology (CIMAGO), Faculty of Medicine, University of Coimbra, 3004-504 Coimbra, Portugal

⁵ Coimbra Institute for Clinical and Biomedical Research (iCBR), Faculty of Medicine, University of Coimbra, 3004-504 Coimbra, Portugal

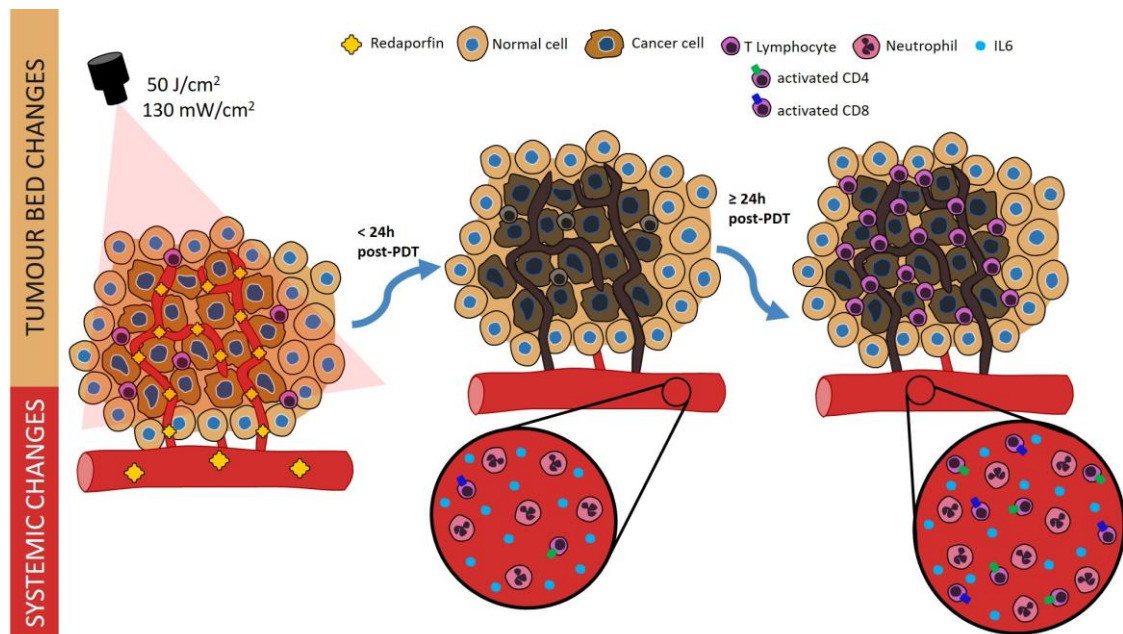
⁶ Center for Innovation in Biomedicine and Biotechnology (CIBB), University of Coimbra, 3004-504 Coimbra, Portugal

⁷ Anatomic Pathology Department, Faculty of Medicine, University of Coimbra, 3004-504 Coimbra, Portugal

3.1 Abstract

Photodynamic therapy (PDT) relies on the administration of a photosensitizer (PS) that is activated, after a certain drug-to-light interval (DLI), by the irradiation of the target tumor with light of a specific wavelength absorbed by the PS. Typically, low light doses are insufficient to eradicate solid tumors and high fluence rates have been described as poorly immunogenic. However, previous work with mice bearing CT26.WT tumors demonstrated that vascular PDT with redaporfin, using a low light dose delivered at a high fluence rate, not only destroys the primary tumor but also reduces the formation of metastasis, thus suggesting antitumor immunity. This work characterizes immune responses triggered by redaporfin-PDT in mice bearing CT26.WT tumors. Our results demonstrate that vascular-PDT leads to a strong neutrophilia (2-24 h), systemic increase of IL-6 (24 h), increased percentage of CD4⁺ and CD8⁺ T cells producing IFN- γ or CD69⁺ (2-24 h) and increased CD4⁺/CD8⁺ T cell ratio (2-4 h). At the tumor bed, T cell tumor infiltration disappeared after PDT but reappeared with a much higher incidence one day later. In addition, it is shown that the therapeutic effect of redaporfin-PDT is highly dependent on neutrophils and CD8⁺ T cells but not on CD4⁺ T cells.

3.1.1 Graphical Abstract



3.2 Introduction

Photodynamic therapy (PDT) combines a photosensitizer (PS) molecule, red or infrared light and molecular oxygen, none of them being individually toxic, to treat solid tumors with selectivity and reduced adverse effects. The PS is administered, after a drug-to-light interval (DLI) the target tissue is illuminated with light absorbed by the PS, and it reacts with molecular oxygen to generate reactive oxygen species (ROS). The oxidative stress locally generated by PDT is highly cytotoxic to cancer cells and to other stromal cells, such as the endothelial cells from angiogenic blood vessels^{38,112}. However, PDT preserves the collagen matrix and is associated with a good cosmetic and functional outcome.

The mechanism of PDT depends considerably on the nature of the PS and on the DLI between the PS administration and the illumination. A DLI ≥ 24 h allows for the distribution of the PS to various tissues at the time of irradiation, and the tumor cells are predominantly killed by the photocytotoxicity of the PS inside the cells (cellular-PDT). The irradiation of the target tissue at DLI < 30 min finds the PS in the vasculature (vascular-PDT) and leads to the occlusion of the tumor vasculature with the subsequent tumor hypoxia, starvation and death⁸⁸. At intermediate DLI, the PS may be also substantially retained within endothelial cells, and approaches that take advantage of this localization can be called endothelial-PDT²³⁶. We recently explored the combined impacts of the polarity of bacteriochlorin photosensitizers and of DLIs on the outcome of PDT²³⁶. More hydrophilic bacteriochlorins showed shorter plasma lifetimes and lower cellular uptake and are more appropriate for use at shorter DLIs. More lipophilic bacteriochlorins can have longer plasma lifetimes and higher accumulation in cells and are indicated for longer DLIs. Amphiphilic bacteriochlorins seemed to be adequate for both vascular- and cellular-PDT, and naturally also for endothelial-PDT.

PDT is not just a local treatment of solid tumors by photocytotoxicity and/or occlusion of the tumor vasculature. PDT also stimulates the host immune system, which contributes to the obliteration of any surviving cancer cells at the irradiated tumor^{37,40,42,66,89,237,238} and to the recognition and destruction of cancer cells at distant locations^{17,36,69}. PDT of basal cell carcinoma provided uncontroversial clinical evidence for the enhancement of systemic antitumor immunity³². The impact of PDT on the host immune system depends on the PDT regimen (eg, DLI, light fluence, light fluence rate) and may range from

Immune responses after vascular PDT with redaporfin

immune enhancing⁶⁶ to immunosuppressive²³⁹. Typically, low light doses and low fluence rates are described to be more prone to stimulate antitumor immunity^{43,66,240}.

Redaporfin (i.e., 5,10,15,20-tetrakis(2,6-difluoro-3-N-methylsulfamoylphenyl)-bacteriochlorin¹⁶) is an amphiphilic bacteriochlorin in clinical trials for head and neck cancer²⁴¹. Vascular-PDT with redaporfin (0.75 mg/kg, DLI=15 min, 50 J/cm² @ 130 mW/cm²) enabled 86 % cures of BALB/c mice with subcutaneously (s.c.) CT26.WT implanted tumors but no cures were achieved in immunocompromised nu/nu mice¹⁷. Although the redaporfin-PDT protocol applied low light doses (50 J/cm²) and high fluence rates (130 mW/cm²), 67 % of the cured mice were protected from developing a new tumor after rechallenge with the same cancer cells on the contra-lateral thigh. Additionally, a significant reduction of distant lung metastasis was noted¹⁷. Other insightful investigations on the stimulation of antitumor immunity with vascular-PDT include the studies by Hamblin and co-workers using verteporfin^{37,78,171} and by Scherz and co-workers using padeliporfin⁸⁹. These studies showed that a functional immune system is essential for successful vascular-PDT, and that vascular-PDT stimulates T-cell dependent antitumor immunity.

Recently, it was also demonstrated that redaporfin has tropism for the Endoplasmic Reticulum (ER) and the Golgi complex triggering signs of ER stress and the main hallmarks of immunogenic cell death namely: the translocation of calreticulin to the cell surface, active release of ATP, the exodus of HMGB1 and the phosphorylation of eIF2 α . In accordance, PDT-killed cancer cells injected subcutaneously into syngeneic mice were able to protect a fraction of the animals against a second re-challenge with live cancer cells of the same type^{242,243}. Currently, redaporfin is in phase I/II clinical trials for head and neck cancer and recently, it was described the case of a patient with advanced head and neck squamous cell cancer, non-responsive to surgery, radiotherapy or chemotherapy, that had strongly benefited from redaporfin-PDT. Three sessions of redaporfin-PDT were enough to destroy all the visible tumor which in further combination with an immune checkpoint blocker (Nivolumab, PD-1) allowed a complete response with the patient, two years later after the PDT, exhibiting no signs of the disease²⁴¹.

Photodynamic stimulation of the immune system may drive PDT to the frontline of cancer immunotherapy²⁵. The critical role of the immune system to the outcome of redaporfin-PDT motivated the design of this study, which aimed at investigating the mechanism of

Immune responses after vascular PDT with redaporfin

immune stimulation triggered by redaporfin-PDT, with a special emphasis on vascular-PDT. The CT26.WT implanted tumor model was selected for this investigation in view of the evidences of immune system stimulation mentioned above¹⁷.

Numerous studies in cancer immunotherapy (including within the PDT field) have described antitumor immune responses. Most of the studies focused mainly on the immune responses at the tumor microenvironment and spleen lymphocytes. However, it was recently demonstrated that effective tumor eradication requires a systemic immune response, which is critical for the therapeutic outcomes²⁴⁴. The detection of systemic immune responses may also offer better opportunities for clinical translation. Monitoring antitumor immunity after PDT in a clinical setting is facilitated by the accessibility of blood sampling. In view of the importance of systemic immune responses and possible availability of blood samples, our study aimed at detecting signs of immune modulation at the blood of mice submitted to a vascular protocol of redaporfin-PDT. The changes in populations of neutrophils, CD8⁺ T cells and CD4⁺ T cells observed in the peripheral blood further motivated an assessment of the depletion of such cells

3.3 Material and Methods

3.3.1 Cell line

CT26.WT cells (ATCC CRL-2638) were cultured in Dulbecco's Modified Eagle's medium (DMEM) (Sigma-Aldrich) supplemented with 10% (v/v) heat-inactivated fetal bovine serum, 100 U/ml penicillin, and 100 ng/ml streptomycin (Invitrogen).

3.3.2 Mouse tumor model and PDT

The Portuguese Animal Health Authority approved the animal experiments (DGAV authorization 0420/000/000/2011). Tumors were established by s.c. injection of 350,000 CT26.WT cells in the right flank of BALB/c (Charles River Laboratories) mice ca. 10 weeks old (20 g). The optimization of vascular-PDT (0.75 mg/kg, DLI=15 min, 50 J/cm² @ 130 mW/cm², 13 mm diameter illumination circle) with redaporfin was described elsewhere¹⁷. The illumination employed an Omicron laser at 748 nm. At different time points after tumor irradiation, mice were anesthetized, and the blood was collected by abdominal artery puncture into heparin-containing tubes.

3.3.3 Lymphocyte analysis by flow cytometry

Leukocytes (20 µL of blood) were stained with the following antibodies: APC anti-CD45, BV 605 anti-GR1 and BV 785 anti-CD11b, Alexa Fluor 647 anti-CD3ε, PE/Cy7 anti-CD4, Alexa Fluor 488 anti-CD8a, PE/Cy5.5 anti-CD19, APC/Cy7 anti-CD11c, Pacific blue anti-CD49b, PerCP/Cy5.5 anti-CD69 and APC/Cy7 anti-CD25. Erythrocytes were depleted with BD FACS Lysing solution (BD Biosciences) and cells were washed 3x with phosphate buffer saline (PBS). All antibodies were purchased from BioLegend. For each sample, 20,000 lymphocytes were acquired using a FACS Canto II flow cytometer (BD Biosciences) or a Novocyte 3000 flow cytometer (ACEA).

3.3.4 Quantification of blood cytokines

Plasma was isolated (2000 rpm; 10 min) from the blood collected at different time points after tumor irradiation. Quantification of IL-2, IL-4, IL-6, IFN-γ, TNF, IL-17A and IL-10 was performed using the BD Cytometric Bead Array (CBA) mouse Th1/Th2/Th17 cytokine kit (BD Bioscience) following the manufacturer's instructions.

3.3.5 Analysis of blood lymphocytes expressing TNF- α , IFN- γ , IL-4 or IL-17A by flow cytometry

PBMC were stained at their surface as previously mentioned followed by intracellular staining with specific antibodies against TNF- α , IFN- γ , IL-4 or IL-17A cytokines. The IL-17A and IL-4 antibodies were conjugated to PE, whereas TNF- α and IFN- γ antibodies were conjugated to PerCP/Cy5.5. FIX & PERM® kit (Invitrogen) was used for cell fixation and permeabilization. For each sample, 20,000 lymphocytes were acquired and further analyzed as described above.

3.3.6 *In vivo* depletion of neutrophils and CD4⁺ or CD8⁺ T lymphocytes

Neutrophils depletion was attained with i.p. administrations of anti-mouse Ly6G/Ly6C monoclonal antibodies (clone NIMP-R14, BioXCell) that were performed one day before PDT (200 μ g/animal) and repeated immediately after and 5 days after irradiation (100 μ g/animal). A control group with administrations of IgG isotype (clone LTF-2, BioXCell) was also included. Blood samples were collected by tail vein puncture 24 h after the first administration and neutropenia was confirmed by flow cytometry. Neutralization of CD4⁺ and CD8⁺ populations were achieved with regular i.p. administration of 500 μ g/animal of anti-mouse CD4 (GK1.5, BioXCell) and CD8 (53-6.7, BioXCell) monoclonal antibodies, respectively. Each antibody was administered 24 h before the PDT protocol and its administration was repeated each 5 days until the end of the assay. Depletion of the target cells was confirmed by flow cytometry in blood samples 24 h after the administration of each antibody. PDT treatments were performed as abovementioned. Tumors were measured twice a week with a caliper and the volume was calculated using the formula $V = \frac{a \cdot b^2}{2}$, where a corresponds to the major diameter and b to the minor diameter.

3.3.7 Histology and Immunohistochemistry (IHC)

Tumors were fixed in formalin (10 %) and then embedded in paraffin. Sections of 4 μ m were stained with hematoxylin and eosin (H&E) for histological analysis. The Image J software was used in the blind evaluation of the necrotic areas present in the tumor sections. The evaluation is expressed as the percentage of the necrotic area in the field of view of each section. For IHC, paraffin slices of tumors were deparanized and hydrated.

Immune responses after vascular PDT with redaporfin

Antigen retrieval was done in 0.1 M citrate buffer (Dako). Endogenous peroxidase was blocked with 10 min incubation with 3 % H₂O₂. Samples were then blocked with 10 % goat (for anti-CD3) or rabbit (for anti-Pax5) serum and incubated, overnight at 4 °C, with a CD3 or Pax5 antibody (Dako). After washing, for CD3 staining, sections were incubated with anti-rabbit EnVision⁺ System-HRP Labelled Polymer (Dako) whereas for Pax5 staining, sections were incubated with a biotinylated secondary antibody, washed and incubated again with HRP containing avidin-biotin complex (VECTASTAIN ABC kit, Vector Laboratories). All sections were revealed with 3,3'-diaminobenzidine and counterstained with Harris' Haematoxylin. Two blinded observers recorded both the total number of cells and the number of CD3⁺ cells in two sections of each tumor separated by at least 600 µm.

3.3.8 Statistical analysis

The results are presented as the mean ± standard deviation (SD). One-way ANOVA with Dunnett's post-test was used to determine statistically significant differences of the means between the control group and the treated groups. Survival analysis was performed by means of a Kaplan-Meier estimator. Statistical differences were presented at probability levels of $p < 0.05$ *, $p < 0.01$ ** and $p < 0.001$ ***.

3.4 Results and Discussion

3.4.1 Redaporfin-PDT induces accentuated neutrophilia and increased levels of the pro-inflammatory cytokine IL-6

Redaporfin-vascular-PDT is currently in phase I/II clinical trials for head and neck cancer which prompted the use of BALB/c mice bearing CT26.WT tumors as the preclinical model. Mice were treated with redaporfin-vascular-PDT (0.75 mg/kg, DLI = 15 min, 50 J/cm², 130 mW/cm², 13 mm diameter illumination circle) as previously described¹⁷. At the indicated time points after tumor irradiation, blood samples were collected, and different immune cell populations and cytokines were quantified. Our results demonstrated that redaporfin-PDT induced a sustained and significant rise in the frequency of granulocytes on the peripheral blood, which peaked 24 h post-PDT (64 ± 6 %) and recovered to pre-treatment values 72 h after the treatments (15 ± 5 %) (Figure 6A). Further evaluations using specific antibodies (GR1⁺ and CD11b⁺) allowed identifying that the major change in the number of granulocytes were due to a 4.2-fold increase in the percentage of neutrophils within the CD45⁺ (common lymphocyte marker) population (Figure 6B). The importance of neutrophilia for vascular-PDT with redaporfin was further assessed by depleting this population through the i.p. administration of monoclonal antibodies against Ly6G/Ly6C one day before PDT and twice post-PDT (immediately after irradiation and 5 days later). Flow cytometry analysis of blood samples confirmed an effective depletion of Gr1⁺ neutrophils (Figure 12), which was correlated with a significant decrease (37.5 %) of the mice survival upon PDT treatments (Figure 6C,D). These results are in agreement with other studies using different photosensitizers^{45,68,105}.

Redaporfin-vascular-PDT inflicts damage to the primary tumor, which is rapidly followed by a strong inflammation within the first hours that is known to be important for the activation of antitumor immunity⁸⁸. This inflammation is expected to alter the normal leukocyte production at the bone marrow by favoring granulopoiesis over lymphopoiesis²⁴⁵ which indeed supports the pronounced neutrophilia observed 2 to 24 h post-PDT. In accordance with the oedema observed in vivo upon PDT, a strong increase of the pro-inflammatory IL-6 cytokine was founded. Its levels were 11-fold higher at 24 h after vascular-PDT than those found in untreated mice (Figure 7). Although increased IL-6 levels are often reported 4-6 h after PDT^{96,238}, the high fluence rate used in this study

Immune responses after vascular PDT with redaporfin

(130 mW/cm²) is typically associated with low IL-6 expression⁴³. The changes in IL-6 levels obtained with redaporfin-vascular-PDT, together with those observed for 2-[1-hexyloxyethyl]-2-devinyl pyropheophorbide-a (HPPH)-PDT using DLI=24 h and 112 mW/cm²⁴³, reveal that IL-6 production occurs more prominently for short DLI, which may contribute to overcome the “non-inflammatory” effect of high fluence rates. Importantly, elevated serum IL-6 is also observed in patients treated with PDT^{108,246,247} and has been correlated with a better prognostic in patients (with primary bile duct cancer) submitted to treatment with hematoporphyrin-PDT²⁴⁷.

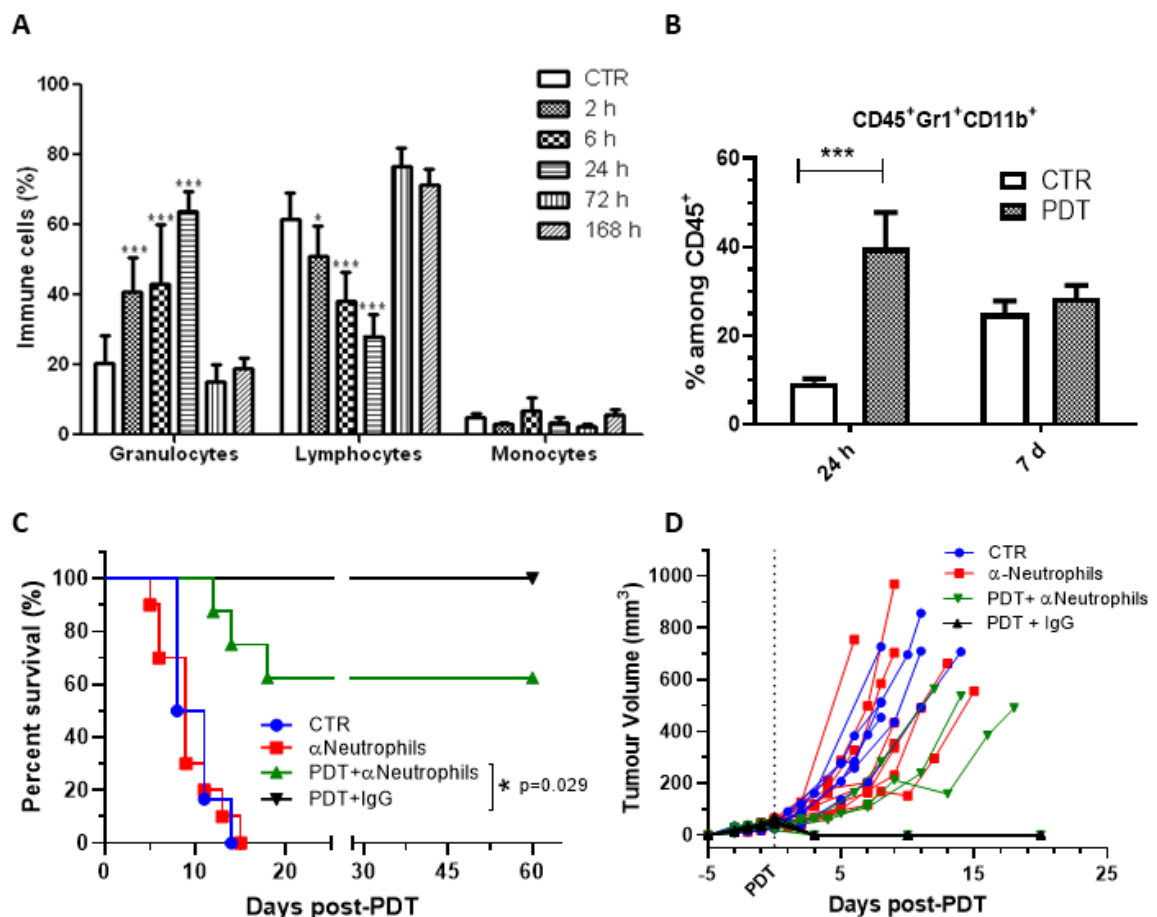


Figure 6. **Redaporfin-PDT induces a strong neutrophilia, which contributes significantly for the treatment efficacy.** A) Relative percentage of blood leukocyte evaluated by flow cytometry at different time points after redaporfin-PDT. B) Relative percentage of neutrophils (CD45⁺, GR1⁺ and CD11b⁺) evaluated by flow cytometry 24 h and 7 days after redaporfin-PDT. Bars are the mean \pm SD of 6 mice. No symbol $p > 0.05$; * $p < 0.05$; ** $p < 0.01$; *** $p < 0.001$. C) Survival curve of mice bearing CT26.WT tumors treated with redaporfin-PDT in normal conditions or upon neutrophils depletion using Ly6G/Ly6C monoclonal antibodies. D) Tumor growth represented individually for each mouse (6-11 mice per group). Survival curve statistics by LogRank (Mantel-Cox) test. No symbol $p > 0.05$; * $p < 0.05$.

Immune responses after vascular PDT with redaporfin

The anti-inflammatory IL-10 cytokine changed in a similar manner, but its increase was rather modest (Figure 7). IL-10 prevents DC maturation and activation cytotoxic T cells²⁴⁸, but as will be shown below, the small and short-lived IL-10 increase was insufficient to prevent the production of IFN- γ by DC or by CD4⁺ and CD8⁺ T cells. In fact, increased IL-10 levels may reflect a compensatory anti-inflammatory response to limit dangerous over-reactive immune responses, thus reducing collateral tissue damage²⁴⁹.

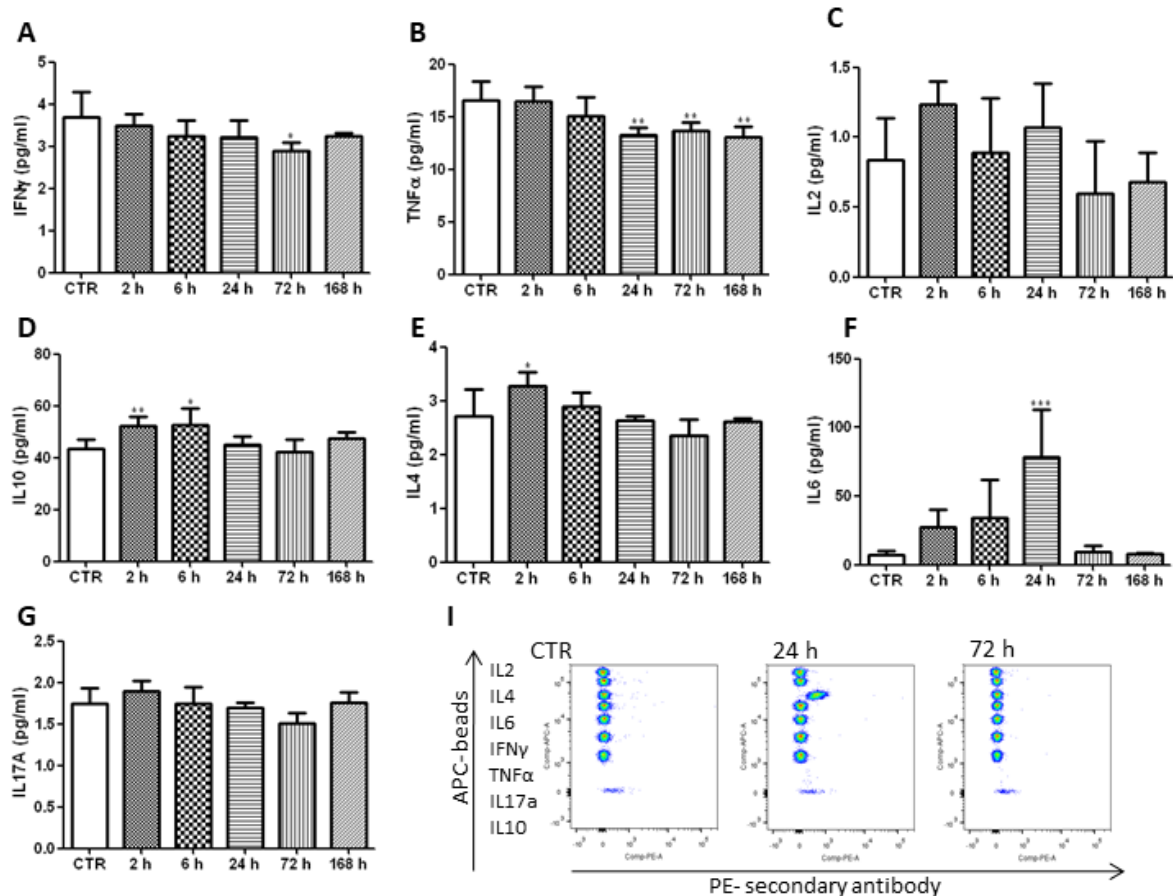


Figure 7. **Redaporfin-PDT increases the blood levels of the pro-inflammatory cytokine IL-6.** The quantification of different cytokines (A - IFN- γ , B - TNF- α , C - IL-2, D - IL-10, E - IL-4, F - IL-6, G - IL-17A) was performed in the blood at different time points after vascular-PDT. I) Representative dot plots that depict the different cytokines in untreated and treated mice. Bars are the mean \pm SD of 5 mice. No symbol $p > 0.05$; * $p < 0.05$; ** $p < 0.01$; *** $p < 0.001$.

3.4.2 Redaporfin-PDT activates the adaptive immune system and depends on CD8⁺ T cells for tumor eradication

The successful transition from innate (non-specific) to adaptive (antigen-specific) immunity determines the therapeutic outcome of different PDT regimens. This prompted

Immune responses after vascular PDT with redaporfin

us to evaluate the peripheral CD4⁺ and CD8⁺ T cells, which are highly specialized cells of the adaptive immune system.

CD4⁺ T cells (also known as helper T cells) recognize the tumor-associated antigens on the surface of antigen-presenting cells (eg dendritic cells, DC) and release cytokines that have a role on the regulation of the adaptive immunity. CD8⁺ T cells (also known as cytotoxic T cells) recognize specific antigens (eg tumor-associated antigen) in cells, which turn on their ability to induce death of those cells (eg cancer cell)²⁵. The vascular protocol herein described presented higher CD4⁺/CD8⁺ T cells ratio within the first hours after tumor irradiation (Figure 8A,B). Importantly, higher CD4⁺/CD8⁺ T cells ratios have been correlated with increased survival rate in cancer patients²⁵⁰. The Very Early Activation Antigen, CD69, which regulates the early events of T cell activation, was upregulated both on CD4⁺ and CD8⁺ T cells. It peaked 6 h after vascular-PDT with 12-fold and 4-fold increases of CD8⁺CD69⁺ and CD4⁺CD69⁺ T cells, respectively (Figure 8C,D). This means that the ratio of the activated CD4⁺CD69⁺ and CD8⁺CD69⁺ T cells is significantly reduced 6 h post-PDT.

Then, the production of different cytokines (IFN- γ , IL-4, TNF- α , and IL-17A) by peripheral immune cells was evaluated at different time points after tumor irradiation. Adaptive immunity can be classified in Th1 and Th2 responses. IFN- γ is the most important marker of Th1 cells, which are important for the elimination of cancer cells and virus- or bacteria-infected cells. IL-4 is secreted by Th2 cells and is typically associated with the differentiation of B cells and antibody production.

Our results demonstrated that the population of CD4⁺ and CD8⁺ T cells secreting IFN- γ increased significantly in the first 24 h after vascular-PDT as well as the ratio between IFN- γ -secreting CD4⁺ T cells and IL-4-producing CD4⁺ T cells (Figure 9A-C). These findings strongly suggest the involvement of the Th1 arm of the adaptive immune system and the activation of CD8⁺ cytotoxic T cells after redaporfin-vascular-PDT. The Th1 cytokine IFN- γ can stimulate phagocytic activity of macrophages and DCs, and to coordinate the transition from innate immunity to adaptive immunity²⁵¹. A significant increase in the percentage of IFN- γ -expressing DC and NK cells was also observed 6 h after vascular-PDT (Figure 9B), which is consistent with the ability of DC, NK and NKT cells of the innate immune system to produce IFN- γ ²⁵². T helper 17 (Th17) cells are a subset of T cells with the ability to produce the pro-inflammatory IL-17 cytokine, which has an important role in the migration of neutrophils into the inflammation site and in the

Immune responses after vascular PDT with redaporfin

stimulation of the granulopoiesis at the bone marrow²⁵³, as well as in the recruitment of IFN- γ -producing CD8⁺ T cells by the tumor²⁵⁴. In fact, our results suggest that IL-17A-producing T cells slightly increased after PDT. This effect was more pronounced in the activated CD69⁺ subset of T cells (Figure 9E,F). Altogether, Th1 CD4⁺ T cells, CD8⁺ cytotoxic T cells, NK, and DC cells, along with their characteristic production of IFN- γ , are important antitumor effectors of our vascular-PDT protocol with redaporfin.

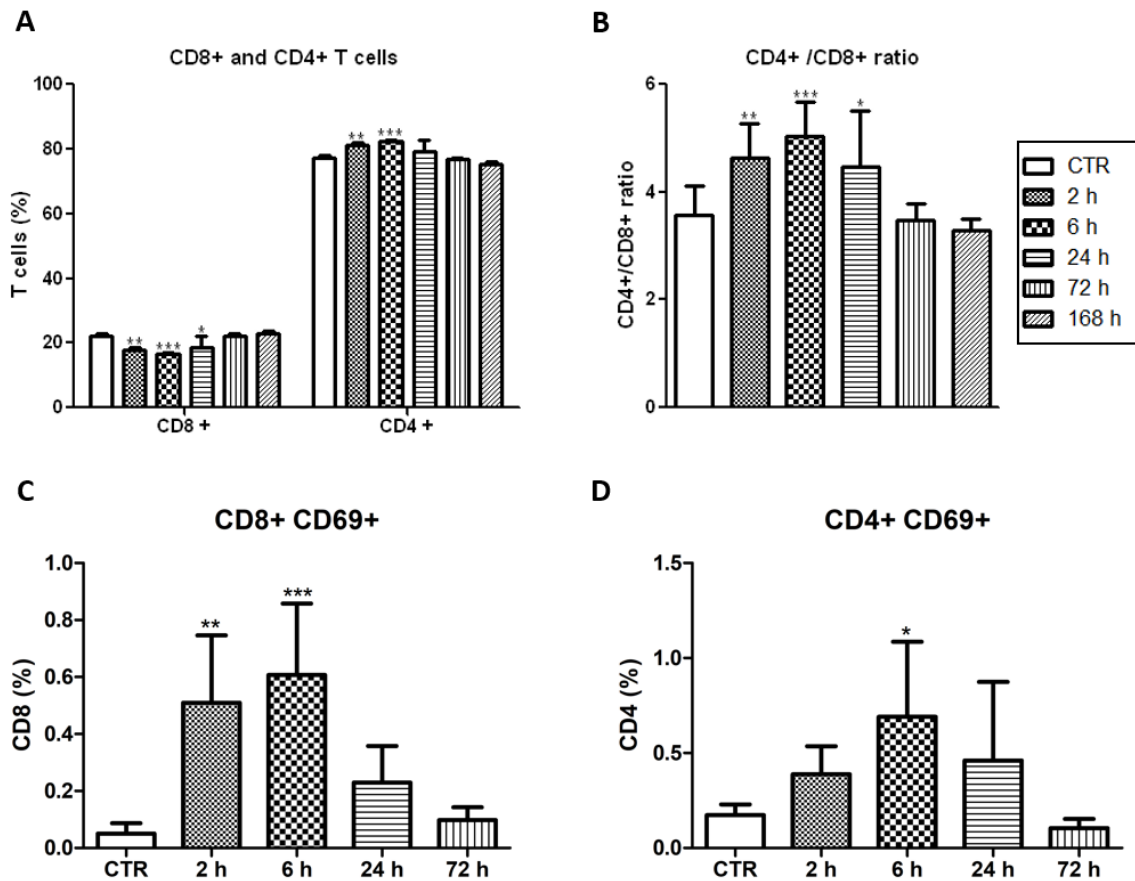


Figure 8. **Activated T cells after vascular-PDT with redaporfin.** **A)** Percentage of CD4⁺ and CD8⁺T cells and **B)** ratio of CD4⁺/CD8⁺ T cells in the blood of mice at different time points after vascular-PDT. **C)** Percentage of CD8⁺ or **D)** CD4⁺ T cells expressing CD69 in the blood of mice at different time points after PDT. Bars are the mean \pm SD of 5 mice. No symbol $p > 0.05$; * $p < 0.05$; ** $p < 0.01$; *** $p < 0.001$.

Immune responses after vascular PDT with redaporfin

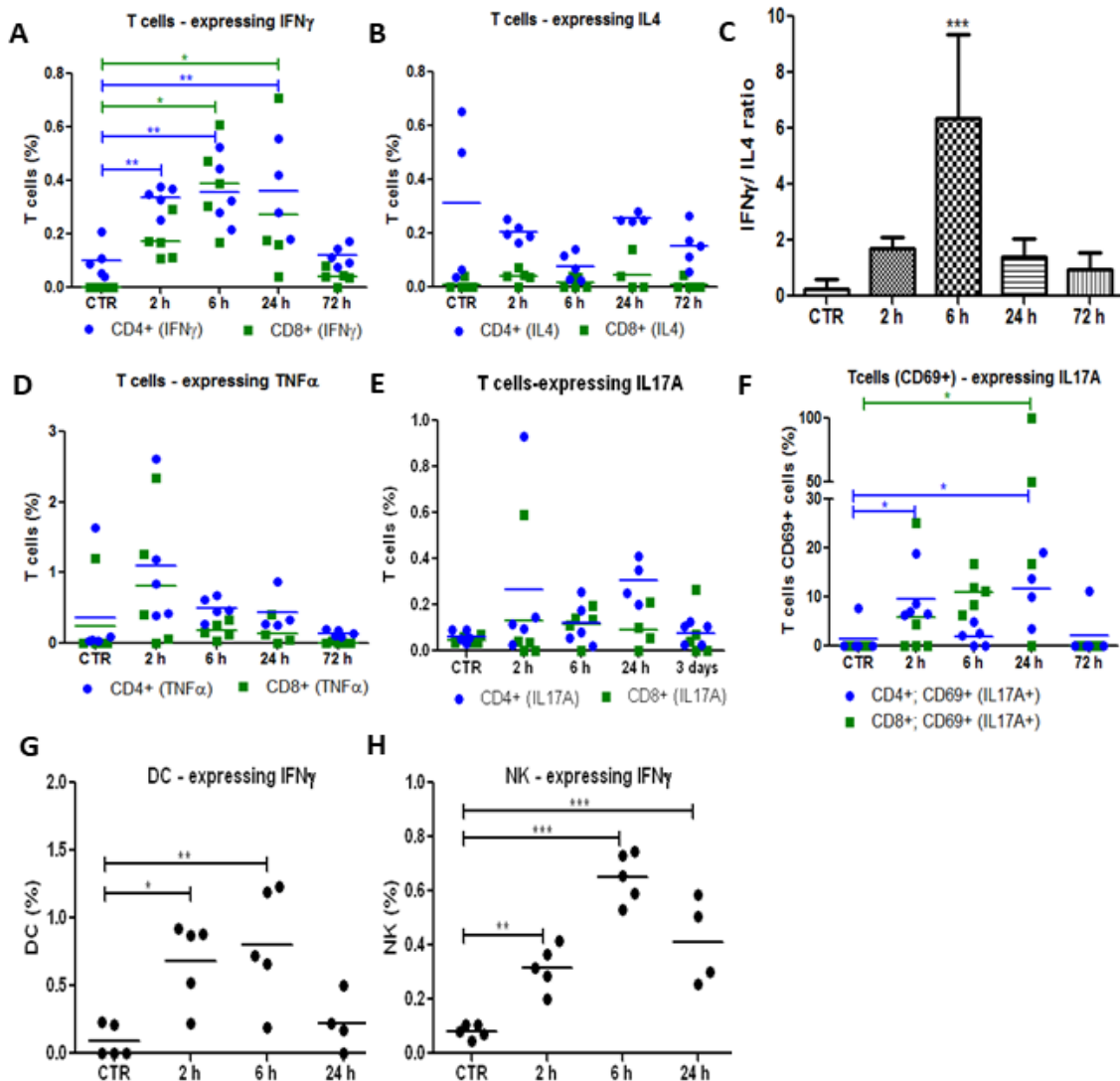


Figure 9. **Redaporfin-PDT stimulates the production of IFN- γ and IL-17A by different immune cells.** Production by T cells CD4 $^{+}$ (●) or CD8 $^{+}$ (■) of **A)** IFN- γ , **B)** IL-4, **D)** TNF- α and **E), F)** IL-17A at different time points after redaporfin-PDT. **C)** IFN- γ /IL-4 ratio, which was obtained by dividing IFN- γ -secreting CD4 $^{+}$ T cells by the IL-4-producing CD4 $^{+}$ T cells. **G)** IFN- γ production by DC and **H)** by NK. Bars are the mean \pm SD of 5 mice. No symbol $p > 0.05$; * $p < 0.05$; ** $p < 0.01$; *** $p < 0.001$.

The importance of CD4 $^{+}$ and CD8 $^{+}$ populations for treatment efficacy was then evaluated by depleting these cell populations through the i.p. administration of specific antibodies against CD4 or CD8. Each antibody was administered 24 h before the PDT protocol and its administration was repeated each 5 days until the end of the assay. Flow cytometry analysis of blood samples confirmed an effective depletion of the target cells (Figure 13). A significant impact was observed when CD8 $^{+}$ population was depleted ($p = 0.046$), with a reduction in the cure rate by half. In contrast, the depletion of CD4 $^{+}$ population had a minimal impact on the tumor growth kinetics that was not statistically significant (Figure

10). These findings suggest that cytotoxic T cells have a major role in the development of the antitumor immune response elicited by redaporfin-PDT, while helper T cells may have just a supportive role. It is interesting to recall that there is a higher increase of activated CD8⁺CD69⁺ T cells in the blood after PDT than of CD4⁺CD69⁺ T cells.

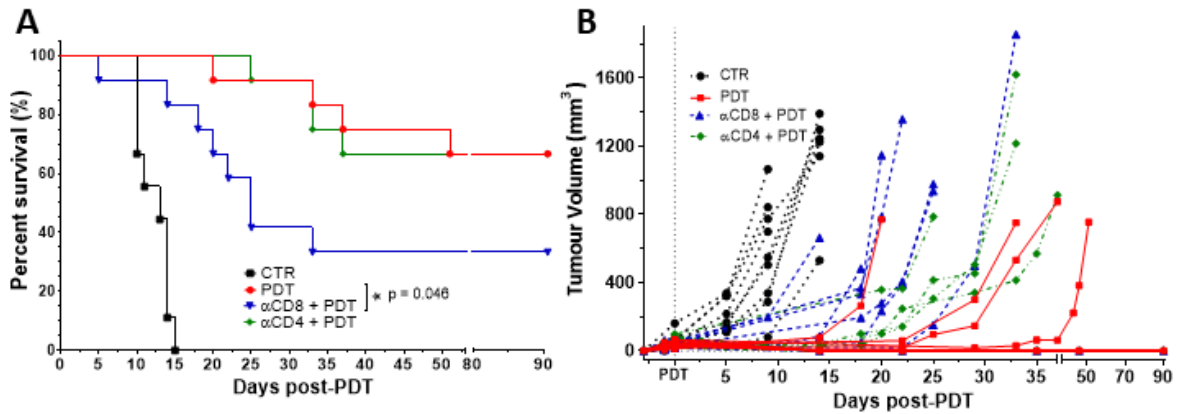


Figure 10. **Tumor eradication by redaporfin-PDT is dependent on CD8⁺ T cells but not on CD4⁺ T cells.** **A)** Survival curve of mice bearing CT26.WT tumors treated with redaporfin-PDT in normal conditions or upon depletion of CD4⁺ or CD8⁺ T cells. **B)** Tumor growth represented individually for each mouse (9-12 mice per group). Survival curve statistics by LogRank (Mantel-Cox) test. No symbol p > 0.05; * p<0.05.

3.4.3 Redaporfin-PDT changes T cells population in the tumor bed but not B cells

Immunohistochemistry of tumors subject to vascular-PDT showed strong hemorrhage and necrosis within 24 h after vascular-PDT, which is consistent with a treatment regime that targets the tumor vasculature (Figure 11A). This observation is in agreement with our previous work that demonstrated the formation of a necrotic eschar that covers the illuminated area 3-4 days after vascular-PDT⁸⁸. Tumor necrosis is evident 24 h post-PDT. T cells infiltration almost disappeared 6 h post-vascular-PDT however, it re-appeared 24 h post-vascular-PDT and reached a higher level than in untreated tumors (Figure 11B)¹⁷. CD3⁺ cells were found mostly in the tumor rim, although some CD3⁺ cells were also found inside the tumor. In contrast, B cell tumor infiltration was not observed (Figure 11C). Cellular-PDT with redaporfin induced less hemorrhage than the one attained with the vascular protocol and no significant changes in T cells or B cells infiltration were observed (data not shown).

The therapeutic dose found in phase I/II clinical trials for head and neck cancer with redaporfin-vascular-PDT (0.75 mg/kg, DLI = 15 min, 50 J/cm² @ 130 mW/cm²) [20] is

Immune responses after vascular PDT with redaporfin

the same as the optimal dose found in preclinical studies with BALB/c mice bearing CT26.WT tumors (0.75 mg/kg, DLI = 15 min, 50 J/cm², 130 mW/cm², 13 mm diameter illumination circle), that cured 86 % of the animals and led to the majority of cured animals rejecting re-challenge with the same tumor model¹⁷. This motivated further use of this animal-model to study immune responses after redaporfin-PDT. Although the use of more than one cell line is desirable to draw general conclusions on antitumor immunity, the appropriate guidance for clinical translation of redaporfin-PDT previously given by immunogenic CT26.WT tumors under the same laser fluence and dosing regimens, may also apply to immune responses in the same clinical setting. Antitumor immunity after redaporfin-PDT was shown using other cell lines, such as TC1 lung cancer cells²⁴².

The successful transition from innate to adaptive immunity depends on the PDT regimen and determines its efficacy. Redaporfin-vascular-PDT inflicts damage to the primary tumor, which is rapidly followed by an acute inflammation. This inflammation alters the normal leukocyte production at the bone marrow by favoring granulopoiesis over lymphopoiesis²⁴⁵, a response that supports the pronounced neutrophilia observed 2 to 24 h post-PDT. This neutrophilia significantly contributes for the efficacy of redaporfin-vascular-PDT as the cure rate decreased from 100 to 62.5 % when the neutrophils were systemically depleted. These results are in agreement with other studies that show neutrophilia after PDT, namely with photofrin and (tetra(m-tetrahydroxyphenyl)chlorin (mTHPC)^{45,68,105}. Selective depletion of neutrophils was previously demonstrated to significantly reduce the cure rate of photofrin-based PDT (DLI = 24 h)⁴⁵. This is explained by the importance of neutrophils for the stimulation of antitumor CD8⁺ T-cell responses, as demonstrated in one study using the photosensitizer 2-[1-hexyloxyethyl]-2-devinyl pyropheophorbide-a¹²⁶.

Consistent with the oedema/inflammation observed in vivo upon PDT, a strong increase of the pro-inflammatory IL-6 cytokine was found in the blood of mice treated by redaporfin-PDT. This result was unanticipated as typically PDT treatments at high fluence rates (as the ones used with our redaporfin-PDT regime, 130 mW/cm²) are associated with low IL-6 levels and with minimal antitumor effects. IL-6 is often found upregulated in cancer²⁵⁵ and has been associated with the tumorigenic process²⁵⁶. However, IL-6 may also have an important antitumor role, for instance, by coordinating the transition from neutrophil to lymphocytes infiltration at the tumor bed, thus leading to the resolution of inflammation and the initiation of T cell-mediated antitumor

Immune responses after vascular PDT with redaporfin

immunity^{255,257}. Indeed, studies with porfimer sodium or with HPPH-PDT demonstrated that IL-6 inhibition significantly impairs the therapeutic outcome of the PDT treatment^{105,238}. Also, increased levels of serum IL-6 have been observed in patients with oesophageal squamous cell carcinoma 7 days after PDT with porfimer sodium (DLI=48 h)^{34,40}, in patients with bile duct cancer submitted to hematoporphyrin-PDT²⁴⁷ and in patients with head and neck squamous cell carcinoma 12 h after PDT with Foscan (DLI=96 h)²⁴⁶, emphasizing the clinical relevance of IL-6 levels.

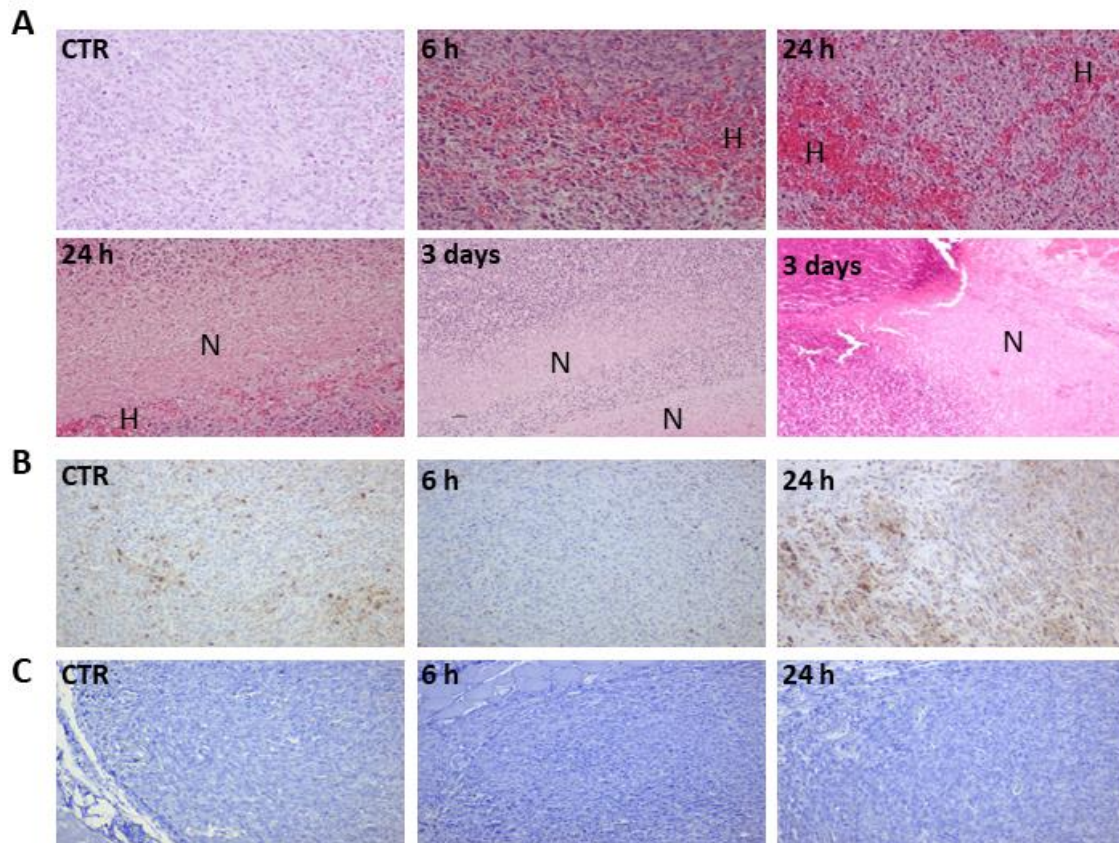


Figure 11. **Redaporfin-PDT induces strong hemorrhage and necrosis that is accompanied by T cells infiltration but not by B cells infiltration** (10x magnification). **A)** Tumors from control and treated mice (at the indicated time points) were stained with H&E, H indicates hemorrhagic areas and N indicates necrotic areas. **B)** T cells (CD3⁺) (brown) infiltration. **C)** Absence of B cells (Pax5) infiltration.

We also found at the peripheral blood that redaporfin-vascular-PDT elicits an immune response mediated by CD4⁺ and CD8⁺ T cells producing IFN- γ . The Th1 cytokine IFN- γ has the ability to stimulate phagocytic activity of macrophages and DCs, and to coordinate the transition from innate immunity to adaptive immunity²⁵¹. Other studies, both with cellular-PDT^{126,171,237} and vascular-PDT^{37,89,91,171} have reported T cell differentiation and enhanced IFN- γ levels after PDT. Redaporfin-PDT efficacy was dependent on T cells

Immune responses after vascular PDT with redaporfin

CD8⁺ but not on CD4⁺. Similar observations have been reported for PDT with photofrin^{40,69}, which was shown to depend on NK cells, and not on CD4⁺ cells, for the activation of T cells CD8⁺ cells. It is tempting to speculate that the same occurs for redaporfin-PDT, yet it remains to be investigated in further detail. Interestingly, Ossendorp and co-workers found that depletion of CD4⁺ T cells in a PDT protocol with DLI = 6 h (“endothelial-PDT”) led to an improved treatment outcome^{195,227}, whereas in our vascular-PDT the depletion of CD4⁺ T cells did not have an impact in the treatment.

Our results, combined with what is known on the enhancement of antitumor immunity by PDT, support the following hypothesis. Neutrophilia (Figure 6) and the strong increase of the pro-inflammatory IL-6 cytokine (Figure 7), which are related to innate immunity, are a non-specific response that occurs within the first hours after tissue damage (acute and sterile inflammation) or pathogen infection. It is well known that neutrophils are the first innate immune responders to PDT and are followed by the recruitment of tumor infiltrating DCs. These act as mediators between the innate immune system and the adaptive immune system. Their main role is to process antigens from the tumor cells and present them on their cell surfaces to lymphocytes initiating adaptive immunity. This process seems to be accelerated in the context of redaporfin-PDT by the induction of immunogenic cell death. Redaporfin-PDT causes the rapid release of cell death-associated molecules that trigger innate immune activation and bridge toward adaptive immunity. In fact, redaporfin-PDT promotes ATP secretion, translocates calreticulin from the endoplasmic reticulum to the cell surface and releases HMGB1 more rapidly than traditional chemotherapy^{242,243}. The release/exposure of DAMPs (calreticulin, HMGB1, ATP, IFN) by cancer cells dying after PDT stimulates the presentation of tumor antigens by dendritic cells and polarizes T cell response towards the production of IFN- γ , which are essential for antitumor immune responses²⁵⁸⁻²⁶⁰. DCs migrate to lymph nodes where they prime tumor-specific cytotoxic CD8⁺ T cells (adaptive immunity). Activated CD8⁺CD69⁺ T cells (Figure 8) can establish immunological memory and may kill cancer cells outside the illumination field. Depletion of CD8⁺ T cells has a dramatic effect on the efficacy of redaporfin-PDT (Figure 10).

3.5 Conclusion

This work demonstrates that redaporfin-vascular PDT induces extensive tissue damage at the primary (irradiated) tumor, which triggers an acute local inflammation characterized by IL-6 expression and neutrophilia that attained a maximum 24 h post-PDT. T cells expressing CD69 attained their maximum at 6 h post-PDT and IFN- γ^+ cells were significantly over-expressed up to 24 h post-PDT, which altogether demonstrates a rapid stimulation of the immune system. B cells were not detected 2 h post-PDT, which may influence the CD4⁺ T cell proliferation²⁶¹. At the same time, the CD3⁺ T cells are depleted at the tumor bed but later, at 24 h post-PDT, a notorious new infiltration of CD3⁺ T cells is attained. The therapeutic effect of redaporfin-PDT is dependent on neutrophils and CD8⁺ T cells but not on CD4⁺ T cells. Redaporfin-PDT can stimulate CD8⁺ T cells even in the absence of CD4⁺ T cells, similarly to photofrin-PDT⁶⁹. The dilemma between tumor-controlling (optimally curative but minimally inflammatory and ineffective to inhibit secondary disease) and immune-enhancing (inflammatory but unable to control primary tumor growth) PDT regimens^{43,66} may be solved with redaporfin-vascular-PDT at high fluence rates ($51 \pm 2 \text{ J/cm}^2$ at 130 mW/cm^2). The effect of currently available immunotherapies seems to be limited by the absence of T cell-based inflammation²⁶². Arguably, major benefits might be achieved with immunostimulating approaches that induce appropriate tissue-based inflammation. Redaporfin-vascular-PDT in a pro-inflammatory regimen achieved a successful transition from innate to adaptive antitumor immunity and transformed the immunosuppressive tumor microenvironment into a more favorable homing for antitumor immunity. This therapy may offer new opportunities to improve systemic cancer treatments.

3.6 Supplementary Material

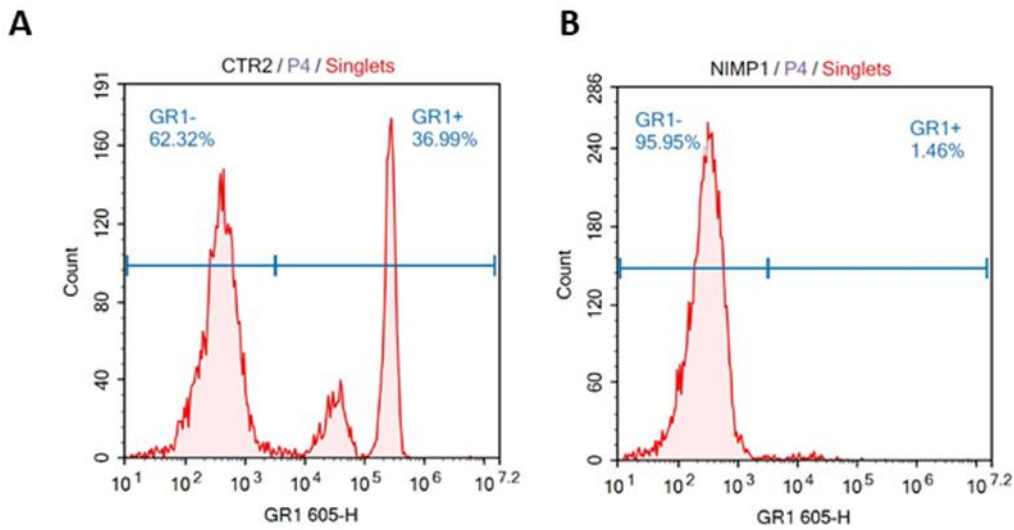


Figure 12. ***In vivo* neutrophil depletion was confirmed by flow cytometry.** Neutrophils depletion was attained with i.p. administrations of anti-mouse Ly6G/Ly6C monoclonal antibodies (NIMP-R14, BioXCell). Blood samples were collected by tail vein puncture 24 h after the first administration and neutropenia was confirmed by flow cytometry. **A, B)** Representative histograms that show the neutrophils level (Gr1⁺ cells) of a control and a neutrophil depleted animal, respectively.

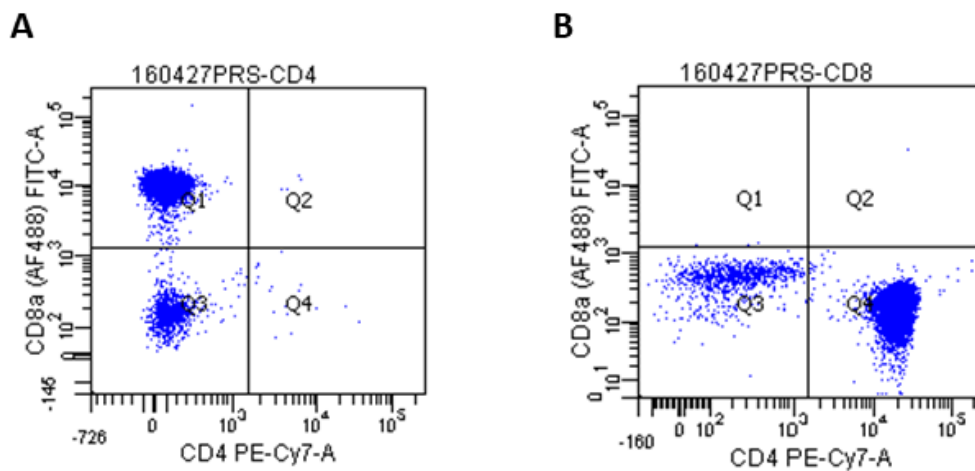


Figure 13. ***In vivo* CD4⁺ and CD8⁺ T cell neutralization was confirmed by flow cytometry.** Neutralization of CD4⁺, CD8⁺ were achieved with regular i.p. administration of anti-mouse CD4 (GK1.5, BioXCell) and CD8 (53-6.7, BioXCell) monoclonal antibodies, respectively. Specific depletion was confirmed by flow cytometry of blood samples collected 24 h after the first administration. **A, B)** Representative dot plots that show the effective depletion of CD4⁺ T and CD8⁺ T cells populations, respectively.

4 OPTIMIZATION OF REDAPORFIN-PDT OF IMMUNOSSUPPRESSIVE TUMOR MODELS

4.1 Abstract

Photodynamic therapy is described as a promising strategy for the treatment of cancer. The immune responses triggered after PDT, which are essential for the success of the treatment, have been considered sufficiently robust to control distant cancer lesions, such as metastasis. Melanoma and mammary carcinoma tumor models are recognized to be more aggressive and difficult to treat than most mouse tumor models, namely colon carcinoma. The response to redaporfin-PDT treatment was evaluated in mouse mammary carcinoma expressing luciferase (4T1-luc2) and in mouse skin melanoma (B16F10) tumor models, and PDT parameters were optimized to maximize the impact on tumors while minimizing treatment lethality. A significant edema that later progresses to necrosis was observed in both tumor models. However, cures were only achieved with the B16F10 tumor model. Imaging with photoacoustic tomography suggested that the lower content of redaporfin in 4T1 tumors is the main reason for the challenging behavior of orthotopic 4T1 model.

4.2 Introduction

Photodynamic therapy (PDT) with photosensitizers such as porfimer sodium, temoporfin and padeliporfin was approved for the treatment of various solid tumors in Europe and elsewhere. Redaporfin is a recently developed photosensitizer for PDT that is currently in phase 2 clinical trials (NCT02070432)²⁴¹. Redaporfin is a photostable bacteriochlorin with intense infrared absorption, high yield of ROS generation, high phototoxicity, low skin photosensitivity and favorable pharmacokinetics^{16,18}. A vascular protocol of redaporfin-PDT allows a high cure rate in CT26.WT subcutaneous tumors implanted in BALB/c mice. Antitumor immune memory and resistance to metastasis were observed in this animal model¹⁷. We have shown that the success of a vascular protocol using redaporfin-PDT depends on the presence of specific cell populations of the immune system, namely cytotoxic lymphocytes¹²⁷. We hypothesize that the combination of redaporfin-PDT with an immune therapy may potentiate the efficacy of both therapies, namely by increasing the response rates of immunotherapies and strengthening the systemic effect of PDT, especially in tumors more difficult to treat.

This chapter reports the optimization of redaporfin-PDT treatment of aggressive tumor models that represent a challenge to PDT and to immunotherapies. Our selection of tumor models focused mainly on tumor immunogenicity, i.e., the ability of the tumor to induce adaptive immune responses, which is mostly mediated by T lymphocytes. Redaporfin-PDT can elicit immunogenic cell death (ICD) and may be able to enhance the immunogenicity of tumor cells. ICD *in vivo* alters the tumor microenvironment leading to an increase in Th1 and Th17 cytokines. This is expected to exacerbate the response of interventions aimed at reactivating tumor-infiltrating leukocytes, such as the administration of anti-cytotoxic T-lymphocyte antigen (CTLA)-4 and anti-PD1 antibodies³⁰. Comprehensive immune profiling of eight murine solid tumors showed that CT26 colon tumor models were the more immunogenic and B16 melanoma models were the least immunogenic of the studied tumor models²⁶³. Redaporfin-PDT of CT26 tumors implanted in the flank of BALB/c mice was optimized using a Kolliphor formulation later translated to the redaporfin clinical trial^{17,241}. Redaporfin-PDT of B16F10 tumors with different intravenous formulations was recently published⁸⁵. Here we revisit this tumor model with the kolliphor formulation in clinical trials. Additionally, this chapter reports redaporfin-PDT of 4T1 mouse mammary carcinoma, to include a moderately immunogenic but rapidly metastasizing tumor.

Optimization of redaporfin-PDT of immunosuppressive tumor models

Melanoma is the most dangerous skin cancer, with a poor prognosis in advance stages. PDT has been evaluated for the treatment of melanoma and revealed promising results. Melanoma presents several challenges to PDT: the absorption of light by the highly-pigmented melanin, the antioxidant effect of melanin the sequestration of PSs inside melanosomes, among many other difficulties²⁶⁴. Melanoma tumors are usually resistant to traditional treatments, such as chemotherapy and radiotherapy.

Metastases are the most often cause of morbidity and mortality of late-stage cancers and new strategies that influence these distant lesions are needful. The 4T1 mammary carcinoma cell line is one of the few breast cancer models that metastasizes via the hematogenous route to the same organs of human breast cancer, including lungs, liver, and bone²⁶⁵. Another advantage presented by 4T1 cell line is the possibility to be implemented in immunocompetent mice which allows to evaluate the tumor-host interactions, namely immune interactions.

Photodynamic therapy efficacy is highly dependent on several parameters that need to be optimized to generate the desired outcome. The right balance between drug dose (DD), light dose (LD), drug-to-light interval (DLI), irradiance and margins of illumination is essential to destroy the target lesion without severe damage in nearby healthy tissues. Additionally, the type and extent of stimulation of the immune system may depend on the protocol applied^{127,236}. Gollnick and coworkers described that different protocols parameters could trigger either an enhanced immune activation and/or the complete control of the primary tumor⁶⁶. Redaporfin-PDT parameters were optimized to create an higher impact in the tumor, which could be further combined with the immunotherapy strategies to potentiate the antitumor immune response. Photoacoustic tomography was used to evaluate redaporfin uptake profile by different tumors.

4.3 Material and Methods

4.3.1 Chemicals

5,10,15,20 - Tetrakis (2,6-difluoro -3-N-methylsulfamoylphenyl) bacteriochlorin (redaporfin) was provided by Luzitin SA (Coimbra, Portugal). Redaporfin for intravenous administration was formulated in NaCl 0.9%: EtOH: Kolliphor (98.8:1:0.2) and the concentration was confirmed by absorption spectra. The appropriate volume of PS was calculated according to the drug dose and the animal weight. Kolliphor EL®, NaCl, absolute ethanol (EtOH), and Matrigel were purchased from Sigma-Aldrich Corp. (St. Louis, MO, USA).

4.3.2 Cell lines

CT26.WT (mouse colon carcinoma) cells (CRL-2638™, ATCC-LCG Standards), 4T1-luc2 cells (Perkin-Elmer) and B16F10 (gently given by IPO, Porto, Portugal) were cultured in Dulbecco's Modified Eagle's medium (DMEM) (Sigma-Aldrich) supplemented with 10 % (v/v) heat-inactivated fetal bovine serum (Gibco), 100 U/ml penicillin and 100 ng/ml streptomycin (Sigma-Aldrich).

4.3.3 Animal tumor models and PDT protocol

The Portuguese Animal Health Authority approved the animal experiments (DGAV authorization 0420/000/000/2011). CT26 tumors were established by s.c. injection of 350,000 CT26.WT cells in the right flank of female BALB/c (Charles River Laboratories) mice ca. 10 weeks old (20 g). B16F10 tumors were established by s.c. injection of 500,000 B16F10 cells in Matrigel:PBS (1:1) in the right flank of female C57BL/6J (Charles River Laboratories) mice ca. 10 weeks old (20 g). 4T1-luc2 tumors were established by s.c. orthotopical injection of 20,000 cells in the right abdominal mammary fat pad of female BALB/c (Charles River Laboratories) mice ca. 10 weeks old (20 g).

The day of PDT treatment is defined when the diameter of the tumors reaches 5-6 mm. PDT parameters (drug dose, light dose, drug-to-light interval, and size of illumination spot) were optimized for each model and all tested protocols are described below. Redaporfin was formulated in Kolliphor EL®:EtOH:saline 0.9 % (98.8:1:0.2) and administered to mice by tail-vein injection. The illumination of tumors employed an Omicron laser at 748 nm. The kinetic of tumor growth was followed after PDT. For

Optimization of redaporfin-PDT of immunosuppressive tumor models

CT26.WT and 4T1-luc2 tumors, two radicular diameters were measured, and the volumes were calculated using the formula $V = \frac{a \cdot b^2}{2}$, where a corresponds to the major diameter and b to the minor diameter. For B16F10 tumors, three radicular diameters were measured, and the volumes were calculated using the formula $V = \frac{a \cdot b \cdot c}{2}$, where a corresponds to the major diameter, b to the minor diameter and c to the tumor height. The endpoint was defined as a tumor diameter higher than 12 mm, or 60 days of tumor-free survival post-PDT, to evaluate the impact of the treatment and the kinetics of tumor growth. Mice without palpable tumor 60 days after the treatment were considered cured.

4.3.4 Photoacoustic Tomography

Redaporfin accumulation on tumor was assessed at several timepoints with the Vevo LAZR-X multimodal imaging system from Fujifilm-VisualSonics (Toronto, Canada). For all imaging procedures, anesthesia was induced and maintained using isoflurane (1.5-2.5%). Each animal was placed in the right position (supine for 4T1 model and prone for CT26.WT model) and tumors region were covered with standard gel for ultrasound. After positioning the transducer in a perpendicular position relative to the center of the tumor, the scanning was initialized. The system was equipped with a 40 MHz central frequency transducer with 40 μ m axial resolution (MX550D). Molecular images were acquired in the PA-mode between 680 and 970 nm with 5 nm steps, and B-mode ultrasound was used to collect anatomical images. Spectra acquisition was acquired in a fixed position, one axial slice, varying the wavelength from 680 nm to 970 nm. 3D multiwavelength (MW) acquisition was performed by scanning the whole tumor at specific wavelengths (680, 740, 750, 765, 924 and 966 nm) and with a 3D step size of 0.5 mm. Both gain values of B and PA mode were set at the beginning of the experiment and maintained through the whole experiment. Unmixing of the MW data was performed with the VevoLab software and took in consideration the PA spectra of redaporfin, oxy- and deoxy-hemoglobin (Figure 16). The PA average value of redaporfin was calculated in the tumor volume and normalized with the blank acquisition performed prior the PS administration.

4.3.5 Statistical Analysis

The results are presented as the mean \pm standard error of the mean (SEM). Survival analysis was performed by means of a Kaplan-Meier estimator and log-rank (Mantel-Cox) test. Two-way ANOVA with Dunnett's post-test was used to determine statistically

Optimization of redaporfin-PDT of immunosuppressive tumor models

significant differences of the means between the groups. Statistical differences were presented at probability levels of $p < 0.05$ *, $p < 0.01$ **, $p < 0.001$ *** and $p < 0.0001$ ****.

4.4 Results and Discussion

4.4.1 PDT optimization of melanoma and mammary carcinoma animal models

Photodynamic therapy of melanomas is generally more challenging due to pigmentation, both present on the tumor cells and on skin of C57BL/6 animals. PDT has potential for a promising treatment of melanoma, but more research is still needed to develop an effective photosensitizer.

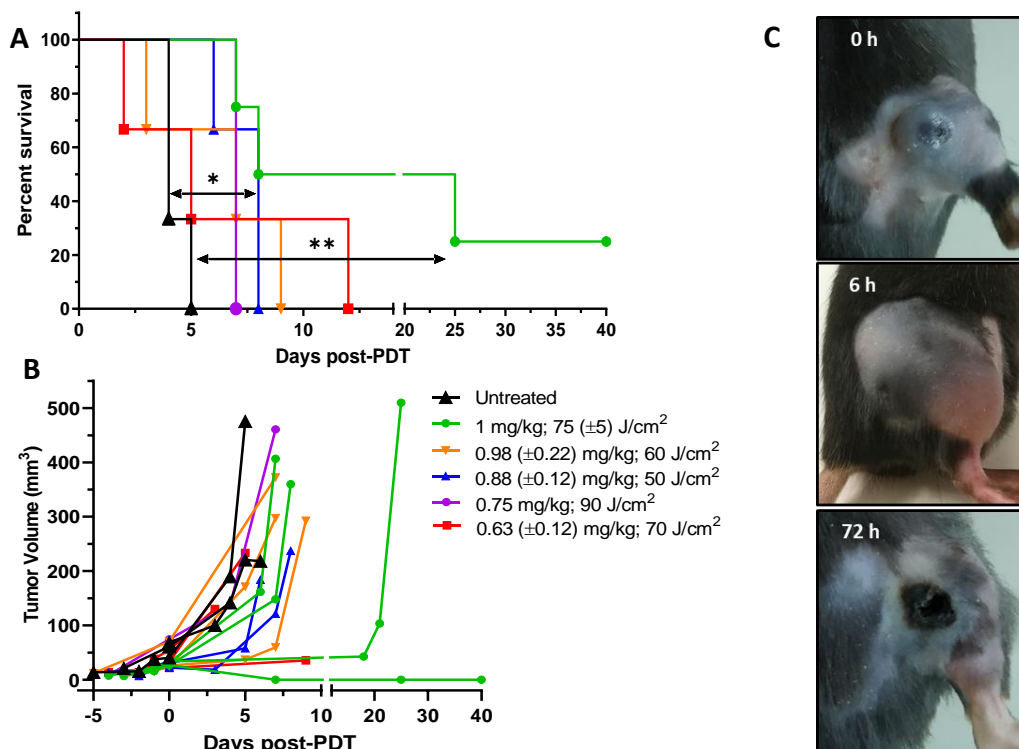


Figure 14. **Redaporfin-PDT treatment optimization of B16F10 animal model.** C57BL/6 mice bearing s.c. B16F10 tumors were treated with different drug and light doses in a vascular protocol of redaporfin-PDT (DLI=15 min). **(A)** Survival plot of the tested PDT protocols. *p* value of log-rank test of: Untreated vs 1mg/kg+75J/cm²: 0.0100; Untreated vs 0.88mg/kg+50J/cm²: 0.0224. **(B)** Individual tumor growth representation of mice. **(C)** Images of tumors before and after PDT illumination. 6h after illumination a strong edema is observed which then turns into necrosis at 24-72 h after illumination.

Redaporfin absorbs in the near-infrared (750 nm) region which represents a good advantage to avoid the melanin absorption spectrum and insufficient light penetration²⁶⁴. Vascular redaporfin-PDT of a melanoma tumor model in male mice was previously reported by Dabrowski and coworkers, where it was demonstrated that higher drug and light doses were needed to trigger an impact on tumors in comparison with CT26.WT

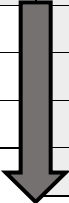
Optimization of redaporfin-PDT of immunosuppressive tumor models

tumors⁸⁵. However, due to the differences in sensitivity between male and female tumor models, direct correlation was not possible to apply.

Five different protocols were tested on the melanoma tumor model with conditions starting from the optimized protocol for CT26.WT tumor model. All the tested procedures were vascular protocols, i.e., with an interval of 15 minutes between administration of the photosensitizer and the illumination of the tumor. Different combinations of drug (0.63-1 mg/kg) and light doses (50-90 J/cm²) were tested to balance efficacy and safety and achieve the best outcome. The size of illumination spot was kept at 13 mm to maintain enough margins around the tumor but also to avoid damage in the surrounding tissues.

Table 6. **Macroscopic evaluation score criteria for PDT treatment impact on primary tumors.**

Edema increased blood vessel wall permeability due to inflammation and obstruction of fluid clearance in the lymphatic system		Necrosis black necrotic tissue formed when healthy tissue dies and becomes dehydrated, typically because of local ischemia	
no edema	0	no necrosis	0
light edema	1	mild erythema	1
strong edema	2	superficial necrosis	2
		deep necrosis	3



After PDT, animals were followed for up to 40 days to evaluate the impact on tumor growth. The assessment of therapeutic efficacy was performed by evaluating the survival plots and by comparing tumor growth kinetics, which are represented in Figure 14. However, the destruction of the primary tumor was not always completely achieved and due to necrosis and edema, measuring tumor boundaries not always seem to be the best evaluation method for this strategy. Regarding this, the impact of PDT on tumors was also macroscopically evaluated in terms of edema and necrosis following the criteria presented on Table 6.

In this study, the protocols designed for melanoma PDT evaluation consist of a DLI of 15 min, similarly to CT26.WT mice, which represents a vascular protocol with the major damages occurring in the vasculature of the tumor. Redaporfin-PDT was tested with gradual small increases of drug or light doses from the optimized protocol for CT26.WT tumors. According with the outcomes achieved in the first studies, alterations were made until a significant and safe impact on tumors was observed. In comparison with colon carcinoma, PDT elicited a stronger edema in B16F10 tumors as soon as 6 h after PDT,

Optimization of redaporfin-PDT of immunosuppressive tumor models

which is demonstrated in Figure 14. Although edema was triggered with low doses of drug/light, considerable signs of necrosis in the tumor were only verified with drug doses of 1 mg/kg and illumination with 75 J/cm².

In general, redaporfin-PDT treatments were well tolerated, animals did not show any severe adverse effects and had no signs of photosensitivity after PDT. Higher drug doses or light doses proved to be harmful for the animals. Furthermore, when light doses increased to 90 J/cm² and drug dose decreased to 0.75 mg/kg, edema and necrosis appeared to be lower, which led us to decide on the previous protocol as the most favorable protocol to treat B16F10 tumor.

Table 7. PDT parameters of the several tested protocols for B16F10 melanoma model. Drug and light doses were tested to obtain the best outcome in terms of impact on treatment. Macroscopic alterations on tumor, as edema and necrosis, were evaluated and scored according to Table 6.

Redaporfin dose (mg/Kg)	Light dose (J/cm ²)	DLI (min)	Spot diameter (cm)	n	Survivals to PDT	PDT Impact Score	
						Edema	Necrosis
0.88 (±0.12)	50	15	1.3	3	100 %	1.33	0.33
0.63 (±0.12)	70	15	1.3	3	100 %	1.67	1.00
0.98 (±0.22)	60	15	1.3	3	100 %	1.33	1.33
1.00	75 (±5)	15	1.3	4	100 %	1.50	2.25
0.75	90	15	1.3	1	100 %	1.00	2.00

Pucelik et al. described a protocol for the treatment of B16F10 on a male tumor model combining 1.5 mg/kg of redaporfin with a light dose of 74 J/cm², leading to remarkable results⁸⁵. The authors demonstrated that the efficacy was dependent on the formulation, possibly by tumor selectivity and ROS generation enhancement. A similar study, with a water-soluble bacteriochlorin, was reported by Dabrowski et al. with a different melanoma cell line, S91. The authors demonstrated that tumors illuminated with 108 J/cm² 24 h after i.p. administration of 10 mg/kg of PS resulted in significant tumor regression²⁶⁶. Schrez and coworkers reported that the best outcomes on a melanoma xenografts model were achieved with a vascular protocol with 9 mg/kg of the photosensitizer WST11 and a light exposure dose of 100 mW/cm²²⁶⁷. This protocol revealed an effective tumor flattening and a high cure rate.

Optimization of redaporfin-PDT of immunosuppressive tumor models

Regarding the mammary carcinoma model, 4T1 cell line models are recognized to be an extremely challenging model for all types of treatment modalities, due to the aggressiveness of the tumor, the immunosuppressive tumor microenvironment and the ability to metastasize to several organs, which in late stage of human breast cancer is the main cause of death the patients. These evidences make the 4T1 an extremely challenging tumor model but also very relevant for the clinics, being extensively studied by the scientific community.

Several strategies were tested and parameters such as drug dose, light dose, DLI, illumination spot size, and fluence were extensively studied to achieve the best protocol. Some of the presented results refers to optimization experiments previously reported elsewhere²⁶⁸. Initial experiments involved a vascular protocol with drug and light doses (protocols from V1 to V4 on Table 8), similar to the optimized parameters for the colon carcinoma model. However, while low doses appear to have no impact on the tumor, slight increases on drug dose (from 0.75 to 1 mg/kg) already created damages in the surrounding healthy organs (liver and kidney necrosis confirmed in mice necropsies), without triggering a considerable effect on the tumor. To minimize the adverse effects on the surrounding organs the illumination spot area was reduced. A complete survival to the treatments were enabled, however no significant impact of PDT on the tumor was observed.

As it has been previously discussed in the literature, the environment where tumor cells grow seem to be highly relevant for the way tumors respond to treatments. Considering this, we evaluated, in parallel to this optimization process, how PDT impact on 4T1 tumors differs when it is subcutaneously implanted in the leg of the animals (protocols V5 and V6 of Table 8) in comparison to when it is orthotopically inoculated in the mammary gland. From the outcomes of the treatments, it was possible to see that the same protocol which revealed almost no impact on orthotopic tumors triggered a strong edema on the subcutaneous model. This suggests that PDT of subcutaneous tumors triggers an higher immune response, however further characterizations of immune infiltrations of both models should be performed to confirm these conclusions. Even though the response on subcutaneous tumors appeared to be significantly better, this model does not correctly mimic the tumor environment of the human disease, which after all, is the main goal in using these strategies. For these reasons, the optimizations were continued on the orthotopic model.

Optimization of redaporfin-PDT of immunosuppressive tumor models

Drug-to-light intervals of 15 minutes means that the photosensitizer is in the circulatory system at the time of irradiation and there was no time to increase selectivity, redaporfin is in circulation in the tumor vasculature but also in the vital organs. From previous studies regarding the deep of necrosis achieved with 750 nm laser light, it was reported that illumination of livers 15 minutes after intravenous administration of redaporfin resulted in a necrosis depth higher than 4 mm for light doses above 25 J/cm^2 ²⁸. This data confirms that if the content of redaporfin in the first millimeters of tissue is not enough to absorb light and work as an inner filter, necrosis in deeper organs with higher content of redaporfin is most likely to occur.

As the balance between the required amount of drug to create an impact on the tumor but without damaging the vital organs seems too hard to attain in vascular protocols, the following strategy was to increase the time between PS administration and the illumination to allow the PS to accumulate on the tumor and be cleared from the circulatory system and vital organs. The tested protocols included DLI from 48 to 96 h, with different doses of redaporfin and light (protocols C1 to C7 of Table 8). This strategy allowed to increase light or drug dose, maintaining the survival of the animals to PDT but increasing the edema after the treatments. However, as no significant necrosis on the tumor was achieved, strategies with increased light and drug doses were tested, but animals did not survive to these PDT conditions. Furthermore, strategies combining different DLIs were also tested but with no significant advantages (protocols CV1- CV5 of Table 8).

Even though higher light penetration represents a huge advantage to treat deeper lesions, our results suggest that light that reaches deeper vital organs was enough to cause severe damages. The strategy to minimize these adverse effects was to change the direction of tumor illumination from a frontal to a transversal illumination, as demonstrated in Figure 15A. This way light was able to go through the tumor with a considerably minimization of phototoxicity on adjacent organs. The protocols implemented with this approach are described in Table 8 (TV1 to TC3). Better results in terms of edema and necrosis were achieved with illumination of the tumor, with 100 J/cm^2 , 72 h after the administration of 1.8 mg/kg of redaporfin.

Optimization of redaporfin-PDT of immunosuppressive tumor models

Table 8. Redaporfin-PDT parameters of the several tested protocols for 4T1-luc2 mammary carcinoma model. Drug and light doses, illumination spot diameter and fluence were tested to obtain the best outcome in terms of impact on treatment. Macroscopic alterations on tumor, as edema and necrosis, were evaluated and scored according to Table 6 criteria. o.t. - orthotopic; s.c. - subcutaneous; Prtel - Protocol: V - vascular protocol; C - cellular protocol; CV - cellular and vascular protocol; TV/TC - transversal irradiation of tumor with vascular/cellular protocol. * optimization protocols previously reported in ²⁶⁸.

Prtel	Model	Drug dose (mg/Kg)	DLI	Light dose (J/cm ²)	Spot diameter (cm)	Fluence (mW/cm ²)	n	Survival to PDT	Impact Score	
									Edema	Necrosis
V1*	o.t.	1.00	15 min	50	1.3	130	7	43 %	0	1
V2*	o.t.	0.75	15 min	50	1.3	130	2	100 %	0	1
V3*	o.t.	0.75	15 min	50	1.1	182	2	100 %	0	1
V4*	o.t.	1.00	15 min	50	1.1	182	1	100 %	0	1
V5	s.c.	1.00	15 min	50	1.3	130	1	100 %	2	0
V6	s.c.	1.00	15 min	100	1.3	130	1	100 %	2	1
C1*	o.t.	1.00	72 h	100	1.3	130	1	100 %	0	2
C2*	o.t.	2.00	72 h	50	1.0	220	6	100 %	2	1
C3*	o.t.	2.00	72 h	75	1.0	131	6	0 %	1	1
C4*	o.t.	2.00	72 h	65	1.0	131	6	0 %	1	1
C5	o.t.	1.00	72 h	100	1.3	130	5	100 %	1	1
C6	o.t.	1.00	72 h	120	1.0	150	6	83 %	0	1
C7	o.t.	1.00	48 h	120	1.0	150	1	0 %	0	1
C8	o.t.	1.00	96 h	120	1.0	150	1	100 %	0	1
CV1*	o.t.	1.00 0.5	72 h 15 min	80	1.3	130	1	0 %	-	-
CV2*	o.t.	1.00 0.5	72 h 15 min	60	1.3	130	1	100 %	1	1
CV3*	o.t.	1.00 0.5	24 h 15 min	50	1.0	220	4	0 %	-	-
CV4*	o.t.	1.00 1.00 0.4	144 h 72 h 15 min	50	1.0	220	3	100 %	1	1
CV5*	o.t.	2.00 0.4	72 h 15 min	50	1.0	220	3	0 %	-	-
TV1	o.t.	1.8	15 min	120	1.1	178	2	100 %	1	1
TC1	o.t.	1.0	48 h	120	1.1	178	4	100 %	1	1
TC2	o.t.	1.8	72 h	100	1.2	137	2	100 %	1	2
TC3	o.t.	1.8	72 h	150	1.2	137	3	100 %	1	2

4.4.2 Accumulation profile of redaporfin is dependent on the tumor models

To further understand the challenges to achieve any impact on mammary carcinoma tumors, the accumulation of redaporfin in 4T1 tumors was compared with CT26 tumors over time with photoacoustic tomography. Redaporfin was intravenously administered to mice with 4T1-luc2 and CT26.WT tumors and at several timepoints tumors were scanned by photoacoustic tomography and multiwavelength acquisitions were performed at seven specific wavelengths from 680 to 970 nm. The unmixing method from VevoLab software, described elsewhere²⁶⁹, allowed to evaluate redaporfin, oxy- and deoxy-hemoglobin content inside tumors and the results are presented in Figure 15B,C.

According to the photoacoustic average of 3D tumor volumes, redaporfin showed a maximum on PS accumulation at 15 minutes after injection, corresponding to the accumulation in tumor vasculature. Later, at 24 h after injection it is possible to identify a new peak which suggests an accumulation in tumor cells. All these findings go in agreement with the uptake profile previously reported for CT26.WT models with biodistribution studies¹⁸. Surprisingly, the photoacoustic signal obtained with 4T1 model revealed to be much lower, which may indicate that even though the same drug doses were administered, the content that reaches the inside of the tumor was much less over time. While in CT26.WT model redaporfin tumor content is higher in the first 24 h, for 4T1 model the accumulation of PS appears to be higher for longer timepoints, as for 48 h and 72 h. These results support the outcomes from the optimization protocols, which indicates that better impacts on the tumor are only achieved for longer timepoints/DLIs.

Optimization of redaporfin-PDT of immunosuppressive tumor models

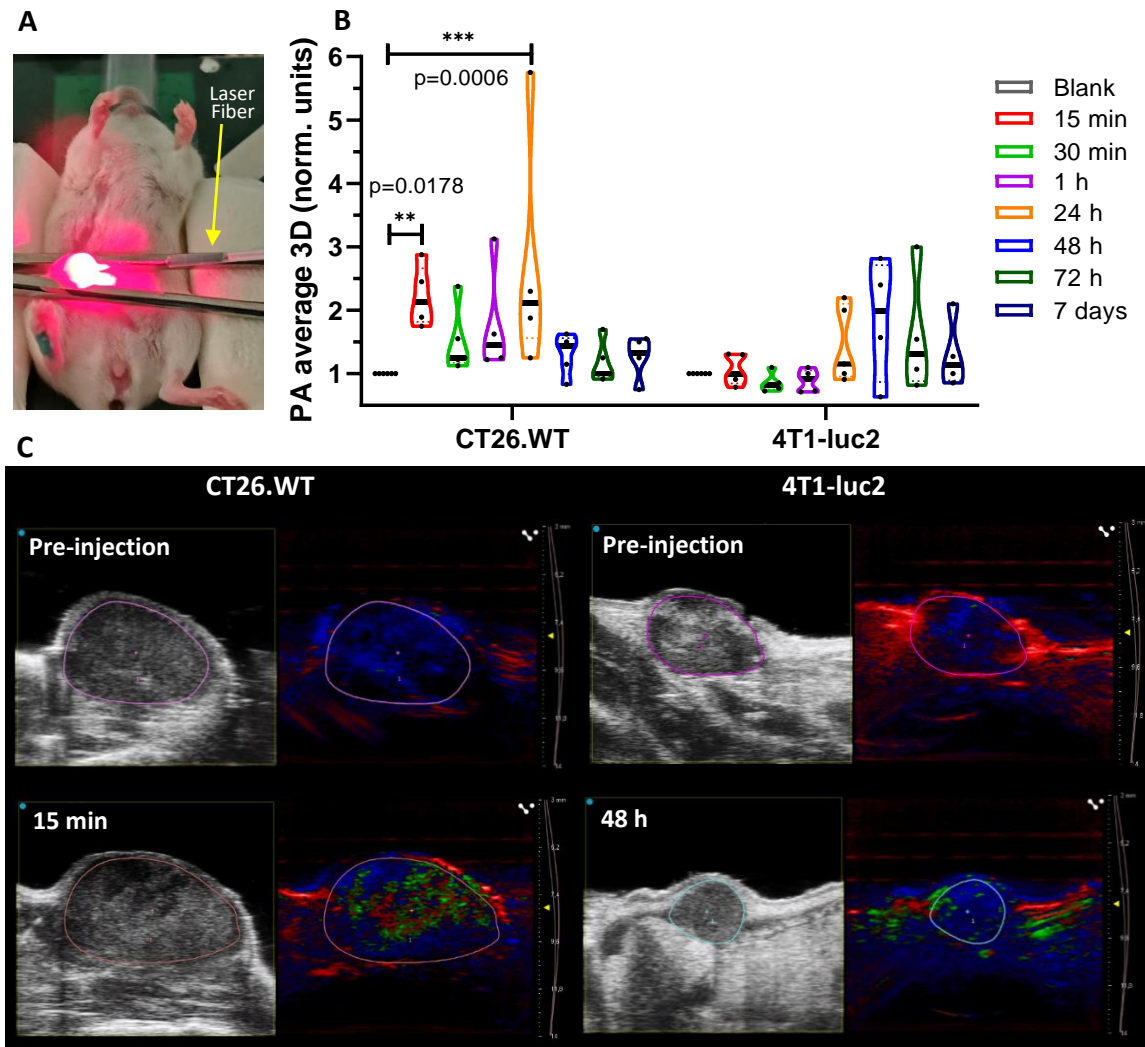


Figure 15. Redaporfin tumor accumulation followed by photoacoustic (PA) tomography. **A**) Transversal irradiation of 4T1-luc2 tumors. **B**) Violin plot representation of redaporfin tumor content. Accumulation of the photosensitizer was assessed after i.v. injection of the formulated redaporfin with a drug dose of 1.65 ± 0.15 mg/kg at several timepoints. Before PS injection, an initial acquisition was performed which is referred as the blank and the following acquisitions were normalized with the blank. Photoacoustic tomography was used to assess the content of redaporfin inside tumors using the unmixing feature of VevoLab and considering as components redaporfin, oxy- and deoxy-hemoglobin. **C**) B-mode and photoacoustic unmixed images of CT26.WT and 4T1-luc2 tumors prior redaporfin injection and at the highest PA average timepoints after i.v. injection. **Color legend:** red - oxyhemoglobin; blue - deoxyhemoglobin; green - redaporfin.

4.5 Conclusion

The present study reports the optimization process of redaporfin-PDT of two different immunosuppressive cancer models. For each model, the drug dose and light dose, drug-to-light interval, area of the illuminated region and fluence were tuned to achieve the best impact on the tumor whilst avoiding effects on healthy tissues. The results show that the same dose that leads to approximately 80 % cures in CT26.WT model revealed to be completely ineffective in the described models. A strong edema which then ended up in a significant necrosis was achieved on B16F10 tumor model with a redaporfin dose of 1 mg/kg and a light dose of 75 J/cm². This protocol increased the median survival time of mice and achieved a percentage of cures of almost 30 %. The mammary carcinoma model revealed to be much more challenging to treat and despite the extensive tries to obtain the suitable protocol, no cures were possible to attain. Nevertheless, a significant impact, with visible edema and necrosis, was attained with 1.8 mg/kg of redaporfin and 100 J/cm². Further studies allowed to elucidate that the ineffectiveness of redaporfin-PDT on 4T1 tumor is related to the low content of redaporfin that manages to accumulate in the tumor. It is suggested that the impact created on tumors by PDT may impact on tumors responsiveness to other therapies, such as immunotherapies. Combinations strategies will be further discussed in chapter 5.

4.6 Supplementary Material

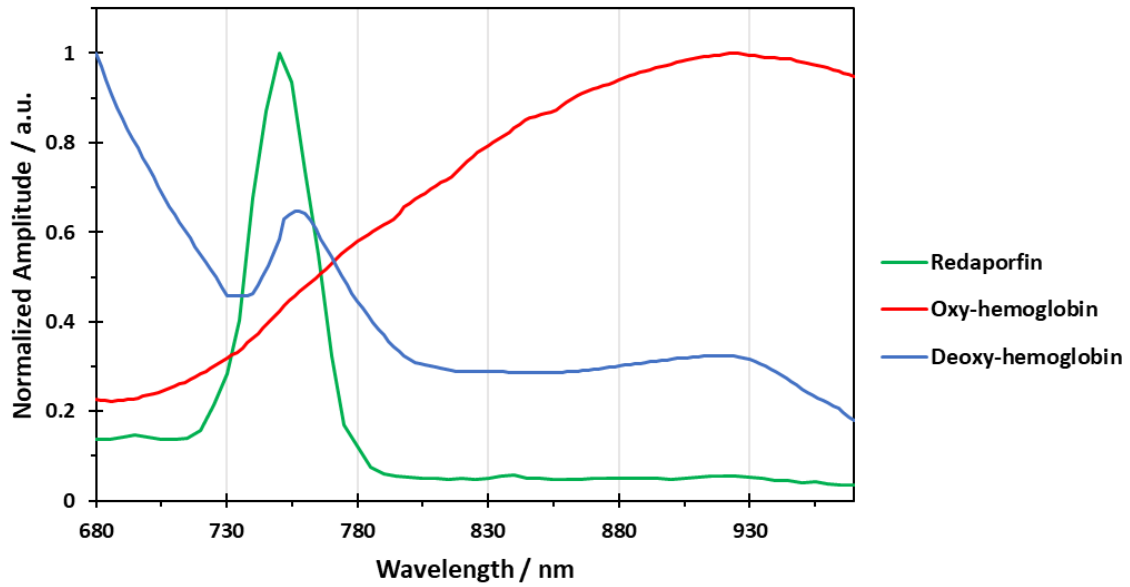


Figure 16. **Normalized photoacoustic spectra of redaporfin, oxy- and deoxy-hemoglobin.** Redaporfin was prepared in *in vivo* formulation and PA spectra was acquired in a phantom apparatus with the Vevo LAZR-X multimodal imaging system. Oxy- and deoxy-hemoglobin are already part of the Vevo LAZR-X analysis software.

5

COMBINATORIAL APPROACHES OF REDAPORFIN-PDT AND IMMUNOTHERAPY

5.1 Abstract

Photodynamic therapy (PDT) has shown great efficacy in treating solid tumors, however it remains a challenge to apply PDT for the treatment of disseminated disease, such as metastatic cancer. The antitumor effect elicited by PDT is in some cases opposed by the immunosuppressive mechanisms elicited by tumor cells which makes the treatment ineffective. Thus, immunotherapies that have as major goal the alleviation of this immunosuppressive tumor environment are interesting to be used in combinatory therapies aiming at higher efficacies with better antitumoral and antimetastatic effects. This chapter reports the use of three different tumor models to test the combination of redaporfin-PDT with immunotherapies using CTLA-4 and PD-1. Treatment outcomes were evaluated by survival percentage, tumor growth kinetics and, for the carcinoma model the observation of metastasis development. This latter case employed bioluminescent imaging. Furthermore, we evaluated the changes on expression of several immune checkpoint molecules triggered by redaporfin-PDT *in vitro*.

Combination of redaporfin-PDT with CTLA-4 immunotherapy, but not with PD-1, led to a significant improvement of survival and a higher cure rate for the colon carcinoma animal model. However, the same was not achieved for the melanoma and breast carcinoma animal models. Expression of immune checkpoint molecules was induced in tumor cells treated *in vitro* with redaporfin-PDT. The most notable changes were observed for CD80 and PD-L1. These results showed that the combination of photodynamic therapy with immunotherapy may be successful for the treatment of

malignant diseases that have resistance to immunotherapies alone. This highlights the fact that a general strategy may not be ideal for every tumor model and an individual optimization must be considered. Combinatorial approaches are not universal and they must be tailored to the specificities of each clinical case.

5.2 Introduction

Malignant cancer diseases usually present a poor diagnosis and outcome caused by their invasiveness and difficulty to treat. PDT is a promising and effective cancer treatment, however some limitations occur when the ambition is to go beyond the local treatment and attempt to destroy isolated tumor cells and distant lesions, such as metastasis.

Redaporfin-PDT is described to create a potent cytotoxic effect with the induction of antitumoral immune response¹⁷. Efficacy of redaporfin-PDT was previously reported to be dependent on cytotoxic T cells¹²⁷. However, low immunogenic tumors or advanced stage conditions are extremely difficult to control, and PDT alone may not be curative.

Tumor microenvironments of low immunogenic models are described by the presence of a high percentage of anergic immune cells that overexpress inhibitory proteins, such as immune checkpoints. Immune checkpoints comprise several immunosuppressive mechanisms that play essential roles in maintaining immune homeostasis and protect the host from exacerbated immune responses to pathogens or even against self-components. These pathways are usually co-opted by tumors as a mechanism to escape from immune attack. The reversion of exhausted T cells is one of the strategies that have been proposed as a promising therapy to combine with PDT. The most studied strategies englobe the blocking of CTLA-4 and PD-1/PD-L1 immune checkpoints pathways, which already have approved drugs in clinical use.

Regarding this, we hypothesized that redaporfin-PDT efficacy could be enhanced through combination with immune checkpoint blockers. The main goal of the work reported here was to combine PDT with immunotherapies and evaluate the impact of these combinations on the overall survival. Furthermore, we evaluated *in vitro* changes in the expression of some molecules involved in the inhibitory checkpoints of the immune system, triggered by redaporfin-PDT.

5.3 Material and Methods

5.3.1 Chemicals

5,10,15,20 - Tetrakis (2,6-difluoro -3-N-methylsulfamoylphenyl) bacteriochlorin (redaporfin) was provided by Luzitin SA (Coimbra, Portugal). Redaporfin for intravenous administration was formulated in NaCl 0.9%: EtOH: Kolliphor (98.8:1:0.2) and the concentration was confirmed by absorption spectra. The appropriate volume of PS was calculated according to the drug dose and the animal weight. Kolliphor EL®, NaCl, absolute ethanol (EtOH), and Matrigel were purchased from Sigma-Aldrich Corp. (St. Louis, MO, USA).

5.3.2 Cell lines

CT26.WT cells (ATCC® CRL-2638™), 4T1 cells (ATCC® CRL-2539™), 4T1-luc2 cells (Perkin-Elmer) and B16F10 (kindly provided by IPO, Porto, Portugal) were cultured in Dulbecco's Modified Eagle's medium (DMEM) (Sigma-Aldrich) supplemented with 10% (v/v) heat-inactivated fetal bovine serum (Gibco), 100 U/ml penicillin and 100 ng/ml streptomycin (Sigma-Aldrich).

5.3.3 Mouse tumor model and PDT

The Portuguese Animal Health Authority approved the animal experiments (DGAV authorization 0420/000/000/2011). CT26.WT tumors were established by s.c. injection of 350,000 cells in the right flank of BALB/c (Charles River Laboratories) mice ca. 10 weeks old (20 g). B16F10 tumors were established by s.c. injection of 500,000 cells in Matrigel:PBS (1:1) in the right flank of C57BL/6J (Charles River Laboratories) mice ca. 10 weeks old (20 g). 4T1-luc2 tumors were established by s.c. orthotopical injection of 20,000 cells in the right abdominal mammary fat pad of BALB/c (Charles River Laboratories) mice ca. 10 weeks old (20 g). The day of each PDT treatment was determined as the day the diameter of each tumor reached 5-6 mm. The protocols for the combinations were deliberately selected not to present efficacy when applied for PDT or immunotherapy alone.

For CT26.WT tumors the protocol was 0.6/0.75 mg/kg of redaporfin, DLI=15 min, 50 J/cm² @ 130 mW/cm², 13 mm diameter illumination circle, orthogonal illumination. For B16F10 tumors the protocol was 1 mg/kg of redaporfin, DLI=15 min, 75 J/cm² @ 130

Combinatorial approaches of redaporfin-PDT and Immunotherapy

mW/cm², 13 mm diameter illumination circle, orthogonal illumination. For 4T1-luc2 tumors the protocol was 1.8 mg/kg of redaporfin, DLI=72 h, 100 J/cm² @ 130 mW/cm², 13 mm diameter illumination circle, transversal illumination to the tumor. The illumination employed an Omicron laser at 748 nm. The kinetic of tumor growth was followed after PDT. The endpoint was defined to evaluate the impact of the treatment and the kinetics of tumor growth with and without the combination with immune checkpoint blockers. The animals were sacrificed when the longest tumor diameter reaches 10-12 mm. Animals without palpable tumor 60-days post-PDT were considered cured.

5.3.4 Immune checkpoint blockade with monoclonal antibodies

Immune checkpoint blockade was performed with monoclonal antibodies for PD-1 and CTLA-4 molecules. mAb were administered 1 day before, 1 and 3 days after PDT or 2 days before, 30 min before, 4 and 8 days after PDT. mAb were administered in the following dosages: anti-PD1 (CD279, clone RMP1-14, BioXCell) – 12.5 mg/kg; anti-CTLA-4 (CD152, clone UC10-4F10-11, BioXCell) – 5 mg/kg; isotype control (IgG2b, Clone MPC-11, BioXCell) – 5 mg/kg.

5.3.5 IVIS Imaging

4T1-luc2 cell line expresses luciferase, which allowed the luminescence imaging of the development of 4T1-luc2 primary tumors and metastasis using the IVIS Lumina XR *in vivo* imaging system (Caliper LifeSciences, Hopkinton, MA, USA). Chemiluminescence data was collected from BALB/c mice with 4T1-luc2 tumors 7 minutes after i.p. administration of D-luciferin (150 mg/kg in PBS) (PerkinElmer, USA) with open emission filter to confirm the establishment of the primary tumor and the development of metastasis. Mice hair in the thorax region was removed with a commercial hair removal cream. To prevent motion, mice were anesthetized immediately after the i.p. injection, and kept under anesthesia during the whole acquisition, with an inhalation anesthetic (isoflurane) using an XGI-8 Gas Anesthesia Delivery System (PerkinElmer, USA). All images were taken in automatic mode and are presented in the same color scale. Bioluminescent signals were quantified using the Living Image 4.5.2 software (IVIS Imaging Systems) and were expressed as radiant efficiency (p/s/cm²/sr)/(μW/cm²). A

region-of-interest (ROI) was drawn in the lung area of each animal (the ROI area was maintained for all images) and compared over time and between treatment groups.

5.3.6 *In vitro* PDT protocol

For *in vitro* experiments, 50,000 cells of CT26.WT, B16F10 and 4T1 were seeded in 24-well plates and left overnight in the incubator to attach. For each cell line, three different concentrations of redaporfin were added according to the IC50 of redaporfin for each cell line (Table 9), to obtain about 40 to 60 % of cell viability. Stock solutions of redaporfin were prepared in DMSO and then diluted in DMEM. After 24 h cells were washed twice, and fresh medium was added to the cells. Illumination of the plates was performed immediately after wash, with the light dose of 0.3 J/cm², required for the desired cell viability, using an irradiation device LEDbox® (BioLambda, Brazil) with 740 nm LED. 6 h after irradiation, one of the conditions per cell line was selected according to morphology observation, and cells were collected to be analyzed by flow cytometry (0.20 μM for CT26.WT, 0.05 μM for B16F10 and 0.02 μM for 4T1).

Table 9. **Redaporfin concentrations and light dose tested in the *in vitro* PDT protocols.** Several redaporfin concentrations were tested *in vitro* with three different cell lines. The concentration in **bold** was the one that was selected to be further analyzed by flow cytometry.

Cell Line	CT26.WT	B16F10	4T1
Redaporfin concentration (μM)	0.20	0.05	0.01
	0.40	0.10	0.02
	0.80	0.20	0.05
Light Dose (J/cm²)	0.3	0.3	0.3

5.3.7 Flow cytometry

The following anti-mouse monoclonal antibodies (mAb) were used for flow cytometry surface staining: Brilliant Violet 650™ anti-mouse CD80 (BioLegend), APC anti-mouse CD152 (BioLegend) and Brilliant Violet 605™ anti-mouse CD274 (B7-H1, PD-L1) (BioLegend). Cells were stained with the Zombie Violet™ Fixable Viability Kit (BioLegend) at room temperature for 20 minutes, washed and resuspended in FACS buffer containing the antibodies for the surface staining, for 30 minutes at 4 °C. Cells were then washed twice, resuspended in FACS buffer, and analyzed by flow cytometry

using a Flow Cytometer NovoCyte® 3000 + NovoSampler® Pro (ACEA Bioscience). The gating strategy implemented is represented in Figure 17.

5.3.8 Statistical Analysis

The results are presented as the mean \pm standard error of the mean (SEM). Survival analysis was performed by means of a Kaplan-Meier estimator and log-rank (Mantel-Cox) test. Two-way ANOVA with Turkey's post-test was used to determine statistically significant differences of the means between groups. Statistical differences were presented at probability levels of $p < 0.05$ *, $p < 0.01$ **, $p < 0.001$ *** and $p < 0.0001$ ****.

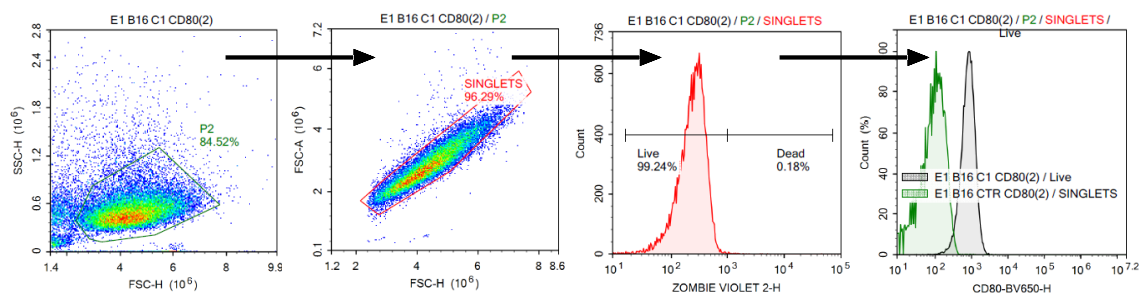


Figure 17. **Gating strategy used to evaluate changes in expression of immune molecules triggered by redaporfin-PDT.** The cell population was selected from the SSC/FSC plot and followed by a gate for the singlet events. Then, death cells, which were positive for the zombie violet assay, were rejected and the mean fluorescence of the dye corresponding to each molecule (CD80, CTLA-4 and PD-L1) was registered and compared with the untreated and unstained samples.

5.4 Results and Discussion

5.4.1 Combinatorial approaches of redaporfin-PDT and immune checkpoint blockers

Redaporfin-PDT was previously described to achieve a remarkable efficacy, in part because it triggers a strong immune response, which was further reported to be dependent on cytotoxic T cells^{17,127}. The desire to increase the fraction of patients that benefit from immunotherapies and to increase the success of redaporfin-PDT in highly aggressive and metastatic cancers motivated the study of combinations between redaporfin-PDT and different immunotherapies.

The most clinically relevant immunotherapies currently involve anti-PD1 and anti-CTLA-4 monoclonal antibodies (mAb) and these were selected for combination with redaporfin-PDT. The tumor models selected to test these combinations were CT26.WT, B16F10 and 4T1-luc2. Redaporfin-PDT was extensively studied with the CT26.WT tumor model, which achieved a high cure rate and a strong antitumoral response. However, when treating larger tumors, the efficacy of PDT is reduced. Furthermore, our motivation was to evaluate the impact of these combinations on aggressive and immunosuppressive tumor models, such as the B16F10 and 4T1-luc2. These models represent a greater challenge for both therapeutic strategies alone. Additionally, these models spontaneously metastasize to distant regions and this is currently one of the major concerns in late-stage diseases.

Redaporfin-PDT treatments of CT26.WT, B16F10 and 4T1-luc2 tumors are presented in Figure 18. The protocols employed are deliberately below the optimal dosage to represent clinical cases of large and metastatic tumors, more difficult to treat with a single dose of redaporfin PDT, except for the case of 4T1. In this tumor model, we did not find conditions that could increase the medium survival time of the animals with treatment-related lethality.

Combinatorial approaches of redaporfin-PDT and Immunotherapy

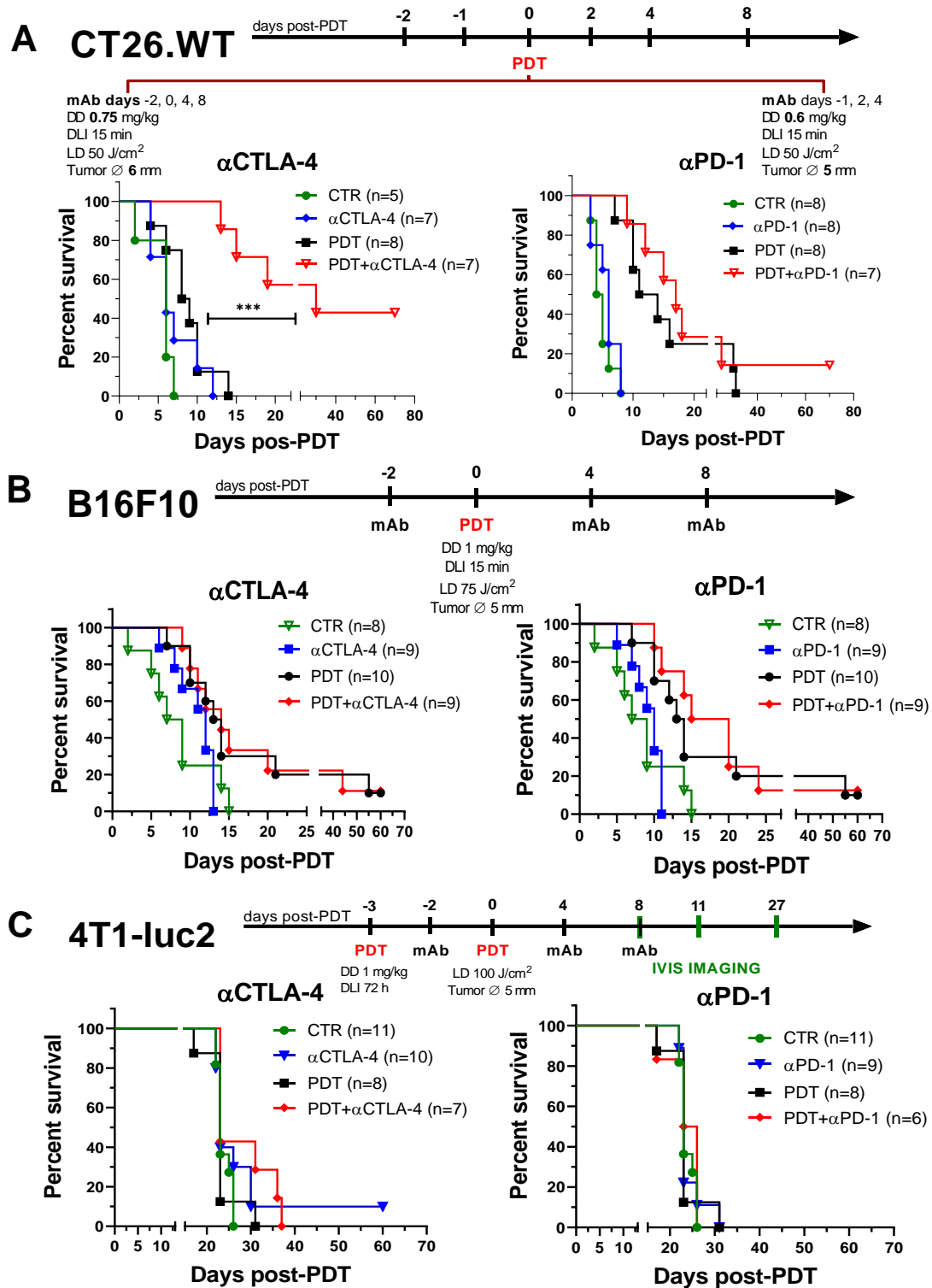


Figure 18. **Survival of combinatory therapeutic strategies of redaporfin-PDT with immunotherapies.** Kaplan Meier representing the survivals proportions of the protocols tested with the immunotherapies CTLA-4 and PD-1 with the (A) CT26.WT, (B) B16F10 and (C) 4T1-luc2 tumor models. The protocol for antibodies administration is represented as a function of the PDT treatment day, and the PDT parameters are described for each model. DD- drug dose; DLI- drug-to-light interval; LD- light dose; mAb- monoclonal antibodies; Tumor Ø- tumor diameter.

Combinatorial approaches of redaporfin-PDT and Immunotherapy

CT26.WT is a colon carcinoma cell line that is extensively used as model for testing immunotherapy protocols and study the host immune responses. CT26.WT is an highly immunogenic tumor which tends to show promising response rates when treated with several commercially available checkpoint inhibitors²⁷⁰. Redaporfin-PDT of CT26.WT tumors achieves 87 % cure rate with a vascular protocol (DLI=15 min), using 0.75 mg/kg of redaporfin and a light dose of 50 J/cm²¹⁷. For the combination strategy, treatments were performed in conditions that PDT alone is not effective. This was achieved by using lower drug doses or treating larger tumors than those of the optimized redaporfin-PDT protocols. The lowering of the drug dose of 0.75 mg/kg to 0.6 mg/kg completely abolished the published cure rate. Nevertheless, PDT alone still improved the median survival time of animals compared to the PD-1 immunotherapy (Figure 18A). However, when combining both treatments, no statistical improvement in survival was observed (p=0.4487). We did observe the cure of one animal in the group of 7 subject to the combination therapy, but this was insufficient for statistical significance. The combination between PDT and CTLA-4 immunotherapy employed tumors with larger dimensions than the optimized PDT protocol. Neither of the two therapies alone changed the survival compared to the untreated mice with such large tumors. However, combining both ineffective treatments uncovered a substantial improve of the therapy outcome (p=0.003). We achieved a 43 % survival with this combination strategy.

This promising outcome encouraged the use of such combination strategy to treat other tumor models, recognized for being much more aggressive and challenging to treat. B16F10 is a murine melanoma cell line from a C57BL/6J mouse and is described as highly metastatic that spontaneously form metastases post implantation into mice²⁷¹. B16F10 tumors are one of the most used cell lines for research in cancer, specifically to analyze metastasis and immunotherapy treatments. Similarly, 4T1 cells is a mammary gland carcinoma cell line, highly aggressive and immunosuppressive. This tumor model is reported to have metastatic spread in mice and mimics the stage IV human breast cancer²⁶⁵.

In the previous chapter, it was extensively reported the challenges faced to optimize PDT parameters for these tumor models. PDT protocols implemented in this study had a visible impact on the tumor, in terms of necrosis and edema, but did not showed a complete curative effect.

Combinatorial approaches of redaporfin-PDT and Immunotherapy

Figure 18 shows that the combination of redaporfin-PDT with the different immunotherapies for the treatment of B16F10 and 4T1 tumor models did not extend the survival of the animals. The kinetics of tumor growth were also followed to evaluate the impact of the treatment in more detail and is represented Figure 19. In agreement with the survival results, the CT26.WT model shows noticeable changes in tumor kinetics when the combinatory approach of PDT with CTLA-4 immunotherapy is employed. The combination with PD-1 immunotherapy was only successful with one animal. It must be recognized that the two combinations are not entirely comparable because the combination with PD-1 employed 0.6 mg/kg and that with CTLA-4 employed 0.75 mg/kg of redaporfin. The latter case produced a stronger impact on the tumor, although it was not curative because the tumor is larger. Nevertheless, we cannot exclude that a stronger PDT impact may stimulate a better combination with immunotherapy.

Regarding the melanoma model, we can see that the immunotherapies alone cause a decrease in the tumor growth. PDT alone has a visible impact in melanoma tumor growth but the combination with the immunotherapies does not significantly improve the therapeutic response. There is an increase in the median survival time with PD-1, but it is not statistically significant (from 13.5 with PDT alone to 17.5 with PDT + α PD1).

Unfortunately, no differences were observed in the kinetic of tumor growth of 4T1 model in treated and untreated animals. 4T1 tumors were orthotopically inoculated in the mammary gland, and this fact limits the dose of PDT because vital organs can be affected by stray light. This location also challenges the measurement of tumor dimensions, as tumors tend to grow internally. These challenges may affect the accuracy of tumor volumes.

Combinatorial approaches of redaporfin-PDT and Immunotherapy

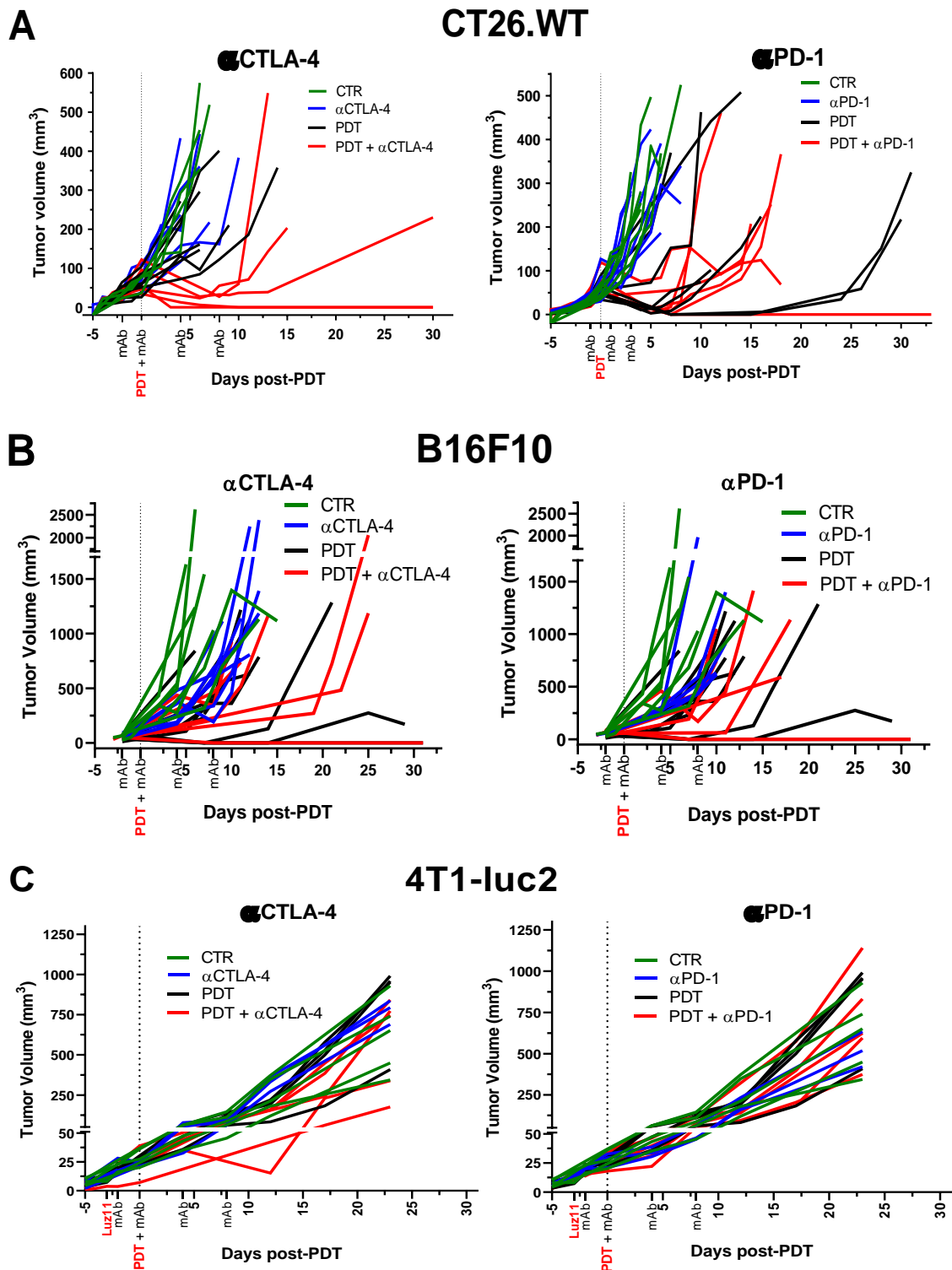


Figure 19. **Tumor volume curves of combinatory approaches of PDT with immunotherapies in three different tumor models.** Tumor volumes are represented individually for each animal with the colors corresponding to the treatment group. Schedule of administrations of immunotherapy antibodies are designated in the X-axis, as well as the PDT treatment day, which was established as the day 0 of the experiment.

Combinatorial approaches of redaporfin-PDT and Immunotherapy

The expression of luciferase by 4T1 cell line allowed the quantification of tumor and metastasis signals using chemiluminescence imaging. Bioluminescence images are represented in Figure 20 and the radiance was further quantified at several timepoints after the treatment (Figure 21). For accurate comparison, all the images are represented at the same color scale. As the treatments did not allowed the elimination of the primary tumor, and to avoid luminescence contamination from this, during metastasis luminescence acquisitions the primary tumor was covered with a black opaque material. Nevertheless, due to the high level of luminescence of the primary tumor and the low luminescence generated by small metastasis, in some cases background signal was still detected and is represented by the dark grey color.

Significant differences in the luminescence from the lung region started to be observed 12 days after PDT treatment. Untreated animals revealed an apparent exponential increase of the luminescence and several metastases were “visually” detected from the 17th day forward. Surprisingly, PD-1 immunotherapy group followed the same kinetics of the untreated mice, and some animals even developed higher levels of metastases compared to untreated. PDT combination with PD-1 immunotherapy slowed these kinetic but no differences were observed between PDT alone and the combination. On the other hand, CTLA-4 immunotherapy significantly delayed the development of distant cancer lesions, both confirmed by metastasis detection, showed in Figure 20, and by the quantification represented in Figure 21. However, the combination of CTLA-4 immunotherapy with PDT, did not revealed a significant reduction of the metastasis development suggesting that PDT did not contribute to improve the effect of the immunotherapy.

Earlier work with redaporfin-PDT and B16F10 melanoma-bearing C57BL/6J mice revealed that a 1.5 mg/kg with 105 J/cm² of light delivered 15 min post i.v. administration was lethal to 80 % of the animals and the animals that survived the treatment were cured⁸⁵. Cures without lethality could only be obtained when the drug formulation was changed from Kolliphor EL to Pluronic P123. In this study we maintained the kolliphor formulation that is currently in clinical use²⁴¹, although the pluronic formulation has the advantage of higher tumor/muscle ratios. We employed a redaporfin dose in the kolliphor formulation of 1 mg/kg and a light dose of 75 J/cm² to avoid lethality. However, this dosage regimen only leads to a 10 % cure rate, as shown in Figure 18B.

Combinatorial approaches of redaporfin-PDT and Immunotherapy

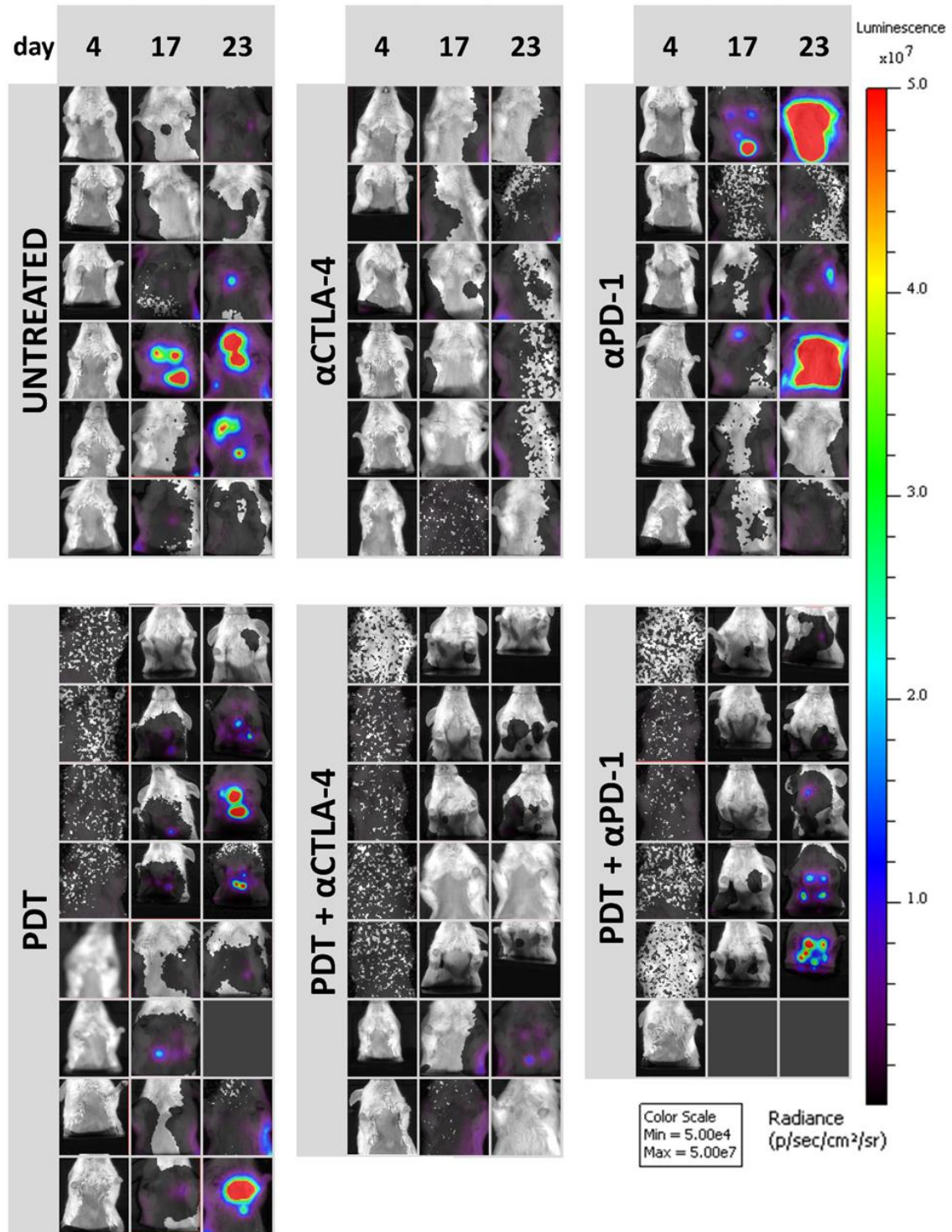


Figure 20. **Bioluminescence imaging of 4T1-luc2 metastases 4, 17 and 23 days post-PDT treatment.** D-luciferin was i.p. administered 7 minutes prior acquisition. For metastasis assessment the primary tumor was covered with an opaque material, however in some acquisitions it was still detected a background luminescent signal which was originated from the primary tumor.

Combinatorial approaches of redaporfin-PDT and Immunotherapy

The extensive steps for the optimization of redaporfin-PDT treatment in the 4T1 model are reported in the previous chapter. Apart from the described difficulty to treat 4T1 tumors, the orthotopic localization of this model turns it even more challenging to treat. However, orthotopic 4T1 tumor models represent with higher accuracy the human breast cancer. Vascular protocols of redaporfin-PDT either revealed to be lethal due to necrosis in adjacent healthy tissues or to have no visible impact on the tumors. Further studies with photoacoustic tomography showed that the presence of redaporfin inside 4T1 tumors is minimal when compared to other tumor types and is higher for longer DLIs (48h-72h). The balance between efficacy and safety led us to consider a cellular protocol, with 1.8 mg/kg of redaporfin administered 72 h before illumination with a light dose of 100 J/cm². Even with this alteration, no significant impact was observed in the survival of animals as represented on Figure 18 and Figure 19.

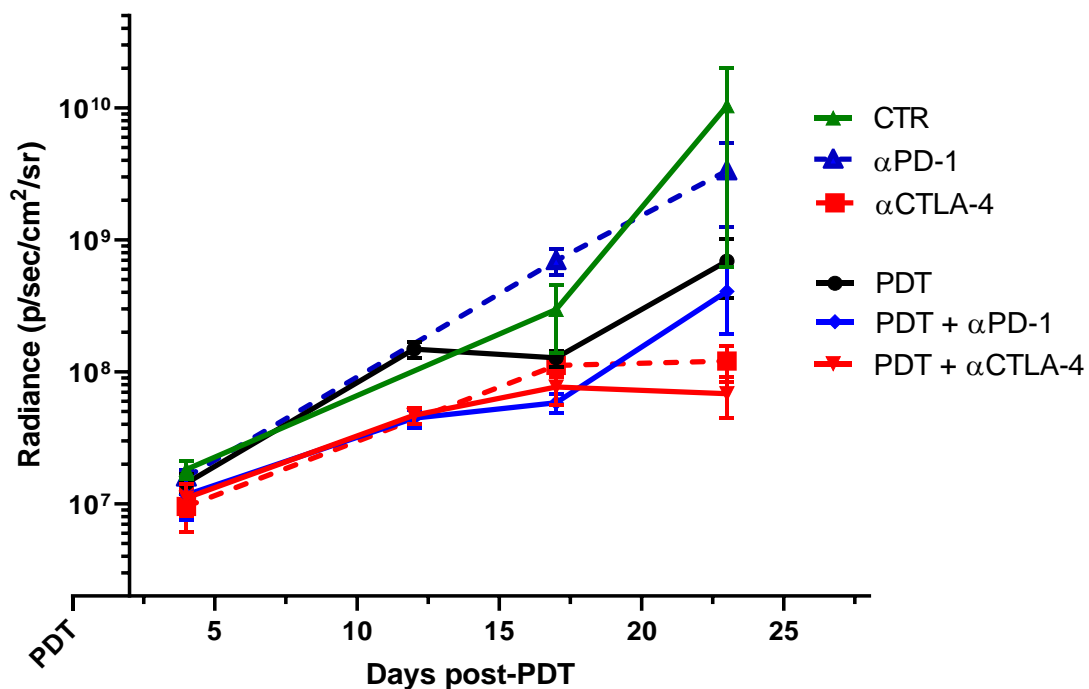


Figure 21. **Assessment of lung metastases development.** Luminescence from the thorax region of animals were quantified by imagiology and followed over time as an indicator of metastases development. Average radiance of each group condition is represented according to the legend.

5.4.2 Redaporfin-PDT alters the expression of immune molecules by tumor cells

PDT is described to induce several changes in the microenvironment of tumors which can induce the upregulation of several proteins^{25,95,272}. We, and others²⁷³, hypothesize that such changes may alter immune checkpoint activity. The release of DAMPs and tumor

Combinatorial approaches of redaporfin-PDT and Immunotherapy

antigens can contribute to trigger an innate immune response, turning PDT into a promising adjuvant for immunotherapies. In view of the results with combinatory approaches, we embarked in an *in vitro* investigation of the expression of molecules involved in the immune checkpoint mechanisms at the surface of tumor cells after PDT. More specifically, we assessed the expression of CD80, CTLA-4 and PD-L1.

PD-1 and CTLA-4 are co-inhibitory receptors expressed on the surface of activated T and B cells. They restrict T cell activity and are referred as immune checkpoints. Antibodies that block CTLA-4 or PD-1, or the PD-1 ligand PD-L1, give durable responses for a fraction of cancer patients. Such antibodies are named immune checkpoint blockers (ICBs).

CTLA-4 is structurally identical to CD28 and both are involved in the regulation of antigen recognition by T cells through the interaction with CD80/CD86. While CD28 transmits a positive costimulation crucial to T cell activation, CTLA-4 inhibits the T cell activation. Apart from the downregulation of T cell activation, CTLA-4 also presents a 100 to 1000-fold higher affinity for CD80 when competing with CD28, which prevents CD28-CD80 binding in the presence of CTLA-4²⁷⁴. Even though CTLA-4 expression is commonly reported in the lymphoid cell lineage, several publications have reported the constitutive expression on tumor cells and suggested that its role/mechanism there may be different²⁷⁵⁻²⁷⁷.

CD80, also known as B7-1, is a costimulatory ligand that has the ability to augment T cell responses through interactions with CD28 expressed on T cells. CD28 is one of the proteins that provide costimulatory signals required for T cell activation and survival. CD80/CD28 interaction augments T cell activation by reducing the number of T cell receptors (TCRs) that must be triggered for T cell activation and also enhances the production of IL-2. CD80 is not considered an immune checkpoint molecule, but as CTLA-4 presents a much higher affinity to bind CD80 than CD28, the low expression of CD80 is one of the many mechanisms that tumor cells use to evade antitumor immunity. Interaction between CTLA-4 and CD80 inhibits T cell responses.

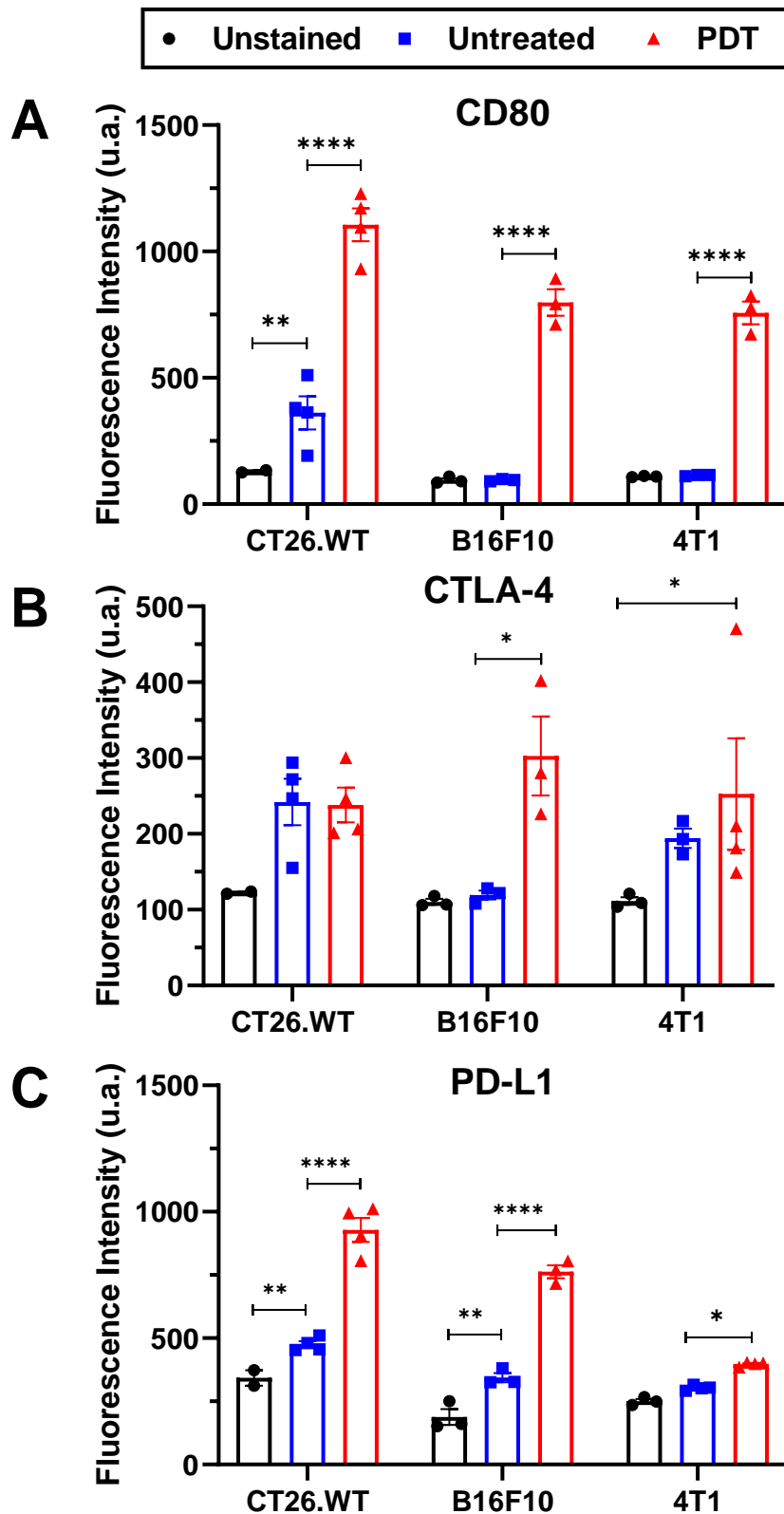


Figure 22. **Expression of different immune checkpoint molecules on tumor cells treated with redaporfin-PDT.** The expression of (A) CD80, (B) CTLA-4 and (C) PD-L1 molecules on three different cell lines were evaluated by flow cytometry and compared to the untreated condition (light only) and to unstained cells. p-values < 0.05 were considered significant with (*), p-values < 0.01 (**), p-values < 0.001 (***), p-values < 0.0001 (****).

Combinatorial approaches of redaporfin-PDT and Immunotherapy

As different cell lines have different IC50 values for redaporfin-PDT, cells were treated with different concentrations of the PS to induce approximately the same percentage of cell death (Table 9). Cells were collected 6 h after the illumination, marked with antibodies for CD80, CTLA4-4 and PD-L1, and analyzed by flow cytometry. The gating strategy applied, Figure 17, started with a selection of the cell population from the SSC/FSC plot and followed by a gate for the singlet events. Next, the dead cells, which were positive for the zombie violet assay, were rejected and the mean fluorescence of the dye corresponding to each immune molecule was registered and compared with the untreated and unstained samples.

Figure 22A demonstrates low or insignificant expression of CD80 on the untreated conditions in all cell lines, which goes in agreement with the reported in literature²⁷⁸. Our results show that redaporfin-PDT significantly increases the *in vitro* expression of CD80 in CT26.WT, B16F10 and 4T1 cells. The higher levels of CD80 are observed in CT26.WT cells post-PDT. This increase in CD80 foster interactions with CD28 and should augment T cell responses. These results are consistent with the stimulation of the immune systems presented in other redaporfin-PDT studies^{17,127}.

PD-1/PD-L1 expression has been evaluated and discussed over the last years and it is not completely understood if there is a direct correlation between expression and treatment prognosis. Despite its association with a poor diagnosis, in the clinical PD-L1 expression emerges as a positive prognostic biomarker for example in breast cancer²⁷⁹. It was suggested that the survival can be due to the presence of a strong antitumor immune response which triggers PD-L1 expression. The variable expression measures and the non-correlations between expression patterns and treatment effect have been similarly reported in the clinics, which led authors to suggest that evaluation of PD-L1 expression on immune and tumor cells for clinical decision-making may not represent a reliable predictive biomarker for approvals of immune checkpoint blockers^{280,281}. As an example, Kim et al. reported that high PD-L1 expression on tumor infiltrating immune cells (TICs), but not on tumor cells (TCs), was an independent favorable prognostic factor for survival of resected head and neck squamous cell cancer²⁸².

PD-L1 is expressed on a wide variety of cell types and can be induced by several inflammatory cytokines. Intratumoral upregulation of PD-L1 was previously described to occur after PDT and was suggested to be associated with IL-6 production²⁷³.

Combinatorial approaches of redaporfin-PDT and Immunotherapy

Anti-PD-1 mAbs are expected to have a greater impact in cancer cells that intrinsically have a higher expression of PD-L1 because anti-PD-1 mAbs will readily block a significant number of ligands and prevent extensive PD-1/PD-L1 interactions. Figure 22C shows that PD-L1 is more expressed in CT26.WT and in B16F10 cells than in 4T1 cells. Figure 18 shows some effect of anti-PD-1 in CT26.WT and B16F10 cell and no effect in 4T1-luc2. At the doses employed in this work, the delay of tumor growth with anti-PD-1 is not statistically significant, but higher doses could increase the trend and render a tumor growth delay statistically significant. This study did not intend to optimize the effect of any therapy alone, and anti-PD-1 immunotherapy was not further optimized.

The interaction between PD-L1 and CD80 occurs exclusively between PD-L1 and CD80 molecules expressed in the same cell, i.e., cis PD-L1/CD80. This cis PD-L1/CD80 disrupts PD-1/PD-L1 interaction between two separate cells, i.e., trans PD-1/PD-L1, and prevents binding of CTLA-4 to CD80. However, cis PD-L1/CD80 does not disrupt binding between CD80 and CD28, and therefore does not prevent its costimulatory effect^{283,284}.

Figure 22C shows that redaporfin-PDT increases the expression of PD-L1. This favors cis PD-L1/CD80 interactions, which will disrupt trans PD-1/PD-L1 interactions and will not prevent the CD80/CD28 costimulatory effect leading to T cell activation. Moreover, in CT26.WT cells, CTLA-4 binding to CD80 is reduced both because cis PD-L1/CD80 prevents binding of CTLA-4 to CD80 and because the expression of CTLA-4 is not increased post-PDT. The higher availability of CD80 after redaporfin-PDT should favorably combine with anti-PD-1 mAbs to increase the median survival time. This trend is visible in Figure 18.

Redaporfin-PDT has a relatively small effect on the expression of PD-L1 in 4T1 cells. The very modest increase in the expression of PD-L1 is not expected to contribute appreciably to cis PD-L1/CD80 interactions. Hence, trans PD-1/PD-L1 interactions are not appreciably perturbed and the combination of redaporfin-PDT with anti-PD-1 mAbs may not have a significant impact in tumor responses.

Redaporfin-PDT significantly increases the expression of CTLA-4 and of PD-L1 in B16F10 cells. Competition between CTLA-4 binding to CD80 and cis PD-L1/CD80 is expected. Anti-CTLA-4 ICBs may shift the competition to favor cis PD-L1/CD80, and eventually disrupt trans PD-1/PD-L1 interactions but meet with the challenge that more

Combinatorial approaches of redaporfin-PDT and Immunotherapy

CTLA-4 must be blocked. Anti-PD-1 ICBs join with cis PD-L1/CD80 interactions to disrupt trans PD-1/PD-L1 interactions and a favorable combination may occur.

Although the role of CTLA-4 in tumor cells is not known yet, we see that the increase in CTLA-4 expression post-PDT in B16F10 and 4T1 cells is associated with combinations with redaporfin-PDT that have no impact in tumor growth. We believe that the increase in CTLA-4 in tumor cells will compete CTLA-4 in lymphocytes for anti-CTLA-4 mAbs. These mAbs will be less available to block trans CTLA-4/CD80 interactions and the benefits of immunotherapy are attenuated.

According to Figure 22B, changes in the CTLA-4 expression were much less significant compared to the other evaluated molecules. Both CT26.WT and B16F10 appear to have mild expression of CTLA-4 on untreated tumor cells, but then rises of its expression were only significant for 4T1 and B16F10 cells. Nevertheless, levels of surface expressed CTLA-4 are extremely well regulated by the cell, and minor changes in surface expression can have major effects on T-cell activations²⁸⁵. It was also reported that most of the CTLA-4 is localized in vesicles of the Golgi apparatus, being then released to cell surface during T cell activation. But even following T-cell activation, only small amounts of CTLA-4 seem to be detected on the cell surface at a given time.

Interestingly, anti-CTLA-4 mAbs combine with redaporfin-PDT to significantly increase survival. Similarly, addition of CTLA-4 blockade prior to Bremachlorin-PDT led to a significant reduction of tumor burden²²⁷. This can be related with the effect of cis PD-L1/CD80 in preventing binding of CTLA-4 to CD80. The combined increase in CD80 and PD-L1 post-PDT in CT26.WT cells allows for abundant cis PD-L1/CD80 interactions that prevent trans CTLA-4/CD80 interactions that are known to restrict T cell activity. This combined increase is more pronounced in CT26.WT cells and less pronounced in 4T1 cells. Hence, we can expect that the combination of redaporfin-PDT with anti-CTLA-4 will be most successful in CT26.WT cells and least successful in 4T1 cells. Figure 18 confirms this prediction.

5.5 Conclusion

The reported studies led to the creation of a combinatory approach which triggered a significant improvement of treatment efficacy and consequent survival of the animals with colon carcinoma tumors in conditions where both treatments alone are ineffective. However, the same results were not possible to achieve with more invasive and aggressive tumor models, such as B16F10 and 4T1 tumor models. The tumor microenvironment associated with these tumor models, which are usually described as immunosuppressive tumors, seems to be the probable cause for the ineffectiveness of the treatments. These results reinforce the concept that each tumor model should be considered and evaluated individually, leading to specific therapeutic strategies to achieve the best outcome in each case. Even though PDT was not effective in the implemented models, significant changes were observed in the expression of specific immune molecules. These findings open new opportunities to evaluate how these changes could be used as methodologies for the design of new combinatory therapeutic strategies.

6

GENERAL CONCLUSIONS AND FINAL REMARKS

Photodynamic therapy (PDT) with redaporfin leads to a remarkable long-term survival rates, effective memory, and control of lung metastasis in a colon carcinoma model of BALB/c mice⁸⁶. The main motivation behind this project was the characterization of the antitumoral immune response triggered by redaporfin-PDT. Besides this, we propose to evaluate its combination with other therapies to treat other tumor models that represent a challenge to the treatments alone.

We demonstrated that redaporfin-vascular PDT induces extensive tissue damage at the illuminated tumor, which triggers an acute local inflammation⁶⁹. This inflammation is characterized by a systemic increase of IL-6 and neutrophils attaining a peak 24 h post-PDT. We also showed an increased percentage of CD4⁺ and CD8⁺ T cells producing IFN- γ or CD69⁺ and increased CD4⁺/CD8⁺ T cell ratio. Altogether these findings demonstrate that redaporfin-PDT stimulates a strong and rapid response from the immune system. At the tumor bed level, 2 h after PDT CD3⁺ T cells are depleted but later, at 24 h post-PDT, a notorious new infiltration of CD3⁺ T cells is attained. These findings showed that redaporfin-PDT achieved a successful transition from innate to adaptive antitumor immunity. We further showed that the therapeutic effect of redaporfin-PDT is dependent on neutrophils and CD8⁺ T cells but not on CD4⁺ T cells. Redaporfin-PDT can stimulate CD8⁺ T cells even in the absence of CD4⁺ T cells, similarly to photofrin-PDT.

Regarding this, we hypothesize that the combination of redaporfin-PDT with an immune therapy may potentiate the efficacy of both therapies. Furthermore, immunotherapies seem to be limited by the absence of T cell-based inflammation²⁶². Arguably, major benefits might be achieved with immunostimulating approaches that induce appropriate tissue-based inflammation. The ambition of this combination is to increase the fraction of

GENERAL CONCLUSIONS AND FINAL REMARKS

patients that benefit from the immunotherapies and increase the success of redaporfin-PDT in highly aggressive and metastatic tumors. Subsequently, the choice of the tested tumor models for this combination took in consideration the ability of redaporfin-PDT to trigger an immunogenic cell death (ICD) which may enhance the immunogenicity of tumor cells.

During this work, we proceeded to an optimization process for the treatment with redaporfin-PDT in two different immunosuppressive cancer models: melanoma (B16F10) and breast carcinoma (4T1-luc2) tumor models. For each model, the conditions of drug dose and light dose, drug-to-light interval, area of the illuminated region and fluence were verified to achieve the best impact on the tumor whilst avoiding effects on healthy tissues.

The optimization results revealed that the same doses used to achieve a high cure rate in CT26.WT model were completely ineffective in the described models. A strong edema which then ended up in a significant necrosis was achieved on B16F10 tumor model with a redaporfin dose of 1 mg/kg and a light dose of 75 J/cm². This protocol increased the median survival time of mice and led to a percentage of cures of almost 30 %. The mammary carcinoma model revealed to be much more challenging to treat and despite the extensive trials to obtain a suitable protocol, no cures were achieved. Nevertheless, a significant impact, with visible edema and necrosis, was attained with 1.8 mg/kg of redaporfin and 100 J/cm². Further studies by photoacoustic tomography allowed to elucidate that the ineffectiveness of redaporfin-PDT on 4T1 tumor is due to the low content of redaporfin that manages to accumulate in the tumor.

It is suggested that the impact created by PDT on tumors may turn them more responsive for other therapies, such as immunotherapies. Considering this, different combination strategies were studied here.

The combinations strategies used included treatment conditions where both treatments alone were ineffective. The conditions applied led to a combinatory approach which triggered a significant improvement of treatment efficacy and consequent survival of the animals with colon carcinoma tumors. However, the same goals were not possible to attain with more invasive and aggressive tumor models, such as B16F10 and 4T1 tumor models.

GENERAL CONCLUSIONS AND FINAL REMARKS

The tumor microenvironments of low immunogenic cancer models are described by the presence of a high percentage of anergic immune cells that overexpress inhibitory proteins, such as immune checkpoints. Even though PDT alone was not effective in the implemented models, significant changes after PDT treatment were observed in the expression of specific immune molecules, such as CD80, CTLA-4 and PD-L1.

The combined increase in CD80 and PD-L1 post-PDT in CT26.WT cells allows for abundant cis PD-L1/CD80 interactions that prevent trans CTLA-4/CD80 interactions that are known to restrict T cell activity. We propose that efficacy of the combination of anti-CTLA-4 with redaporfin-PDT results from the combined increased of CD80 and PD-L1, which is more pronounced in CT26.WT cells.

These findings open new opportunities to evaluate how these changes could be used to design new combinatory therapeutic strategies. Even though, it is necessary to perform additional studies to characterize the changes triggered on tumor cell infiltrates and circulatory immune cells after PDT treatment. This will bring more elucidations on the mechanisms behind redaporfin-PDT.

7

APPENDIX

i. Redaporfin *in vivo* formulation

Formulation for *in vivo* studies was prepared by dissolving redaporfin powder in ethanol:Kolliphor®EL (5:1). Complete solubilization was achieved by 3 cycles of 10 minutes in ultrasound bath followed by 1 minute of vortex mixing, After that, the stock in ethanol: Kolliphor®EL was added to a saline solution (0.9 % NaCl), achieving a final ratio of saline:ethanol:Kolliphor®EL of 98.8:1:0.2. Redaporfin is soluble in the ethanol:Kolliphor®EL solution and immediately form micelles when added to the saline solution. Micelles size was further evaluated by light scattering measurements, Figure 23 (Zetasizer NanoS, Malvern). The concentration of redaporfin was always confirmed by the absorption spectra of the photosensitizer, represented in Figure 24, and following the Beer-Lambert law. The molar absorption coefficient of redaporfin in this formulation is $\epsilon = 121.700 \text{ M}^{-1}\text{cm}^{-1}$ at 749 nm¹⁶. The appropriate dose of redaporfin was slowly delivered by intravenous administration in the mice tail vein, in a volume correspondent to 10 $\mu\text{L/g}$ of mouse body weight. The formulation was selected based on previous studies that evaluated the stability of redaporfin and tolerance in the organism¹⁸.

ii. Light Delivery Laser

PDT *in vivo* treatments employed a laser Omicron diode laser system (Rodgau, Germany), model LDM750.300.CWA.L.M with laser head 1201-07-D and 1201-08-D, maximum output power of 300 mW and wavelength of 749 nm \pm 3 nm, connected to a glass optical fiber with microlens tip from Medlight (Ecublens, Switzerland), model FD with 2 mm of diameter and 4 m of overall length, which was held in a fixed position and directed perpendicularly, unless stated otherwise, to the tumor to produce an illumination circle concentric with the tumor. The energy of the laser was always checked before illumination with a handheld laser power meter LaserCheck (Coherent Inc, Santa Clara,

CA, USA). The position of the fiber was fixed previously to the treatment to obtain an illumination circle concentric with the tumor and with a set diameter.

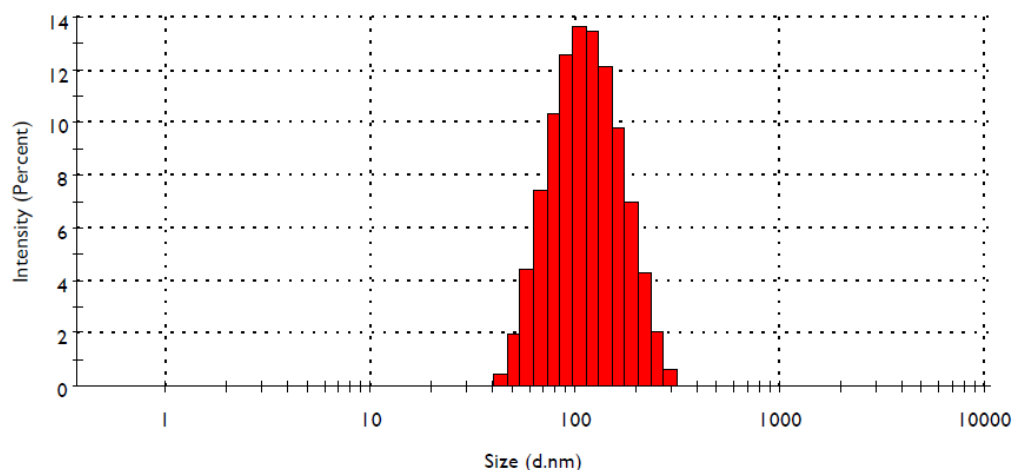


Figure 23. **DLS intensity-based size distribution histograms.** Size distribution of redaporfin formulation micelles measured by light scattering technique (average size = 122 ± 48.44 nm)

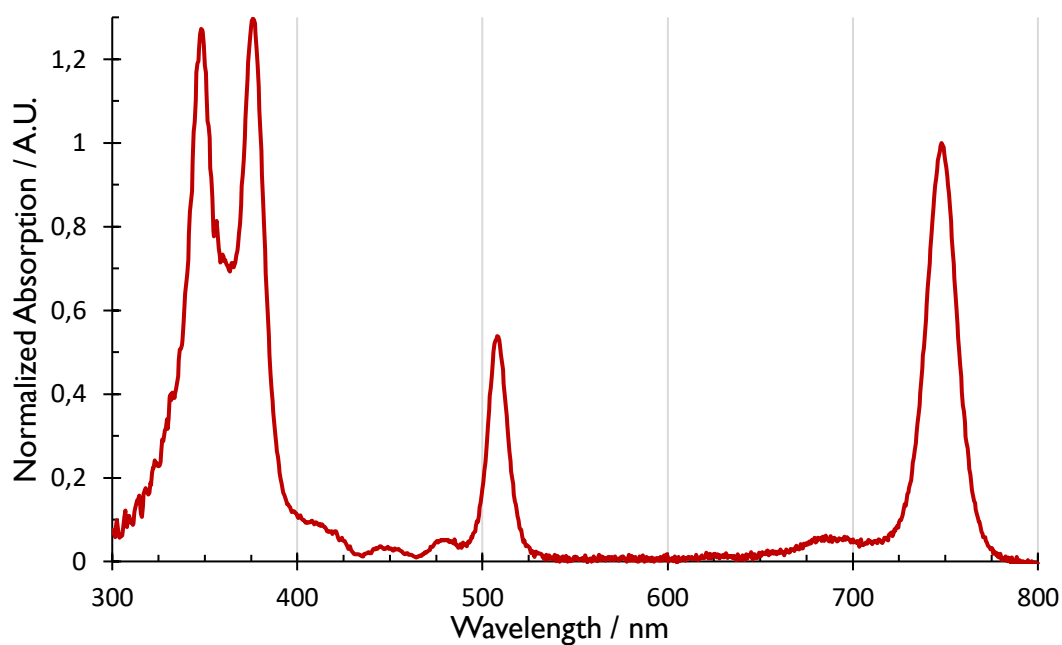


Figure 24. **Absorption spectra of redaporfin in *in vivo* formulation.** Formulation for *in vivo* intravenous administration was prepared by dissolving redaporfin powder in ethanol:Kolliphor®EL (5:1) and then diluted in saline 0.9 % achieving a final ratio of saline:ethanol:Kolliphor®EL of 98.8:1:0.2.

iii. List of Figures

- Figure 1. **Jablonski energy diagram illustrating the main events of PDT mechanism, leading to the generation of reactive oxygen species (ROS).** The photosensitizer molecule (PS) is excited from ground state to excited singlet states (S_1, S_2, \dots) by the absorption of light at a specific wavelength. The excited molecule (PS^*) can either decay to the ground state by radiative (fluorescence and/or phosphorescence) or nonradiative processes (internal conversion and/or intersystem crossing to the triplet state). The PS triplet excited state (T_1) can further trigger the local production of cytotoxic ROS, such as singlet oxygen (1O_2), superoxide radical anion ($O_2^{\cdot-}$), hydrogen peroxide (H_2O_2) and hydroxyl radical (HO^{\cdot})..... 22
- Figure 2. **Phototherapeutic window for PDT.** Endogenous chromophores, such as hemoglobin and melanin have absorption until the 650 nm, while water absorbs from the 900 nm. Over 850 nm, light does not present enough energy to excite the molecular oxygen and generate ROS. These facts lead to the definition of the phototherapeutic window, from 650 to 850 nm, which is also corroborated by the optical penetration depth of light into skin. Adapted from¹⁹..... 24
- Figure 3. **Antitumor immune mechanism triggered by Photodynamic Therapy.** The cytotoxic effect of PDT induces a local inflammation, with recruitment of innate immune cells to the illuminated area. Innate immune cells, such as DCs, phagocytize tumor antigens and DAMPS released by damaged tumor cells and present them to T cells in the lymph nodes. This stimulation activates the adaptive arm of the immune system, generating the proliferation of effector T cells capable of recognize and destroy the remaining tumor cells. 31
- Figure 4. **Innate immune response mechanism triggered by Photodynamic Therapy.** Shortly after the light activation, the release of DAMPs, cytokines and other components lead to the development of a strong inflammation with infiltration of innate immune cells, such as macrophages, neutrophils, dendritic cells (DCs) and NK cells. The recognition of the tumor antigens by APCs and further presentation to T cells in the lymph nodes activated the adaptive immune response. 34
- Figure 5. **Immune checkpoint mechanisms and respective blockade therapy.** T cell activity can be impaired by immune checkpoint protein to maintain the immune homeostasis of the organism. However, these mechanisms are exploited by tumor cells to evade antitumor immune responses. Binding of CTLA-4 to CD80/CD86 prevents the

costimulation of CD28, crucial for effective T cell activation. In a similar manner, binding of PD-L1 to PD-1 generates a negative stimulation, causing T cell anergy. Blockade of these proteins with specific monoclonal antibodies represents a therapeutic strategy to increase the effector function of the immune system. 61

Figure 6. Redaporfin-PDT induces a strong neutrophilia, which contributes significantly for the treatment efficacy. A) Relative percentage of blood leukocyte evaluated by flow cytometry at different time points after redaporfin-PDT. B) Relative percentage of neutrophils (CD45⁺, GR1⁺ and CD11b⁺) evaluated by flow cytometry 24 h and 7 days after redaporfin-PDT. Bars are the mean \pm SD of 6 mice. No symbol $p > 0.05$; * $p < 0.05$; ** $p < 0.01$; *** $p < 0.001$. C) Survival curve of mice bearing CT26.WT tumors treated with redaporfin-PDT in normal conditions or upon neutrophils depletion using Ly6G/Ly6C monoclonal antibodies. D) Tumor growth represented individually for each mouse (6-11 mice per group). Survival curve statistics by LogRank (Mantel-Cox) test. No symbol $p > 0.05$; * $p < 0.05$ 78

Figure 7. Redaporfin-PDT increases the blood levels of the pro-inflammatory cytokine IL-6. The quantification of different cytokines (A - IFN- γ , B - TNF- α , C - IL-2, D - IL-10, E - IL-4, F - IL-6, G - IL-17A) was performed in the blood at different time points after vascular-PDT. I) Representative dot plots that depict the different cytokines in untreated and treated mice. Bars are the mean \pm SD of 5 mice. No symbol $p > 0.05$; * $p < 0.05$; ** $p < 0.01$; *** $p < 0.001$ 79

Figure 8. Activated T cells after vascular-PDT with redaporfin. A) Percentage of CD4⁺ and CD8⁺ T cells and B) ratio of CD4⁺/CD8⁺ T cells in the blood of mice at different time points after vascular-PDT. C) Percentage of CD8⁺ or D) CD4⁺ T cells expressing CD69 in the blood of mice at different time points after PDT. Bars are the mean \pm SD of 5 mice. No symbol $p > 0.05$; * $p < 0.05$; ** $p < 0.01$; *** $p < 0.001$ 81

Figure 9. Redaporfin-PDT stimulates the production of IFN- γ and IL-17A by different immune cells. Production by T cells CD4⁺ (•) or CD8⁺ (▪) of A) IFN- γ , B) IL-4, D) TNF- α and E, F) IL-17A at different time points after redaporfin-PDT. C) IFN- γ /IL-4 ratio, which was obtained by dividing IFN- γ -secreting CD4⁺ T cells by the IL-4-producing CD4⁺ T cells. G) IFN- γ production by DC and H) by NK. Bars are the mean \pm SD of 5 mice. No symbol $p > 0.05$; * $p < 0.05$; ** $p < 0.01$; *** $p < 0.001$ 82

Figure 10. Tumor eradication by redaporfin-PDT is dependent on CD8⁺ T cells but not on CD4⁺ T cells. A) Survival curve of mice bearing CT26.WT tumors treated with redaporfin-PDT in normal conditions or upon depletion of CD4⁺ or CD8⁺ T cells. B)

Tumor growth represented individually for each mouse (9-12 mice per group). Survival curve statistics by LogRank (Mantel-Cox) test. No symbol $p > 0.05$; * $p < 0.05$ 83

Figure 11. **Redaporfin-PDT induces strong hemorrhage and necrosis that is accompanied by T cells infiltration but not by B cells infiltration** (10x magnification).

A) Tumors from control and treated mice (at the indicated time points) were stained with H&E, H indicates hemorrhagic areas and N indicates necrotic areas. **B)** T cells (CD3⁺) (brown) infiltration. **C)** Absence of B cells (Pax5) infiltration. 85

Figure 12. **In vivo neutrophil depletion was confirmed by flow cytometry.** Neutrophils depletion was attained with i.p. administrations of anti-mouse Ly6G/Ly6C monoclonal antibodies (NIMP-R14, BioXCell). Blood samples were collected by tail vein puncture 24 h after the first administration and neutropenia was confirmed by flow cytometry. **A, B)** Representative histograms that show the neutrophils level (Gr1⁺ cells) of a control and a neutrophil depleted animal, respectively. 88

Figure 13. **In vivo CD4⁺ and CD8⁺ T cell neutralization was confirmed by flow cytometry.** Neutralization of CD4⁺, CD8⁺ were achieved with regular i.p. administration of anti-mouse CD4 (GK1.5, BioXCell) and CD8 (53-6.7, BioXCell) monoclonal antibodies, respectively. Specific depletion was confirmed by flow cytometry of blood samples collected 24 h after the first administration. **A, B)** Representative dot plots that show the effective depletion of CD4⁺ T and CD8⁺ T cells populations, respectively.... 88

Figure 14. **Redaporfin-PDT treatment optimization of B16F10 animal model.** C57BL/6 mice bearing s.c. B16F10 tumors were treated with different drug and light doses in a vascular protocol of redaporfin-PDT (DLI=15 min). **(A)** Survival plot of the tested PDT protocols. *p* value of log-rank test of: Untreated vs 1mg/kg+75J/cm²: 0.0100; Untreated vs 0.88mg/kg+50J/cm²: 0.0224. **(B)** Individual tumor growth representation of mice. **(C)** Images of tumors before and after PDT illumination. 6h after illumination a strong edema is observed which then turns into necrosis at 24-72 h after illumination. 96

Figure 15. **Redaporfin tumor accumulation followed by photoacoustic (PA) tomography.** **A)** Transversal irradiation of 4T1-luc2 tumors. **B)** Violin plot representation of redaporfin tumor content. Accumulation of the photosensitizer was assessed after i.v. injection of the formulated redaporfin with a drug dose of 1.65±0.15 mg/kg at several timepoints. Before PS injection, an initial acquisition was performed which is referred as the blank and the following acquisitions were normalized with the blank. Photoacoustic tomography was used to assess the content of redaporfin inside tumors using the unmixing feature of VevoLab and considering as components

redaporfin, oxy- and deoxy-hemoglobin. C) B-mode and photoacoustic unmixed images of CT26.WT and 4T1-luc2 tumors prior redaporfin injection and at the highest PA average timepoints after i.v. injection. **Color legend:** red - oxyhemoglobin; blue - deoxyhemoglobin; green - redaporfin. 103

Figure 16. **Normalized photoacoustic spectra of redaporfin, oxy- and deoxy-hemoglobin.** Redaporfin was prepared in *in vivo* formulation and PA spectra was acquired in a phantom apparatus with the Vevo LAZR-X multimodal imaging system. Oxy- and deoxy-hemoglobin are already part of the Vevo LAZR-X analysis software. 105

Figure 17. **Gating strategy used to evaluate changes in expression of immune molecules triggered by redaporfin-PDT.** The cell population was selected from the SSC/FSC plot and followed by a gate for the singlet events. Then, death cells, which were positive for the zombie violet assay, were rejected and the mean fluorescence of the dye corresponding to each molecule (CD80, CTLA-4 and PD-L1) was registered and compared with the untreated and unstained samples..... 112

Figure 18. **Survival of combinatory therapeutic strategies of redaporfin-PDT with immunotherapies.** Kaplan Meier representing the survivals proportions of the protocols tested with the immunotherapies CTLA-4 and PD-1 with the (A) CT26.WT, (B) B16F10 and (C) 4T1-luc2 tumor models. The protocol for antibodies administration is represented as a function of the PDT treatment day, and the PDT parameters are described for each model. DD- drug dose; DLI- drug-to-light interval; LD- light dose; mAb- monoclonal antibodies; Tumor \varnothing - tumor diameter. 114

Figure 19. **Tumor volume curves of combinatory approaches of PDT with immunotherapies in three different tumor models.** Tumor volumes are represented individually for each animal with the colors corresponding to the treatment group. Schedule of administrations of immunotherapy antibodies are designated in the X-axis, as well as the PDT treatment day, which was established as the day 0 of the experiment. 117

Figure 20. **Bioluminescence imaging of 4T1-luc2 metastases 4, 17 and 23 days post-PDT treatment.** D-luciferin was i.p. administered 7 minutes prior acquisition. For metastasis assessment the primary tumor was covered with an opaque material, however in some acquisitions it was still detected a background luminescent signal which was originated from the primary tumor. 119

- Figure 21. **Assessment of lung metastases development.** Luminescence from the thorax region of animals were quantified by imagiology and followed over time as an indicator of metastases development. Average radiance of each group condition is represented according to the legend..... 120
- Figure 22. **Expression of different immune checkpoint molecules on tumor cells treated with redaporfin-PDT.** The expression of (A) CD80, (B) CTLA-4 and (C) PD-L1 molecules on three different cell lines were evaluated by flow cytometry and compared to the untreated condition (light only) and to unstained cells. p-values < 0.05 were considered significant with (*), p-values < 0.01 (**), p-values < 0.001 (***), p-values < 0.0001 (****)..... 122
- Figure 23. **DLS intensity-based size distribution histograms.** Size distribution of redaporfin formulation micelles measured by light scattering technique (average size = 122 ± 48.44 nm)..... 134
- Figure 24. **Absorption spectra of redaporfin in *in vivo* formulation.** Formulation for *in vivo* intravenous administration was prepared by dissolving redaporfin powder in ethanol:Kolliphor®EL (5:1) and then diluted in saline 0.9 % achieving a final ratio of saline:ethanol:Kolliphor®EL of 98.8:1:0.2..... 134

iv. List of Tables

Table 1. Molecular structures of some photosensitizers for PDT, as well as their excitation wavelength.	11
Table 2. Description of terms and abbreviations referred over this thesis.	13
Table 3. Cell lines description. Description of several cell lines implemented <i>in vitro</i> and <i>in vivo</i> experiments to evaluate the efficacy of photodynamic therapy and reported in this thesis.	17
Table 4. List of animal models. Description of animal models implemented in photodynamic therapy <i>in vivo</i> experiments and reported over this thesis.	19
Table 5. PDT protocols with several photosensitizers and tumor models uncovering the importance of the immune system for the outcome of the treatment. Rechallenge refers to the ability of PDT treated animals acquire immune memory and reject a rechallenge with untreated tumor cells. Immunization refers to experiments where PDT treated cancer cells are administered to healthy animals and confer protection to rechallenge. Percentages refers to percentage of cures.	32
Table 6. Macroscopic evaluation score criteria for PDT treatment impact on primary tumors.	97
Table 7. PDT parameters of the several tested protocols for B16F10 melanoma model. Drug and light doses were tested to obtain the best outcome in terms of impact on treatment. Macroscopic alterations on tumor, as edema and necrosis, were evaluated and scored according to Table 6.....	98
Table 8. Redaporfin-PDT parameters of the several tested protocols for 4T1-luc2 mammary carcinoma model. Drug and light doses, illumination spot diameter and fluence were tested to obtain the best outcome in terms of impact on treatment. Macroscopic alterations on tumor, as edema and necrosis, were evaluated and scored according to Table 6 criteria. o.t. - orthotopic; s.c. - subcutaneous; Prtcl - Protocol: V - vascular protocol; C - cellular protocol; CV - cellular and vascular protocol; TV/TC - transversal irradiation of tumor with vascular/cellular protocol. * optimization protocols previously reported in ²⁶⁸	101
Table 9. Redaporfin concentrations and light dose tested in the <i>in vitro</i> PDT protocols. Several redaporfin concentrations were tested <i>in vitro</i> with three different cell lines. The concentration in bold was the one that was selected to be further analyzed by flow cytometry.....	111

8

REFERENCES

- (1) Dolmans, D. E. J. G. J.; Fukumura, D.; Jain, R. K. Photodynamic Therapy for Cancer. *Nat. Rev. Cancer* **2003**, *3* (5), 380–387 doi:10.1038/nrc1071.
- (2) Silva, E. F. F.; Serpa, C.; Dąbrowski, J. M.; Monteiro, C. J. P.; Formosinho, S. J.; Stochel, G.; Urbanska, K.; Simões, S.; Pereira, M. M.; Arnaut, L. G. Mechanisms of Singlet-Oxygen and Superoxide-Ion Generation by Porphyrins and Bacteriochlorins and Their Implications in Photodynamic Therapy. *Chem. - A Eur. J.* **2010**, *16* (30), 9273–9286 doi:10.1002/chem.201000111.
- (3) Abrahamse, H.; Hamblin, M. R. New Photosensitizers for Photodynamic Therapy. *Biochem. J.* **2016**, *473* (4), 347–364 doi:10.1042/BJ20150942.
- (4) Castano, A. P.; Demidova, T. N.; Hamblin, M. R. Mechanisms in Photodynamic Therapy: Part One - Photosensitizers, Photochemistry and Cellular Localization. *Photodiagnosis Photodyn. Ther.* **2004**, *1* (4), 279–293 doi:10.1016/S1572-1000(05)00007-4.
- (5) Plaetzer, K.; Krammer, B.; Berlanda, J.; Berr, F.; Kiesslich, T. Photophysics and Photochemistry of Photodynamic Therapy: Fundamental Aspects. *Lasers Med. Sci.* **2009**, *24* (2), 259–268 doi:10.1007/s10103-008-0539-1.
- (6) Dougherty, T. J.; Kaufman, J. E.; Goldfarb, A.; Weishaupt, K. R.; Boyle, D.; Mittleman, A. Photoradiation Therapy for the Treatment of Malignant Tumors. *Cancer Res.* **1978**, *38* (8), 2628–2635.
- (7) Divaris, D. X. G.; Kennedy, J. C.; Pottier, R. H. Phototoxic Damage to Sebaceous Glands and Hair Follicles of Mice after Systemic Administration of 5-Aminolevulinic Acid Correlates with Localized Protoporphyrin IX Fluorescence. *Am. J. Pathol.* **1990**, *136* (4), 891–897.
- (8) el-Sharabasy, M.; El-Waseef, A.; Hafez, M.; Salim, S. Porphyrin Metabolism in Some Malignant Diseases. *Br. J. Cancer* **1992**, *65* (3), 409–412 doi:10.1038/bjc.1992.83.
- (9) Ma, L.; Moan, J.; Berg, K. Evaluation of a New Photosensitizer, Meso-tetra-

- hydroxyphenyl-chlorin, for Use in Photodynamic Therapy: A Comparison of Its Photobiological Properties with Those of Two Other Photosensitizers. *Int. J. Cancer* **1994**, *57* (6), 883–888 doi:10.1002/ijc.2910570618.
- (10) Rezzoug, H.; Barberi-Heyob, M.; Merlin, J. L.; Bolotine, L.; Lignon, D.; Guillemin, F. In Vitro Comparison of the Photodynamic Activity of Meso-Tetra (m-Hydroxyphenyl) Chlorin and Hematoporphyrin Derivative. *Bull. Cancer* **1996**, *83* (10), 816–822.
- (11) Kato, H.; Furukawa, K.; Sato, M.; Okunaka, T.; Kusunoki, Y.; Kawahara, M.; Fukuoka, M.; Miyazawa, T.; Yana, T.; Matsui, K.; Shiraishi, T.; Horinouchi, H. Phase II Clinical Study of Photodynamic Therapy Using Mono-l-Aspartyl Chlorin E6 and Diode Laser for Early Superficial Squamous Cell Carcinoma of the Lung. *Lung Cancer* **2003**, *42* (1), 103–111 doi:10.1016/S0169-5002(03)00242-3.
- (12) Scott, L. J.; Goa, K. L. Verteporfin. *Drugs Aging* **2000**, *16* (2), 139–146 doi:10.2165/00002512-200016020-00005.
- (13) Richter, A.; Waterfield, E.; Jain, A.; Allison, B.; Sternberg, E.; Dolphin, D.; Levy, J. Photosensitising Potency of Structural Analogues of Benzoporphyrin Derivative (BPD) in a Mouse Tumour Model. *Br. J. Cancer* **1991**, *63* (1), 87–93 doi:10.1038/bjc.1991.18.
- (14) Brandis, A.; Mazor, O.; Neumark, E.; Rosenbach-Belkin, V.; Salomon, Y.; Scherz, A. Novel Water-Soluble Bacteriochlorophyll Derivatives for Vascular-Targeted Photodynamic Therapy: Synthesis, Solubility, Phototoxicity, and the Effect of Serum Proteins. *Photochem. Photobiol.* **2005**, *81* (4), 983–993 doi:10.1562/2004-12-01-RA-389.
- (15) Mazor, O.; Brandis, A.; Plaks, V.; Neumark, E.; Rosenbach-Belkin, V.; Salomon, Y.; Scherz, A. WST11, A Novel Water-Soluble Bacteriochlorophyll Derivative; Cellular Uptake, Pharmacokinetics, Biodistribution, and Vascular Targeted Photodynamic Activity Against Melanoma Tumors. *Photochem. Photobiol.* **2004**, *81* (2), 342–351 doi:10.1562/2004-06-14-RA-199.
- (16) Arnaut, L. G.; Pereira, M. M.; Dąbrowski, J. M.; Silva, E. F. F. F.; Schaberle, F. A.; Abreu, A. R.; Rocha, L. B.; Barsan, M. M.; Urbańska, K.; Stochel, G.; Brett, C. M. A. a. Photodynamic Therapy Efficacy Enhanced by Dynamics: The Role of Charge Transfer and Photostability in the Selection of Photosensitizers. *Chem. - A Eur. J.* **2014**, *20* (18), 5346–5357 doi:10.1002/chem.201304202.

- (17) Rocha, L. B.; Gomes-da-Silva, L. C.; Dąbrowski, J. M.; Arnaut, L. G. Elimination of Primary Tumours and Control of Metastasis with Rationally Designed Bacteriochlorin Photodynamic Therapy Regimens. *Eur. J. Cancer* **2015**, *51* (13), 1822–1830 doi:10.1016/j.ejca.2015.06.002.
- (18) Saavedra, R.; Rocha, L. B.; Dabrowski, J. M.; Arnaut, L. G. Modulation of Biodistribution, Pharmacokinetics, and Photosensitivity with the Delivery Vehicle of a Bacteriochlorin Photosensitizer for Photodynamic Therapy. *ChemMedChem* **2014**, *9* (2), 390–398 doi:10.1002/cmdc.201300449.
- (19) Bashkatov, a N.; Genina, E. a; Kochubey, V. I.; Tuchin, V. V. Optical Properties of Human Skin, Subcutaneous and Mucous Tissues in the Wavelength Range from 400 to 2000 Nm. *J. Phys. D. Appl. Phys.* **2005**, *38* (15), 2543–2555 doi:10.1088/0022-3727/38/15/004.
- (20) Mallidi, S.; Anbil, S.; Bulin, A. L.; Obaid, G.; Ichikawa, M.; Hasan, T. Beyond the Barriers of Light Penetration: Strategies, Perspectives and Possibilities for Photodynamic Therapy. *Theranostics* **2016**, *6* (13), 2458–2487 doi:10.7150/thno.16183.
- (21) Triesscheijn, M.; Baas, P.; Schellens, J. H. M.; Stewart, F. A. Photodynamic Therapy in Oncology. *Oncologist* **2006**, *11* (9), 1034–1044 doi:10.1634/theoncologist.11-9-1034.
- (22) Moan, J.; Berg, K. The Photodegradation of Porphyrins in Cells Can Be Used To Estimate the Lifetime of Singlet Oxygen. *Photochem. Photobiol.* **1991**, *53* (4), 549–553 doi:10.1111/j.1751-1097.1991.tb03669.x.
- (23) Liao, J. C.; Roider, J.; Jay, D. G. Chromophore-Assisted Laser Inactivation of Proteins Is Mediated by the Photogeneration of Free Radicals. *Proc. Natl. Acad. Sci.* **1994**, *91* (7), 2659–2663 doi:10.1073/pnas.91.7.2659.
- (24) da Silva, E. F. F.; Pedersen, B. W.; Breitenbach, T.; Toftegaard, R.; Kuimova, M. K.; Arnaut, L. G.; Ogilby, P. R. Irradiation- and Sensitizer-Dependent Changes in the Lifetime of Intracellular Singlet Oxygen Produced in a Photosensitized Process. *J. Phys. Chem. B* **2012**, *116* (1), 445–461 doi:10.1021/jp206739y.
- (25) Donohoe, C.; Senge, M. O.; Arnaut, L. G.; Gomes-da-Silva, L. C. Cell Death in Photodynamic Therapy: From Oxidative Stress to Anti-Tumor Immunity. *Biochim. Biophys. Acta - Rev. Cancer* **2019**, *1872* (2), 188308 doi:10.1016/j.bbcan.2019.07.003.
- (26) Pakos-Zebrucka, K.; Koryga, I.; Mnich, K.; Ljujic, M.; Samali, A.; Gorman, A.

- M. The Integrated Stress Response. *EMBO Rep.* **2016**, *17* (10), 1374–1395
doi:10.15252/embr.201642195.
- (27) Broekgaarden, M.; Weijer, R.; van Gulik, T. M.; Hamblin, M. R.; Heger, M. Tumor Cell Survival Pathways Activated by Photodynamic Therapy: A Molecular Basis for Pharmacological Inhibition Strategies. *Cancer Metastasis Rev.* **2015**, *34* (4), 643–690 doi:10.1007/s10555-015-9588-7.
- (28) Rocha, L. B.; Soares, H. T.; Mendes, M. I. P.; Cabrita, A.; Schaberle, F. A.; Arnaut, L. G. Necrosis Depth and Photodynamic Threshold Dose with Redaporfin-PDT. *Photochem. Photobiol.* **2020**, *96* (3), 692–698
doi:10.1111/php.13256.
- (29) Galluzzi, L.; Vitale, I.; Aaronson, S. A.; Abrams, J. M.; Adam, D.; Agostinis, P.; Alnemri, E. S.; Altucci, L.; Amelio, I.; Andrews, D. W.; Annicchiarico-Petruzzelli, M.; Antonov, A. V.; Arama, E.; Baehrecke, E. H.; Barlev, N. A.; Bazan, N. G.; Bernassola, F.; Bertrand, M. J. M.; Bianchi, K.; Blagosklonny, M. V.; Blomgren, K.; Borner, C.; Boya, P.; Brenner, C.; Campanella, M.; Candi, E.; Carmona-Gutierrez, D.; Cecconi, F.; Chan, F. K.-M.; Chandel, N. S.; Cheng, E. H.; Chipuk, J. E.; Cidlowski, J. A.; Ciechanover, A.; Cohen, G. M.; Conrad, M.; Cubillos-Ruiz, J. R.; Czabotar, P. E.; D'Angiolella, V.; Dawson, T. M.; Dawson, V. L.; De Laurenzi, V.; De Maria, R.; Debatin, K.-M.; DeBerardinis, R. J.; Deshmukh, M.; Di Daniele, N.; Di Virgilio, F.; Dixit, V. M.; Dixon, S. J.; Duckett, C. S.; Dynlacht, B. D.; El-Deiry, W. S.; Elrod, J. W.; Fimia, G. M.; Fulda, S.; García-Sáez, A. J.; Garg, A. D.; Garrido, C.; Gavathiotis, E.; Golstein, P.; Gottlieb, E.; Green, D. R.; Greene, L. A.; Gronemeyer, H.; Gross, A.; Hajnoczky, G.; Hardwick, J. M.; Harris, I. S.; Hengartner, M. O.; Hetz, C.; Ichijo, H.; Jäättelä, M.; Joseph, B.; Jost, P. J.; Juin, P. P.; Kaiser, W. J.; Karin, M.; Kaufmann, T.; Kepp, O.; Kimchi, A.; Kitsis, R. N.; Klionsky, D. J.; Knight, R. A.; Kumar, S.; Lee, S. W.; Lemasters, J. J.; Levine, B.; Linkermann, A.; Lipton, S. A.; Lockshin, R. A.; López-Otín, C.; Lowe, S. W.; Luedde, T.; Lugli, E.; MacFarlane, M.; Madeo, F.; Malewicz, M.; Malorni, W.; Manic, G.; Marine, J.-C.; Martin, S. J.; Martinou, J.-C.; Medema, J. P.; Mehlen, P.; Meier, P.; Melino, S.; Miao, E. A.; Molkenin, J. D.; Moll, U. M.; Muñoz-Pinedo, C.; Nagata, S.; Nuñez, G.; Oberst, A.; Oren, M.; Overholtzer, M.; Pagano, M.; Panaretakis, T.; Pasparakis, M.; Penninger, J. M.; Pereira, D. M.; Pervaiz, S.; Peter, M. E.; Piacentini, M.; Pinton, P.; Prehn, J. H. M.; Puthalakath, H.;

- Rabinovich, G. A.; Rehm, M.; Rizzuto, R.; Rodrigues, C. M. P.; Rubinsztein, D. C.; Rudel, T.; Ryan, K. M.; Sayan, E.; Scorrano, L.; Shao, F.; Shi, Y.; Silke, J.; Simon, H.-U.; Sistigu, A.; Stockwell, B. R.; Strasser, A.; Szabadkai, G.; Tait, S. W. G.; Tang, D.; Tavernarakis, N.; Thorburn, A.; Tsujimoto, Y.; Turk, B.; Vanden Berghe, T.; Vandenabeele, P.; Vander Heiden, M. G.; Villunger, A.; Virgin, H. W.; Vousden, K. H.; Vucic, D.; Wagner, E. F.; Walczak, H.; Wallach, D.; Wang, Y.; Wells, J. A.; Wood, W.; Yuan, J.; Zakeri, Z.; Zhivotovsky, B.; Zitvogel, L.; Melino, G.; Kroemer, G. Molecular Mechanisms of Cell Death: Recommendations of the Nomenclature Committee on Cell Death 2018. *Cell Death Differ.* **2018**, *25* (3), 486–541 doi:10.1038/s41418-017-0012-4.
- (30) Kroemer, G.; Galluzzi, L.; Kepp, O.; Zitvogel, L. Immunogenic Cell Death in Cancer Therapy. *Annu. Rev. Immunol.* **2013**, *31* (1), 51–72 doi:10.1146/annurev-immunol-032712-100008.
- (31) Galluzzi, L.; Humeau, J.; Buqué, A.; Zitvogel, L.; Kroemer, G. Immunostimulation with Chemotherapy in the Era of Immune Checkpoint Inhibitors. *Nat. Rev. Clin. Oncol.* **2020** doi:10.1038/s41571-020-0413-z.
- (32) Kabingu, E.; Oseroff, A. R.; Wilding, G. E.; Gollnick, S. O. Enhanced Systemic Immune Reactivity to a Basal Cell Carcinoma Associated Antigen Following Photodynamic Therapy. *Clin. Cancer Res.* **2009**, *15* (13), 4460–4466 doi:10.1158/1078-0432.CCR-09-0400.
- (33) Anzengruber, F.; Avci, P.; de Freitas, L. F.; Hamblin, M. R. T-Cell Mediated Anti-Tumor Immunity after Photodynamic Therapy: Why Does It Not Always Work and How Can We Improve It? *Photochem. Photobiol. Sci.* **2015**, *14* (8), 1492–1509 doi:10.1039/C4PP00455H.
- (34) Reginato, E.; Lindenmann, J.; Langner, C.; Schweintzger, N.; Bambach, I.; Smolle-Jüttner, F.; Wolf, P. Photodynamic Therapy Downregulates the Function of Regulatory T Cells in Patients with Esophageal Squamous Cell Carcinoma. *Photochem. Photobiol. Sci.* **2014**, *13* (9), 1281–1289 doi:10.1039/c4pp00186a.
- (35) Castano, A. P.; Liu, Q.; Hamblin, M. R. A Green Fluorescent Protein-Expressing Murine Tumour but Not Its Wild-Type Counterpart Is Cured by Photodynamic Therapy. *Br. J. Cancer* **2006**, *94* (3), 391–397 doi:10.1038/sj.bjc.6602953.
- (36) Mroz, P.; Szokalska, A.; Wu, M. X.; Hamblin, M. R. Photodynamic Therapy of Tumors Can Lead to Development of Systemic Antigen-Specific Immune Response. *PLoS One* **2010**, *5* (12) doi:10.1371/journal.pone.0015194.

- (37) Mroz, P.; Vatansever, F.; Muchowicz, A.; Hamblin, M. R. Photodynamic Therapy of Murine Mastocytoma Induces Specific Immune Responses against the Cancer/Testis Antigen P1A. *Cancer Res.* **2013**, *73* (21), 6462–6470 doi:10.1158/0008-5472.CAN-11-2572.
- (38) Dąbrowski, J. M.; Arnaut, L. G. Photodynamic Therapy (PDT) of Cancer: From Local to Systemic Treatment. *Photochem. Photobiol. Sci.* **2015**, *14* (10), 1765–1780 doi:10.1039/C5PP00132C.
- (39) Cantl, G.; Lattuada, D.; Nicolin, A.; Taroni, P.; Valentinl, G.; Cubeddu, R. Antitumor Immunity Induced by Photodynamic Therapy with Aluminum Disulfonated Phthalocyanines and Laser Light. *Anticancer. Drugs* **1994**, *5* (4), 443–447 doi:10.1097/00001813-199408000-00009.
- (40) Korbelik, M. M.; Krosł, G.; Krosł, J.; Dougherty, G. J. The Role of Host Lymphoid Populations in the Response of Mouse EMT6 Tumor to Photodynamic Therapy. *Cancer Res.* **1996**, *56* (24), 5647–5652.
- (41) Korbelik, M. Induction of Tumor Immunity by Photodynamic Therapy. *J. Clin. Laser Med. Surg.* **1996**, *14* (5), 329–334.
- (42) Korbelik, M.; Dougherty, G. J. Photodynamic Therapy-Mediated Immune Response against Subcutaneous Mouse Tumors. *Cancer Res.* **1999**, *59* (8), 1941–1946.
- (43) Henderson, B. W.; Gollnick, S. O.; Snyder, J. W.; Busch, T. M.; Kousis, P. C.; Cheney, R. T.; Morgan, J. Choice of Oxygen-Conserving Treatment Regimen Determines the Inflammatory Response and Outcome of Photodynamic Therapy of Tumors. *Cancer Res.* **2004**, *64* (6), 2120–2126 doi:10.1158/0008-5472.CAN-03-3513.
- (44) De Vree, W. J. A.; Essers, M. C.; De Bruijn, H. S.; Star, W. M.; Koster, J. F.; Sluiter, W. Evidence for an Important Role of Neutrophils in the Efficacy of Photodynamic Therapy in Vivo. *Cancer Res.* **1996**, *56* (13), 2908–2911.
- (45) Korbelik, M.; Cecic, I. Contribution of Myeloid and Lymphoid Host Cells to the Curative Outcome of Mouse Sarcoma Treatment by Photodynamic Therapy. *Cancer Lett.* **1999**, *137* (1), 91–98 doi:10.1016/S0304-3835(98)00349-8.
- (46) Hendrzak-Henion, J. A.; Knisely, T. L.; Cincotta, L.; Cincotta, E.; Cincotta, A. H. Role of the Immune System in Mediating the Antitumor Effect of Benzophenothiazine Photodynamic Therapy. *Photochem. Photobiol.* **1999**, *69* (5), 575–581 doi:10.1111/j.1751-1097.1999.tb03330.x.

- (47) Hwang, H. S.; Shin, H.; Han, J.; Na, K. Combination of Photodynamic Therapy (PDT) and Anti-Tumor Immunity in Cancer Therapy. *J. Pharm. Investig.* **2018**, *48* (2), 143–151 doi:10.1007/s40005-017-0377-x.
- (48) Korbelik, M. PDT-Associated Host Response and Its Role in the Therapy Outcome. *Lasers Surg. Med.* **2006**, *38* (5), 500–508 doi:10.1002/lsm.20337.
- (49) Korbelik, M.; Sun, J.; Cecic, I. Photodynamic Therapy-Induced Cell Surface Expression and Release of Heat Shock Proteins: Relevance for Tumor Response. *Cancer Res.* **2005**, *65* (3), 1018–1026.
- (50) Zaidi, S. I. A.; Mukhtar, H.; Oleinick, N. L. Phospholipase Activation Triggers Apoptosis in Photosensitized Mouse Lymphoma Cells. *Cancer Res.* **1993**.
- (51) Korbelik, M. Role of Toll-like Receptors in Photodynamic-Therapy-Elicited Host Response. In *Laser Interaction with Tissue and Cells XV*; Jacques, S. L., Roach, W. P., Eds.; 2004; Vol. 5319, p 87 doi:10.1117/12.529783.
- (52) Korbelik, M.; Cecic, I. Deposition of Complement Proteins on Cells Treated by Photodynamic Therapy in Vitro. *J. Environ. Pathol. Toxicol. Oncol.* **2006**, *25* (1–2), 189–204 doi:10.1615/JEnvironPatholToxicolOncol.v25.i1-2.110.
- (53) Korbelik, M.; Cecic, I.; Merchant, S.; Sun, J. Acute Phase Response Induction by Cancer Treatment with Photodynamic Therapy. *Int. J. Cancer* **2008**, *122* (6), 1411–1417 doi:10.1002/ijc.23248.
- (54) Xie, Y.; Wei, Z.-B.; Zhang, Z.; Wen, W.; Huang, G.-W.; Huang. Effect of 5-ALA-PDT on VEGF and PCNA Expression in Human NPC-Bearing Nude Mice. *Oncol. Rep.* **2009**, *22* (06), 1365–1371 doi:10.3892/or_00000576.
- (55) Wang, X.; Ji, J.; Zhang, H.; Fan, Z.; Zhang, L.; Shi, L.; Zhou, F.; Chen, W. R.; Wang, H.; Wang, X. Stimulation of Dendritic Cells by DAMPs in ALA-PDT Treated SCC Tumor Cells. *Oncotarget*, **2015**, *6* (42), 44688.
- (56) Bhatta, A. K.; Wang, P.; Keyal, U.; Zhao, Z.; Ji, J.; Zhu, L.; Wang, X.; Zhang, G. Therapeutic Effect of Imiquimod Enhanced ALA-PDT on Cutaneous Squamous Cell Carcinoma. *Photodiagnosis Photodyn. Ther.* **2018**, *23* (June), 273–280 doi:10.1016/j.pdpdt.2018.07.010.
- (57) Kammerer, R.; Buchner, A.; Palluch, P.; Pongratz, T.; Oboukhovskij, K.; Beyer, W.; Johansson, A.; Stepp, H.; Baumgartner, R.; Zimmermann, W. Induction of Immune Mediators in Glioma and Prostate Cancer Cells by Non-Lethal Photodynamic Therapy. *PLoS One* **2011**, *6* (6), e21834 doi:10.1371/journal.pone.0021834.

- (58) Ji, J.; Fan, Z.; Zhou, F.; Wang, X. X.; Shi, L.; Zhang, H.; Wang, P.; Yang, D.; Zhang, L.; Chen, W. R.; Wang, X. X. Improvement of DC Vaccine with ALA-PDT Induced Immunogenic Apoptotic Cells for Skin Squamous Cell Carcinoma. *Oncotarget* **2015**, *6* (19), 17135–17146 doi:10.18632/oncotarget.3529.
- (59) Zhang, H.; Wang, P.; Wang, X.; Shi, L.; Fan, Z.; Zhang, G.; Yang, D.; Bahavar, C. F.; Zhou, F.; Chen, W. R.; Wang, X. Antitumor Effects of DC Vaccine With ALA-PDT-Induced Immunogenic Apoptotic Cells for Skin Squamous Cell Carcinoma in Mice. *Technol. Cancer Res. Treat.* **2018**, *17*, 1–10 doi:10.1177/1533033818785275.
- (60) Ji, J.; Zhang, Y.; Chen, W. R.; Wang, X. DC Vaccine Generated by ALA-PDT-Induced Immunogenic Apoptotic Cells for Skin Squamous Cell Carcinoma. *Oncoimmunology* **2016**, *5* (6), e1072674 doi:10.1080/2162402X.2015.1072674.
- (61) Sanovic, R.; Verwanger, T.; Hartl, A.; Krammer, B. Low Dose Hypericin-PDT Induces Complete Tumor Regression in BALB/c Mice Bearing CT26 Colon Carcinoma. *Photodiagnosis Photodyn. Ther.* **2011**, *8* (4), 291–296 doi:10.1016/j.pdpdt.2011.04.003.
- (62) Blank, M.; Lavie, G.; Mandel, M.; Keisari, Y. Effects of Photodynamic Therapy With Hypericin in Mice Bearing Highly Invasive Solid Tumors. *Oncol. Res. Featur. Preclin. Clin. Cancer Ther.* **2001**, *12* (9), 409–418 doi:10.3727/096504001108747864.
- (63) Zheng, Y.; Yin, G.; Le, V.; Zhang, A.; Chen, S. Y.; Liang, X.; Liu, J. W. Photodynamic-Therapy Activates Immune Response by Disrupting Immunity Homeostasis of Tumor Cells, Which Generates Vaccine for Cancer Therapy. *Int. J. Biol. Sci.* **2016**, *12* (1), 120–132 doi:10.7150/ijbs.12852.
- (64) Bhuvaneswari, R.; Yuen, G. Y.; Chee, S. K.; Olivo, M. Hypericin-Mediated Photodynamic Therapy in Combination with Avastin (Bevacizumab) Improves Tumor Response by Downregulating Angiogenic Proteins. *Photochem. Photobiol. Sci.* **2007**, *6* (12), 1275 doi:10.1039/b705763f.
- (65) Wang, X.; Hu, J.; Wang, P.; Zhang, S.; Liu, Y.; Xiong, W.; Liu, Q. Analysis of the In Vivo and In Vitro Effects of Photodynamic Therapy on Breast Cancer by Using a Sensitizer, Sinoporphyrin Sodium. *Theranostics* **2015**, *5* (7), 772–786 doi:10.7150/thno.10853.
- (66) Shams, M.; Owczarczak, B.; Manderscheid-Kern, P.; Bellnier, D. A.; Gollnick, S. O. Development of Photodynamic Therapy Regimens That Control Primary

- Tumor Growth and Inhibit Secondary Disease. *Cancer Immunol. Immunother.* **2015**, *64* (3), 287–297 doi:10.1007/s00262-014-1633-9.
- (67) Wu, D.; Liu, Z.; Fu, Y.; Zhang, Y.; Tang, N.; Wang, Q.; Tao, L. Efficacy of 2-(1-Hexyloxyethyl)-2-Devinyl Pyrropeophorbide-a in Photodynamic Therapy of Human Esophageal Squamous Cancer Cells. *Oncol. Lett.* **2013**, *6* (4), 1111–1119 doi:10.3892/ol.2013.1493.
- (68) Cecic, I.; Parkins, C. S.; Korbelik, M. Induction of Systemic Neutrophil Response in Mice by Photodynamic Therapy of Solid Tumors. *Photochem. Photobiol.* **2001**, *74* (5), 712 doi:10.1562/0031-8655(2001)074<0712:IOSNRI>2.0.CO;2.
- (69) Kabingu, E.; Vaughan, L.; Owczarczak, B.; Ramsey, K. D.; Gollnick, S. O. CD8+ T Cell-Mediated Control of Distant Tumours Following Local Photodynamic Therapy Is Independent of CD4+ T Cells and Dependent on Natural Killer Cells. *Br. J. Cancer* **2007**, *96* (12), 1839–1848 doi:10.1038/sj.bjc.6603792.
- (70) Korbelik, M.; Sun, J.; Zeng, H. Ischaemia-Reperfusion Injury in Photodynamic Therapy-Treated Mouse Tumours. *Br. J. Cancer* **2003**, *88* (5), 760–766 doi:10.1038/sj.bjc.6600792.
- (71) Gomer, C. J.; Ferrario, A.; Murphree, A. L. The Effect of Localized Porphyrin Photodynamic Therapy on the Induction of Tumour Metastasis. *Br. J. Cancer* **1987**, *56* (1), 27–32 doi:10.1038/bjc.1987.147.
- (72) Peterson, C. M.; Reed, R.; Jolles, C. J.; Jones, K. P.; Straight, R. C.; Poulson, A. M. Photodynamic Therapy of Human Ovarian Epithelial Carcinoma, OVCAR-3, Heterotransplanted in the Nude Mouse. *Am. J. Obstet. Gynecol.* **1992**, *167* (6), 1852–1855 doi:10.1016/0002-9378(92)91786-A.
- (73) Adams, K.; Rainbow, A. J.; Wilson, B. C.; Singh, G. In Vivo Resistance to Photofrin-Mediated Photodynamic Therapy in Radiation-Induced Fibrosarcoma Cells Resistant to in Vitro Photofrin-Mediated Photodynamic Therapy. *J. Photochem. Photobiol. B Biol.* **1999**, *49* (2–3), 136–141 doi:10.1016/S1011-1344(99)00047-0.
- (74) Tong, Z.; Miao, P.; Liu, T.; Jia, Y.; Liu, X. Enhanced Antitumor Effects of BPD-MA-Mediated Photodynamic Therapy Combined with Adriamycin on Breast Cancer in Mice. *Acta Pharmacol. Sin.* **2012**, *33* (10), 1319–1324 doi:10.1038/aps.2012.45.

- (75) Muchowicz, A.; Wachowska, M.; Stachura, J.; Tonecka, K.; Gabrysiak, M.; Wołosz, D.; Pilch, Z.; Kilarski, W. W.; Boon, L.; Klaus, T. J.; Golab, J. Inhibition of Lymphangiogenesis Impairs Antitumour Effects of Photodynamic Therapy and Checkpoint Inhibitors in Mice. *Eur. J. Cancer* **2017**, *83*, 19–27 doi:10.1016/j.ejca.2017.06.004.
- (76) Samkoe, K. S.; Chen, A.; Rizvi, I.; O'Hara, J. A.; Hoopes, P. J.; Pereira, S. P.; Hasan, T.; Pogue, B. W. Imaging Tumor Variation in Response to Photodynamic Therapy in Pancreatic Cancer Xenograft Models. *Int. J. Radiat. Oncol.* **2010**, *76* (1), 251–259 doi:10.1016/j.ijrobp.2009.08.041.
- (77) Reginato, E.; Mroz, P.; Chung, H.; Kawakubo, M.; Wolf, P.; Hamblin, M. R. Photodynamic Therapy plus Regulatory T-Cell Depletion Produces Immunity against a Mouse Tumour That Expresses a Self-Antigen. *Br. J. Cancer* **2013**, *109* (8), 2167–2174 doi:10.1038/bjc.2013.580.
- (78) Castano, A. P.; Mroz, P.; Wu, M. X.; Hamblin, M. R. Photodynamic Therapy plus Low-Dose Cyclophosphamide Generates Antitumor Immunity in a Mouse Model. *Proc. Natl. Acad. Sci.* **2008**, *105* (14), 5495–5500 doi:10.1073/pnas.0709256105.
- (79) Molpus, K. L.; Kato, D.; Hamblin, M. R.; Lilge, L.; Bamberg, M.; Hasan, T. Intraperitoneal Photodynamic Therapy of Human Epithelial Ovarian Carcinomatosis in a Xenograft Murine Model. *Cancer Res.* **1996**, *56* (5), 1075–1082.
- (80) Korbelik, M.; Sun, J. Photodynamic Therapy-Generated Vaccine for Cancer Therapy. *Cancer Immunol. Immunother.* **2006**, *55* (8), 900–909 doi:10.1007/s00262-005-0088-4.
- (81) Gil, M.; Bieniasz, M.; Seshadri, M.; Fisher, D.; Ciesielski, M. J.; Chen, Y.; Pandey, R. K.; Kozbor, D. Photodynamic Therapy Augments the Efficacy of Oncolytic Vaccinia Virus against Primary and Metastatic Tumours in Mice. *Br. J. Cancer* **2011**, *105* (10), 1512–1521 doi:10.1038/bjc.2011.429.
- (82) Grossman, C. E.; Pickup, S.; Durham, A.; Wileyto, E. P.; Putt, M. E.; Busch, T. M. Photodynamic Therapy of Disseminated Non-Small Cell Lung Carcinoma in a Murine Model. *Lasers Surg. Med.* **2011**, *43* (7), 663–675 doi:10.1002/lsm.21102.
- (83) Korbelik, M.; Sun, J. Cancer Treatment by Photodynamic Therapy Combined with Adoptive Immunotherapy Using Genetically Altered Natural Killer Cell

- Line. *Int. J. Cancer* **2001**, *93* (2), 269–274 doi:10.1002/ijc.1326.
- (84) Separovic. Enhanced Tumor Cures after Foscan Photodynamic Therapy Combined with the Ceramide Analog LCL29. Evidence from Mouse Squamous Cell Carcinomas for Sphingolipids as Biomarkers of Treatment Response. *Int. J. Oncol.* **2011**, *38* (2) doi:10.3892/ijo.2010.863.
- (85) Pucelik, B.; Arnaut, L. G.; Stochel, G.; Dabrowski, J. M. Design of Pluronic-Based Formulation for Enhanced Redaporfin-Photodynamic Therapy against Pigmented Melanoma. *ACS Appl. Mater. Interfaces* **2016**, *8* (34), 22039–22055 doi:10.1021/acsami.6b07031.
- (86) Rocha, L. B.; Schaberle, F.; Dąbrowski, J. M.; Simões, S.; Arnaut, L. G. Intravenous Single-Dose Toxicity of Redaporfin-Based Photodynamic Therapy in Rodents. *Int. J. Mol. Sci.* **2015**, *16* (12), 29236–29249 doi:10.3390/ijms161226162.
- (87) Karwicka, M.; Pucelik, B.; Gonet, M.; Elas, M.; Dąbrowski, J. M. Effects of Photodynamic Therapy with Redaporfin on Tumor Oxygenation and Blood Flow in a Lung Cancer Mouse Model. *Sci. Rep.* **2019**, *9* (1), 1–15 doi:10.1038/s41598-019-49064-6.
- (88) Krzykawska-Serda, M.; Dąbrowski, J. M.; Arnaut, L. G.; Szczygieł, M.; Urbańska, K.; Stochel, G.; Elas, M. The Role of Strong Hypoxia in Tumors after Treatment in the Outcome of Bacteriochlorin-Based Photodynamic Therapy. *Free Radic. Biol. Med.* **2014**, *73*, 239–251 doi:10.1016/j.freeradbiomed.2014.05.003.
- (89) Preise, D.; Oren, R.; Glinert, I.; Kalchenko, V.; Jung, S.; Scherz, A.; Salomon, Y. Systemic Antitumor Protection by Vascular-Targeted Photodynamic Therapy Involves Cellular and Humoral Immunity. *Cancer Immunol. Immunother.* **2009**, *58* (1), 71–84 doi:10.1007/s00262-008-0527-0.
- (90) Corradi, R. B.; LaRosa, S.; Jebiwott, S.; Murray, K. S.; Rosenzweig, B.; Somma, A. J.; Gomez, R. S.; Scherz, A.; Kim, K.; Coleman, J. A. Effectiveness of the Combination of Vascular Targeted Photodynamic Therapy and Anti-Cytotoxic T-Lymphocyte-Associated Antigen 4 in a Preclinical Mouse Model of Urothelial Carcinoma. *Int. J. Urol.* **2019**, *26* (3), 414–422 doi:10.1111/iju.13878.
- (91) Yeung, H. Y.; Lo, P. C.; Ng, D. K. P.; Fong, W. P. Anti-Tumor Immunity of BAM-SiPc-Mediated Vascular Photodynamic Therapy in a BALB/c Mouse Model. *Cell. Mol. Immunol.* **2017**, *14* (2), 223–234 doi:10.1038/cmi.2015.84.

- (92) Leung, S. C. H.; Lo, P.-C.; Ng, D. K. P.; Liu, W.-K.; Fung, K.-P.; Fong, W.-P. Photodynamic Activity of BAM-SiPc, an Unsymmetrical Bisamino Silicon(IV) Phthalocyanine, in Tumour-Bearing Nude Mice. *Br. J. Pharmacol.* **2008**, *154* (1), 4–12 doi:10.1038/bjp.2008.82.
- (93) Saji, H.; Song, W.; Furumoto, K.; Kato, H.; Engleman, E. G. Systemic Antitumor Effect of Intratumoral Injection of Dendritic Cells in Combination with Local Photodynamic Therapy. *Clin. Cancer Res.* **2006**, *12* (8), 2568–2574 doi:10.1158/1078-0432.CCR-05-1986.
- (94) Yang, Y.; Hu, Y.; Wang, H. Targeting Antitumor Immune Response for Enhancing the Efficacy of Photodynamic Therapy of Cancer: Recent Advances and Future Perspectives. *Oxid. Med. Cell. Longev.* **2016**, *2016* (1) doi:10.1155/2016/5274084.
- (95) Mroz, P.; Hashmi, J. T.; Huang, Y.-Y.; Lange, N.; Hamblin, M. R. Stimulation of Anti-Tumor Immunity by Photodynamic Therapy. *Expert Rev. Clin. Immunol.* **2011**, *7* (1), 75–91 doi:10.1586/eci.10.81.
- (96) Gollnick, S. O.; Evans, S. S.; Baumann, H.; Owczarczak, B.; Maier, P.; Vaughan, L.; Wang, W. C.; Unger, E.; Henderson, B. W. Role of Cytokines in Photodynamic Therapy-Induced Local and Systemic Inflammation. *Br. J. Cancer* **2003**, *88* (11), 1772–1779 doi:10.1038/sj.bjc.6600864.
- (97) Evans, S.; Matthews, W.; Perry, R.; Fraker, D.; Norton, J.; Pass, H. I. Effect of Photodynamic Therapy on Tumor Necrosis Factor Production by Murine Macrophages. *J. Natl. Cancer Inst.* **1990**, *82* (1), 34–39 doi:10.1093/jnci/82.1.34.
- (98) Kick, G.; Messer, G.; Goetz, A.; Plewig, G.; Kind, P. Photodynamic Therapy Induces Expression of Interleukin 6 by Activation of AP-1 but Not NF-KB DNA Binding. *Cancer Res.* **1995**, *55* (11), 2373–2379.
- (99) Gollnick, S. O.; Liu, X.; Owczarczak, B.; Musser, D. A.; Henderson, B. W. Altered Expression of Interleukin 6 and Interleukin 10 as a Result of Photodynamic Therapy in Vivo. *Cancer Res.* **1997**, *57* (18), 3904–3909.
- (100) Cecic, I.; Stott, B.; Korbelik, M. Acute Phase Response-Associated Systemic Neutrophil Mobilization in Mice Bearing Tumors Treated by Photodynamic Therapy. *Int. Immunopharmacol.* **2006**, *6* (8), 1259–1266 doi:10.1016/j.intimp.2006.03.008.
- (101) Cecic, I.; Serrano, K.; Gyongyossy-Issa, M.; Korbelik, M. Characteristics of Complement Activation in Mice Bearing Lewis Lung Carcinomas Treated by

- Photodynamic Therapy. *Cancer Lett.* **2005**, 225 (2), 215–223
doi:10.1016/j.canlet.2004.11.059.
- (102) Stott, B.; Korbelik, M. Activation of Complement C3, C5, and C9 Genes in Tumors Treated by Photodynamic Therapy. *Cancer Immunol. Immunother.* **2007**, 56 (5), 649–658 doi:10.1007/s00262-006-0221-z.
- (103) Cecic, I.; Sun, J.; Korbelik, M. Role of Complement Anaphylatoxin C3a in Photodynamic Therapy-Elicited Engagement of Host Neutrophils and Other Immune Cells. *Photochem. Photobiol.* **2006**, 82 (2), 558 doi:10.1562/2005-09-09-ra-681.
- (104) De Vree, W. J. A.; Essers, M. C.; Koster, J. F.; Sluiter, W. Role of Interleukin 1 and Granulocyte Colony-Stimulating Factor in Photofrin-Based Photodynamic Therapy of Rat Rhabdomyosarcoma Tumors. *Cancer Res.* **1997**, 57 (13), 2555–2558.
- (105) Cecic, I.; Korbelik, M. Mediators of Peripheral Blood Neutrophilia Induced by Photodynamic Therapy of Solid Tumors. *Cancer Lett.* **2002**, 183 (1), 43–51 doi:10.1016/S0304-3835(02)00092-7.
- (106) Zióikowski, P.; Symonowicz, K.; Milach, J.; Zawirska, B.; Szkudlarek, T. In Vivo Tumor Necrosis Factor-Alpha Induction Following Chlorin E6-Photodynamic Therapy in Buffalo Rats. *Neoplasma* **1997**.
- (107) Nseyo, U. O.; Whalen, R. K.; Duncan, M. R.; Berman, B.; Lundahl, S. L. Urinary Cytokines Following Photodynamic Therapy for Bladder Cancer a Preliminary Report. *Urology* **1990** doi:10.1016/0090-4295(90)80220-H.
- (108) Yom, S. S.; Busch, T. M.; Friedberg, J. S.; Wileyto, E. P.; Smith, D.; Glatstein, E.; Hahn, S. M. Elevated Serum Cytokine Levels in Mesothelioma Patients Who Have Undergone Pleurectomy or Extrapleural Pneumonectomy and Adjuvant Intraoperative Photodynamic Therapy. *Photochem. Photobiol.* **2003**, 78 (1), 75 doi:10.1562/0031-8655(2003)078<0075:ESCLIM>2.0.CO;2.
- (109) Granville, D. J.; McManus, B. M.; Hunt, D. W. C. Photodynamic Therapy: Shedding Light on the Biochemical Pathways Regulating Porphyrin-Mediated Cell Death. *Histol. Histopathol.* **2001**, 16 (1), 309–317 doi:10.14670/HH-16.309.
- (110) Nowis, D.; Makowski, M.; Stokłosa, T.; Legat, M.; Issat, T.; Gołab, J. Direct Tumor Damage Mechanisms of Photodynamic Therapy. *Acta Biochim. Pol.* **2005**, 52 (2), 339–352 doi:10.18388/abp.2005_3447.
- (111) Hunt, D. W.; Levy, J. G. Immunomodulatory Aspects of Photodynamic Therapy.

- Expert Opin. Investig. Drugs* **1998**, 7 (1), 57–64 doi:10.1517/13543784.7.1.57.
- (112) Agostinis, P.; Berg, K.; Cengel, K. A.; Foster, T. H.; Girotti, A. W.; Gollnick, S. O.; Hahn, S. M.; Hamblin, M. R.; Juzeniene, A.; Kessel, D.; Korbelik, M.; Moan, J.; Mroz, P.; Nowiz, D.; Piette, J. J.; Willson, B. C.; Golab, J.; Nowis, D.; Piette, J. J.; Wilson, B. C.; Golab, J.; Nowiz, D.; Piette, J. J.; Willson, B. C.; Golab, J. Photodynamic Therapy of Cancer : An Update. *Am. Cancer Soc.* **2011**, 61 (4), 250–281 doi:10.3322/caac.20114.Available.
- (113) Sun, J.; Cecic, I.; Parkins, C. S.; Korbelik, M. Neutrophils as Inflammatory and Immune Effectors in Photodynamic Therapy-Treated Mouse SCCVII Tumours. *Photochem. Photobiol. Sci.* **2002**, 1 (9), 690–695 doi:10.1039/b204254a.
- (114) Chen, G. Y.; Nuñez, G. Sterile Inflammation: Sensing and Reacting to Damage. *Nat. Rev. Immunol.* **2010**, 10 (12), 826–837 doi:10.1038/nri2873.
- (115) Brackett, C. M.; Muhitch, J. B.; Evans, S. S.; Gollnick, S. O. IL-17 Promotes Neutrophil Entry into Tumor-Draining Lymph Nodes Following Induction of Sterile Inflammation. *J. Immunol.* **2013**, 191 (8), 4348–4357 doi:10.4049/jimmunol.1103621.
- (116) Janeway, C. A.; Travers, P.; Walport, M.; Shlomchik, M. J. The Complement System and Innate Immunity. In *Immunobiology: The Immune System in Health and Disease*; Garland Science: New York, 2001.
- (117) Cecic, I.; Minchinton, A. I.; Korbelik, M. The Impact of Complement Activation on Tumor Oxygenation During Photodynamic Therapy. *Photochem. Photobiol.* **2007**, 83 (5), 1049–1055 doi:10.1111/j.1751-1097.2007.00161.x.
- (118) Kajita, T.; Hugli, T. E. C5a-Induced Neutrophilia: A Primary Humoral Mechanism for Recruitment of Neutrophils. *Am. J. Pathol.* **1990**, 137 (2), 467–477.
- (119) Korbelik, M.; Sun, J.; Cecic, I.; Serrano, K. Adjuvant Treatment for Complement Activation Increases the Effectiveness of Photodynamic Therapy of Solid Tumors. *Photochem. Photobiol. Sci.* **2004**, 3 (8), 812 doi:10.1039/b315663j.
- (120) Korbelik, M.; Cooper, P. D. Potentiation of Photodynamic Therapy of Cancer by Complement: The Effect of γ -Inulin. *Br. J. Cancer* **2007**, 96 (1), 67–72 doi:10.1038/sj.bjc.6603508.
- (121) Akramienė, D.; Gražalienė, G.; Didžiapetrienė, J.; Kėvelaitis, E. Treatment of Lewis Lung Carcinoma by Photodynamic Therapy and Glucan from Barley. *Medicina (B. Aires).* **2009** doi:10.3390/medicina45060063.

- (122) Akramiene, D.; Aleksandraviciene, C.; Grazeliene, G.; Zalinkevicius, R.; Suziedelis, K.; Didziapetriene, J.; Simonsen, U.; Stankevicius, E.; Kevelaitis, E. Potentiating Effect of β -Glucans on Photodynamic Therapy of Implanted Cancer Cells in Mice. *Tohoku J. Exp. Med.* **2010** doi:10.1620/tjem.220.299.
- (123) Maeding, N.; Verwanger, T.; Krammer, B. Boosting Tumor-Specific Immunity Using PDT. *Cancers (Basel)*. **2016**, 8 (10), 91 doi:10.3390/cancers8100091.
- (124) Brackett, C. M.; Gollnick, S. O. Photodynamic Therapy Enhancement of Anti-Tumor Immunity. *Photochem. Photobiol. Sci.* **2011**, 10 (5), 649–652 doi:10.1039/c0pp00354a.
- (125) Krosi, G.; Korbelik, M.; Dougherty, G. J. Induction of Immune Cell Infiltration into Murine SCCVII Tumour by Photofrin-Based Photodynamic Therapy. *Br. J. Cancer* **1995**, 71 (3), 549–555 doi:10.1038/bjc.1995.108.
- (126) Kousis, P. C.; Henderson, B. W.; Maier, P. G.; Gollnick, S. O. Photodynamic Therapy Enhancement of Antitumor Immunity Is Regulated by Neutrophils. *Cancer Res.* **2007**, 67 (21), 10501–10510 doi:10.1158/0008-5472.CAN-07-1778.
- (127) Lobo, A. C. S.; Gomes-da-Silva, L. C.; Rodrigues-Santos, P.; Cabrita, A.; Santos-Rosa, M.; Arnaut, L. G. Immune Responses after Vascular Photodynamic Therapy with Redaporfin. *J. Clin. Med.* **2020**, 9 (1), 104 doi:10.3390/jcm9010104.
- (128) Krosi, G.; Korbelik, M.; Krosi, J.; Dougherty, G. J. Potentiation of Photodynamic Therapy-Elicited Antitumor Response by Localized Treatment with Granulocyte-Macrophage Colony-Stimulating Factor. *Cancer Res.* **1996**, 56 (14), 3281–3286.
- (129) Gołab, J.; Wilczyński, G.; Zagożdżon, R.; Stokłosa, T.; Dąbrowska, A.; Rybczyńska, J.; Wąsik, M.; Machaj, E.; Oldak, T.; Kozar, K.; Kamiński, R.; Giermasz, A.; Czajka, A.; Lasek, W.; Feleszko, W.; Jakóbisiak, M. Potentiation of the Anti-Tumour Effects of Photofrin®- Based Photodynamic Therapy by Localized Treatment with G-CSF. *Br. J. Cancer* **2000**, 82 (8), 1485–1491 doi:10.1054/bjoc.1999.1078.
- (130) de Bruijn, H. S.; Sluiter, W.; van der Ploeg-van den Heuvel, A.; Sterenborg, H. J. C. M.; Robinson, D. J. Evidence for a Bystander Role of Neutrophils in the Response to Systemic 5-Aminolevulinic Acid-Based Photodynamic Therapy. *Photodermatol. Photoimmunol. Photomed.* **2006**, 22 (5), 238–246 doi:10.1111/j.1600-0781.2006.00240.x.
- (131) Vivier, E.; Tomasello, E.; Baratin, M.; Walzer, T.; Ugolini, S. Functions of

- Natural Killer Cells. *Nat. Immunol.* **2008**, 9 (5), 503–510 doi:10.1038/ni1582.
- (132) Marshall, J. F.; Chan, W. S.; Hart, I. R. Effect of Photodynamic Therapy on Anti-Tumor Immune Defenses: Comparison of the Photosensitizers Hematoporphyrin Derivative and Chloro-Aluminum Sulfonated Phthalocyanine. *Photochem. Photobiol.* **1989**, 49 (5), 627–632 doi:10.1111/j.1751-1097.1989.tb08434.x.
- (133) Firczuk, M.; Nowis, D.; Gołąb, J. PDT-Induced Inflammatory and Host Responses. *Photochem. Photobiol. Sci.* **2011**, 10 (5), 653 doi:10.1039/c0pp00308e.
- (134) Mills, C. D.; Kincaid, K.; Alt, J. M.; Heilman, M. J.; Hill, A. M. Pillars Article: M-1/M-2 Macrophages and the Th1/Th2 Paradigm. *J. Immunol.* **2017**, 199 (7), 2194–2201 doi:10.4049/jimmunol.1701141.
- (135) Zhou, F.; Xing, D.; Chen, W. R. Regulation of HSP70 on Activating Macrophages Using PDT-Induced Apoptotic Cells. *Int. J. Cancer* **2009** doi:10.1002/ijc.24520.
- (136) Korbelik, M.; Naraparaju, V. R.; Yamamoto, N. Macrophage-Directed Immunotherapy as Adjuvant to Photodynamic Therapy of Cancer. *Br. J. Cancer* **1997**, 75 (2), 202–207 doi:10.1038/bjc.1997.34.
- (137) Steubing, R. W.; Yeturu, S.; Tuccillo, A.; Sun, C. H.; Berns, M. W. Activation of Macrophages by Photofrin II during Photodynamic Therapy. *J. Photochem. Photobiol. B Biol.* **1991**, 10 (1–2), 133–145 doi:10.1016/1011-1344(91)80218-7.
- (138) Reiter, I.; Schwamberger, G.; Krammer, B. Activation of Macrophage Tumoricidal Activity by Photodynamic Treatment in Vitro - Indirect Activation of Macrophages by Photodynamically Killed Tumor Cells. *J. Photochem. Photobiol. B Biol.* **1999**, 50 (2–3), 99–107 doi:10.1016/S1011-1344(99)00078-0.
- (139) Korbelik, M.; Kroszl, G. Enhanced Macrophage Cytotoxicity Against Tumor Cells Treated With Photodynamic Therapy. *Photochem. Photobiol.* **1994**, 60 (5), 497–502 doi:10.1111/j.1751-1097.1994.tb05140.x.
- (140) Yamamoto, N.; Sery, T. W.; Hooper, J. K.; Willett, N. P.; Lindsay, D. D. Effectiveness of Photofrin II in Activation of Macrophages and in Vitro Killing of Retinoblastoma Cells. *Photochem. Photobiol.* **1994**, 60 (2), 160–164 doi:10.1111/j.1751-1097.1994.tb05084.x.
- (141) Coutier, S.; Bezdetnaya, L.; Marchal, S.; Melnikova, V.; Belitchenko, I.; Merlin, J. L.; Guillemin, F. Foscan® (MTHPC) Photosensitized Macrophage Activation: Enhancement of Phagocytosis, Nitric Oxide Release and Tumour Necrosis

- Factor- α -Mediated Cytolytic Activity. *Br. J. Cancer* **1999**, *81* (1), 37–42
doi:10.1038/sj.bjc.6690648.
- (142) Yamamoto, N.; Hooper, J. K.; Yamamoto, N.; Yamamoto, S. Tumoricidal Capacities of Macrophages Photodynamically Activated With Hematoporphyrin Derivative. *Photochem. Photobiol.* **1992**, *56* (2), 245–250 doi:10.1111/j.1751-1097.1992.tb02153.x.
- (143) Qin, B.; Selman, S. H.; Payne, K. M.; Keck, R. W.; Metzger, D. W. Enhanced Skin Allograft Survival after Photodynamic Therapy. Association with Lymphocyte Inactivation and Macrophage Stimulation. *Transplantation* **1993**, *56* (6), 1481–1486 doi:10.1097/00007890-199312000-00038.
- (144) Yamamoto, N.; Homma, S.; Sery, T. W.; Donoso, L. A.; Kenneth Hooper, J. Photodynamic Immunopotential: In Vitro Activation of Macrophages by Treatment of Mouse Peritoneal Cells with Haematoporphyrin Derivative and Light. *Eur. J. Cancer Clin. Oncol.* **1991**, *27* (4), 467–471 doi:10.1016/0277-5379(91)90388-T.
- (145) Gollnick, S. O.; Owczarczak, B.; Maier, P. Photodynamic Therapy and Anti-Tumor Immunity. *Lasers Surg. Med.* **2006**, *38* (5), 509–515
doi:10.1002/lsm.20362.
- (146) Henderson, B. W.; Donovan, J. M. Release of Prostaglandin E2 from Cells by Photodynamic Treatment in Vitro. *Cancer Res.* **1989**, *49* (1 ml), 6896–6900.
- (147) Reiter, I.; Schwamberger, G.; Krammer, B. Effect of Photodynamic Pretreatment on the Susceptibility of Murine Tumor Cells to Macrophage Antitumor Mechanisms. *Photochem. Photobiol.* **1997**, *66* (3), 384–388 doi:10.1111/j.1751-1097.1997.tb03162.x.
- (148) Korbelik, M.; Hamblin, M. R. The Impact of Macrophage-Cancer Cell Interaction on the Efficacy of Photodynamic Therapy. *Photochem. Photobiol. Sci.* **2015**, *14* (8), 1403–1409 doi:10.1039/c4pp00451e.
- (149) Song, S.; Zhou, F.; Chen, W. R.; Xing, D. PDT-Induced HSP70 Externalization up-Regulates NO Production via TLR2 Signal Pathway in Macrophages. *FEBS Lett.* **2013**, *587* (2), 128–135 doi:10.1016/j.febslet.2012.11.026.
- (150) Demidova, T. N.; Hamblin, M. R. Macrophage-Targeted Photodynamic Therapy. *Int. J. Immunopathol. Pharmacol.* **2004**, *17* (2), 117–126
doi:10.1177/039463200401700203.
- (151) Hayashi, N.; Hiromi Kataoka; Yano, S.; Tanaka, M.; Moriwaki, K.; Akashi, H.;

- Suzuki, S.; Mori, Y.; Kubota, E.; Tanida, S.; Takahashi, S.; Joh, T. A Novel Photodynamic Therapy Targeting Cancer Cells and Tumor-Associated Macrophages. *Mol Cancer Ther.* **2015**, *14* (2), 452–460 doi:10.1158/1535-7163.MCT-14-0348.
- (152) Chan, C. W.; Housseau, F. The “kiss of Death” by Dendritic Cells to Cancer Cells. *Cell Death and Differentiation.* 2008 doi:10.1038/sj.cdd.4402235.
- (153) Gouwy, M.; Struyf, S.; Leutenez, L.; Pörtner, N.; Sozzani, S.; Van Damme, J. Chemokines and Other GPCR Ligands Synergize in Receptor-Mediated Migration of Monocyte-Derived Immature and Mature Dendritic Cells. *Immunobiology* **2014**, *219* (3), 218–229 doi:10.1016/j.imbio.2013.10.004.
- (154) Pearce, E. L. Metabolism in T Cell Activation and Differentiation. *Curr Opin Immunol.* **2015**, *22* (3), 314–320 doi:10.1016/j.coi.2010.01.018.Metabolism.
- (155) Garg, A. D.; Martin, S.; Golab, J.; Agostinis, P. Danger Signalling during Cancer Cell Death: Origins, Plasticity and Regulation. *Cell Death Differ.* **2014**, *21* (1), 26–38 doi:10.1038/cdd.2013.48.
- (156) Dudek, A. M.; Garg, A. D.; Krysko, D. V.; De Ruyscher, D.; Agostinis, P. Inducers of Immunogenic Cancer Cell Death. *Cytokine Growth Factor Rev.* **2013**, *24* (4), 319–333 doi:10.1016/j.cytogfr.2013.01.005.
- (157) Basu, S.; Binder, R. J.; Ramalingam, T.; Srivastava, P. K. CD91 Is a Common Receptor for Heat Shock Proteins Gp96, Hsp90, Hsp70, and Calreticulin. *Immunity* **2001** doi:10.1016/S1074-7613(01)00111-X.
- (158) Clark, E. A. A Short History of the B-Cell-Associated Surface Molecule CD40. *Front. Immunol.* **2014** doi:10.3389/fimmu.2014.00472.
- (159) Gao, L.; Zhang, C.; Gao, D.; Liu, H.; Yu, X.; Lai, J.; Wang, F.; Lin, J.; Liu, Z. Enhanced Anti-Tumor Efficacy through a Combination of Integrin Avβ6-Targeted Photodynamic Therapy and Immune Checkpoint Inhibition. *Theranostics* **2016**, *6* (5), 627–637 doi:10.7150/thno.14792.
- (160) Kushibiki, T.; Tajiri, T.; Tomioka, Y.; Awazu, K. Photodynamic Therapy Induces Interleukin Secretion from Dendritic Cells. *Int. J. Clin. Exp. Med.* **2010**, *3* (2), 110–114.
- (161) Ashley, C. E.; Carnes, E. C.; Phillips, G. K.; Padilla, D.; Durfee, P. N.; Brown, P. A.; Hanna, T. N.; Liu, J.; Phillips, B.; Carter, M. B.; Carroll, N. J.; Jiang, X.; Dunphy, D. R.; Willman, C. L.; Petsev, D. N.; Evans, D. G.; Parikh, A. N.; Chackerian, B.; Wharton, W.; Peabody, D. S.; Brinker, C. J. The Targeted

- Delivery of Multicomponent Cargos to Cancer Cells by Nanoporous Particle-Supported Lipid Bilayers. *Nat. Mater.* **2011**, *10* (5), 389–397
doi:10.1038/nmat2992.
- (162) Dudek, A. M.; Martin, S.; Garg, A. D.; Agostinis, P. Immature, Semi-Mature, and Fully Mature Dendritic Cells: Toward a DC-Cancer Cells Interface That Augments Anticancer Immunity. *Frontiers in Immunology*. 2013
doi:10.3389/fimmu.2013.00438.
- (163) Strioga, M.; Schijns, V.; Powell, D. J.; Pasukoniene, V.; Dobrovolskiene, N.; Michalek, J. Dendritic Cells and Their Role in Tumor Immunosurveillance. *Innate Immunity*. 2013 doi:10.1177/1753425912449549.
- (164) Cheong, T. C.; Shin, E. P.; Kwon, E. K.; Choi, J. H.; Wang, K. K.; Sharma, P.; Choi, K. H.; Lim, J. M.; Kim, H. G.; Oh, K.; Jeon, J. H.; So, I.; Kim, I. G.; Choi, M. S.; Kim, Y. K. Y. R.; Seong, S. Y.; Kim, Y. K. Y. R.; Cho, N. H. Functional Manipulation of Dendritic Cells by Photoswitchable Generation of Intracellular Reactive Oxygen Species. *ACS Chem. Biol.* **2015**, *10* (3), 757–765
doi:10.1021/cb5009124.
- (165) King, D. E.; Jiang, H.; Simkin, G. O.; Obochi, M. O. K.; Levy, J. G.; Hunt, D. W. C. Photodynamic Alteration of the Surface Receptor Expression Pattern of Murine Splenic Dendritic Cells. *Scand. J. Immunol.* **1999**, *49* (2), 184–192
doi:10.1046/j.1365-3083.1999.00498.x.
- (166) Hryhorenko, E. A.; Oseroff, A. R.; Morgan, J.; Rittenhouse-Diakun, K. Antigen Specific and Nonspecific Modulation of the Immune Response by Aminolevulinic Acid Based Photodynamic Therapy. *Immunopharmacology* **1998**, *40* (3), 231–240 doi:10.1016/S0162-3109(98)00047-2.
- (167) Jalili, A.; Makowski, M.; Świtaj, T.; Nowis, D.; Wilczyński, G. M.; Wilczek, E.; Chorąży-Massalska, M.; Radzikowska, A.; Maśliński, W.; Biały, Ł.; Sieńko, J.; Sieroń, A.; Adamek, M.; Basak, G.; Mróz, P.; Krasnodębski, I. W.; Jakóbisiak, M.; Gołąb, J. Effective Photoimmunotherapy of Murine Colon Carcinoma Induced by the Combination of Photodynamic Therapy and Dendritic Cells. *Clin. Cancer Res.* **2004**, *10* (13), 4498–4508 doi:10.1158/1078-0432.CCR-04-0367.
- (168) Reginato, E.; Wolf, P.; Hamblin, M. R. Immune Response after Photodynamic Therapy Increases Anti-Cancer and Anti-Bacterial Effects. *World J. Immunol.* **2014**, *4* (1), 1–11 doi:10.5411/wji.v4.i1.1.
- (169) Eagar, T. N.; Miller, S. D. 16 - Helper T-Cell Subsets and Control of the

- Inflammatory Response; Rich, R. R., Fleisher, T. A., Shearer, W. T., Schroeder, H. W., Frew, A. J., Weyand, C. M. B. T.-C. I. (Fifth E., Eds.; Content Repository Only! London, 2019; pp 235-245.e1 doi:10.1016/B978-0-7020-6896-6.00016-8.
- (170) Knutson, K. L.; Disis, M. L. Tumor Antigen-Specific T Helper Cells in Cancer Immunity and Immunotherapy. *Cancer Immunol. Immunother.* **2005**, *54* (8), 721–728 doi:10.1007/s00262-004-0653-2.
- (171) Wachowska, M.; Gabrysiak, M.; Muchowicz, A.; Bednarek, W.; Barankiewicz, J.; Rygiel, T.; Boon, L.; Mroz, P.; Hamblin, M. R.; Golab, J. 5-Aza-2'-Deoxycytidine Potentiates Antitumour Immune Response Induced by Photodynamic Therapy. *Eur. J. Cancer* **2014**, *50* (7), 1370–1381 doi:10.1016/j.ejca.2014.01.017.
- (172) Castellino, F.; Germain, R. N. COOPERATION BETWEEN CD4 + AND CD8 + T CELLS: When, Where, and How. *Annu. Rev. Immunol.* **2006**, *24* (1), 519–540 doi:10.1146/annurev.immunol.23.021704.115825.
- (173) Zou, W. Regulatory T Cells, Tumour Immunity and Immunotherapy. *Nat Rev Immunol.* **2006**, *6* (4), 295–307.
- (174) Campbell, D. J.; Koch, M. A. Phenotypical and Functional Specialization of FOXP3+ Regulatory T Cells. *Nat. Rev. Immunol.* **2011**, *11* (2), 119–130 doi:10.1038/nri2916.
- (175) Sakaguchi, S.; Wing, K.; Onishi, Y.; Prieto-Martin, P.; Yamaguchi, T. Regulatory T Cells: How Do They Suppress Immune Responses? *Int. Immunol.* **2009**, *21* (10), 1105–1111 doi:10.1093/intimm/dxp095.
- (176) Chen, W.; Jin, W.; Hardegen, N.; Lei, K.; Li, L.; Marinos, N.; McGrady, G.; Wahl, S. M. Conversion of Peripheral CD4+CD25– Naive T Cells to CD4+CD25+ Regulatory T Cells by TGF- β Induction of Transcription Factor Foxp3. *J. Exp. Med.* **2003**, *198* (12), 1875–1886 doi:10.1084/jem.20030152.
- (177) Roychoudhuri, R.; Eil, R. L.; Restifo, N. P. The Interplay of Effector and Regulatory T Cells in Cancer. *Curr. Opin. Immunol.* **2015**, *33*, 101–111 doi:10.1016/j.coi.2015.02.003.
- (178) Chen, M.-L.; Pittet, M. J.; Gorelik, L.; Flavell, R. A.; Weissleder, R.; von Boehmer, H.; Khazaie, K. Regulatory T Cells Suppress Tumor-Specific CD8 T Cell Cytotoxicity through TGF- Signals in Vivo. *Proc. Natl. Acad. Sci.* **2005**, *102* (2), 419–424 doi:10.1073/pnas.0408197102.
- (179) Awate, S.; Babiuk, L. A.; Mutwiri, G. Mechanisms of Action of Adjuvants.

- Front. Immunol.* **2013**, *4* (MAY), 1–10 doi:10.3389/fimmu.2013.00114.
- (180) Myers, R. C.; Lau, B. H. S.; Kunihiro, D. Y.; Torrey, R. R.; Woolley, J. L.; Tosk, J. Modulation of Hematoporphyrin Derivative-Sensitized Phototherapy with *Corynebacterium Parvum* in Murine Transitional Cell Carcinoma. *Urology* **1989**, *33* (3), 230–235 doi:10.1016/0090-4295(89)90399-3.
- (181) Korbelik, M.; Cecic, I. Enhancement of Tumour Response to Photodynamic Therapy by Adjuvant Mycobacterium Cell-Wall Treatment. *J. Photochem. Photobiol. B Biol.* **1998**, *44* (2), 151–158 doi:10.1016/S1011-1344(98)00138-9.
- (182) Korbelik, M.; Sun, J.; Posakony, J. J. Interaction Between Photodynamic Therapy and BCG Immunotherapy Responsible for the Reduced Recurrence of Treated Mouse Tumors. *Photochem. Photobiol.* **2001**, *73* (4), 403 doi:10.1562/0031-8655(2001)073<0403:IBPTAB>2.0.CO;2.
- (183) Cho, Y.-H.; Straight, R. C.; Smith, J. A. Effects of Photodynamic Therapy in Combination with Intravesical Drugs in a Murine Bladder Tumor Model. *J. Urol.* **1992**, *147* (3 Part 1), 743–746 doi:10.1016/S0022-5347(17)37370-6.
- (184) Szygula, M.; Pietrusa, A.; Adamek, M.; Wojciechowski, B.; Kawczyk-Krupka, A.; Cebula, W.; Duda, W.; Sieron, A. Combined Treatment of Urinary Bladder Cancer with the Use of Photodynamic Therapy (PDT) and Subsequent BCG-Therapy: A Pilot Study. *Photodiagnosis Photodyn. Ther.* **2004**, *1* (3), 241–246 doi:10.1016/S1572-1000(04)00067-5.
- (185) Uehara, M.; Sano, K.; Wang, Z.-L.; Sekine, J.; Ikeda, H.; Inokuchi, T. Enhancement of the Photodynamic Antitumor Effect by Streptococcal Preparation OK-432 in the Mouse Carcinoma. *Cancer Immunol. Immunother.* **2000**, *49* (8), 401–409 doi:10.1007/s002620000134.
- (186) Kroszl, G.; Korbelik, M. Potentiation of Photodynamic Therapy by Immunotherapy: The Effect of Schizophyllan (SPG). *Cancer Lett.* **1994**, *84* (1), 43–49 doi:10.1016/0304-3835(94)90356-5.
- (187) Chen, W. R.; Korbelik, M.; Bartels, K. E.; Liu, H.; Sun, J.; Nordquist, R. E. Enhancement of Laser Cancer Treatment by a Chitosan-Derived Immunoadjuvant. *Photochem. Photobiol.* **2004**, *81* (1), 190 doi:10.1562/2004-07-20-RA-236.
- (188) Xia, Y.; Gupta, G. K.; Castano, A. P.; Mroz, P.; Avci, P.; Hamblin, M. R. CpG Oligodeoxynucleotide as Immune Adjuvant Enhances Photodynamic Therapy Response in Murine Metastatic Breast Cancer. *J. Biophotonics* **2014**, *7* (11–12),

- 897–905 doi:10.1002/jbio.201300072.
- (189) Korbelik, M.; Banáth, J.; Zhang, W.; Gallagher, P.; Hode, T.; Lam, S. S. K.; Chen, W. R. N-Dihydrogalactochitosan as Immune and Direct Antitumor Agent Amplifying the Effects of Photodynamic Therapy and Photodynamic Therapy-Generated Vaccines. *Int. Immunopharmacol.* **2019**, *75* (July), 105764 doi:10.1016/j.intimp.2019.105764.
- (190) Marrache, S.; Choi, J. H.; Tundup, S.; Zaver, D.; Harn, D. A.; Dhar, S. Immune Stimulating Photoactive Hybrid Nanoparticles for Metastatic Breast Cancer. *Integr. Biol.* **2013**, *5* (1), 215–223 doi:10.1039/c2ib20125a.
- (191) Im, S.; Lee, J.; Park, D.; Park, A.; Kim, Y.-M.; Kim, W. J. Hypoxia-Triggered Transforming Immunomodulator for Cancer Immunotherapy via Photodynamically Enhanced Antigen Presentation of Dendritic Cell. *ACS Nano* **2019**, *13* (1), 476–488 doi:10.1021/acsnano.8b07045.
- (192) Bellnier, D. A. Potentiation of Photodynamic Therapy in Mice with Recombinant Human Tumor Necrosis Factors- α . *J. Photochem. Photobiol. B Biol.* **1991**, *8* (2), 203–210 doi:10.1016/1011-1344(91)80060-U.
- (193) Bellnier, D. A.; Gollnick, S. O.; Camacho, S. H.; Greco, W. R.; Cheney, R. T. Treatment with the Tumor Necrosis Factor-Alpha-Inducing Drug 5,6-Dimethylxanthenone-4-Acetic Acid Enhances the Antitumor Activity of the Photodynamic Therapy of RIF-1 Mouse Tumors. *Cancer Res.* **2003**, *63* (22), 7584–7590.
- (194) Korbelik, M.; Banáth, J.; Saw, K. M.; Zhang, W.; Čiplyš, E. Calreticulin as Cancer Treatment Adjuvant: Combination with Photodynamic Therapy and Photodynamic Therapy-Generated Vaccines. *Front. Oncol.* **2015**, *5* (FEB), 1–7 doi:10.3389/fonc.2015.00015.
- (195) Kleinovink, J. W.; van Driel, P. B.; Snoeks, T. J.; Prokopi, N.; Fransen, M. F.; Cruz, L. J.; Mezzanotte, L.; Chan, A.; Löwik, C. W.; Ossendorp, F. Combination of Photodynamic Therapy and Specific Immunotherapy Efficiently Eradicates Established Tumors. *Clin. Cancer Res.* **2016**, *22* (6), 1459–1468 doi:10.1158/1078-0432.CCR-15-0515.
- (196) Onizuka, S.; Tawara, I.; Shimizu, J.; Sakaguchi, S.; Fujita, T.; Nakayama, E. Tumor Rejection by in Vivo Administration of Anti-CD25 (Interleukin-2 Receptor α) Monoclonal Antibody. *Cancer Res.* **1999**, *59* (13), 3128–3133.
- (197) Whiteside, T. L. Immune Suppression in Cancer: Effects on Immune Cells,

- Mechanisms and Future Therapeutic Intervention. *Semin. Cancer Biol.* **2006**, *16* (1), 3–15 doi:10.1016/j.semcancer.2005.07.008.
- (198) Gollnick, S. O.; Vaughan, L.; Henderson, B. W. Generation of Effective Antitumor Vaccines Using Photodynamic Therapy. *Cancer Res.* **2002**, *62* (6), 1604–1608.
- (199) Korbelik, M.; Stott, B.; Sun, J. Photodynamic Therapy-Generated Vaccines: Relevance of Tumour Cell Death Expression. *Br. J. Cancer* **2007**, *97* (10), 1381–1387 doi:10.1038/sj.bjc.6604059.
- (200) Zhang, H.; Ma, W.; Li, Y. Generation of Effective Vaccines against Liver Cancer by Using Photodynamic Therapy. *Lasers Med. Sci.* **2009**, *24* (4), 549–552 doi:10.1007/s10103-008-0609-4.
- (201) Bae, S.-M.; Kim, Y.-W.; Kwak, S.-Y.; Kim, Y.-W.; Ro, D.-Y.; Shin, J.-C.; Park, C.-H.; Han, S.-J.; Oh, C.-H.; Kim, C.-K.; Ahn, W.-S. Photodynamic Therapy-Generated Tumor Cell Lysates with CpG-Oligodeoxynucleotide Enhance Immunotherapy Efficacy in Human Papillomavirus 16 (E6/E7) Immortalized Tumor Cells. *Cancer Sci.* **2007**, *98* (5), 747–752 doi:10.1111/j.1349-7006.2007.00447.x.
- (202) Cornwall, S. M. J.; Wikstrom, M.; Musk, A. W.; Alvarez, J.; Nowak, A. K.; Nelson, D. J. Human Mesothelioma Induces Defects in Dendritic Cell Numbers and Antigen-Processing Function Which Predict Survival Outcomes. *Oncoimmunology* **2016**, *5* (2), e1082028 doi:10.1080/2162402X.2015.1082028.
- (203) Sur, B. W.; Nguyen, P.; Sun, C.-H.; Tromberg, B. J.; Nelson, E. L. Immunophototherapy Using PDT Combined with Rapid Intratumoral Dendritic Cell Injection. *Photochem. Photobiol.* **2008**, *84* (5), 1257–1264 doi:10.1111/j.1751-1097.2008.00356.x.
- (204) Garg, A. D.; Vandenberk, L.; Koks, C.; Verschuere, T.; Boon, L.; Gool, S. W. Van; Agostinis, P. Dendritic Cell Vaccines Based on Immunogenic Cell Death Elicit Danger Signals and T Cell-Driven Rejection of High-Grade Glioma. *Sci Transl Med* **2016**, *8* (328), 328ra27 doi:10.1126/scitranslmed.aae0105.
- (205) Jung, N.; Jung, H.; Kang, M.; Lee, J.; Song, J.; Geuk, H.; Bae, Y.; Lim, D. Photodynamic Therapy-Mediated DC Immunotherapy Is Highly Effective for the Inhibition of Established Solid Tumors. *Cancer Lett.* **2012**, *324* (1), 58–65 doi:10.1016/j.canlet.2012.04.024.
- (206) Ferrario, A.; von Tiehl, K. F.; Rucker, N.; Schwarz, M. A.; Gill, P. S.; Gomer, C.

- J. Antiangiogenic Treatment Enhances Photodynamic Therapy Responsiveness in a Mouse Mammary Carcinoma. *Cancer Res.* **2000**, *60* (15), 4066–4069.
- (207) del Carmen, M. G.; Rizvi, I.; Chang, Y.; Moor, A. C. E. E.; Oliva, E.; Sherwood, M.; Pogue, B.; Hasan, T. Synergism of Epidermal Growth Factor Receptor–Targeted Immunotherapy With Photodynamic Treatment of Ovarian Cancer In Vivo. *JNCI J. Natl. Cancer Inst.* **2005**, *97* (20), 1516–1524
doi:10.1093/jnci/dji314.
- (208) Fisher, C.; Obaid, G.; Niu, C.; Foltz, W.; Goldstein, A.; Hasan, T.; Lilge, L. Liposomal Lapatinib in Combination with Low-Dose Photodynamic Therapy for the Treatment of Glioma. *J. Clin. Med.* **2019**, *8* (12), 2214
doi:10.3390/jcm8122214.
- (209) Zhou, Q.; Olivo, M.; Lye, K. Y. K.; Moore, S.; Sharma, A.; Chowbay, B. Enhancing the Therapeutic Responsiveness of Photodynamic Therapy with the Antiangiogenic Agents SU5416 and SU6668 in Murine Nasopharyngeal Carcinoma Models. *Cancer Chemother. Pharmacol.* **2005**, *56* (6), 569–577
doi:10.1007/s00280-005-1017-0.
- (210) Jiang, F.; Zhang, X.; Kalkanis, S. N.; Zhang, Z.; Yang, H.; Katakowski, M.; Hong, X.; Zheng, X.; Zhu, Z.; Chopp, M. Combination Therapy with Antiangiogenic Treatment and Photodynamic Therapy for the Nude Mouse Bearing U87 Glioblastoma. *Photochem. Photobiol.* **2007**, *84* (1), 071018085748008-??? doi:10.1111/j.1751-1097.2007.00208.x.
- (211) Korbelik, M.; Banáth, J.; Zhang, W. Mreg Activity in Tumor Response to Photodynamic Therapy and Photodynamic Therapy-Generated Cancer Vaccines. *Cancers (Basel)*. **2016**, *8* (10), 94 doi:10.3390/cancers8100094.
- (212) Kobayashi, H.; Choyke, P. L. Near-Infrared Photoimmunotherapy of Cancer. *Acc. Chem. Res.* **2019**, *52* (8), 2332–2339 doi:10.1021/acs.accounts.9b00273.
- (213) Goff, B.; Blake, J.; Bamberg, M.; Hasan, T. Treatment of Ovarian Cancer with Photodynamic Therapy and Immunoconjugates in a Murine Ovarian Cancer Model. *Br. J. Cancer* **1996**, *74* (8), 1194–1198 doi:10.1038/bjc.1996.516.
- (214) Del Governatore, M.; Hamblin, M. R.; Shea, C. R.; Rizvi, I.; Molpus, K. G.; Tanabe, K. K.; Hasan, T. Experimental Photoimmunotherapy of Hepatic Metastases of Colorectal Cancer with a 17.1A Chlorin(E6) Immunoconjugate. *Cancer Res.* **2000**, *60* (15), 4200–4205.
- (215) Mitsunaga, M.; Ogawa, M.; Kosaka, N.; Rosenblum, L. T.; Choyke, P. L.;

- Kobayashi, H. Cancer Cell–Selective in Vivo near Infrared Photoimmunotherapy Targeting Specific Membrane Molecules. *Nat. Med.* **2011**, *17* (12), 1685–1691 doi:10.1038/nm.2554.
- (216) Savellano, M. D. Photochemical Targeting of Epidermal Growth Factor Receptor: A Mechanistic Study. *Clin. Cancer Res.* **2005**, *11* (4), 1658–1668 doi:10.1158/1078-0432.CCR-04-1902.
- (217) Savellano, M. D.; Hasan, T. Targeting Cells That Overexpress the Epidermal Growth Factor Receptor with Polyethylene Glycolated BPD Verteporfin Photosensitizer Immunoconjugates. *Photochem. Photobiol.* **2003**, *77* (4), 431 doi:10.1562/0031-8655(2003)077<0431:TCTOTE>2.0.CO;2.
- (218) Vrouenraets, M. B.; Visser, G. W. M.; Stewart, F. A.; Stigter, M.; Oppelaar, H.; Postmus, P. E.; Snow, G. B.; Dongen, G. A. M. S. van. Development of Meta-Tetrahydroxyphenylchlorin-Monoclonal Antibody Conjugates for Photoimmunotherapy. *Exp. Ther.* **1999**, *59* (7), 1505–1513.
- (219) Vrouenraets, M. B.; Visser, G. W. M.; Stigter, M.; Oppelaar, H.; Snow, G. B.; van Dongen, G. A. Targeting of Aluminum (III) Phthalocyanine Tetrasulfonate by Use of Internalizing Monoclonal Antibodies: Improved Efficacy in Photodynamic Therapy. *Cancer Res.* **2001**, *61* (5), 1970–1975.
- (220) Ishida, M.; Kagawa, S.; Shimoyama, K.; Takehara, K.; Noma, K.; Tanabe, S.; Shirakawa, Y.; Tazawa, H.; Kobayashi, H.; Fujiwara, T. Trastuzumab-Based Photoimmunotherapy Integrated with Viral HER2 Transduction Inhibits Peritoneally Disseminated HER2-Negative Cancer. *Mol. Cancer Ther.* **2016**, *15* (3), 402–411 doi:10.1158/1535-7163.MCT-15-0644.
- (221) Soukos, N. S.; Hamblin, M. R.; Keel, S.; Fabian, R. L.; Deutsch, T. F.; Hasan, T. Epidermal Growth Factor Receptor-Targeted Immunophotodiagnosis and Photoimmunotherapy of Oral Precancer in Vivo. *Cancer Res.* **2001**, *61* (11), 4490–4496.
- (222) Mitsunaga, M.; Nakajima, T.; Sano, K.; Choyke, P. L.; Kobayashi, H. Near-Infrared Theranostic Photoimmunotherapy (PIT): Repeated Exposure of Light Enhances the Effect of Immunoconjugate. *Bioconjug. Chem.* **2012**, *23* (3), 604–609 doi:10.1021/bc200648m.
- (223) Sato, K.; Sato, N.; Xu, B.; Nakamura, Y.; Nagaya, T.; Choyke, P. L.; Hasegawa, Y.; Kobayashi, H. Spatially Selective Depletion of Tumor-Associated Regulatory T Cells with near-Infrared Photoimmunotherapy. *Sci. Transl. Med.* **2016**, *8* (352),

- 352ra110-352ra110 doi:10.1126/scitranslmed.aaf6843.
- (224) Sharpe, A. H.; Pauken, K. E. The Diverse Functions of the PD1 Inhibitory Pathway. *Nat. Rev. Immunol.* **2018**, *18* (3), 153–167 doi:10.1038/nri.2017.108.
- (225) Buchbinder, E. I.; Desai, A. CTLA-4 and PD-1 Pathways Similarities, Differences, and Implications of Their Inhibition. *Am. J. Clin. Oncol. Cancer Clin. Trials* **2016**, *39* (1), 98–106 doi:10.1097/COC.0000000000000239.
- (226) Vaddepally, R. K.; Kharel, P.; Pandey, R.; Garje, R.; Chandra, A. B. Review of Indications of FDA-Approved Immune Checkpoint Inhibitors per NCCN Guidelines with the Level of Evidence. *Cancers (Basel)*. **2020**, *12* (3), 738 doi:10.3390/cancers12030738.
- (227) Kleinovink, J. W.; Fransen, M. F.; Löwik, C. W.; Ossendorp, F. Photodynamic-Immune Checkpoint Therapy Eradicates Local and Distant Tumors by CD8+ T Cells. *Cancer Immunol. Res.* **2017**, *5* (10), 832–838 doi:10.1158/2326-6066.CIR-17-0055.
- (228) O’Shaughnessy, M. J.; Murray, K. S.; La Rosa, S. P.; Budhu, S.; Merghoub, T.; Somma, A.; Monette, S.; Kim, K.; Corradi, R. B.; Scherz, A.; Coleman, J. A. Systemic Antitumor Immunity by PD-1/PD-L1 Inhibition Is Potentiated by Vascular-Targeted Photodynamic Therapy of Primary Tumors. *Clin. Cancer Res.* **2018**, *24* (3), 592–599 doi:10.1158/1078-0432.CCR-17-0186.
- (229) Lan, G.; Ni, K.; Xu, Z.; Veroneau, S. S.; Song, Y.; Lin, W. Nanoscale Metal-Organic Framework Overcomes Hypoxia for Photodynamic Therapy Primed Cancer Immunotherapy. *J. Am. Chem. Soc.* **2018**, *140* (17), 5670–5673 doi:10.1021/jacs.8b01072.
- (230) Duan, X.; Chan, C.; Guo, N.; Han, W.; Weichselbaum, R. R.; Lin, W. Photodynamic Therapy Mediated by Nontoxic Core–Shell Nanoparticles Synergizes with Immune Checkpoint Blockade To Elicit Antitumor Immunity and Antimetastatic Effect on Breast Cancer. *J. Am. Chem. Soc.* **2016**, *138* (51), 16686–16695 doi:10.1021/jacs.6b09538.
- (231) Shao, Y.; Liu, B.; Di, Z.; Zhang, G.; Sun, L.; Li, L.; Yan, C. Engineering of Upconverted Metal-Organic Frameworks for Engineering of Upconverted Metal-Organic Frameworks for Near- Infrared Light-Triggered Combinational Photodynamic- / Chemo- / Immuno-Therapy Against Hypoxic Tumors. *J. Am. Chem. Soc.* **2020**, *142* (8), 3939–3946 doi:10.1021/jacs.9b12788.
- (232) Wang, D.; Wang, T.; Liu, J.; Yu, H.; Jiao, S.; Feng, B.; Zhou, F.; Fu, Y.; Yin, Q.;

- Zhang, P.; Zhang, Z.; Zhou, Z.; Li, Y. Acid-Activatable Versatile Micelleplexes for PD-L1 Blockade-Enhanced Cancer Photodynamic Immunotherapy. *Nano Lett.* **2016**, *16* (9), 5503–5513 doi:10.1021/acs.nanolett.6b01994.
- (233) Dai, L.; Li, K.; Li, M.; Zhao, X.; Luo, Z.; Lu, L.; Luo, Y.; Cai, K. Size/Charge Changeable Acidity-Responsive Micelleplex for Photodynamic-Improved PD-L1 Immunotherapy with Enhanced Tumor Penetration. *Adv. Funct. Mater.* **2018**, *28* (18), 1707249 doi:10.1002/adfm.201707249.
- (234) Uyttenhove, C.; Pilotte, L.; Théate, I.; Stroobant, V.; Colau, D.; Parmentier, N.; Boon, T.; Van den Eynde, B. J. Evidence for a Tumoral Immune Resistance Mechanism Based on Tryptophan Degradation by Indoleamine 2,3-Dioxygenase. *Nat. Med.* **2003**, *9* (10), 1269–1274 doi:10.1038/nm934.
- (235) Lu, K.; He, C.; Guo, N.; Chan, C.; Ni, K.; Weichselbaum, R. R.; Lin, W. Chlorin-Based Nanoscale Metal–Organic Framework Systemically Rejects Colorectal Cancers via Synergistic Photodynamic Therapy and Checkpoint Blockade Immunotherapy. *J. Am. Chem. Soc.* **2016**, *138* (38), 12502–12510 doi:10.1021/jacs.6b06663.
- (236) Pucelik, B.; Arnaut, L. G.; Dąbrowski, J. M. Lipophilicity of Bacteriochlorin-Based Photosensitizers as a Determinant for PDT Optimization through the Modulation of the Inflammatory Mediators. *J. Clin. Med.* **2019**, *9* (1), 8 doi:10.3390/jcm9010008.
- (237) Li, F.; Cheng, Y.; Lu, J.; Hu, R.; Wan, Q.; Feng, H. Photodynamic Therapy Boosts Anti-Glioma Immunity in Mice: A Dependence on the Activities of T Cells and Complement C3. *Journal of Cellular Biochemistry.* 2011, pp 3035–3043 doi:10.1002/jcb.23228.
- (238) Wei, L.-H.; Baumann, H.; Tracy, E.; Wang, Y.; Hutson, A.; Rose-John, S.; Henderson, B. W. Interleukin-6 Trans Signalling Enhances Photodynamic Therapy by Modulating Cell Cycling. *Br. J. Cancer* **2007**, *97* (11), 1513–1522 doi:10.1038/sj.bjc.6604073.
- (239) Mroz, P.; Hamblin, M. R. The Immunosuppressive Side of PDT. *Photochem. Photobiol. Sci.* **2011**, *10* (5), 751–758 doi:10.1039/c0pp00345j.
- (240) Gollnick, S. O. Photodynamic Therapy and Antitumor Immunity. *J. Natl. Compr. Cancer Netw.* **2012**, *10* (Suppl_2), S-40-S-43 doi:10.6004/jnccn.2012.0173.
- (241) Santos, L. L.; Oliveira, J.; Monteiro, E.; Santos, J.; Sarmiento, C. Treatment of Head and Neck Cancer with Photodynamic Therapy with Redaporfin: A Clinical

- Case Report. *Case Rep. Oncol.* **2018**, *11* (3), 769–776 doi:10.1159/000493423.
- (242) Gomes-da-Silva, L. C.; Zhao, L.; Bezu, L.; Zhou, H.; Sauvat, A.; Liu, P.; Durand, S.; Leduc, M.; Souquere, S.; Loos, F.; Mondragón, L.; Sveinbjörnsson, B.; Rekdal, Ø.; Boncompain, G.; Perez, F.; Arnaut, L. G.; Kepp, O.; Kroemer, G. Photodynamic Therapy with Redaporfin Targets the Endoplasmic Reticulum and Golgi Apparatus. *EMBO J.* **2018**, *37* (13) doi:10.15252/emj.201798354.
- (243) Gomes-da-Silva, L. C.; Zhao, L.; Arnaut, L. G.; Kroemer, G.; Kepp, O. Redaporfin Induces Immunogenic Cell Death by Selective Destruction of the Endoplasmic Reticulum and the Golgi Apparatus. *Oncotarget* **2018**, *9* (58), 31169–31170 doi:10.18632/oncotarget.25798.
- (244) Spitzer, M. H.; Carmi, Y.; Reticker-Flynn, N. E.; Kwek, S. S.; Madhireddy, D.; Martins, M. M.; Gherardini, P. F.; Prestwood, T. R.; Chabon, J.; Bendall, S. C.; Fong, L.; Nolan, G. P.; Engleman, E. G. Systemic Immunity Is Required for Effective Cancer Immunotherapy. *Cell* **2017**, *168* (3), 487–502.e15 doi:10.1016/j.cell.2016.12.022.
- (245) Ueda, Y.; Kondo, M.; Kelsoe, G. Inflammation and the Reciprocal Production of Granulocytes and Lymphocytes in Bone Marrow. *J. Exp. Med.* **2005**, *201* (11), 1771–1780 doi:10.1084/jem.20041419.
- (246) Theodoraki, M. N.; Lorenz, K.; Lotfi, R.; Fürst, D.; Tsamadou, C.; Jaekle, S.; Mytilineos, J.; Brunner, C.; Theodorakis, J.; Hoffmann, T. K.; Laban, S.; Schuler, P. J. Influence of Photodynamic Therapy on Peripheral Immune Cell Populations and Cytokine Concentrations in Head and Neck Cancer. *Photodiagnosis Photodyn. Ther.* **2017**, *19* (May), 194–201 doi:10.1016/j.pdpdt.2017.05.015.
- (247) Cheon, Y. K.; Cho, Y. D.; Moon, J. H.; Jang, J. Y.; Kim, Y. S. Y. S.; Kim, Y. S. Y. S.; Lee, M. S.; Lee, J. S.; Shim, C. S. Diagnostic Utility of Interleukin-6 (IL-6) for Primary Bile Duct Cancer and Changes in Serum IL-6 Levels Following Photodynamic Therapy. *Am. J. Gastroenterol.* **2007**, *102* (10), 2164–2170 doi:10.1111/j.1572-0241.2007.01403.x.
- (248) Mosser, D. M.; Zhang, X. Interleukin-10: New Perspectives on an Old Cytokine. *Immunol. Rev.* **2008**, *226* (1), 205–218 doi:10.1111/j.1600-065X.2008.00706.x.
- (249) Ng, T. H. S.; Britton, G. J.; Hill, E. V.; Verhagen, J.; Burton, B. R.; Wraith, D. C. Regulation of Adaptive Immunity; The Role of Interleukin-10. *Front. Immunol.* **2013**, *4* doi:10.3389/fimmu.2013.00129.
- (250) Shah, W.; Yan, X.; Jing, L.; Zhou, Y.; Chen, H.; Wang, Y. A Reversed

- CD4/CD8 Ratio of Tumor-Infiltrating Lymphocytes and a High Percentage of CD4+FOXP3+ Regulatory T Cells Are Significantly Associated with Clinical Outcome in Squamous Cell Carcinoma of the Cervix. *Cell. Mol. Immunol.* **2011**, 8 (1), 59–66 doi:10.1038/cmi.2010.56.
- (251) Schroder, K.; Hertzog, P. J.; Ravasi, T.; Hume, D. A. Interferon- γ : An Overview of Signals, Mechanisms and Functions. *J. Leukoc. Biol.* **2004**, 75 (2), 163–189 doi:10.1189/jlb.0603252.
- (252) Berner, V.; Liu, H.; Zhou, Q.; Alderson, K. L.; Sun, K.; Weiss, J. M.; Back, T. C.; Longo, D. L.; Blazar, B. R.; Witrout, R. H.; Welniak, L. A.; Redelman, D.; Murphy, W. J. IFN- γ Mediates CD4+ T-Cell Loss and Impairs Secondary Antitumor Responses after Successful Initial Immunotherapy. *Nat. Med.* **2007**, 13 (3), 354–360 doi:10.1038/nm1554.
- (253) Witowski, J.; Ksiazek, K.; Jorres, A. Interleukin-17: A Mediator of Inflammatory Responses. *Cell. Mol. Life Sci.* **2004**, 61 (5), 567–579 doi:10.1007/s00018-003-3228-z.
- (254) Ma, Y.; Aymeric, L.; Locher, C.; Mattarollo, S. R.; Delahaye, N. F.; Pereira, P.; Boucontet, L.; Apetoh, L.; Ghiringhelli, F.; Casares, N.; Lasarte, J. J.; Matsuzaki, G.; Ikuta, K.; Ryffel, B.; Benlagha, K.; Tesnière, A.; Ibrahim, N.; Déchanet-Merville, J.; Chaput, N.; Smyth, M. J.; Kroemer, G.; Zitvogel, L. Contribution of IL-17–Producing $\Gamma\delta$ T Cells to the Efficacy of Anticancer Chemotherapy. *J. Exp. Med.* **2011**, 208 (3), 491–503 doi:10.1084/jem.20100269.
- (255) Fisher, D. T.; Appenheimer, M. M.; Evans, S. S. The Two Faces of IL-6 in the Tumor Microenvironment. *Semin. Immunol.* **2014**, 26 (1), 38–47 doi:10.1016/j.smim.2014.01.008.
- (256) Taniguchi, K.; Karin, M. IL-6 and Related Cytokines as the Critical Lynchpins between Inflammation and Cancer. *Semin. Immunol.* **2014**, 26 (1), 54–74 doi:10.1016/j.smim.2014.01.001.
- (257) Fielding, C. A.; McLoughlin, R. M.; McLeod, L.; Colmont, C. S.; Najdovska, M.; Grail, D.; Ernst, M.; Jones, S. A.; Topley, N.; Jenkins, B. J. IL-6 Regulates Neutrophil Trafficking during Acute Inflammation via STAT3. *J. Immunol.* **2008**, 181 (3), 2189–2195 doi:10.4049/jimmunol.181.3.2189.
- (258) Zitvogel, L.; Kepp, O.; Kroemer, G. Decoding Cell Death Signals in Inflammation and Immunity. *Cell* **2010**, 140 (6), 798–804 doi:10.1016/j.cell.2010.02.015.

- (259) Garg, A. D.; Krysko, D. V.; Verfaillie, T.; Kaczmarek, A.; Ferreira, G. B.; Marysael, T.; Rubio, N.; Firczuk, M.; Mathieu, C.; Roebroek, A. J. M.; Annaert, W.; Golab, J.; de Witte, P.; Vandenabeele, P.; Agostinis, P. A Novel Pathway Combining Calreticulin Exposure and ATP Secretion in Immunogenic Cancer Cell Death. *EMBO J.* **2012**, *31* (5), 1062–1079 doi:10.1038/emboj.2011.497.
- (260) Krysko, D. V.; Garg, A. D.; Kaczmarek, A.; Krysko, O.; Agostinis, P.; Vandenabeele, P. Immunogenic Cell Death and DAMPs in Cancer Therapy. *Nat. Rev. Cancer* **2012**, *12* (12), 860–875 doi:10.1038/nrc3380.
- (261) Lund, F. E.; Randall, T. D. Effector and Regulatory B Cells: Modulators of CD4+ T Cell Immunity. *Nat. Rev. Immunol.* **2010**, *10* (4), 236–247 doi:10.1038/nri2729.
- (262) Gajewski, T. F.; Schreiber, H.; Fu, Y.-X. Innate and Adaptive Immune Cells in the Tumor Microenvironment. *Nat. Immunol.* **2013**, *14* (10), 1014–1022 doi:10.1038/ni.2703.
- (263) Lechner, M. G.; Karimi, S. S.; Barry-Holson, K.; Angell, T. E.; Murphy, K. A.; Church, C. H.; Ohlfest, J. R.; Hu, P.; Epstein, A. L. Immunogenicity of Murine Solid Tumor Models as a Defining Feature of In Vivo Behavior and Response to Immunotherapy. *J. Immunother.* **2013**, *36* (9), 477–489 doi:10.1097/01.cji.0000436722.46675.4a.
- (264) Huang, Y.-Y.; Vecchio, D.; Avci, P.; Yin, R.; Garcia-Diaz, M.; Hamblin, M. R. Melanoma Resistance to Photodynamic Therapy: New Insights. *Biol. Chem.* **2013**, *394* (2), 239–250 doi:10.1515/hsz-2012-0228.
- (265) Tao, K.; Fang, M.; Alroy, J.; Sahagian, G. G. Imagable 4T1 Model for the Study of Late Stage Breast Cancer. *BMC Cancer* **2008**, *8* (1), 228 doi:10.1186/1471-2407-8-228.
- (266) Dąbrowski, J. M.; Urbanska, K.; Arnaut, L. G.; Pereira, M. M.; Abreu, A. R.; Simões, S.; Stochel, G. Biodistribution and Photodynamic Efficacy of a Water-Soluble, Stable, Halogenated Bacteriochlorin against Melanoma. *ChemMedChem* **2011**, *6* (3), 465–475 doi:10.1002/cmdc.201000524.
- (267) Mazor, O.; Brandis, A.; Plaks, V.; Neumark, E.; Rosenbach-Belkin, V.; Salomon, Y.; Scherz, A. WST11, A Novel Water-Soluble Bacteriochlorophyll Derivative; Cellular Uptake, Pharmacokinetics, Biodistribution and Vascular-Targeted Photodynamic Activity Using Melanoma Tumors as a Model¶. *Photochem. Photobiol.* **2005**, *81* (2), 342 doi:10.1562/2004-06-14-ra-199.1.

- (268) S. Lobo, A. C. Impact of Photodynamic Therapy with the Photosensitizer Redaporfin in Distant Metastasis, University of Coimbra, 2015.
- (269) Lobo, C. S.; Tomé, V. A.; Schaberle, F. A.; Calvete, M. J. F.; Pereira, M. M.; Serpa, C.; Arnaut, L. G. Biocompatible Ring-Deformed Indium Phthalocyanine Label for near-Infrared Photoacoustic Imaging. *Inorganica Chim. Acta* **2021**, *514*, 119993 doi:10.1016/j.ica.2020.119993.
- (270) Zhong, W.; Myers, J. S.; Wang, F.; Wang, K.; Lucas, J. J.; Rosfjord, E.; Lucas, J. J.; Hooper, A. T.; Yang, S.; Lemon, L. A.; Guffroy, M.; May, C.; Bienkowska, J. R.; Rejto, P. A. Comparison of the Molecular and Cellular Phenotypes of Common Mouse Syngeneic Models with Human Tumors. *BMC Genomics* **2020**, *21* (1), 2 doi:10.1186/s12864-019-6344-3.
- (271) Fidler, I. J. Biological Behavior of Malignant Melanoma Cells Correlated to Their Survival In Vivo. *Cancer Res.* **1975**, *35*, 218–224.
- (272) Galluzzi, L.; Buqué, A.; Kepp, O.; Zitvogel, L.; Kroemer, G. Immunogenic Cell Death in Cancer and Infectious Disease. *Nat. Rev. Immunol.* **2017**, *17* (2), 97–111 doi:10.1038/nri.2016.107.
- (273) Cramer, G. M.; Moon, E. K.; Cengel, K. A.; Busch, T. M. Photodynamic Therapy and Immune Checkpoint Blockade. *Photochem. Photobiol.* **2020**, *96* (5), 954–961 doi:10.1111/php.13300.
- (274) van der Merwe, P. A.; Bodian, D. L.; Daenke, S.; Linsley, P.; Davis, S. J. CD80 (B7-1) Binds Both CD28 and CTLA-4 with a Low Affinity and Very Fast Kinetics. *J. Exp. Med.* **1997**, *185* (3), 393–404 doi:10.1084/jem.185.3.393.
- (275) Mao, H.; Zhang, L.; Yang, Y.; Zuo, W.; Bi, Y.; Gao, W.; Deng, B.; Sun, J.; Shao, Q.; Qu, X. New Insights of CTLA-4 into Its Biological Function in Breast Cancer. *Curr. Cancer Drug Targets* **2010**, *10* (7), 728–736.
- (276) Pistillo, M. P. CTLA-4 Is Not Restricted to the Lymphoid Cell Lineage and Can Function as a Target Molecule for Apoptosis Induction of Leukemic Cells. *Blood* **2003**, *101* (1), 202–209 doi:10.1182/blood-2002-06-1668.
- (277) Contardi, E.; Palmisano, G. L.; Tazzari, P. L.; Martelli, A. M.; Falà, F.; Fabbi, M.; Kato, T.; Lucarelli, E.; Donati, D.; Polito, L.; Bolognesi, A.; Ricci, F.; Salvi, S.; Gargaglione, V.; Mantero, S.; Alberghini, M.; Ferrara, G. B.; Pistillo, M. P. CTLA-4 Is Constitutively Expressed on Tumor Cells and Can Trigger Apoptosis upon Ligand Interaction. *Int. J. Cancer* **2005**, *117* (4), 538–550 doi:10.1002/ijc.21155.

- (278) Tirapu, I.; Huarte, E.; Guiducci, C.; Arina, A.; Zaratiegui, M.; Murillo, O.; Gonzalez, A.; Berasain, C.; Berraondo, P.; Fortes, P.; Prieto, J.; Colombo, M. P.; Chen, L.; Melero, I. Low Surface Expression of B7-1 (CD80) Is an Immunoescape Mechanism of Colon Carcinoma. *Cancer Res.* **2006**, *66* (4), 2442–2450 doi:10.1158/0008-5472.CAN-05-1681.
- (279) Baptista, M. Z.; Sarian, L. O.; Derchain, S. F. M.; Pinto, G. A.; Vassallo, J. Prognostic Significance of PD-L1 and PD-L2 in Breast Cancer. *Hum. Pathol.* **2016**, *47* (1), 78–84 doi:10.1016/j.humpath.2015.09.006.
- (280) Davis, A. A.; Patel, V. G. The Role of PD-L1 Expression as a Predictive Biomarker: An Analysis of All US Food and Drug Administration (FDA) Approvals of Immune Checkpoint Inhibitors. *J. Immunother. Cancer* **2019**, *7* (1), 278 doi:10.1186/s40425-019-0768-9.
- (281) Dyck, L.; Mills, K. H. G. Immune Checkpoints and Their Inhibition in Cancer and Infectious Diseases. *Eur. J. Immunol.* **2017**, *47* (5), 765–779 doi:10.1002/eji.201646875.
- (282) Kim, H. R.; Ha, S.; Hong, M. H.; Heo, S. J.; Koh, Y. W.; Choi, E. C.; Kim, E. K.; Pyo, K. H.; Jung, I.; Seo, D.; Choi, J.; Cho, B. C.; Yoon, S. O. PD-L1 Expression on Immune Cells, but Not on Tumor Cells, Is a Favorable Prognostic Factor for Head and Neck Cancer Patients. *Sci. Rep.* **2016**, *6* (1), 36956 doi:10.1038/srep36956.
- (283) Patsoukis, N.; Wang, Q.; Strauss, L.; Boussiotis, V. A. Revisiting the PD-1 Pathway. *Sci. Adv.* **2020**, *6* (38), eabd2712 doi:10.1126/sciadv.abd2712.
- (284) Sugiura, D.; Maruhashi, T.; Okazaki, I.; Shimizu, K.; Maeda, T. K.; Takemoto, T.; Okazaki, T. Restriction of PD-1 Function by Cis -PD-L1/CD80 Interactions Is Required for Optimal T Cell Responses. *Science (80-.)*. **2019**, *364* (6440), 558–566 doi:10.1126/science.aav7062.
- (285) Schneider, H.; Rudd, C. E. Diverse Mechanisms Regulate the Surface Expression of Immunotherapeutic Target CTLA-4. *Front. Immunol.* **2014**, *5* doi:10.3389/fimmu.2014.00619.